Experimental studies of forward in situ combustion.

Alshalabe, Maysoon Ismaeil

Award date:
1985

Awarding institution:
University of Bath

EXPERIMENTAL STUDIES OF FORWARD *IN SITU* COMBUSTION

Submitted by Maysoon Ismaeil Alshalabe

for the degree of Doctor of Philosophy

of the University of Bath

1985

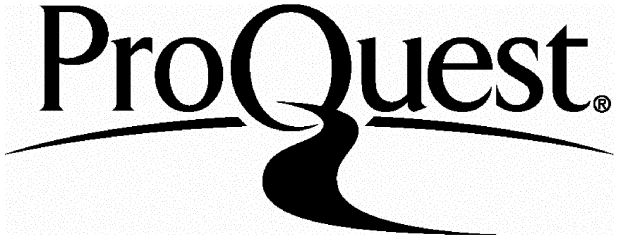

To my husband, Mohammed

ACKNOWLEDGEMENTS

The author expresses her most sincere gratitude to Dr. M. Greaves, for his guidance and counsel as research supervisor.

The author is also indebted to Dr. R.W. Field, who was a frequent source of helpful suggestions and stimulating discussion.

Thanks are also due to Professor W.J. Thomas, for providing research equipment and facilities.

The generous provision of crude oils by the British Petroleum Company (BP Research Centre) is gratefully acknowledged.

The kind assistance of Mr. T. Walton and all the technical staff is also gratefully acknowledged.

Similarly, the author owes her gratitude to Mrs. Paula Keilthy, for typing the thesis.

ABSTRACT

Investigation of forward *in situ* combustion have been carried out in a 7.3 cm diameter tube having a length of 0.869 m. Experiments at pressures up to 50 psig were made to study combustion characteristics and enhanced oil recovery of three different crude oils, namely North Sea Forties (36.6 °API), Maya Isthmus (32.4 °API) and Maya (22.1 °API). Sand packs were prepared with oil saturations in the range 38-44.32%.

Close adiabatic control of the combustion tube was achieved for both dry and wet combustion modes. Detailed production history and overall mass balances are presented. Correlation in both graphical and tabular form is given for air-fuel ratio, oxygen utilisation and normalised combustion velocity. In this respect, the results of the present work show good agreement with those of other workers.

Normal wet, partial quenched modes of combustion were produced using WARs up to 3.75 m^3/Mm^3(STP). The combustion front temperature was not significantly affected by the cooling effect of the injected water. Under partially quenched conditions, high combustion-steam zone temperatures were achieved. For wet combustion, the oxygen utilisation generally improved slightly. Air requirement, air-oil ratio and fuel consumption all decreased with increased water-air ratio and increased with increased clay content.

The velocity of the combustion front (normalised with respect to the air flux) increased in a linear manner as the WAR increased. Increasing the clay content, however, gave rise to a decrease in the

combustion front velocity. High oil recovery, at 79.37%, was achieved during normal wet combustion of Forties oil.

In sand mixtures containing amorphous silica powder, the combustion exhibited virtually 100% oxygen utilisation, with higher carbon burning rates compared with runs using clay addition. These effects are attributed to the nature and magnitude of the surface area of solid additives, which play an important role in the oxidation mechanisms.

NOMENCLATURE

A	Arrhenius constant, cm^3/g mole.s
°API	American Petroleum Institute Gravity, $°API = \frac{141.5}{sp\ gr} - 131.5$
AFR	Air-fuel-ratio, standard cubic meter of air per kilogram of fuel burned.
AOR	Air-oil-ratio, standard cubic meter of air per cubic meter of produced oil.
BV	Bulk volume, dimensionless
C	Fuel concentration, g fuel/100 g sand
cal/g CHX	Calorie per one gram of fuel
cal/g sand	Calorie per one gram of sand
E	Activation energy, J/g mole
K	Rate constant, $(sec - psi)^{-1}$
kJ/kg sand	Kilojoule per kilogram sand
M	Thousand in English Engineering units
$m^3(st)$	Standard cubic meter (at STP)
PO_2	Oxygen partial pressure, psi (KPa)
PV	Pore volume, dimensionless
R	Gas constant, J/(g mole) (°C)
R_C	Combustion rate g fuel/(100 g sand).s
S	Saturation, dimensionless
STP	Standard conditions for S.I.: 15 °C and 101.325 KPa Standard conditions for English Engineering units: 60 °F and 14.696 psia
t	Time, seconds
T	Absolute temperature, °F (°C)
WAR	Water-air-ratio, m^3 water/Mm^3(STP) air
w/w	Weight ratio

Superscript

n	reaction order with respect to coke, constant

Subscripts

m	reaction order with respect to oxygen, constant
o	oil
w	water

Abbreviations

COFCAW	combination of forward combustion and water-flooding
LTO	low temperature oxidation
OOIP	original oil in-place
TGA	thermogravimetric analysis
DSC	differential scanning calorimetry

CONTENTS

CONTENTS (Continued)

CHAPTER 1

INTRODUCTION

In the longer term, the demand for crude oil is set to increase. High exploration costs, particularly off-shore, and marginal economic performance of some secondary recovery projects, however, places an upper limit on recoverable reserves. These facts have been strongly recognised by the major oil companies and other research organisations, who are now devoting considerable attention to developing improved methods of oil recovery. Enhanced oil recovery (EOR), therefore, aims to recover the oil which is left "unrecovered" by conventional reservoir production techniques. This represents a considerable challenge, since, on a world-wide basis, the unrecovered oil averages about 50-60%, or more, of the original oil in place.

Thermal processes constitute an important sector of enhanced oil recovery techniques. The basic principle is one of applying heat, either at the surface or underground, to raise the internal energy of the reservoir. Increasing the temperature of the reservoir reduces the viscosity of the oil, which increases its ability to flow. In turn, improving the mobility ratio between the oil and the displacing fluid enhances the displacement process. Thermal processes are not limited by heterogeneity of the formation, because heat can penetrate by conduction into the less permeable and porous parts of the reservoir. This effect contributes to an improvement in the overall volumetric sweep efficiency. Other possible effects of applying heat may include the reduction in the interfacial tension between the fluid phases, and alteration of the wettability characteristics of the reservoir.

There are four basic types of thermal recovery processes used to introduce heat into a reservoir. These include hot fluid injection, forward combustion, reverse combustion, and conduction "downhole heating". In addition to these, other methods have been used which combine two or more of these basic processes. All the methods have been field tested with varying degrees of success. Theoretical and experimental laboratory work by industry, universities and research institutes has contributed to the development of field projects.

A great deal of attention has been directed recently to the study of forward combustion as a very promising oil recovery technique. In this sense, it can be considered as a primary, secondary, or tertiary recovery process. Forward combustion should be applied to a reservoir as soon as it is economically justified and where the reservoir properties are favourable to combustion.

The process of forward combustion involves igniting the oil in the reservoir by injecting a continuous supply of air. In this way, a burning front is propagated through the formation in the direction of the air flow. Distillation and cracking of some of this oil leaves behind residual fuel, which, in turn, provides the main source of fuel for the burning zone. The mobile oil is driven forward by a vigorous gas drive produced by the combustion gases and an accompanying water drive, due to recondensed formation water and water from the combustion. Some oil is also vaporised by the approaching heat wave carried forward by the combustion gases. This is recondensed upon contact with the cooler regions of the reservoir, where it is again subjected to gas and water displacement.

One of the most important parameters governing the forward combustion process is the fuel availability. In heavier crude oils having sufficient

naphthenic and asphaltic compounds, the fuel is produced in the form of coke, which deposits on the sand grains of the porous reservoir rock. Due to the critical importance of the above parameter, there has been some speculation concerning the applicability of forward combustion to light oil reservoirs. This is because insufficient fuel deposition may take place to sustain combustion.

Fuel availability is a function of many factors, not the least of which is the nature of the reservoir rock itself (Ramey, 1971). It has been found that reservoir lithology can, in many cases, be more significant than oil gravity in determining fuel concentration. Laboratory studies by Bousaid and Ramey (1968) normally indicate that to sustain vigorous combustion, higher fuel concentration is obtained with a natural reservoir matrix, compared with clean unconsolidated sands. However, Guvenir (1980) showed that combustion could not be sustained in sand mixtures alone without the addition of clay. Recent studies by Vossoughi *et al.* (1981, 1982a) revealed that the addition of clay influenced the amount of fuel deposition in the combustion process, specifically its catalytic and surface area effect on the crude oil oxidation reaction.

Many oil reservoir formations are known to contain substantial amounts of fines, which include considerable amounts of clay minerals. Successful application of enhanced recovery techniques depends, to a large extent, on the mobility and reactivity of the clays in the formation (Somerton and Radke, 1980). Thus, the clay content of reservoir rocks has an important bearing on fuel deposition in the combustion process, due to the high reactive surface area. On the other hand, clay minerals, when in contact with water, may give rise to formation damage or plugging problems. This situation can occur with a wet forward-combustion technique, because of the steam or fresh water from condensing steam.

It is considered that montmorillonite is the principal clay mineral causing reduced permeability in the reservoir. However, Gray and Rex (1966) have shown that other clay minerals also cause formation damage. Mungen (1965) has also demonstrated that permeability reduction can occur in formations containing non-swelling clays, such as illite and kaolinite, when there is a change in the pH of the flowing fluid.

Many studies are limited to the water sensitivity of the formation clay towards other enhanced oil recovery processes, such as surfactant flooding and chemical flooding. Unfortunately, the author was not able to locate any work relevant to the role of clay mineral in formations in which wet forward combustion is applied. Preliminary experiments showed that a self-sustained combustion front could be established only when clay was present in the sand mixture.

The main objective of the present study was to investigate the factor governing wet forward combustion, with special emphasis on the use of high water to air ratios and conditions when certain amounts of clay material were added to the sand matrix. Comparative studies were also made under dry combustion conditions with amorphous silica incorporated into the sand mixture. The results, including air requirement, air to oil ratios, combustion front velocities, production histories and oxygen utilisation, were obtained using two light crude oils (Forties and Maya Isthmus) and a medium gravity crude oil (Maya).

CHAPTER 2

LITERATURE REVIEW

There is a wide body of literature concerning forward combustion processes. This review covers works carried out on the processes of wet and dry forward combustion, derived mainly from combustion tube experiments, associated kinetic studies and field *in situ* combustion projects.

2.1 Forward *in situ* combustion

In forward *in situ* combustion, air is injected into the reservoir through an injection well. Ignition is obtained at the injection well, either spontaneously or by assisted means, and a combustion zone is propagated within the reservoir rock towards the producing wells. The process is initiated first by injecting air for a short period, to establish a continuous gas path between the injection and producing wells, which could lead to a spontaneous ignition. If spontaneous ignition does not occur, then it is necessary to introduce heat into the formation. Artificial ignition ensures a more uniform initial burning zone in the reservoir and also serves to reduce air compression costs (Strange, 1964). As the air is continuously injected, the combustion front progresses further away from the injection well.

Figure 2.1 shows a schematic diagram of the forward *in situ* combustion process (McNiel and Nelson, 1959). The upper portion of this drawing represents the temperature profile as a function of the distance between the injection and producing wells. In the zone between the injection well and the burning front, the temperature varies from that of the injection air temperature to a maximum at the burning front. Part of the heat from the hot zone is recovered by the air as it moves towards the burning front, but this is limited by the poor heat carrying capacity of the air. The

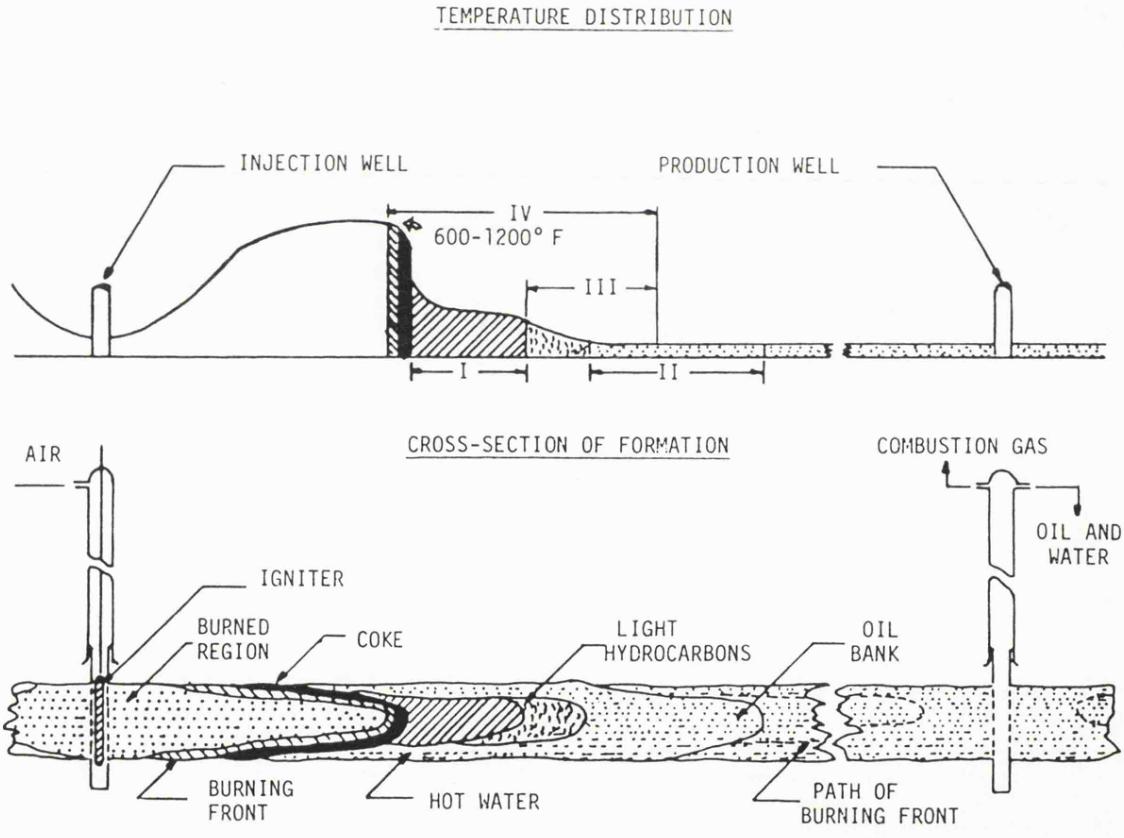

Figure 2.1 Schematic diagram of *in situ* combustion process

remaining heat is lost to the overlaying and underlaying strata. The temperature of the combustion zone is about 600-1200° F (315-650° C). Residual fuel, or coke, is produced as a result of thermal cracking and distillation of the crude oil, which takes place just ahead of the burning front. This fuel is necessary to sustain the moving combustion front.

Immediately ahead of the burning zone, the temperature increases rapidly through the cracking and evaporation zones. In these, all of the liquid water and light oil components are vaporised. Downstream of the cracking and evaporation zones is the condensing steam zone (so-called steam plateau), which is characterised by a flat temperature profile. This zone consists of steam, combustion gases and vaporised oil, in association with the flowing liquid water and oil.

The lower temperature ahead of the steam plateau causes the steam and vaporised oil to condense, creating a condensation zone. Further downstream, an oil bank is formed, due to oil being displaced by the burning front. Ahead of this lies the undisturbed formation containing virgin oil and the temperature is at the original reservoir value.

Oil displacement in the forward combustion process is the result of a combination of all mechanisms mentioned above, *i.e.*, condensing steam drive, gas drive, miscible drive and the thermal drive. A full description of these mechanisms can be found in Al-Saadoon (1970) and McNiel and Nelson (1959).

Forward combustion can be further subdivided into dry and wet forward processes. In wet forward combustion, water is added together with the air, either continuously, or in an intermittent manner. Addition of water increases the sensible heat in the injection stream, so that greater heat utilisation is achieved. A more comprehensive description will be given in the following section.

2.2 Wet forward combustion

This process involves simultaneous, or cyclic, injection of water with the air, thus enabling the heat from the hot sand behind the combustion front to be recovered. If sufficient water is injected, it is possible to cool or quench the trailing edge of the combustion zone before all the fuel has been burned. This, in turn, causes the combustion front to move at a faster rate through the reservoir, so that more oil is recovered per unit of air injected. This method is known by the abbreviation "COFCAW", first described by Parrish and Craig (1969) for the combination of forward combustion and water flooding. Later, Buxton and Craig (1973) described COFCAW as shown in Figure 2.2, with an injection well on the left and a producing well on the right. Moving out from the injection well, one first encounters an air-water zone in which injected air and water are flowing. The air and water saturations in this region are established by the relative permeability characteristics of the rock and the injected air-water ratio. Some residual coke saturation exists, due to incomplete fuel consumption. The cooling effect of the water reduces the temperature to its original level.

The next zone which is encountered is the combustion zone, where essentially all of the oxygen is consumed. The temperature here may range from approximately 800-1200° F (425-650° C). The size of this zone is negligible in terms of field dimensions. Ahead of the combustion zone is the steam zone, in which gas (mainly nitrogen and carbon dioxide), steam and water, together with vaporised hydrocarbons, are flowing. A non-flowing hydrocarbon saturation exists, but part of this will be vaporised, or cracked, and part will be consumed as fuel. The residue will remain as unrecovered oil. The temperature of the steam zone is essentially that of boiling water at the prevailing reservoir pressure.

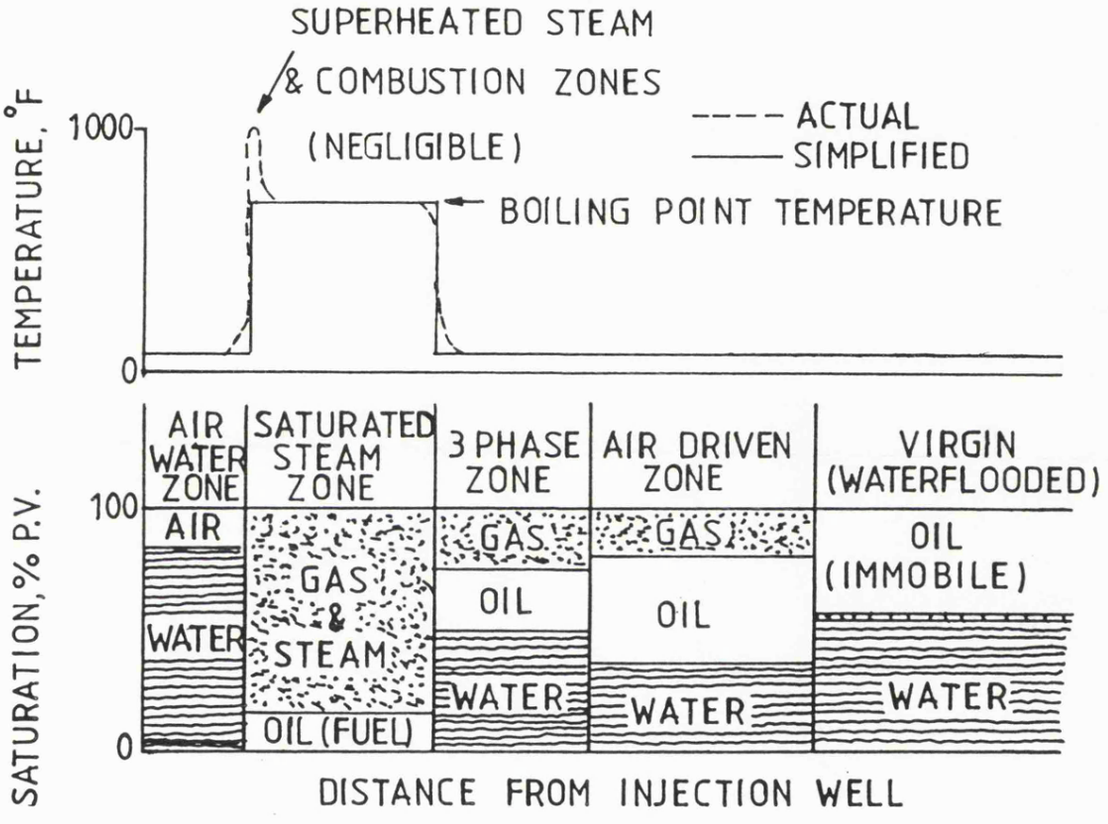

Figure 2.2 Schematic drawing of COFCAW saturation and temperature profiles (Buxton and Craig, 1973).

Downstream of the steam zone the temperature falls off fairly rapidly to the original reservoir temperature. Here there is a region in which oil, water and gas are flowing. The three phase flow results in a high pressure drop throughout this region.

Further downstream is a gas drive zone, again containing oil, water and combustion gases. In a tertiary recovery operation, the water saturation is reduced from that which existed after the water flooding. In this case, the initial oil saturation may be immobile. In non-flooded reservoirs, the water saturation is at connate water saturation and the flowing phases are gas and oil.

A number of investigators (Dietz and Weijdema, 1968; Burger and Sahuquet, 1973) have identified different types of wet combustion. Dietz and Weijdema (1968) have further refined the understanding of wet combustion by classifying it according to the injected water-air ratio. These are known as normal wet, optimal and partially quenched combustion. In normal wet combustion (moderate water injection rates) super heated steam forms upon contact with the hot sand before the combustion front. In limited cases, the water evaporation front travels at just the same velocity as the combustion front, but does not overtake it. This is optimal normal wet combustion. Although it would seem that wet combustion should be limited to conditions which do not allow water to over-run the combustion zone (due to extinction), the combustion is only quenched locally. Therefore, the combustion evaporation zone is still propagated when the evaporation front over-runs the combustion front, and the residual oil burns at the steam temperature. They also showed that hydrogen is preferentially burned at a temperature of about 200° C, but a temperature of 400° C is necessary to burn the carbonaceous residue completely. Thus,

a very fast travelling front is established as a result of the heat wave from steam, the heat recovered from the formation, and the heat released by combustion.

Wet combustion has been differently classified by Burger and Sahuquet (1973). They defined three types of wet combustion, according to the temperature of the saturation profile - normal wet, incomplete, and super wet combustion. In normal wet combustion, all of the coke is burned, but with incomplete wet combustion, some may be left unburned. For both of these cases, the evaporation front remains behind the combustion front so that steam passes through the burning zone. The third type, super wet combustion, takes place when sufficient water enters the combustion zone to cause the peak combustion temperature to disappear. However, several possibilities exist between the two extremes of water injection. The effect of water volume has been studied thoroughly by Buxton and Craig (1973).

2.3 Development of *in situ* combustion

The idea of using heat to stimulate oil production is not a recent innovation. The use of downhole-heating for the purpose of melting parafinic accumulations in the vicinity of the well bore was practiced as early as 1920 (Hester and Menzie, 1954). Russian workers were the first to carry out field trials in subsurface combustion. They achieved this by igniting shallow oil with glowing charcoal and then feeding this into the well together with injected air. The first English translation of this report appeared in 1938.

The first United States patents to mention *in situ* combustion were granted to Howard (1923) and Wolcott (1923) (Standard Development Company). Following this, experiments were conducted in a shallow, pressure-depleted reservoir during the period 1933-1935. This confirmed that combustion in an oil

bearing sand could be initiated and maintained and significant amounts of oil recovered. After World War II, with the increased interest in developing new recovery methods, field experiments with underground combustion were started in the U.S.A. In 1953, the Magnolia Petroleum Company reported some laboratory and field test information on combustion methods (Kuhn and Koch, 1953). Whilst Magnolia were testing their field experiments, Sinclair Research Laboratories Inc. were conducting a large-scale field test in the Delaware-Childers field in Oklahoma. This work had begun in 1947, but it was first published by Grant and Szasz in 1954. In addition, in 1957, a combination of steam drive and *in situ* combustion processes was reported by Walters (1957), as a result of a field test in Illinois.

Following these developments, a co-operative venture, involving twelve oil companies, working in the South Belridge field in California, published their results in 1958 (Gates and Ramey, 1958). This test involved a pattern of almost commercial well spacing for a low API gravity crude oil of 12.9°. Observations revealed that spontaneous ignition occurred near the injection well. This was due to low temperature oxidation by air, at a pressure of 200 p.s.i. Since the Belridge experiment, a number of other field tests have been undertaken with different well patterns and field conditions (Moss *et al.*, 1959; Holbrook *et al.*, 1959; Fuchida, 1959; Emery, 1962; Parrish *et al.*, 1962). Of particular interest in this area is the work of Fuchida (1959), in which *in situ* combustion was successfully conducted in a reservoir having a high water saturation, as well as a strong natural water drive. This led to the conclusion that *in situ* combustion could be applied as a tertiary recovery technique in watered-out reservoirs.

Not all of the field tests have been successful. For example, Holbrook *et al.* (1959) describe an abortive attempt to ignite a high gravity paraffinic crude in a reservoir with poor permeability. Moreover, extinction of the flame front has occurred in other tests shortly after ignition. In order to define the physical limit of combustion and extinction, several investigators have undertaken both theoretical and laboratory studies of the process concurrent with the field tests.

2.4 Combustion tube experiments

2.4.1 Dry forward combustion

An extensive programme of research has been carried out in the laboratory, in order to understand the mechanics of dry forward combustion and to delineate the process variables which are necessary for successful propagation of the combustion front.

Sheinman and Sergeev (1958) conducted combustion studies in unconsolidated media and concluded that a stable combustion zone is achieved when the coke residue is greater than 1.5% by weight of the sand. Presumably, when coke concentration is less than this amount, extinction will occur. However, Bailey and Larkin (1960) predicted a lower limit of approximately 0.6% coke by weight. Other laboratory experiments by Martin *et al.* (1958) have also demonstrated that stable combustion can be achieved at lower fuel concentrations than those given by Sheinman and Sergeev.

A technique for determining the fuel availability or coke laydown, and the corresponding theoretical air requirement for *in situ* combustion was reported by Alexander *et al.* (1962). Their method involved a fire flood-pot technique. Using both consolidated and unconsolidated media, the authors found that crushed core material gave essentially the same

fuel availability as the original consolidated core. They also concluded that the amount of fuel available for *in situ* combustion varied with crude oil and porous medium characteristics, oil saturation, air flux and time-temperature relationships. Fuel availability, determined using clean porous media, was lower than that obtained using natural reservoir rock material when the oil saturation was high. An increase in the initial oil saturation from 5.0 to 10.0 weight percent caused an increase in the fuel of only 0.15 weight percent (ranging from 1.05 to 1.2).

One of the important characteristics of crude oils is the API gravity. Research by Showalter (1963) has shown that as the API gravity of oil decreased, the fuel concentration increases, which leads to a greater air requirement. Showalter established, therefore, that air requirement for forward combustion was a function of the API gravity of the oil. Other factors which could affect the air requirement, are increase in the hydrogen-carbon ratio of the fuel and the percentage of oxygen in the exit gases. It was further determined that an increase in pressure resulted in a slight increase in fuel concentration. The fuel concentration was, however, insensitive to the rate of burning of the fuel.

Another study concerning a high API gravity of oil of 32.1-44.3° was conducted by Sterner and Wertman (1976). Their result confirmed that *in situ* combustion is applicable to both asphaltic- and paraffinic-based high gravity oils under suitable conditions.

Combustion tube tests carried out by Buesse (1971) showed that fuel deposition increases with higher air rates and also as the surface area of the solid matrix increases. Although pressure did not noticeably affect fuel consumption, an increase in the peak temperature was observed. The relationship between oil saturation and fuel deposition was found to be linear.

Garon and Wygal (1974) have reported the results of tests carried out on twelve different crude oils which included 32.8°, 37.3°, 40.2° and 48.2° API gravity crudes. These showed that all of the crude oils, except the lightest (48.2° API), sustained dry forward combustion, both at atmospheric and 6895 KPa pressure. In another experiment using a high gravity 40° API oil, some difficulty was experienced in sustaining combustion with a synthetic matrix (Harding *et al.*, 1972). However, vigorous combustion was maintained when natural core material was used. The data obtained indicated that *in situ* combustion variables for high gravity crude oil were greatly influenced by the mineral composition of the host matrix. According to Poettman *et al.* (1967), the specific surface area of the matrix has a direct effect on the fuel concentration, especially if the surface area is less than 2 m^2/g.

Dabbous and Fulton (1974) have also detected some surface effects of the clay additives on the reaction rate, but they were not measured. In other works, by Bousaid and Ramey (1968) and by Burger and Sahuquet (1972), it has been noticed that the reaction rate is proportional to the specific surface area of the matrix raised to the power 10 to 1. Certain soils and metallic derivatives also exhibit catalytic affects (Buesse, 1971; Sterner and Wertman, 1976; Garon and Wygal, 1974). Al-Saadoon (1970) has shown a definite dependence of fuel deposition on the surface area. The mineral composition of the matrix rock, type of crude oil and chemical composition of the oil all have an important effect on fuel deposition (Okandan *et al.*, 1982).

Mekhtibeili and Sultanov (1978), who studied the effect of rock mineral on the oxidation reaction, found that an unexpected decomposition of carbonates rock took place below 700° C, due to the presence of substantial

pyrites. In addition, sulphur components of the porous medium tend to react with the carbonate. In fact, certain crudes may provide a source of sulphur dioxide. It was concluded that higher air consumption in rocks containing sulphur-bearing crude was to be expected.

2.4.2 Wet forward combustion

In forward combustion, about one-fifth of the heat generated is taken up by the air stream as it contacts the hot zone of the reservoir through which the burning zone has passed. Owing to the high cost of the compressed air required per barrel of recoverable oil, and also the relatively inefficient heat utilisation, methods have been sought to improve the efficiency of the dry forward combustion process.

The first modification was reported by Scott (1960), who suggested injecting water simultaneously with air. Before Scott's patent, Kuhn and Koch (1953) had also mentioned facilitating heat transfer by injecting water with the air. In the combustion tube experiment carried by Langnes and Beeson (1964), the switch-over from air to water was made after the flame front had travelled over 60% of the sand pack. Compared with simultaneous injection of air and water, this method suffers from a number of disadvantages. Oil recovery from the water flooded zone is much less and a larger amount of heat may be lost to the adjacent formations prior to water injection. Thus, injection of water is most advantageous when undertaken at the earliest opportunity.

Generally, wet combustion is characterised by a lower air requirement and air-oil ratio, in comparison with dry combustion. In laboratory experiments, Smith and Perkin (1973) confirmed the feasibility of reduced air requirement and the improved heat utilisation by water injection. Because of the apparently high transient nature of wet combustion, they

showed that stable combustion may not be achieved until the front has travelled a distance greater than the length of most laboratory combustion tubes. This suggests that even with perfectly adiabatic combustion tube conditions, where normal tube lengths are concerned, the result of wet combustion tests may be misleading. Garon and Wygal (1974) showed that such combustion tube problems can be overcome by a proper design and operation. In particular, the transient effects were reduced by establishing an expected temperature profile by using an ignition heater prior to combustion.

Research has shown that wet forward combustion can be sustained under suitable conditions. Garon and Wygal found that normal wet combustion of high gravity crude oils could not be sustained at atmospheric pressure, because distillation residues were too low. However, with 32.8° and 48.2° API gravity crude oils, wet combustion was sustained at 6895 and 13790 KPa pressure, respectively. Prior to this, Parrish and Craig (1969) had published the first wet forward combustion laboratory studies with high gravity crude oils, of 35.2°, 38.9° and 40.9° API. They concluded that the air requirement and fuel consumption were significantly lower, compared with dry forward combustion. Using higher water:air ratios also produced higher recoveries. Ejiogu (1978) found that a natural core could deposit enough fuel to sustain combustion, even when the residual oil saturation was as low as 28.9° percent, using a water:air ratio as high as 0.00273m^3/m^3 (st). He suggested that it was important to obtain a mineral analysis of pre- and post-burn samples, for possible correction of carbon dioxide generated by decarbonation of such minerals as calcite, dolomite, and siderite when using natural core.

Laboratory studies have also been concerned with low API gravity oils. Harding *et al.* (1976) conducted wet forward combustion tube experiments using high bitumen saturations in Alberta sand. These tests were characterised by high pressure drops (even with preheating), high fuel consumption and high air:oil ratios. The 'tight' emulsions which were produced gave rise to difficult operational problems and were formed by the heavy oil, together with cracked light ends, and condensed steam and formation of water. Difficulty in separating the emulsion produced can lead to inaccuracies in the oil mass balances and hence determined air:oil ratios. Wet combustion tests using heavy oils as low as 9.6°, 16°, and 13.5° API gravity, have been carried out by Burger and Sahuquet, 1973; Garon and Wygal, 1974; and Parrish and Craig, 1969.

2.5 Field projects

Several field projects have indicated the usefulness of co-ordination between laboratory research and field experimentation in carrying out combustion projects. An example is the Caddo Pine Island field project (Horne *et al.*, 1982), which was carried out in a thin oil column underlaid by water. Laboratory tube tests used the reservoir matrix to determine the optimal water to air ratio, which was later required in developing the project design. The conducting combustion project in the Romanian field of Suplacu de Barcau and Balaria (Gadelle *et al.*, 1981) is another good example of the use of laboratory combustion tube results. This provided data on the chemical reaction kinetics, fuel availability, air requirement and many other parameters. The kinetic studies on the core samples showed firstly, how the reaction rates were affected by the properties of the oil and core material; secondly, the effect of any catalytic material present in the oil or in the matrix and finally, the effect of organic material associated with the core. These results were also helpful in deciding

whether to use dry or wet combustion and what optimal water:air ratio to use in the field project.

Laboratory combustion tube tests gave favourable results for the flank of sand 5 (a major oil reservoir in the West Heidelburg Cotton Valley Sands Unit, Jasper County, M.S., U.S.A.) (Huffman *et al.*, 1983). This could mean that, if developed, it will probably be the world's deepest *in situ* combustion project (the Cotton Valley Sands occurring at an average depth of 3475 m, or 11400 ft).

It should be emphasised that for application in field projects, reliable laboratory evaluation can only be obtained for experiments using a natural core material. This is mainly due to possible catalytic effects to which actual core material may contribute. In the case of the May-Libby project (Hardingetal., 1972), a series of combustion tests has shown that it was difficult to sustain combustion with synthetic material, whereas no such difficulty was encountered when the natural core was used (restored to post-water flooded saturation).

The condition of the natural core has also been cited as another factor affecting laboratory test results. In these cases, preliminary tests with reservoir crude, using Berea sandstone and an old, unpreserved Estes reservoir core (West Texas, U.S.A.) were not favourable. However, favourable results were obtained when resaturated and water-flooded fresh cores were used. It was further concluded that *in situ* combustion was applicable in a watered-out sandstone reservoir containing a light gravity crude oil (Anthony *et al.*, 1982).

2.6 Effect of clay minerals on forward *in situ* combustion

Clay minerals play a major role in the physico-chemical processes of oil production. This is primarily because of their platelike structure

(Somerton and Radke, 1980). The response of a formation to an *in situ* combustion process may be dominated by the reaction of these clay minerals. Part 1 of this section reviews the clay composition of some oil producing reservoirs and some important characteristics of clay mineral, while Part 2 deals more specifically with the effect of clay minerals and other additives on the reaction mechanism of the combustion process.

2.6.1 Clay in oil producing formations

The clay mineral composition can be distinctive for a particular horizon of a sedimentary sequence and may be used for correlation purposes. According to the clay mineral concept, clay minerals are essentially composed of extremely small crystalline particles of one or more members of a smaller group of minerals. These minerals are basically hydrous aluminium silicates, with magnesium or iron acting as proxy, wholly or in part, for aluminium in some cases (Grim, 1962).

All clay minerals exhibit various physical properties, such as surface activity, ion exchange capacity and a tendency to swell. The degree or capacity of any particular property is specific to the particular type of clay mineral.

Clay minerals can be present in substantial amounts in many producing reservoirs. This has been shown by a lithographic/mineralogy study performed on representative samples of Nacatoch formation in the Caddo Pine Island field, Los Angeles, U.S.A. (Horne *et al.*, 1982). The samples were found to contain an average of 15% authogenic and allogenic kaolinite clay and minor amounts of illite. Another example is that of the Yates formation sand of the North Ward-Estes field in Texas, U.S.A. (Anthony *et al.*, 1982), in which the clay represents approximately 10% of the rock volume. The clay consists of 80-85% montmorillonite, 5-10% illite and 1-5% chlorite.

In Athabasca tar sand (Alberta, Canada), the fines contain about 32% clay, which is equal to 7% of the total content of sand (Dabbous, 1971; Guvenir, 1980). Amyx *et al.* (1960) showed that kaolinite and montmorillonite occur in high proportions in the cementation material in the arkose sandstone of Stevens, California oil sand. Amyx also reported that illite is the principal clay mineral in graywacke sediments in the Frio formation (Gulf coast of Texas and Louisiana).

Clay catalysts are frequently used in the petroleum processing industry for the cracking of petroleum and the manufacture of gasoline (Grim, 1962). The types of clay used in catalyst manufacture are produced from bentonite, which is composed of montmorillonite and kaolinite clays. There are several possible ways of preparing satisfactory catalysts from kaolinite clays. Mills (1947) claimed that the surface area of the kaolin can be increased without acid treatment to produce an efficient catalytic product. However, it is also argued that an adequate catalyst does not require a very large surface area. Also, Grim (1962) pointed out that there is no direct correlation between the catalytic activity and the amount of surface area.

The Computer Modelling Group (1982: 110-119) have shown that the catalytic property of the rock matrix is strongly related to its composition. Table 2.1 indicates that as the surface area increases, the amount of coke decreases. This is found to be consistent for both silica sand and pre-treated stainless steel shavings. In Table 2.2, the coke content decreases with clay fraction .

The swelling tendency, flocculation and dispersion characteristics of clay minerals may cause serious plugging of pores, with consequent reduction of the permeability. A study in this field, concerning fresh

Table 2.1 Computer Modelling Group 1982

SURFACE AREA EFFECT

Name	Athabasca Bitumen	Atha. Bitumen & Silica Sand (200 mesh) Surface Area 8.5 m^2/g	Atha. Bitumen & Silica Sand (25 mesh) Surface Area 4.3 m^2/g	Atha. Bitumen & Pretreated Stainless Steel Shavings Surface Area 6.1 m^2/g
Coke	9.1	5.1	6.2	5.6
Asphaltenes	11.9	12.2	12.4	12.0
Light Oil	27.1	30.5	30.7	30.1
Heavy Oil	46.7	46.3	44.0	47.3
Gas	5.3	5.0	5.3	4.7
H_2	5.0	5.2	5.2	5.2
CH_4	35.8	36.3	40.6	41.6
CO	1.9	2.7	2.0	4.0
CO_2	1.8	1.6	1.6	2.4
C_2H_4	0.58	0.71	0.52	0.95
C_2H_6	15.0	15.2	16.7	19.8
H_2S	23.7	21.7	19.6	--
COS	0.33	0.29	0.15	--
C_3H_6	--	--	--	--
C_3H_8	9.8	10.3	8.7	13.9
$i\text{-}C_4H_{10}$	1.2	1.2	0.95	1.8
$n\text{-}C_4H_{10}$	3.1	3.0	3.0	6.7
$i\text{-}C_5H_{12}$	0.52	0.57	0.33	1.0
$n\text{-}C_5H_{12}$	0.91	1.0	0.65	1.9
C_6H_{14}	0.23	0.27	0.04	0.79
Gas Vol.	--	--	--	--
Aver. M.W.	28.2	28.1	26.7	29.0
TOTAL**	100.1	99.1	98.6	99.7

** *TOTAL refers to the sum of the calculated mass percents for components coke, asphaltenes, light oil, heavy oil, and gas.*

Table 2.2 Computer Modelling Group 1982

EFFECT OF NATIVE CLAY

Name	Bitumen & Core*	Bitumen & Core* Washed**	Bitumen Core* & H_2O	Bitumen & Core Ignited 1000°C
Coke	8.4	6.2	8.1	7.2
Asphaltene	13.1	12.7	12.3	10.8
Light Oil	25.1	27.6	23.0	27.0
Heavy Oil	49.2	48.7	51.8	50.1
Gas	5.3	5.1	5.5	5.0
H_2	5.1	5.1	6.1	5.5
CH_4	38.3	37.5	38.1	37.6
CO	1.1	1.6	0.40	1.2
CO_2	3.3	2.3	5.4	2.7
C_2H_4	0.52	0.66	0.32	0.52
C_2H_6	16.4	16.0	16.1	15.9
H_2S	18.8	20.2	17.6	20.6
COS	0.18	0.37	0.01	0.20
C_3H_6	--	--	--	--
C_3H_8	9.3	9.5	9.0	9.3
$i\text{-}C_4H_{10}$	1.2	1.1	1.5	1.2
$n\text{-}C_4H_{10}$	3.7	3.8	3.4	3.6
$i\text{-}C_5H_{12}$	0.58	0.54	0.71	0.51
$n\text{-}C_5H_{12}$	1.1	1.1	1.1	0.97
C_6H_{14}	0.34	0.31	0.33	0.26
Aver. M.W.	28.1	28.1	28.0	27.9
TOTAL***	101.1	100.3	100.7	100.1

* *Ignited at 320°C.*

** *Part of clay removed*

*** *Total refers to sum of calculated mass percents for components coke, asphaltenes, light oil, heavy oil and gas.*

water sensitivity, has been published by Nahin *et al.* (1951). Their identification of clay minerals in the Steven and Gutchell sand cores of Californian oil-bearing reservoirs, has led them to conclude that the predominance of illite and/or montmorillonite in the Stevens zone core is in harmony with the observed sensitivity of these strata to fresh water. Likewise, the predominance of kaolin as kaolinite or anauxite, or both, is in accord with the relative immunity of the Gatchell sand to such damage.

2.6.2 Reaction mechanisms in porous media in the presence of clay minerals and metallic derivatives

In the combustion drive, the least desirable part of the original oil in-place (OOIP) is burnt as fuel. The fuel laydown (*i.e.*, coke) is produced by cracking, pyrolysis and distillation. Due to the importance of fuel in controlling the reaction rate of crude oil in porous media, extensive work has been carried out concerning the kinetic studies of *in situ* combustion.

In general, the combustion rate R_C of crude oil in a porous medium, as described by Wilson *et al.*, 1963; Bousaid and Ramey, 1968; and Burger and Sahuquet, 1972, is given by:

$$R_C = -\frac{dC_m}{dt} = k\, p_{O_2}^{m}\, C_m^{n}$$

The reaction constant, k, is often a function of temperature:

$$k = A \exp(-E/RT)$$

where A is the Arrhenius constant and is a function of the surface area of the rock.

Early studies by Bousaid and Ramey (1968) have shown that the activation energy is reasonably insensitive to the gravity of the crude oil. For two oils which were studied (13.9 and 22.1° API gravity), the activation energy decreased from 26600 to *ca.* 20500 Btu/lb mole, with a 20% addition of clay to the sand. As clay was added to the system, they found that the amount of fuel deposited increased. Fassihi *et al.* (1980a, 1980b, 1984) concluded that metallic additives such as copper, nickel, vanadium, iron, and clay, *etc.*, have a catalytic effect on the oxidation reactions. Clay also enhances the deposition of higher amounts of fuel, due to its adsorption characteristics.

Vossuoghi *et al.* (1982b) investigated the effect of surface area using both combustion tube tests as well as a thermogravimetric analysis (TGA) and also differential scanning calorimeter (DSC). They showed that a minimum specific area should be available for a given crude oil to establish a self-sustained combustion front in clean, unconsolidated sand packs, but the clay mineral would have additional catalytic effects.

A new criterion for the selection of the candidate reservoir for the combustion process has been considered by Kharrat and Vossoughi (1984). A minimum oil content of the reservoir rock ought to be available to establish a self-sustained combustion front. However, measurement of the effects of the surface area of the rock should be carried out independently, or along with the new criterion. Drici and Vossoughi (1984) concluded that surface area of the additives affects the crude oil combustion, regardless of the composition of the additives, using surface areas ranging from 30 cm^2/g to 24.3 m^2/g. However, the nature of the surface area, as well as the availability of large surfaces, may play a vital role in determining the effectiveness of the additives.

CHAPTER 3

COMBUSTION TUBE EQUIPMENT AND EXPERIMENTAL PROCEDURE

3.1 Experimental equipment

The laboratory *in situ* combustion comprises five major components. These are the combustion tube and the pressure jacket, the fluid injection and control system, the fluid production system, gas analysis, and temperature control and display system.

A flow diagram of the combustion tube assembly is shown in Figure 3.1. A brief description of the location and purpose of each component in the flow diagram is given in the following sections, while detailed tabular forms are shown in Appendix A.

3.1.1 Fluid injection system

This is made up of two parts - gas injection and water injection. The gas injection system delivers nitrogen and air to the combustion tube from high pressure cylinders equipped with two regulators (I_1 and I_2 in Figure 3.1). Nitrogen is used prior to ignition to prevent low temperature oxidation (LTO) during the period when the temperature of the sand pack is increasing up to ignition temperature. Air is supplied to start the ignition and is necessary to sustain combustion. After completion of a combustion run, nitrogen is used to cool down the combustion tube. A Nupro check valve (V_1 in Figure 3.1) is used between the two gas cylinders to prevent any disturbance of flow when switching from one gas to another.

The lines from the gas cylinders to the inlet of the flowmeters were ¼" nylon tubing. From the flowmeters to the inlet of the combustion tube, they were ¼" copper tubing. As shown in Figure 3.1, I_3 is a

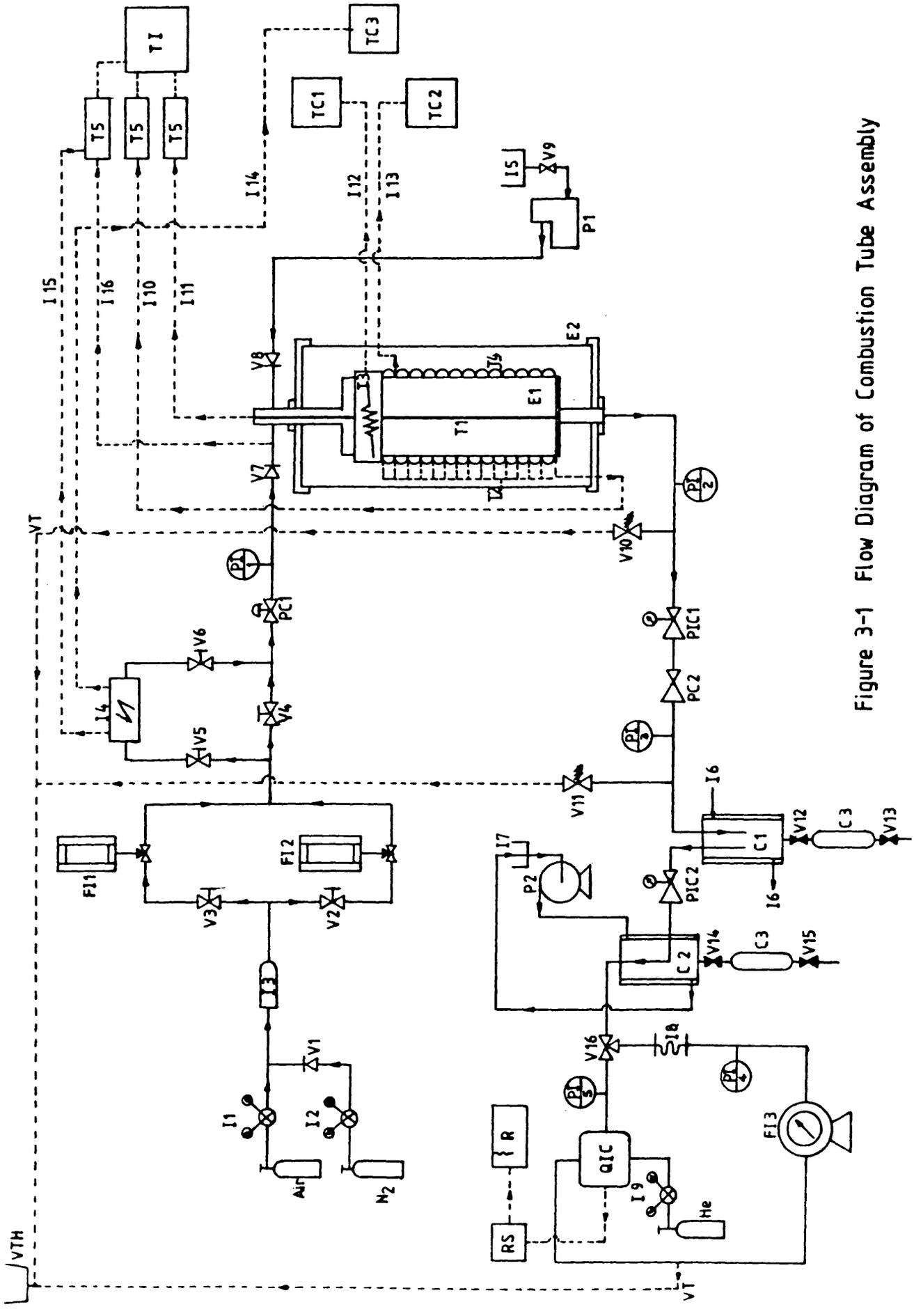

Figure 3-1 Flow Diagram of Combustion Tube Assembly

tubular section packed with molecular sieve granules which serve to dry the inlet air. There are two shut-off valves (V_2 and V_3), which are used to direct the gas flow to the desired flowmeter.

The inlet gas flowmeters (FI_1 and FI_2) are Fisher controls, series 1100. Flowmeter FI_2 has a flowrate from 0-1.8 st lit/min and a maximum operating pressure of 75 psig and temperature of 60° C. Flowmeter FI_2 has a range of 1-15 lit/h, calibrated at atmospheric pressure and temperature of 15° C. The accuracy of these instruments is ±2% of indicated flow, or ±0.2% of full scale reading. A Whitey valve (V_4) is used to shut off the air supply to the combustion tube in case of an emergency and is located on the instrument panel. An optional shut-off valve (V_5) was used to bypass valve V when it needed to preheat the injected air by the electrical furnace (optional I_4 in Figure 3.1) during some preliminary tests. In addition, it can be used to bypass the combustion tube in order to calibrate the flowmeters, or to send the inlet gases by a separate line to the gas chromatograph in case oxygen enriched gas was used.

In order to provide precise pressure regulation of the inlet gases to the combustion tube, a miniature regulator (pc 1) was installed in the panel. This regulator has a maximum inlet pressure of 1-60 psi. A separate diagram of the control panel is shown in Figure 3.2. A pressure gauge (PI_1 in Figure 3.1) is used to monitor the gas pressure to the combustion tube.

In order to prevent back flow of the gases from the combustion tube into the gas cylinders, a safety non-return valve (V_7 in Figure 3.1) was installed in the inlet line.

As shown in Figure 3.1, the water injection system consists of a metering pump (p_1), which is fed from a separate water storage tank (I_5).

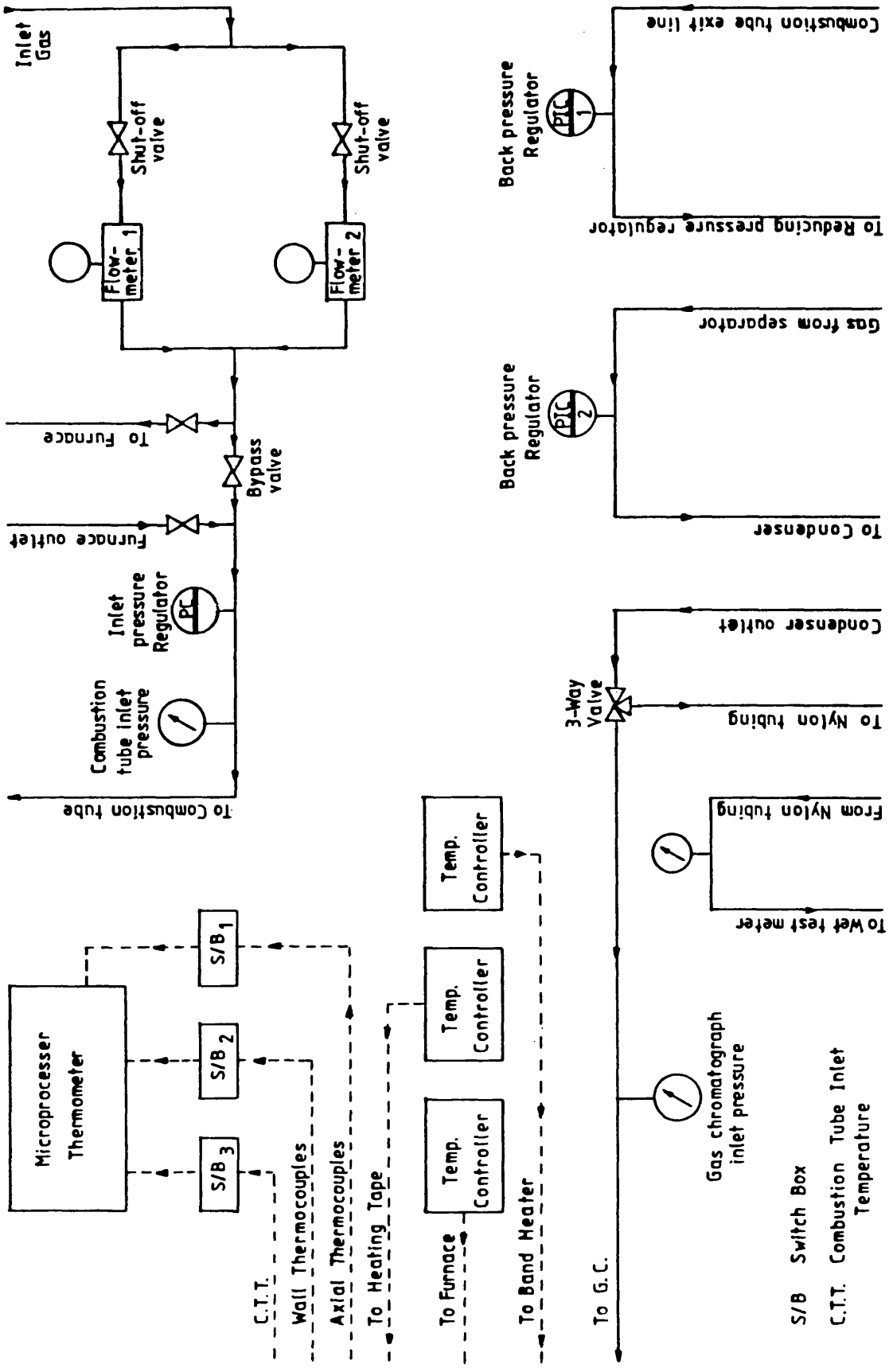

Figure 3-2 Schematic Diagram Describing the Control Panel

The metering pump delivers the water directly to the top inlet assembly of the combustion tube. The precise water injection rate can be selected by adjusting the stroke of the pump in conjunction with a calibration curve. A non-return valve (V_8) is installed in the water line to prevent back flow of the gases into the metering pump.

3.1.2 Combustion tube and pressure jacket

The combustion assembly, comprising a pressure jacket and a thin-walled combustion tube, is shown in Figure 3.3. The combustion tube is of type 321 schedule 10 stainless steel with a wall thickness of 0.3 cm (0.12"). It has an internal diameter of 7.3 cm (2.875") and a length of 86.9 cm (34.2"). Two 11.2 cm stainless steel flanges are welded onto the top and the bottom of the combustion tube (Figure 3.4a,b). The two end flanges are attached to the receiving weld neck pipe flanges utilising six 8 mm bolts in order to secure them against a high temperature gasket. "Unilion" 434.1 gasket jointing material was used, which has a working temperature of up to 550° C and is manufactured by James Walker Limited. A 3 cm outside diameter stainless steel tube is welded to the top flange, which serves as the air inlet to the combustion tube (Figure 3.5).

The production line from the combustion tube is a 5 cm (2") tube, which is welded to the bottom of the flange. This tube also supports the combustion tube, as shown in Figure 3.6(a). The combustion tube is contained in an outer pressure shell constructed of 16.8 cm (6.625") outside diameter, 114.3 cm in length and 0.63 cm (¼") wall thickness SD tube. The top flanges have six 11 mm holes equally spaced, whereas the bottom flange (Figure 3.6b) contains twelve equally spaced ⅛" BSP holes (tapered). The latter serve to take the pressure glands for the wall thermocouples. The production line from the pressure jacket is a 3.4 cm (1.35") tube, which is connected to an 0.63 cm (¼") reducer. This outer pressure

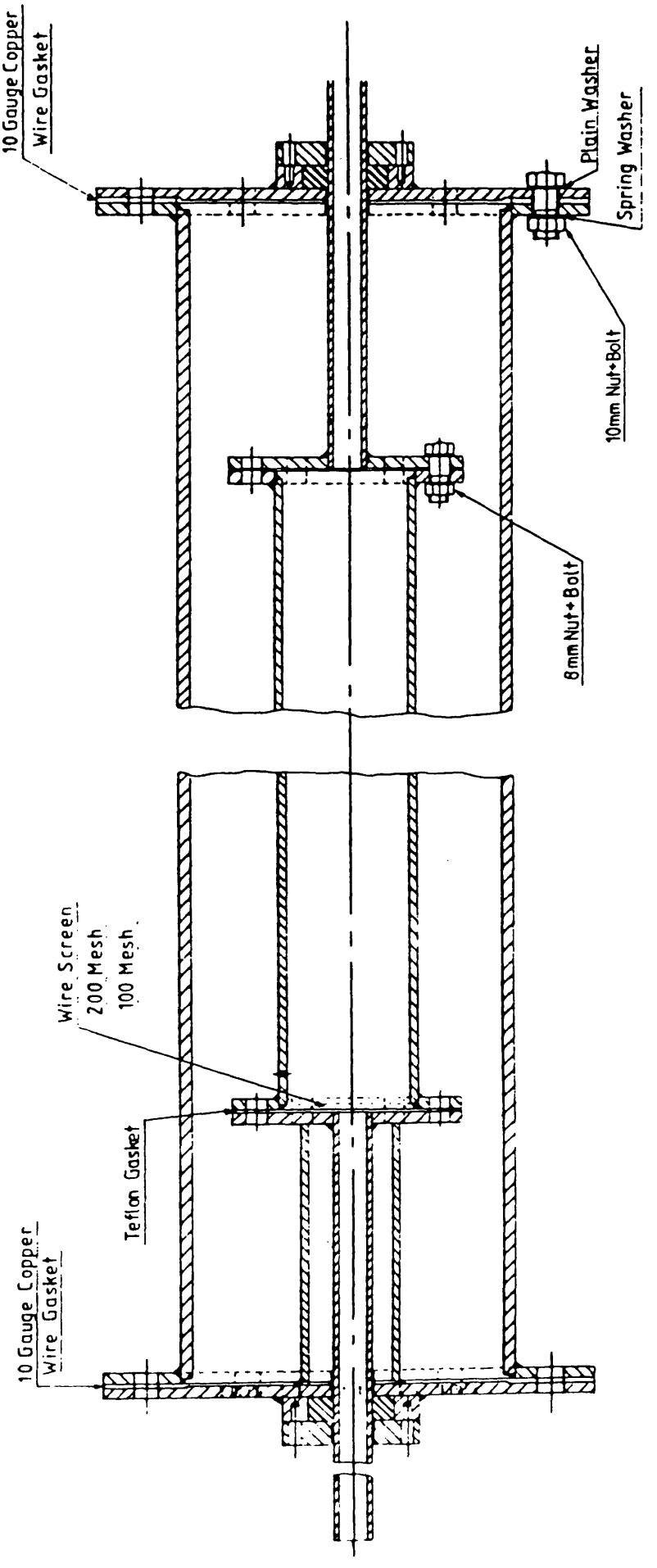

Figure 3.3 Combustion tube and pressure jacket assembly

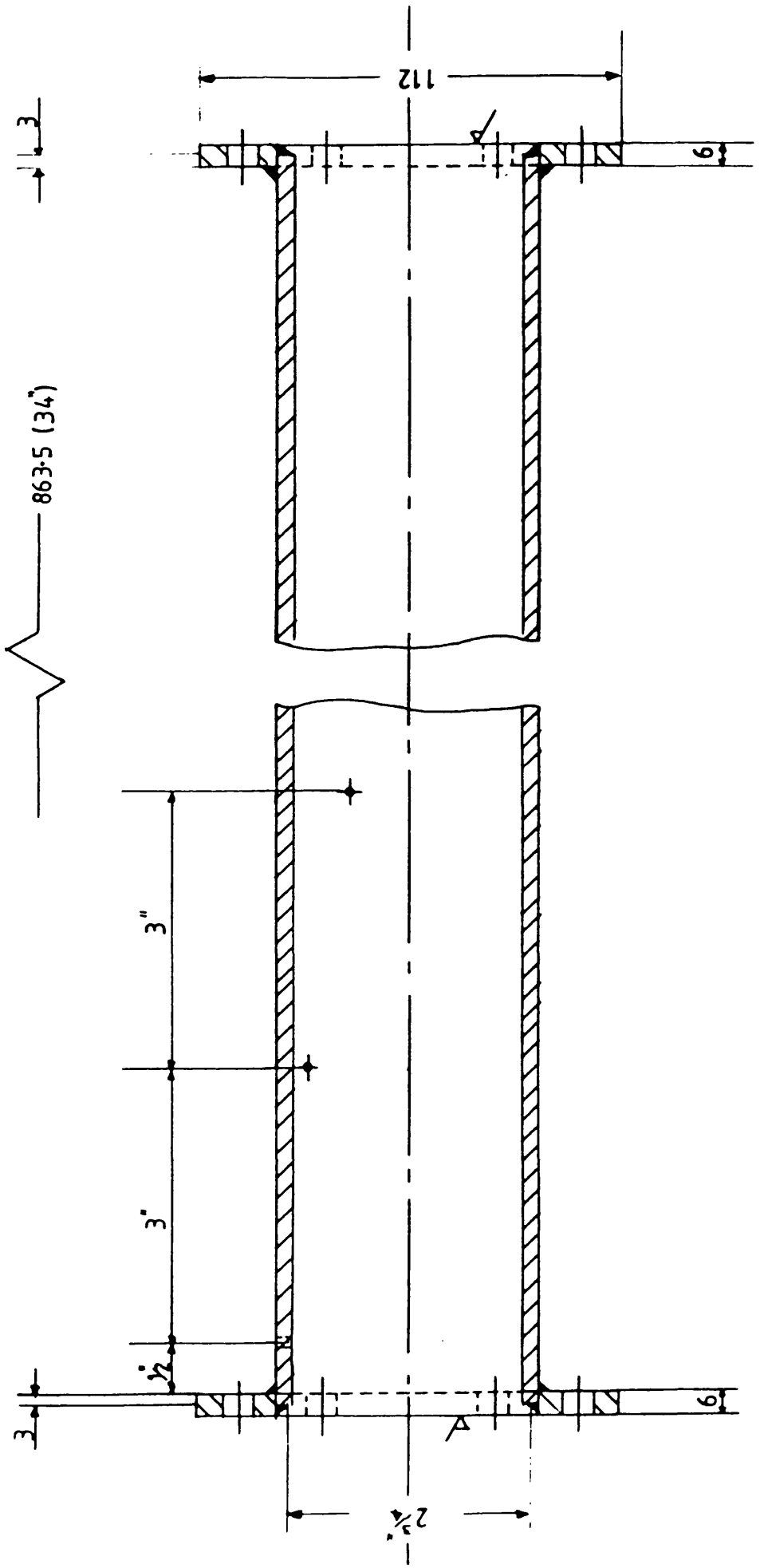

Figure 3.4(a) Combustion tube, back and front flanges

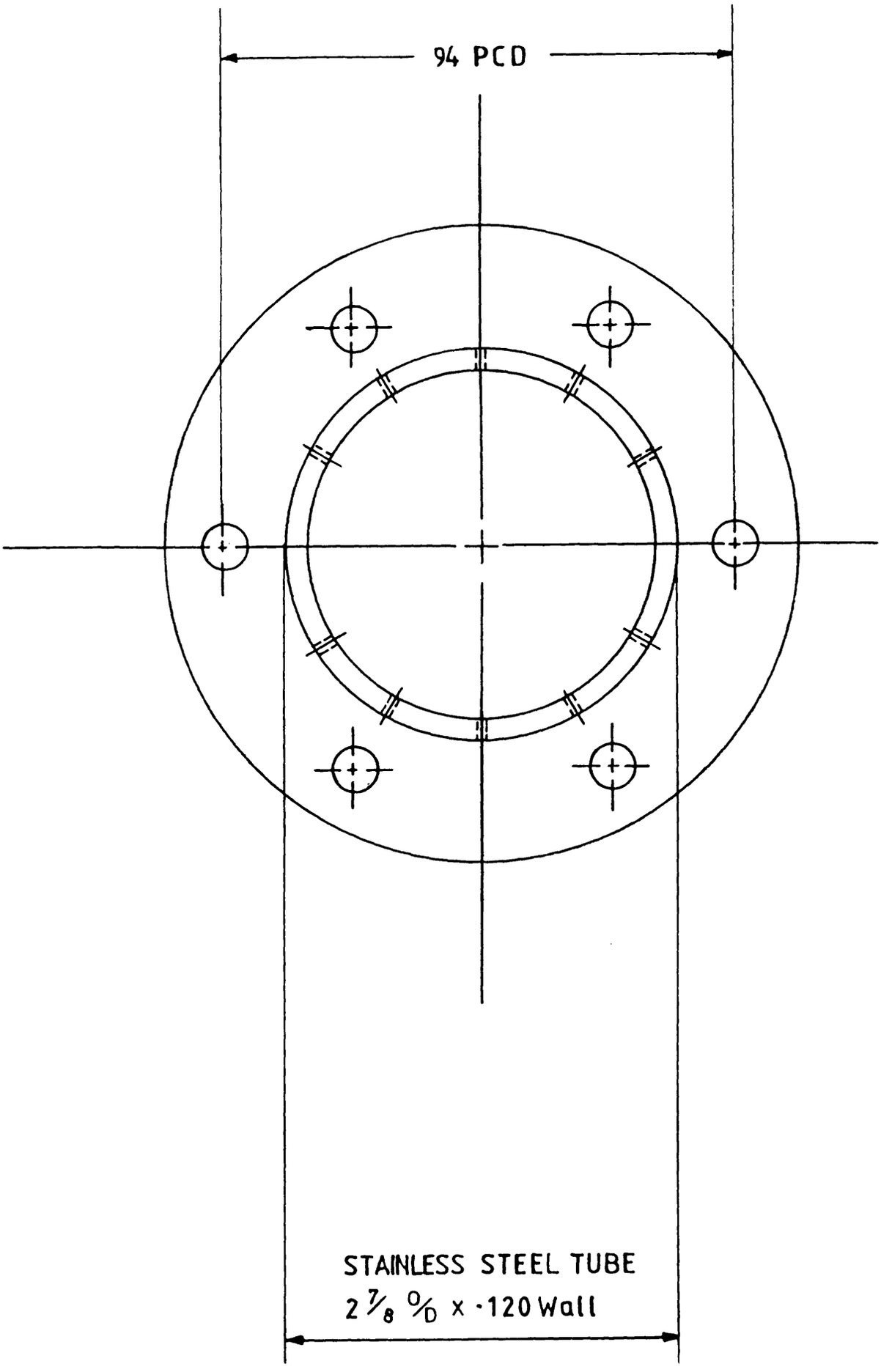

Figure 3.4(b) Top view of the combustion tube flange

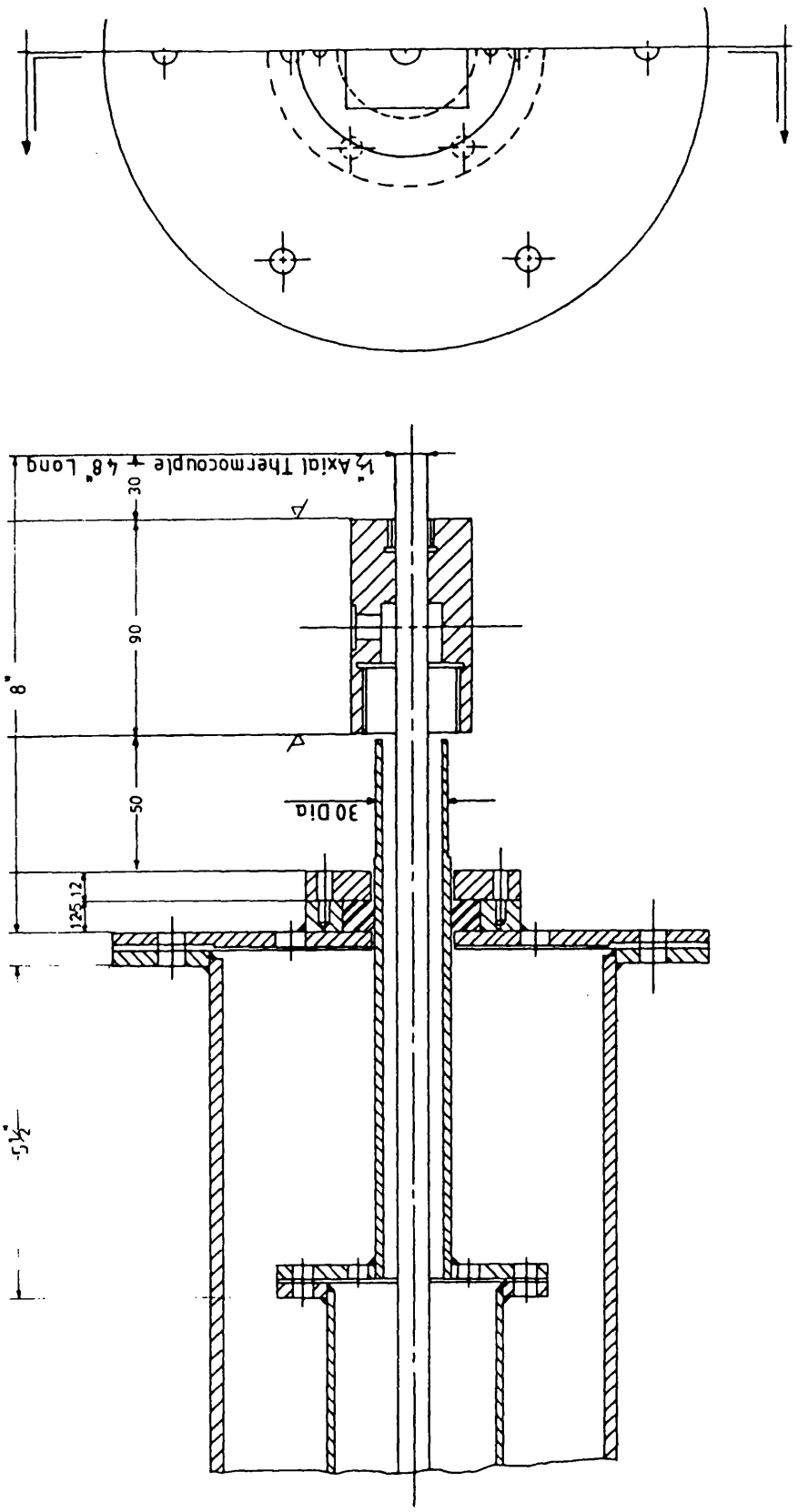

Figure 3.5 Pressure vessel assembly/top half

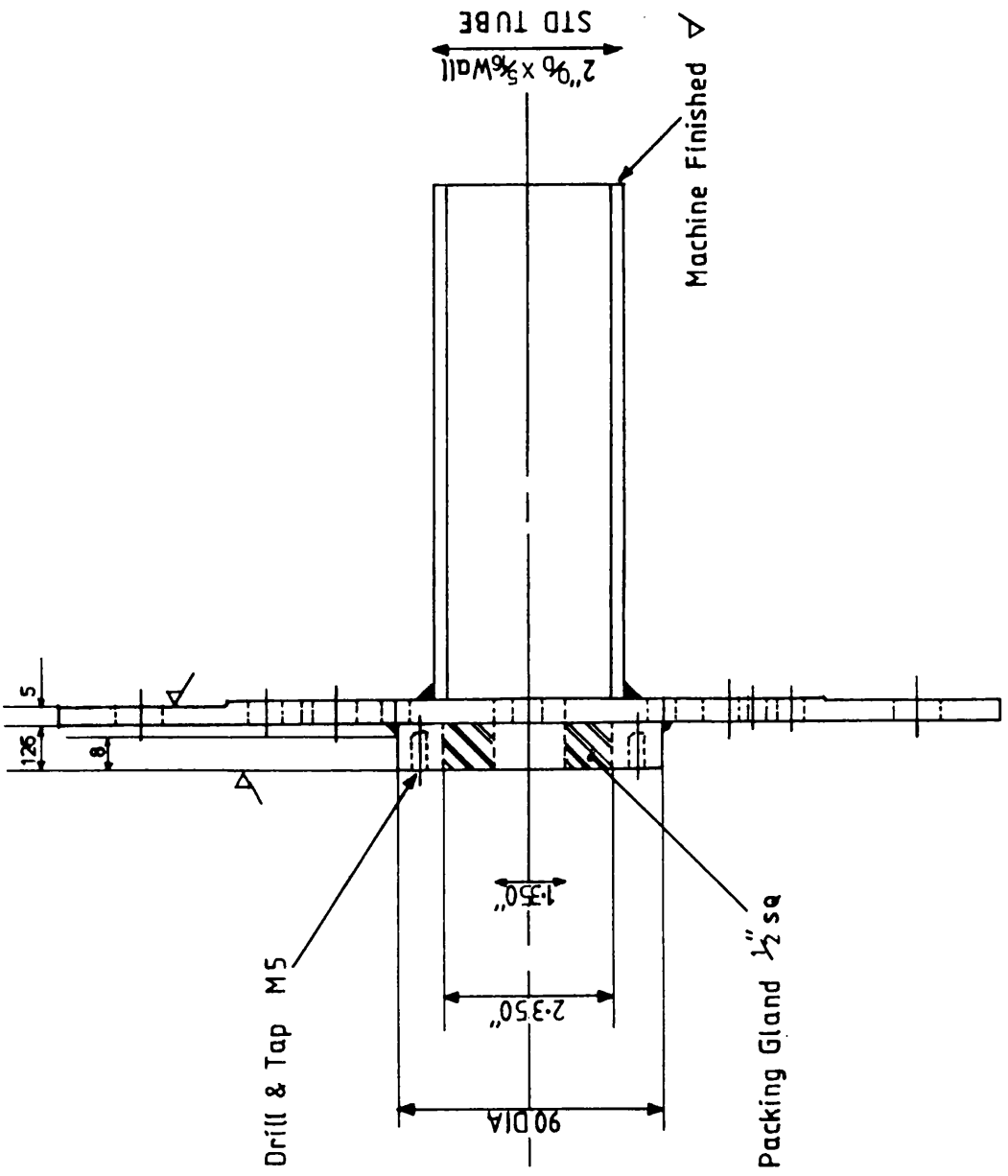

Figure 3.6(a) Combustion tube production end and pressure jacket bottom flange

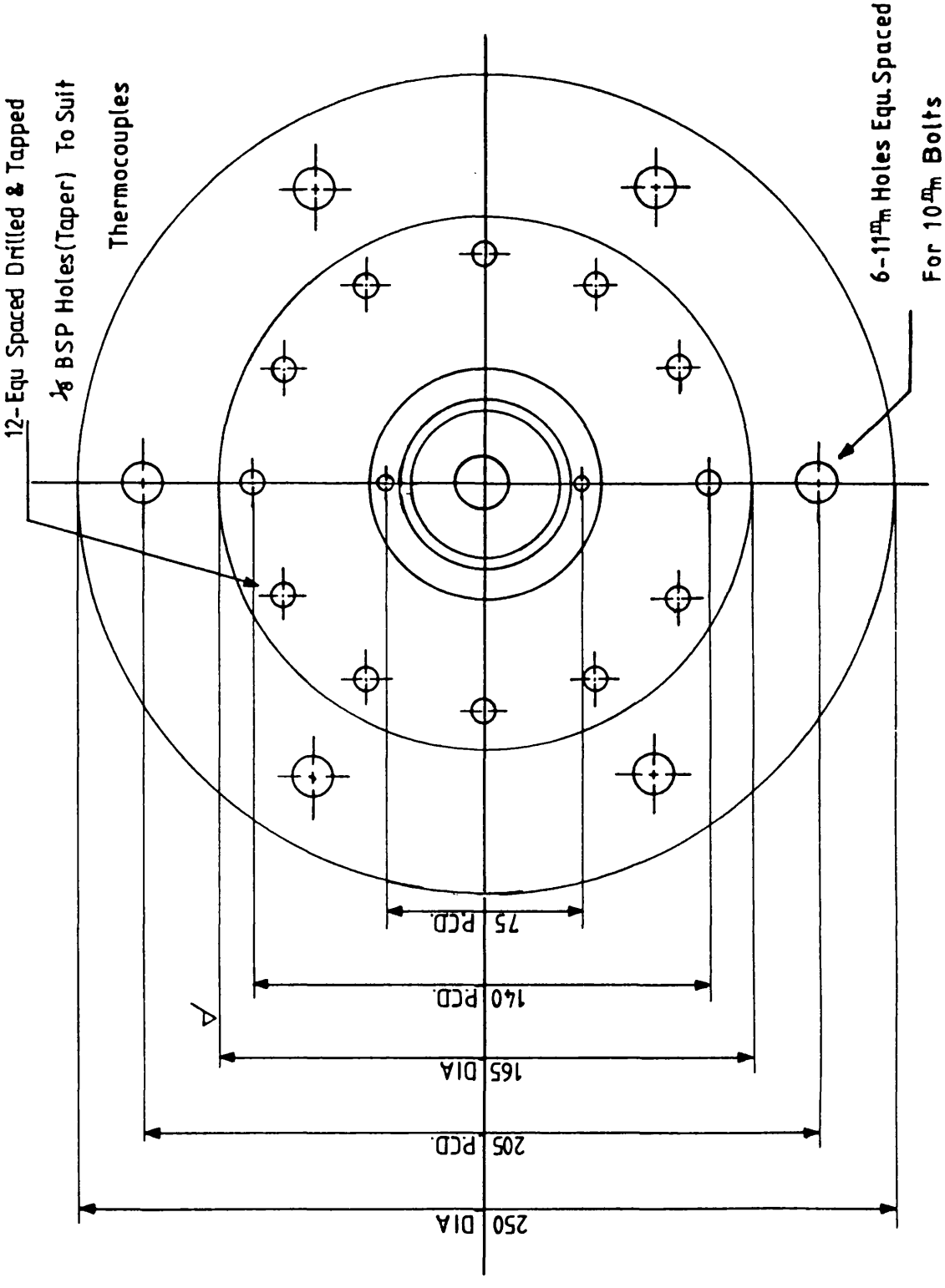

Figure 3.6(b) Pressure jacket bottom flange

jacket is mounted in a cradle stand at mid-length, allowing it to be rotated from a vertical to a horizontal position (see Figure 3.7).

The entire combustion assembly is earthed as a safety precaution.

A knuckle-type band heater is clamped on the top end of the combustion tube. This acts to raise this section of the tube up to the required ignition temperature. It has a ceramic body fitted with a terminal cover and braided leads 24" long.

Twelve chromel alumel thermocouples are soldered to the wall of the combustion tube at 3" intervals, with the first and last thermocouples located ½" from the top and bottom flanges respectively. All the thermocouple extension leads are brought out through the pressure glands in the bottom flange. These thermocouples, which are of different lengths, are fitted with ferrules for compression glands type TGB ⅛ BSPT, 1.5 mm.

An axial thermowell containing twelve thermocouples is inserted through the top flange through the centre of the combustion tube. The twelve thermocouple positions correspond exactly with the position of the twelve wall thermocouples. This stainless steel thermowell is 122 cm (48") in length and 1.27 cm (½") in diameter. Both axial and wall thermocouples are equipped with plugs and sockets which permit the leads to be disconnected when the combustion assembly is taken apart.

In order to compensate for heat losses and hence maintain the process as near adiabatic conditions as possible, the combustion tube was wound with 17.5' of 1" heating tape. It has a voltage rate of 15 v/ft. As a safety precaution, the heating tape is inserted into a 'refrasil' sleeving and is secured along its length by 'refrasil' tape. The 'refrasil' material is electrical insulation and is effective at high temperatures (see Appendix A.6 for details).

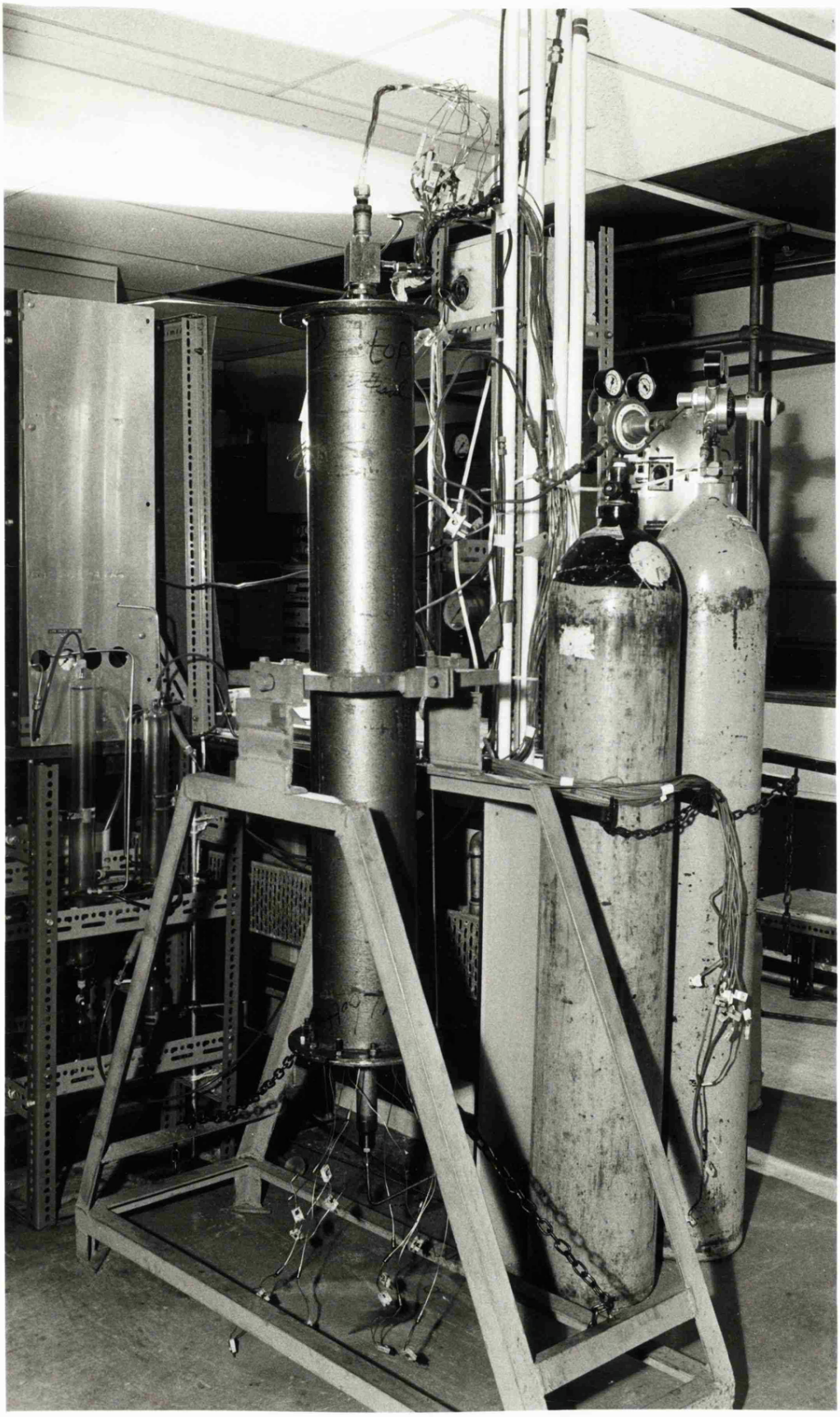

FIGURE 3.7 COMBUSTION TUBE and PRESSURE JACKET

In order to reduce heat losses through the annulus further and to protect the heaters' power supply leads from high temperature, the heaters are wrapped with 'Triton Kaowool' ceramic fibre blanket. The annular space between the insulating blanket and the pressure jacket is filled with a very fine vermiculite insulation.

3.1.3 The fluid production lines

The fluids produced during a combustion run are controlled as follows:

As shown in Figure 3.1, the exit pressure gauge (PI_2) is used to monitor the pressure at the exit (bottom) of the combustion tube.

A Nupro series 4CA relief valve (V_{10}) is used to relieve any excess pressure which may have developed in the producing lines.

The desired back pressure on the combustion tube is set by the back pressure regulator (PCI_1). This BPR regulator has a maximum inlet pressure of 100 psi and adjustable outlet pressure from 2-50 psi.

The glass separator and condenser in the exit line must be protected from high pressures. This is achieved by the pressure regulator (PC_2), which reduces the pressure to 5 psi (dead end) for an inlet pressure below 150 psi. The inlet pressure of the separator is monitored by a small pressure gauge (PI_3). Another adjustable in-line relief valve (V_{11}) is installed just before the separator as a further protection.

The liquid gas separator (C_1 in Figure 3.1) was constructed in the University of Bath Glassblowing Workships, of 40 mm ID Pyrex glass. It was fitted with a sintered glass disc at the top end and a bubble cap in the bottom end to prevent any entrainment of the liquid droplets with the gas stream. The separator has a water jacket to cool the gases and liquids which are produced.

A second back pressure regulator (PCI_2) is installed to maintain the desired pressure in the separator. It has a maximum inlet pressure of 100 psi and an adjustable outlet pressure of 1-10 psi.

Gaseous components which were not condensed in the previous separator are passed to an ice-water jacketted condenser (C_2). Cold water is recycled to the condenser by means of a small pump (P_2).

A Dralliam series 40 four-port valve (3-way) is installed after the condenser to send the exit gases either to the wet test meter or to the gas chromatograph.

The wet test meter (FI_3) was manufactured by Alexander Wright and was their model DM3D. This provides an accurate measurement of the cumulative gas volume. It is also fitted with a remote read-out facility which can be fed into a computer or other control system if required. In order to operate this instrument within the recommended pressure of ±48 millibar, 25' of ⅛" nylon tubing (I_8 in Figure 3.1) was installed before the wet test meter, to reduce the upstream pressure to less than 1 psi, which is monitored by a small pressure gauge (PI_4).

3.1.4 Gas analysis

A Pye Unicam series 104 gas chromatograph, fitted with a thermal conductivity detector head, was used to analyse the composition of the gases produced. The analysis of carbon dioxide, nitrogen, oxygen, carbon monoxide and methane is completed in less than 6 min at ambient temperature using a new version of the CTR column. This concentric column was packed with a blend of Porapak polymers in the inner column and molecular sieve 13X in the annular space. The column was supplied by Alltech Associates Inc. with product number 8700. Figure 3.8 shows a chromatogram of the gaseous mixture from such a column. The first peak is a composite of oxygen,

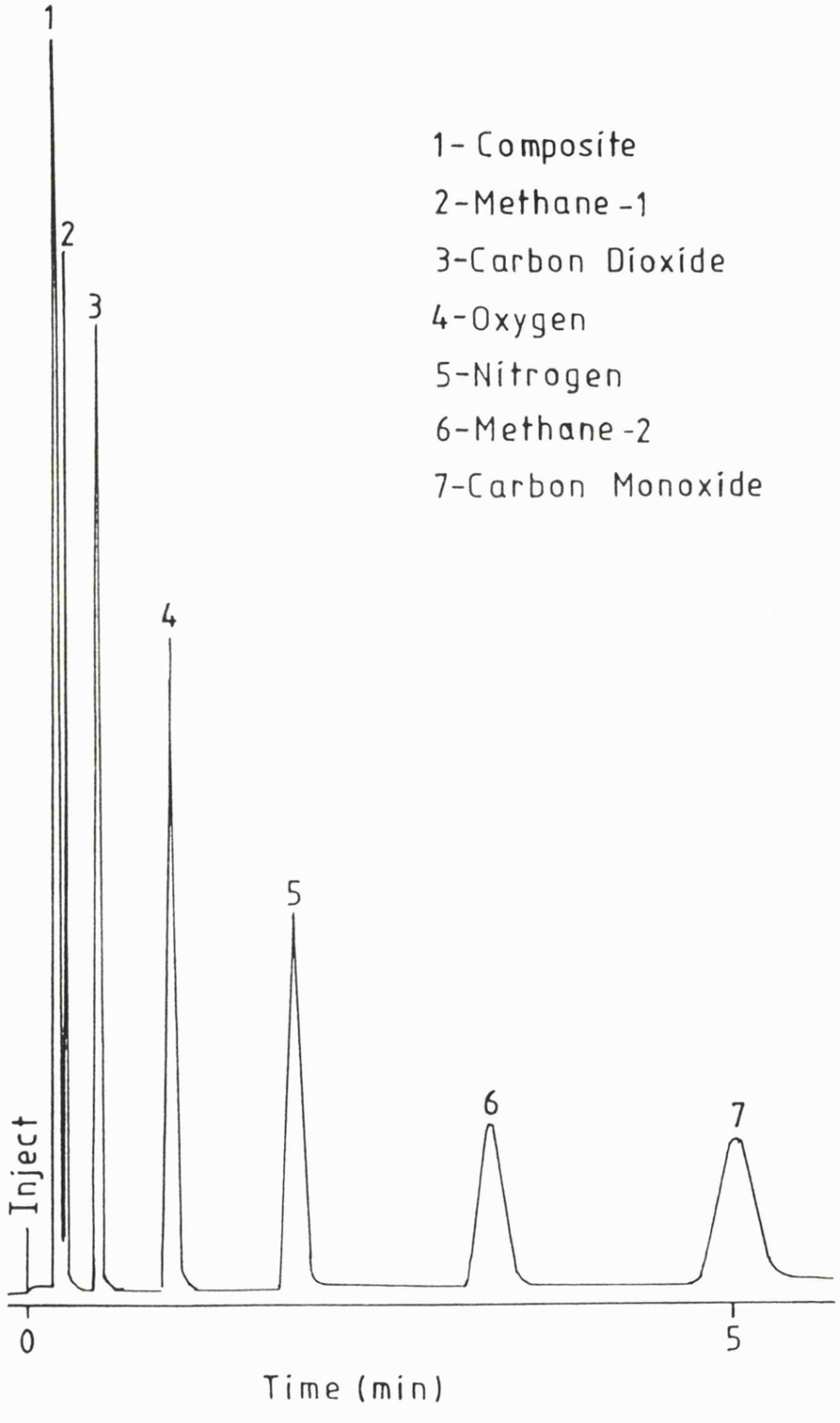

Figure 3.8 CTR column. ¼" annular space with molecular sieve 13X; ⅛" section packed with Porapak P, detector 35° C. Helium at 75 ml/min. TCD detector at 200 ma, oven temperature at ambient, 1 ml sample, chart speed 2 cm/min.

nitrogen and carbon monoxide. Peaks 1,2 and 3 are all from the Porapak P. Finally, peaks 4, 5, 6 and 7 elute from the molecular sieve 13X. With helium carrier gas, hydrogen elutes just before oxygen from the molecular sieve 13X.

The gas chromatography trace was recorded on a Pye Vitatron recorder (R in Figure 3.1), which was connected to a Labdata instrument digital integrator (RS) to compute the area of each individual gas component, which gives the mole fraction.

3.1.5 Temperature control and display system

As shown in Figure 3.1, the temperature of the heating tape (T_4) was controlled by a power regulator (TC_2). A Pye mini ether controller (TC_1), having a maximum set point of 600° C, was used to regulate the band heater temperature, which was detected by a separate thermocouple.

The 24 extension cables (12 axial and 12 wall thermocouples) are connected to a Digitron multipoint switch, each switch having 12 thermocouples input. The thermocouples are connected through the multipoint switch to a Comark 6600 microprocessor thermometer. The specification of this instrument is given in Table 3.1.

Figure 3.9 shows the control panel, where a network of valves, pressure gauges and temperature controllers are mounted. It also shows the separator and the condenser to the right and a part of the gas analysis system to the left.

3.2 Experimental procedures

The following procedures were employed in conducting the combustion tube runs. The water injection procedure used for the wet combustion runs is described in the section dealing with operational procedures.

Table 3.1

Microprocessor thermometer analogue output specification

D.C. output	1 v out = 100° or 1 mv 1 v out = 1000° or 10 mv
Resolution	On temperature ranges 0.1 to 700° C, 1° above
Linearity	Monotonic
Accuracy	± 0.25% of full scale
Output resistance	< 1 Ω
Output current	-8 mA to +8 mA
Temperature coefficient	±0.05% per °C
K type thermocouple characterising accuracy range	-200-500° C; <0.15 (max.error ±°C) 500-1150 °C; <0.05 (max.error ±°C)
Termination	Miniature jack socket on back panel

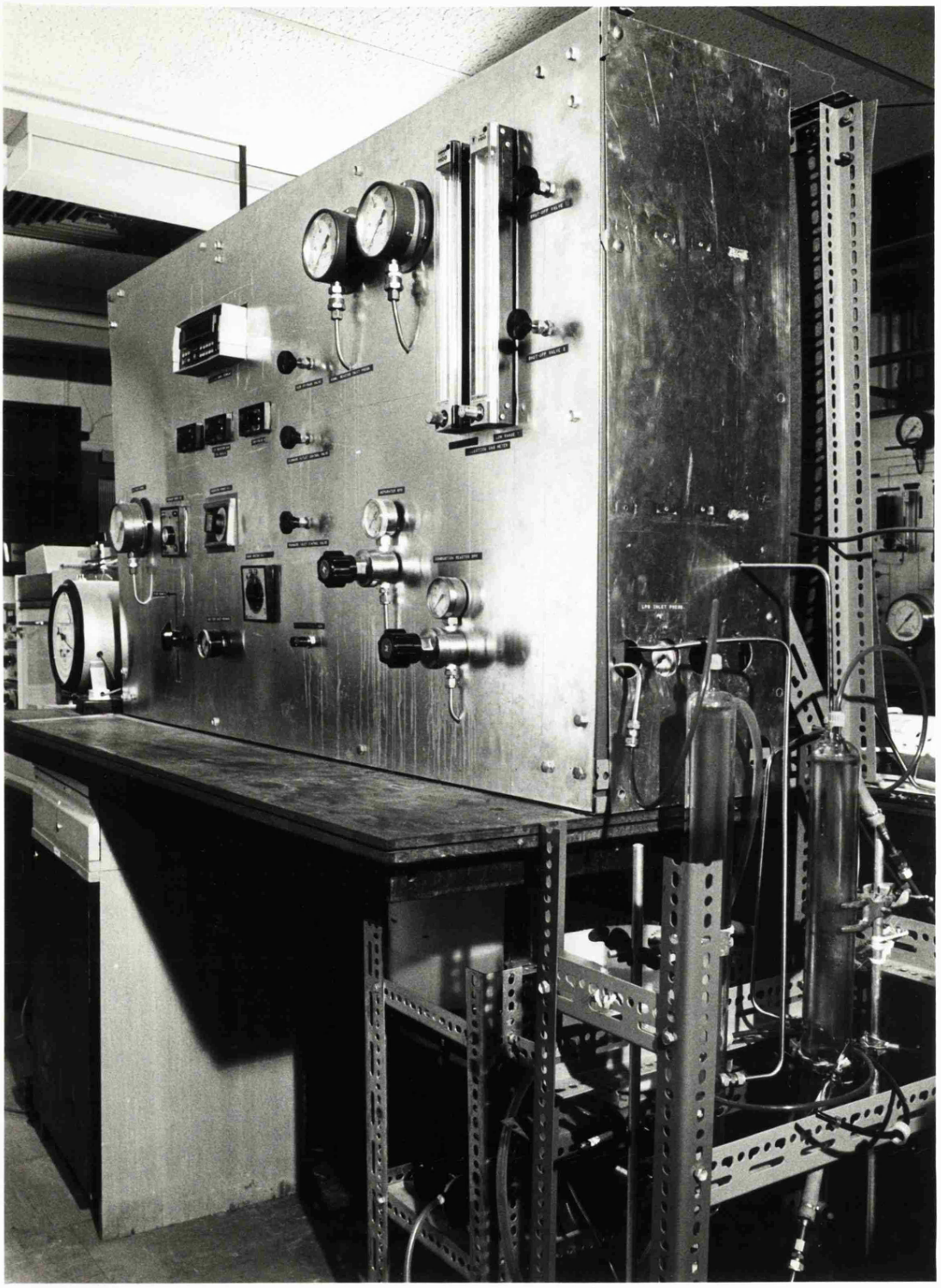

FIGURE 3.9 CONTROL PANEL

3.2.1 Preparation of combustion tube and material

The premixed method has been used in preparing the sand packs mixture. In most cases, the porous media consisted of a commercially washed silica sand and kaolin clay, the latter having a reduced swelling tendency compared with other clay minerals. A particular clay to sand ratio was selected for each individual run. The properties of the material used in the sand mixtures are given in Tables 3.2 and 3.3.

Two light crude oils (Forties °API = 36.6 and Maya-Isthmus, °API = 32.4) and a medium heavy crude (Maya, °API = 22.1) were used in this investigation. The physical properties of these crudes are presented in Table 3.4.

Mixing of the oil and water with the sand-clay mixture was performed manually in a large container. The prepared mixture was then tamped carefully into the combustion tube by means of a disc which was attached to a metal rod. For the ignition sequence, 3-4 g of linseed oil were poured on the surface of the sand at the top of the combustion tube, in order to ensure a uniform and faster ignition. After packing of the tube was completed, the surfaces of the top flanges of the combustion tube were cleaned and polished. In order to ensure a good seal of the high temperature gasket against the flanges, high temperature silicon rubber was used between the gasket and the surface of the flanges. The top flange was then bolted down and the axial thermowell inserted. All the connectiong fittings were cleaned and the inlet air and water lines were connected to the top end of the combustion tube assembly. The vermiculte insulation was then poured into the annulus of the pressure jacket and the top flange was secured.

Table 3.2

Properties of the silica sand

Geological type:	lower green sand of the cretaceous period
Location:	Reigate, Surrey
Grain shape:	sub-angular

Chemical Analysis*

SiO_2	99.5%
Al_2O_3	0.1%
Fe_2O_3	0.09%
CaO	0.07%
K_2O	0.08%
Na_2O	0.02%
Loss on ignition	0.17%
Clay fraction	0.1%

*Provided by Buckland Sand and Silica Co. Ltd., Surrey.

Table 3.3

Chemical analysis of kaolin clay and particle size distribution of amorphous silica

Kaolin light b.p.*	
Loss on drying	0.9%
Loss on ignition	12.7%
Chloride	<350 ppm
Heavy metals	< 20 ppm
Arsenic	< 2 ppm
Soluble matter	4.6 mg/g
Coarse particles	0.3 mg/g
Fine particles	76.2%
Amorphous silica (silicon dioxide SiO_2)	
Particle size distribution:	0.5-10 micron
Approximately 80% between:	1-5 micron
Specific surface area†	20,216 cm^2/gm

*Supplied by Dearborn Chemicals Limited.

†Provided by Sigma Chemical Company

Table 3.4

Physical properties of crude oils[a]

Forties crude (North sea)[b]		Maya Isthmus crude (Mexico)			Maya crude (Mexico)[c]	
Gravity, API	36.6	Gravity, API (BP assay)		32.4	Gravity, API	22.1
Sulphur, wt%	0.3	Density, gm/cm^3		0.8649	Sulphur, wt%	3.91
Viscosity, cst (at 10° C)	9.6	Viscosity, cst (Brookfield digital viscometer)	at 40° C	11.42	Kinematic viscosity, cst	
(at 21.1° C)	6.81		at 100° C	8.71	(at 10° C)	406
Pour point, °C	-3				(at 20° C)	203
Wax, wt%	7.0				Pour point, °C	-27
Carbon residue, wt%	2.2				Carbon residue, wt%	11.0
Asphaltenes, wt%	0.2				Asphaltenes, wt%	9.4
Vanadium/nickel ppm	3/2				Vanadium, ppm	267
Watson K factor	11.9				Nickel, ppm	52
C_1-C_4, wt%	2.74				C_1-C_4, wt%	1.3

[a] Crude oils supplied by British Petroleum (BP) Research Centre, Sunbury-on-Thames, Middlesex.
[b] Published by Aalund (1983), see reference.
[c] British Petroleum Research Centre.

A period of at least 24 h was allowed for complete curing of the silicon rubber sealing, before pressurising the combustion tube. This procedure was very important in order to prevent leaks from the flanges.

3.2.2 Start-up and operational procedure

Before starting a combustion run, the thermal conductivity detector of the gas chromatograph was activated for at least 3 h. Once stabilised, the chromatograph was calibrated by injecting samples of standard gas mixtures. Regeneration of the CTR column is necessary after completion of two or three combustion runs. This is to avoid deactivation of the molecular sieve by carbon dioxide and water vapour in the production gases. The recommended procedure for regeneration and calculation of individual gas components has been published by Rendle *et al.* (1980).

Both axial and wall thermocouples are checked by the microprocessor thermometer for any open circuit condition. The heaters also are again checked for any possible short circuit, or any other faults.

Cooling water is fed to the separator and the recycling pump is turned on to circulate the iced water to the condenser. All the instrument power supplies and necessary valves are turned on.

The oil-sand pack is heated up to approximately 120° F (50° C) by turning on the heating tape. At the same time, nitrogen is injected into the tube at approximately 0.5 lit/min in order to displace the air. This is to reduce low temperature oxidation (LTO), which can occur below 600° F (315° C). The top band heater is turned on to raise the temperature at the inlet of the sand pack up to ignition temperature, which is usually about 340-350° C. Once this temperature is reached, the nitrogen is switched to air. Ignition is confirmed both by development of a combustion temperature front and by analysis for CO, CO_2 and O_2 in the exit gases.

The combustion front is monitored by temperature traverse along the combustion tube every 30 min, and supplemented by frequent analysis of the produced gases.

All wet combustion tests were started as dry combustion until conditions were stable, then water was injected. The major problem encountered during the operation of wet combustion tests with high water:air ratios was that of early steam breakthrough, which made it extremely difficult to control the pressure and the high temperature of the flowing fluid in the production line. However, cooling of the production line by the circulating water has eased this problem.

In order to keep the process as nearly adiabatic as possible, the wall temperature needs to be kept at about 15-20° F (10° C) higher than the corresponding axial temperature in the bed. This was achieved by activating the top band heater and the heating tap manually.

The resultant liquids were collected in centrifuge tubes directly from the sampling cylinder. The gases which had been produced were analysed continuously by gas chromatograph every 15 min. The cumulative volume of the exit gases was measured by the wet test meter every 15 min.

3.2.3 Shut-down procedure

A run is usually terminated when the last thermocouple from the production end reaches a temperature of about 650° F (345° C). This is necessary in order to avoid coke formation on the stainless steel mesh and as a precaution against any fire breakthrough in the product line. Air injection is then switched to nitrogen and the combustion tube is allowed to cool down. All heaters are switched off. The microprocessor thermometer is turned off. The combustion tube is then dismantled, after first removing the axial thermocouple tube. Selected samples of the burned sand are removed from the ignition, middle and coke zones for post-burn analysis.

3.2.4 Post-burn analysis

The produced liquids are separated by means of a high speed centrifuge. Clay production occurred in most of the collected samples, giving rise to severe emulsion formation. Breaking of stable emulsions could be improved considerably by the addition of toluene.

The oil densities were measured by a DMA 35 vibrating u-tube, which has a resolution of ±0.001 g/cm.

The coke percentage, or fuel availability, is determined by burning samples that have been removed from the coke zone. The carbonaceous residue is burned in a crucible in a muffle furnace at 815° C, cooled and then weighed. Reproducibility of the results is achieved by repeating the heating and weighing until consecutive readings differ by no more than 0.5 mg. The difference in weight as a percentage of the original sample weight gives the percentage of coke. The coke percentage was also determined using the extraction method.

An extraction unit has been designed and operated according to the Bureau of Mines specification (Rall and Taliaferro, 1946), for the determination of oil and water residual saturation. Complete extraction of the remaining oil was achieved in 2 h. In order to obtain maximum accuracy, the samples should be subjected to continuous refluxing. In other words, a longer extraction time is required. The measured volume of water is subtracted from the total weight lost, to determine the weight of the extracted oil.

3.2.5 Operation conditions

In order to study the effect of the various injected water to air ratios and the composition of the porous media on the forward combustion oil process, all runs were made under the same initial conditions (see Table 3.5).

Table 3.5

Summary of initial test conditions

Sand	washed silica sand retained on 52 BS mesh or 50 US mesh
Clay	kaolin
Oil to (sand + clay) ratio	11.2%
Water to (sand + clay) ratio	1.8 %
Inlet pressure	50 psig
Air flux	14.57 m^3 (st)/m^2.h
Initial pack temperature	100-120° F (38-48° C)

The weight ratio of crude oil to sand gave an oil saturation of approximately 38% to 44%. The selected water to sand and clay ratio was fixed for all runs, giving a water saturation of approximately 5% to 6%.

A summary description of the properties of the oil sand packs used in the combustion tube runs is given in Table 3.6.

Table 3.6

Description of the characteristics of the oil-sand mixtures

Run No.	Crude oil	Gravity (API)	Composition of the porous media	Porosity (BV)	S_O (%PV)	S_W (%PV)	Length of pack (m)
1	Maya Isthmus	32.4	95% sand + 5% clay	46.83	38.0	5.43	0.711
2	Maya Isthmus	32.4	95% sand + 5% clay	44.26	42.0	5.87	0.724
3	Maya Isthmus	32.4	95% sand + 5% clay	45.6	39.76	5.55	0.736
4	Maya Isthmus	32.4	95% sand + 5% clay	45.76	39.46	5.55	0.728
5	Maya Isthmus	32.4	90% sand + 10% clay	44.56	41.42	5.80	0.724
6	Forties	36.6	95% sand + 5% clay	47.33	38.0	5.20	0.749
7	Maya	22.1	95% sand + 5% clay	45.0	38.84	5.68	0.736
8	Maya Isthmus	32.4	90% sand + 10% amorphous silica	40.3	44.32	6.18	0.750

CHAPTER 4

RESULTS OF FORWARD COMBUSTION EXPERIMENTS

Altogether, seventeen *in situ* combustion experiments were made. Nine of these were assessed to be only partially successful, either on account of the preliminary nature of the tests, or because of operational problems which were encountered during the experimental runs. The remaining eight runs were judged to be successful, and the results for these are described in detail.

4.1 Preliminary experiments

Extensive tests were made in order to establish an effective procedure for carrying out the combustion experiments. The major problem which arose was that of establishing a self-sustained combustion front in the oil-sand mixtures which contained only washed silica sand.

The first attempts to rectify this involved changing the operating conditions, *i.e.*, the air flux, ignition procedure and the oil-sand mixture properties. A different ignition procedure was employed by injecting nitrogen prior to air, in order to eliminate LTO reactions which could occur while raising the temperature of the bed and, at the same time, the air flux was varied from 12-18 m^3 (st)/m^2 h. Three crude oils were used with different API gravity (Forties, Maya Isthmus and heavy Maya). In addition, the surface area of the porous medium was changed by passing the sand through a 100 mesh sieve to reduce the coarse grains in an attempt to increase the surface area. In all these tests, the oil saturation was 35-45% PV and the water saturation 11-17% PV.

Following this, 10 w/w % of fine silica flour, of less than 50 micron particle size was incorporated into the sand mixture.

With this modification, the combustion front travelled 8" from the inlet end, then died away. This extinction was revealed by the increasing oxygen concentration in the exit gas, which eventually reached the inlet value of 21%.

In another test, a successful combustion run was achieved by incorporating 8.5 w/w % of natural soil into the sand matrix. The soil was first dried and after cooling, it was passed through a 100 mesh sieve. The self-sustained combustion front produced an average peak temperature of 780-800° F (415-425° C) and the oxygen utilisation was approximately 81%. Complete results for this run were not obtained, however, due to its preliminary nature and also because of the unknown composition of the soil.

In all of the tests in which the combustion front could not be sustained, the sand samples which were taken from the combustion tube afterwards were very dark in colour. They were also very hard in texture compared with the samples obtained from successful combustion runs. These hard, almost consolidated sand packs, were very difficult to remove from the combustion tube. Normally, they could only be removed by drilling the coke. The reason for this change in composition of the sand pack is most probably due to LTO reaction of the oil. This can significantly alter the properties of the coke formed, giving rise to increased surface roughness of the porous medium (Dabbous, 1971).

Following on from the success obtained with the natural soil, the effect of adding clay (kaolin) was investigated (see Table 3.6). This proved to be successful in maintaining self-supporting combustion in all subsequent experiments.

4.1.1 Main combustion experiments

Each type of run had as a target the study of a particular area of the forward combustion process. Table 4.1 shows the water injection rate and the water:air ratio for each combustion tube experiment. The classification according to Dietz and Weijdema, 1968; Garon and Wygal, 1974, and McKay, 1982, was used to determine whether a particular run was normally wet, or partially quenched. For the first four runs using the Maya Isthmus crude, dry, normal wet and partially quenched modes of combustion were investigated. The other two runs at the same clay content of 5 w/w % kaolin (6 and 7) are both in the normal mode, but using different crude oils, namely Forties and the medium heavy Maya. Runs 5 and 8 were conducted with increased amounts of clay or amorphous silica (run 8) added to the sand matrix. These runs were respectively partially quenched, and dry, combustion runs for the Maya Isthmus crude oil.

In this chapter, the general features of the combustion results, *i.e.*, the temperature profiles, exit gas composition, oxygen utilisation and peak temperature, the H/C and CO/CO_2 ratio and the fuel consumption are presented, whilst detailed discussion of the specific air requirement, mass balance and fluid production history are treated in Chapter 5.

4.2 Temperature profiles

The temperature profiles for the dry run (run 1) are shown in Figures 4.1(a) and (b). Figure 4.1(a) shows a very distinctive steam plateau, as characterised by the flat profile occurring at 15:30, which is 2.2 h after ignition. The temperature of this plateau is approximately 240° F (115° C). No other plateau effect was observed during any other periods of the run. This is mainly because of the low initial water saturation and the relatively

Table 4.1

Combustion tube experiments (water injection rate and water:air ratios)

Run No.	Crude oil	Clay content (%)	Water:air ratio [m^3/Mm^3 (STP)]	Water injection rate (cm^3/min)	Mode of combustion
1	Maya Isthmus	5	0.0	0.0	dry
2	Maya Isthmus	5	1.25	1	normal wet
3	Maya Isthmus	5	2.5	2	normal wet
4	Maya Isthmus	5	3.75	3	partially quenched
5	Maya Isthmus	10	3.75	3	partially quenched
6	Forties	5	1.25	1	normal wet
7	Maya	5	1.25	1	normal wet
8	Maya Isthmus	10% amorphous silica	0.0	0.0	dry

Operating pressure = 50 psig; initial bed temperature 100-120° F; STP refers to standard condition at 1 atmosphere and 60° F.

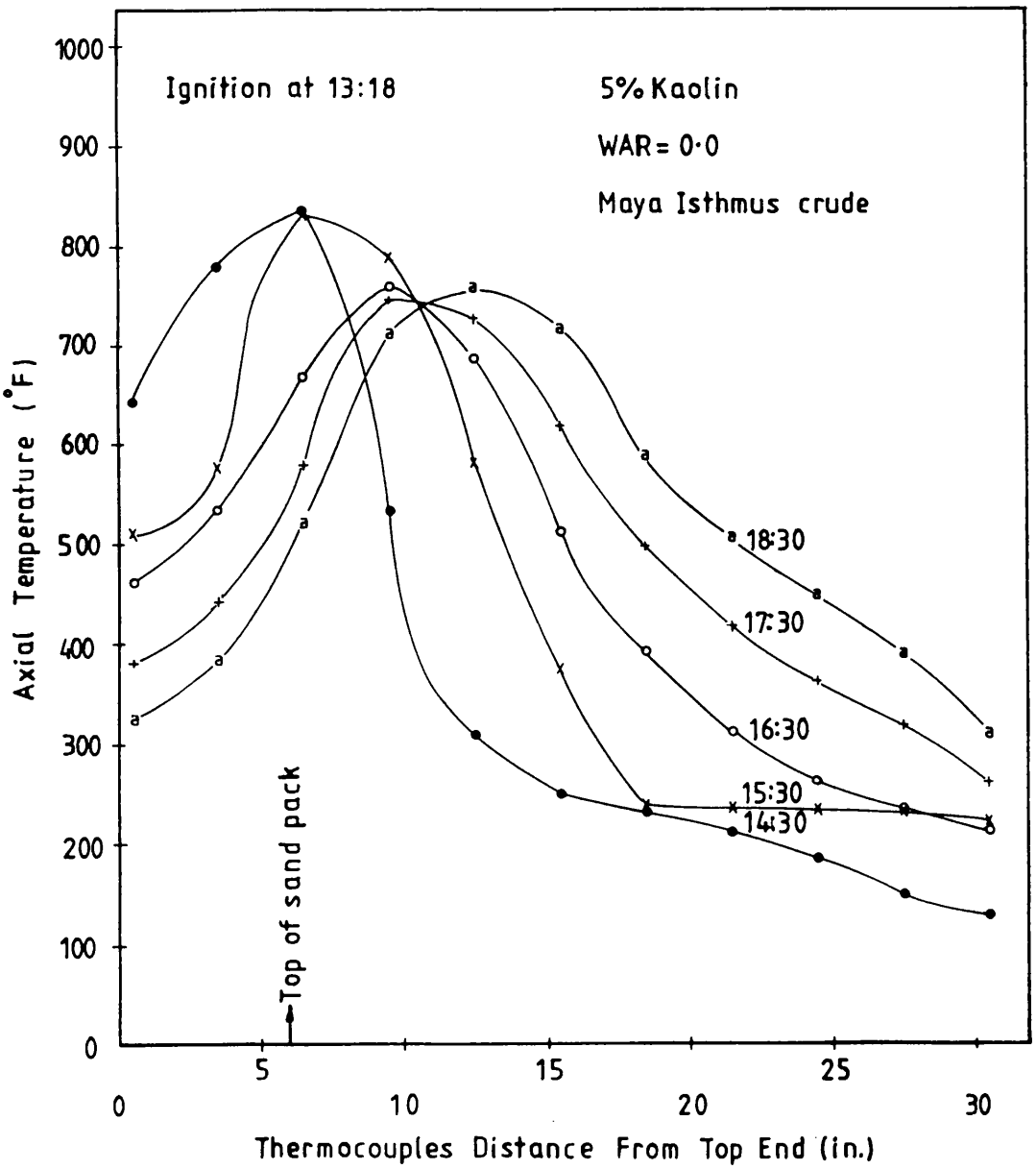

Figure 4.1(a) Axial temperature of sand *versus* distance along the combustion tube (run No.1)

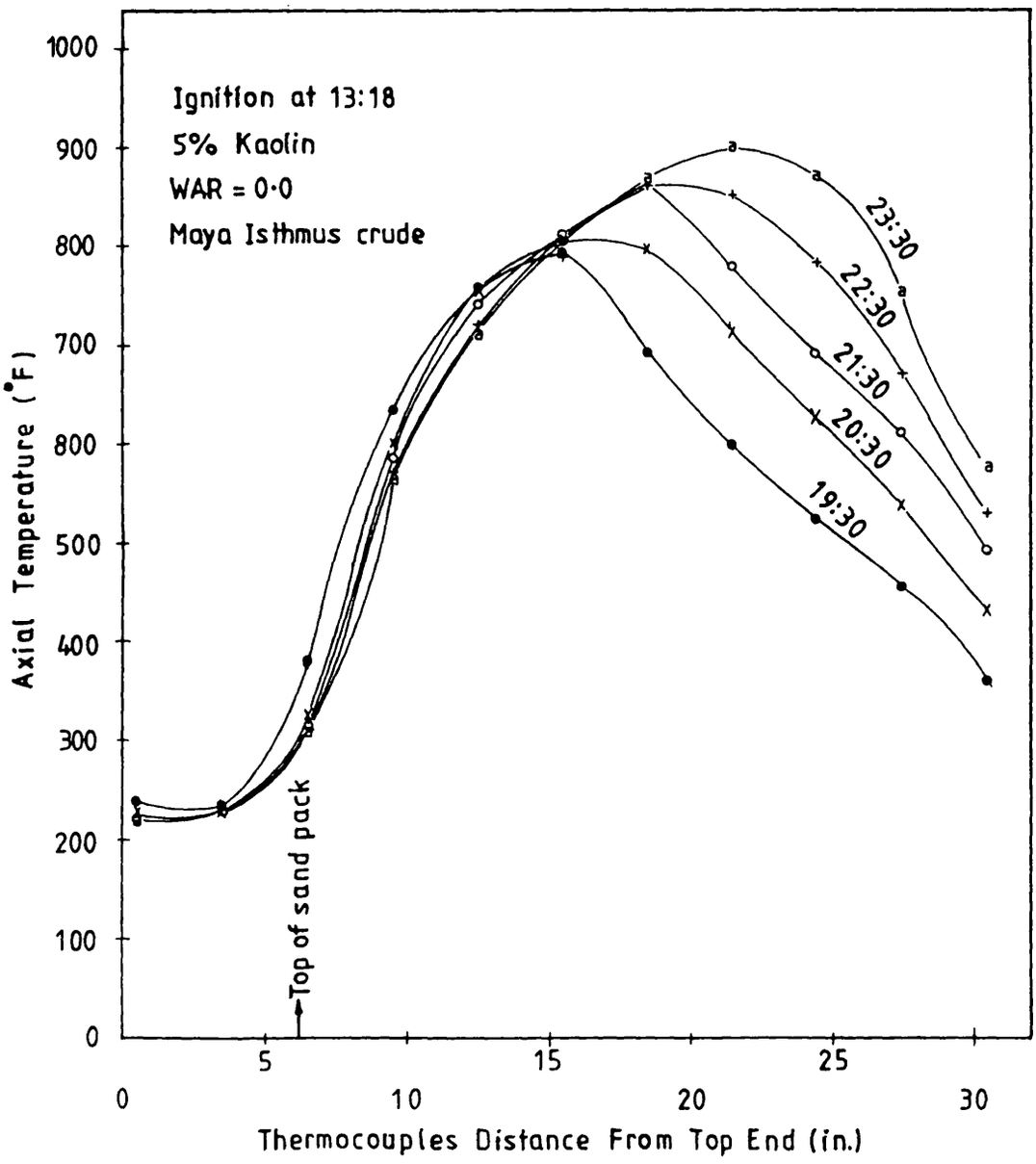

Figure 4.1(b) Axial temperature of sand pack *versus* distance along the combustion tube (run No.1).

high bed temperature achieved with dry combustion. Thus the only water available for the formation of steam in the bed is that formed from combustion of the fuel. Figure 4.1(b) shows that a self-sustained combustion front in the range 775-800° F (410-415° C) moves slowly downstream, reaching a maximum temperature of 906.2° F (485° C) at 10.2 h after ignition (clock time 23:30). This high peak temperature occurrence towards the end of the run is due to the preheating effect in passing through the burnt upstream zone of the bed. The combustion gases convectively transport heat downstream of the combustion zone, further enhancing this effect.

In run 2, which was a normal wet combustion run, the shape of the temperature profiles before water was injected are essentially the same as those for run 1 and are shown in Figure 4.2. During the period of wet combustion, however, the profiles become steeper behind the combustion zone. The increased temperature gradient is due to scavenging of heat from upstream of the combustion zone by the injected water. This effect increases at higher levels of water flux, or more specifically, as the local water:air ratio increases at the combustion front. This distinction is important, because some of the injected water is used to fill the porous volume of the bed.

The cooling action of the water is also obvious, since the temperature at the injection end of the combustion tube drops quickly down to a low temperature, in the region of 200° F (93° C). This is characterised by the relatively flat section close to the entrance of the tube. Despite the cooling effect of the water, wet combustion produces relatively high temperatures, due to the much larger steam bank which is formed. This reduces the rate of heat loss in the immediate neighbourhood of the combustion front, so that there is a reduced temperature gradient towards the

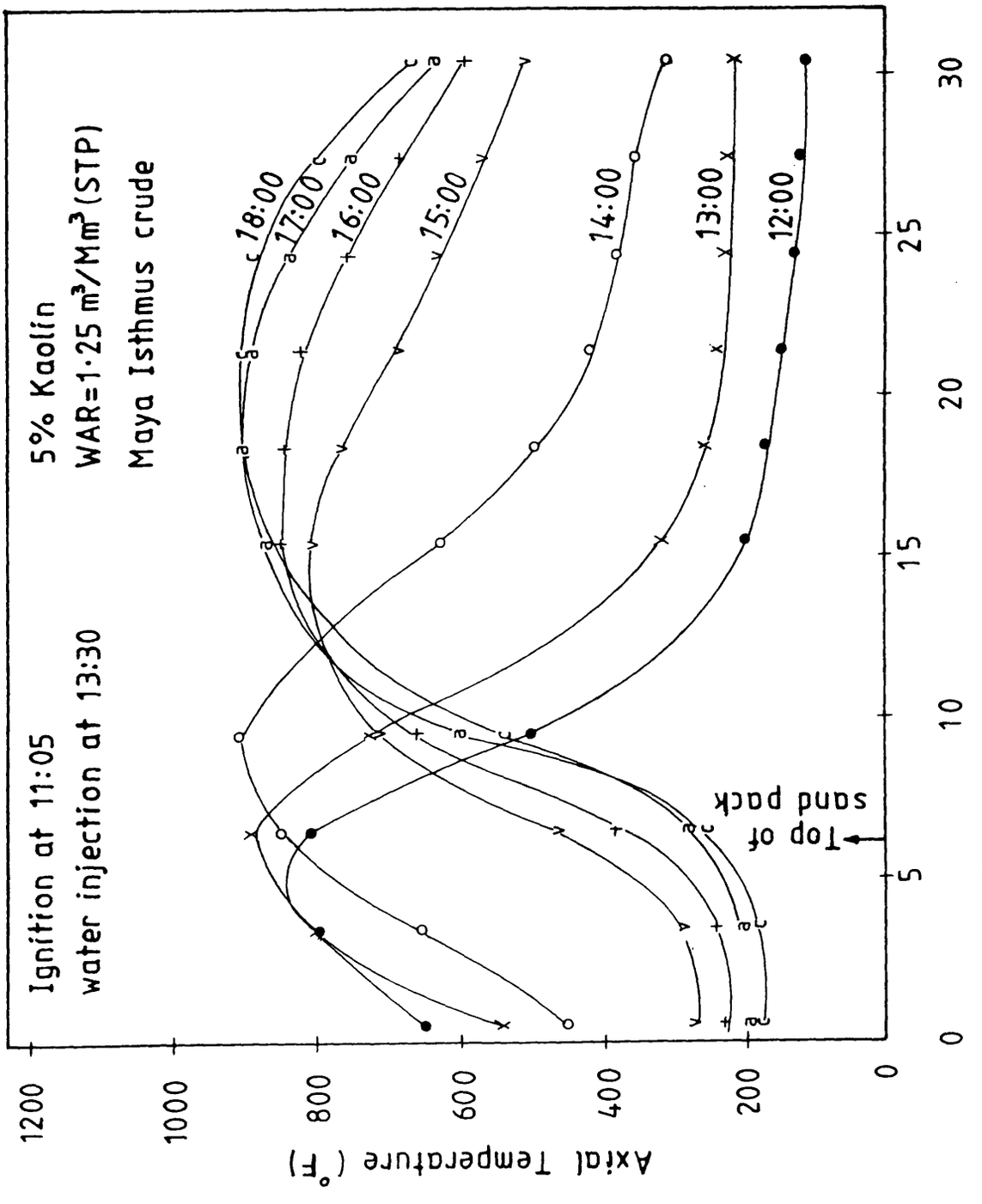

Figure 4.2 Axial temperature of sand pack *versus* distance along the combustion tube (run No.2).

steam zone. The temperature profiles occurring at time 16:00, 17:00 and 18:00 (5, 6 and 7 h respectively, after ignition) indicates that the combustion zone and steam zone are travelling at essentially the same rate. No condensation was observed at the trailing edge of the steam zone, owing to the fast expansion of this zone causing a large amount of heat to be carried downstream. With a longer combustion tube, a transient effect of this type would probably not occur and instead, the formation of a condensation zone would be observed in the temperature profile. The average peak temperature for this run was about 885° F (475° C), as shown in Table 4.2.

The conditions for run 3 with WAR of 2.5 m^3/Mm^3 (STP), represent the upper limit of the normal wet combustion mode. The shape of the temperature profiles in Figure 4.3 shows a similar trend to that of run 2, for which the WAR was only 1.25 m^3/Mm^3 (STP). A more distinctive combustion-steam zone is formed 5.4 h after ignition (clock time 18:36), in temperatures ranging from 790 to 800° F (420-425° C). However, the average peak temperature is much lower than that for run 2 (Table 4.2).

Temperature profiles for run 4, in which the WAR was three times that of run 2, are as shown in Figure 4.4. In this case, the water:air ratio had increased to a sufficiently large value to cause partial quenching of the combustion front, *i.e.*, part of the water passing through the combustion zone, remains in a liquid state. The notable feature of this condition is that the combustion zone moves through the pack in the form of a steam bank. Again, though, the temperature depends on the local water:air ratio, pressure and the oxidation characteristics of the crude oil (Computer Modelling Group, 1982). The profiles at 3.6 and 4 h after ignition (clock time 17:00 and 17:30, as shown in Figure 4.4) show the typical partially quenched condition.

Table 4.2

Average peak combustion temperatures

Run No.	Crude oil	Sand mixture characteristics	Mode of combustion	Peak temperature (° F)
1	Maya Isthmus	5% kaolin	dry	844
2	Maya Isthmus	5% kaolin	normal wet	885
3	Maya Isthmus	5% kaolin	normal wet	797
4	Maya Isthmus	5% kaolin	partially quenched	844
5	Maya Isthmus	10% kaolin	partially quenched	875
6	Forties	5% kaolin	normal wet	829
7	Maya	5% kaolin	normal wet	846
8	Maya Isthmus	10% amorphous silica	dry	865

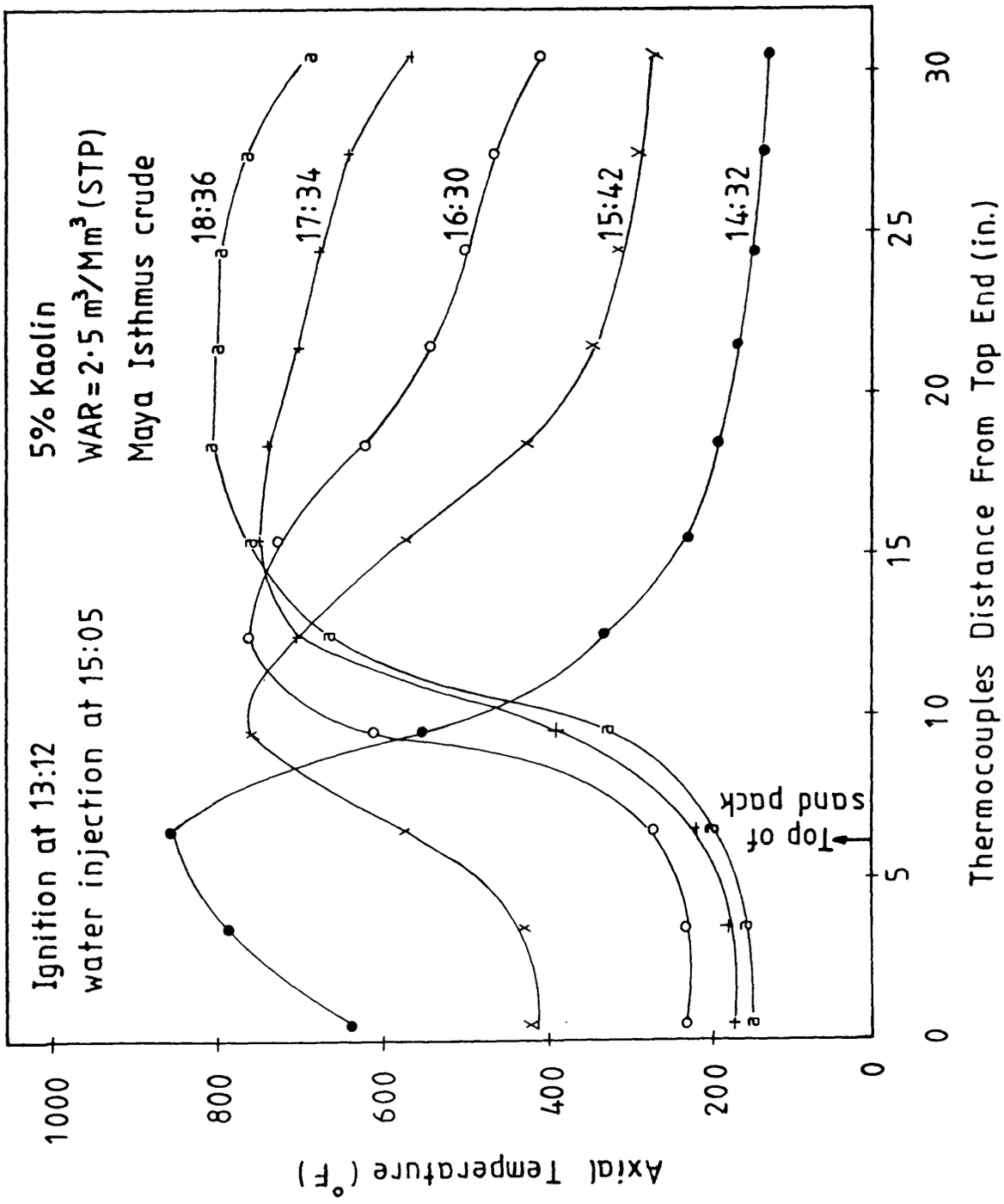

Figure 4.3 Axial temperature of sand pack *versus* distance along the combustion tube (run No.3).

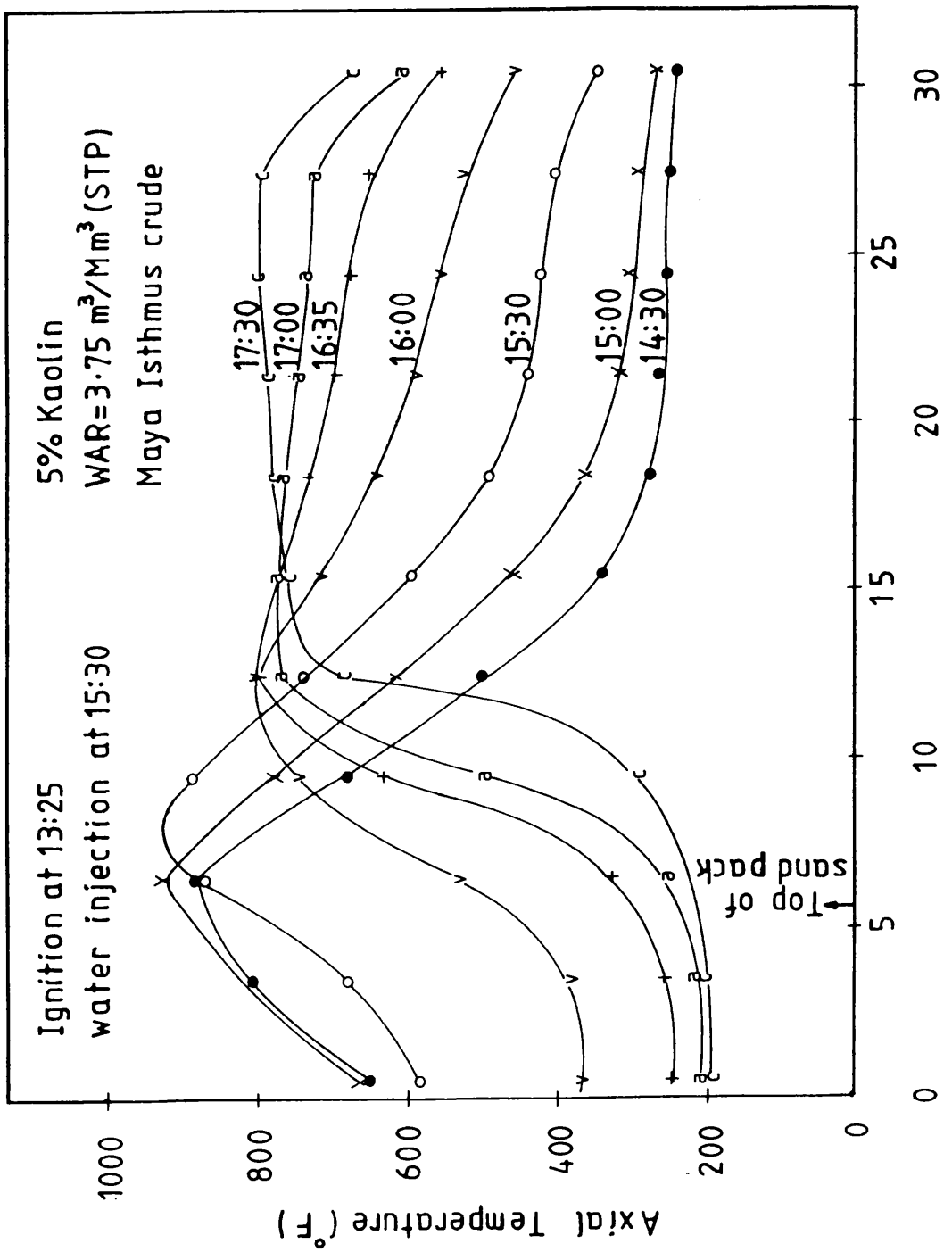

Figure 4.4 Axial temperature of sand pack *versus* distance along the combustion tube (run No.4).

There is no possibility of transition to a condensation zone in this case, because of the extended size of the steam zone, which causes the early breakthrough of steam. Approximately four hours after ignition (clock time 17:30), a superheated steam region exists at a temperature of 800° F (425° C), which is almost the same as the temperature of the steam zone in run 3. However, the average peak temperature is 40° F higher than that of run 3 (Table 4.2). Although the combustion front was partially quenched, considerable amounts of oxygen were consumed at this steam temperature, as evidenced by the composition of the produced gases (treated in the next section).

Figure 4.5 illustrates the temperature profiles for run 5, in which 10% of kaolin was present in the sand mixture. The other conditions were the same as in run 4. The steam plateau for the dry combustion period is slightly wider (clock times 17:00 and 18:00 respectively), 0.87 and 1.87 h after ignition, compared with run 4, which used a mixture containing 5% of kaolin. However, the temperature profiles during the quenched period of combustion are different from those observed for run 4 (see Figure 4.4). The less flat profile for run 5 (clock time 21:00 and 22:00) are evidence of a significant pressure drop developing with the sand pack, due primarily to the migration of fine clay material.

Figure 4.6 shows that the temperature profiles for normal wet combustion of Forties crude (run 6). These are essentially the same as those obtained using Maya Isthmus crude (run 2), apart from the fact that the average peak temperature is lower (829 ° F). The normal wet combustion profiles for the medium heavy Maya crude (Figure 4.7) show a narrower steam plateau. For the same WAR (Table 4.2), the average peak temperature is higher than that obtained in run 6, but is still lower than that in run 2. An

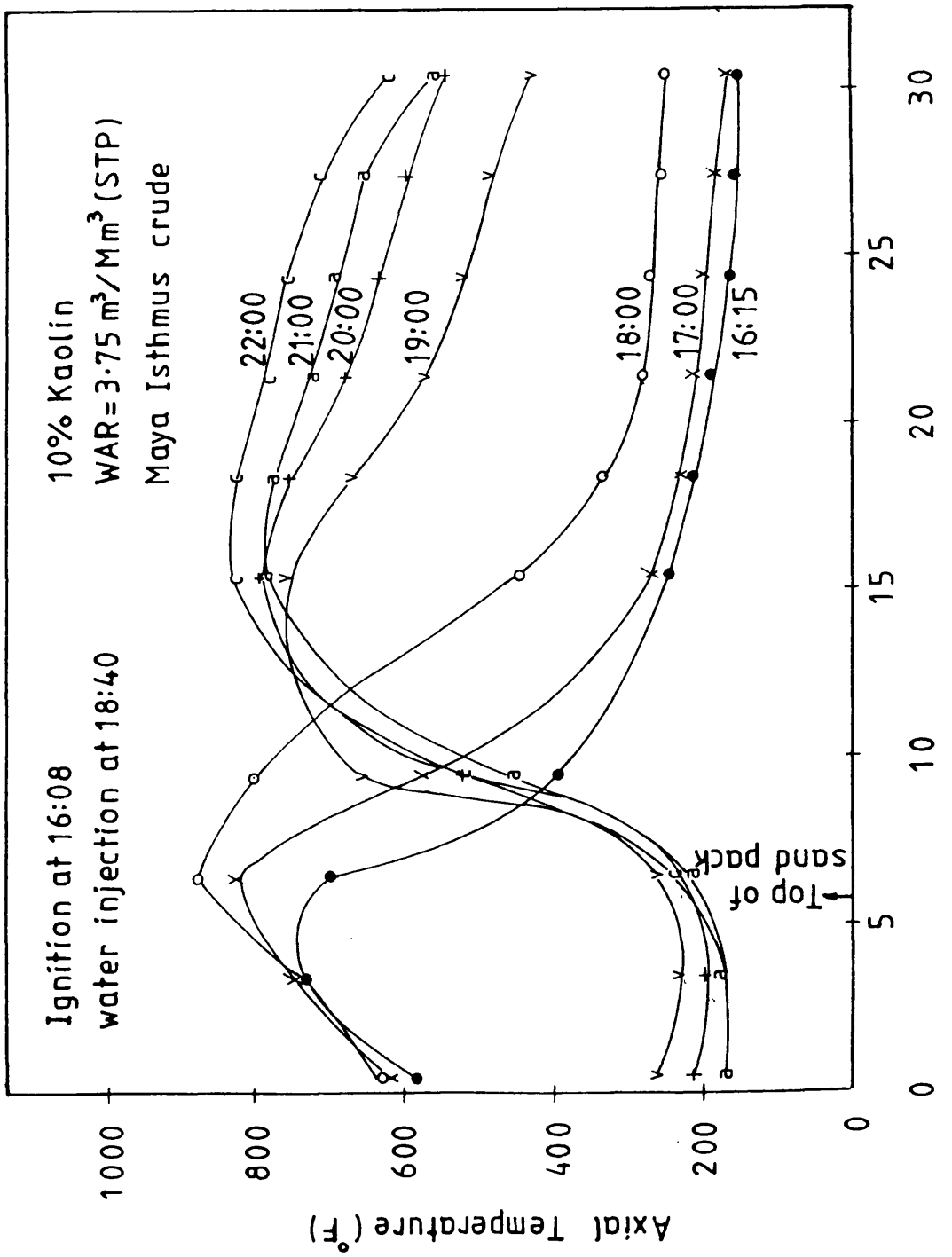

Figure 4.5 Axial temperature of sand pack *versus* distance along the combustion tube (run No.5).

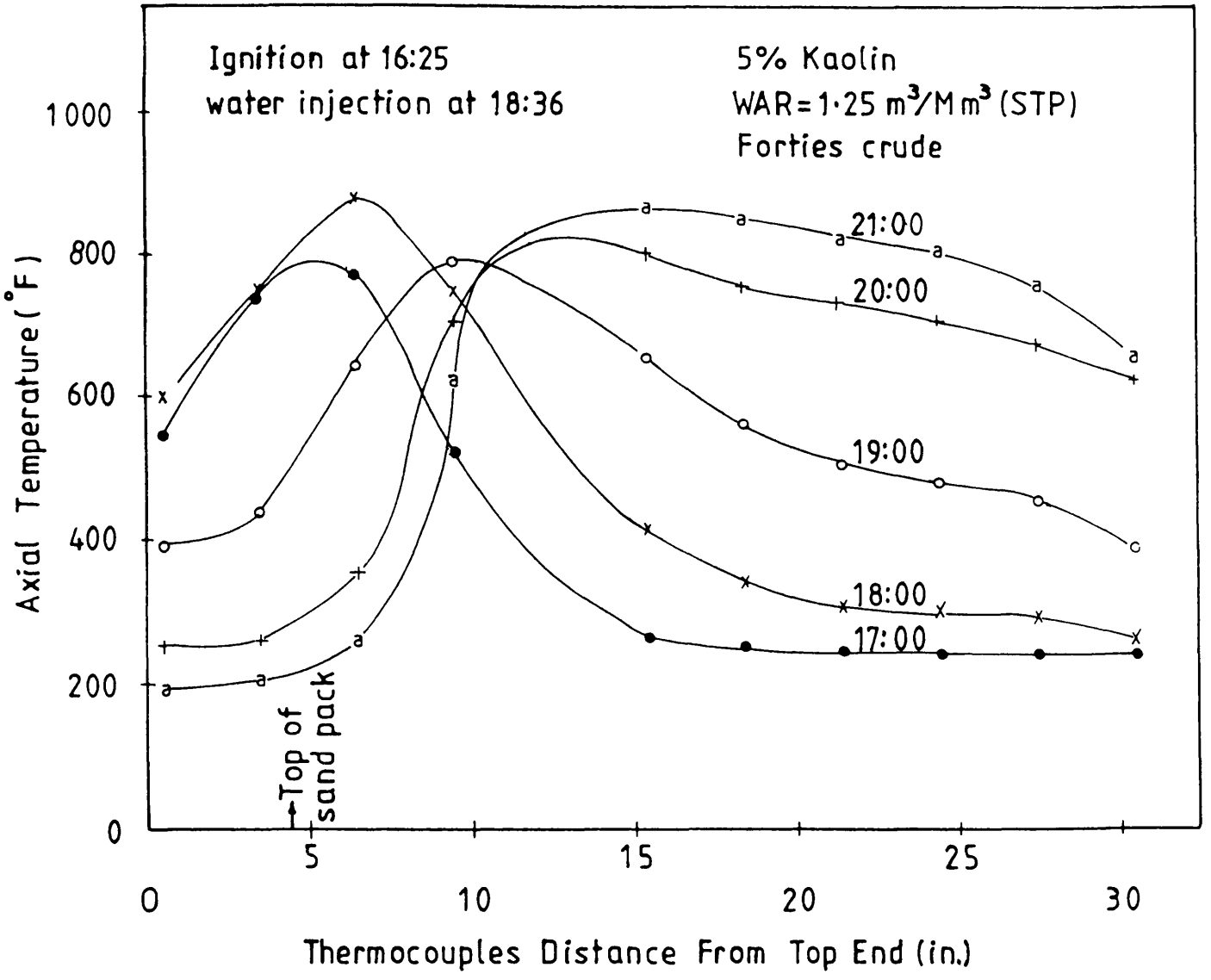

Figure 4.6 Axial temperature of sand pack *versus* distance along the combustion tube (run No.6).

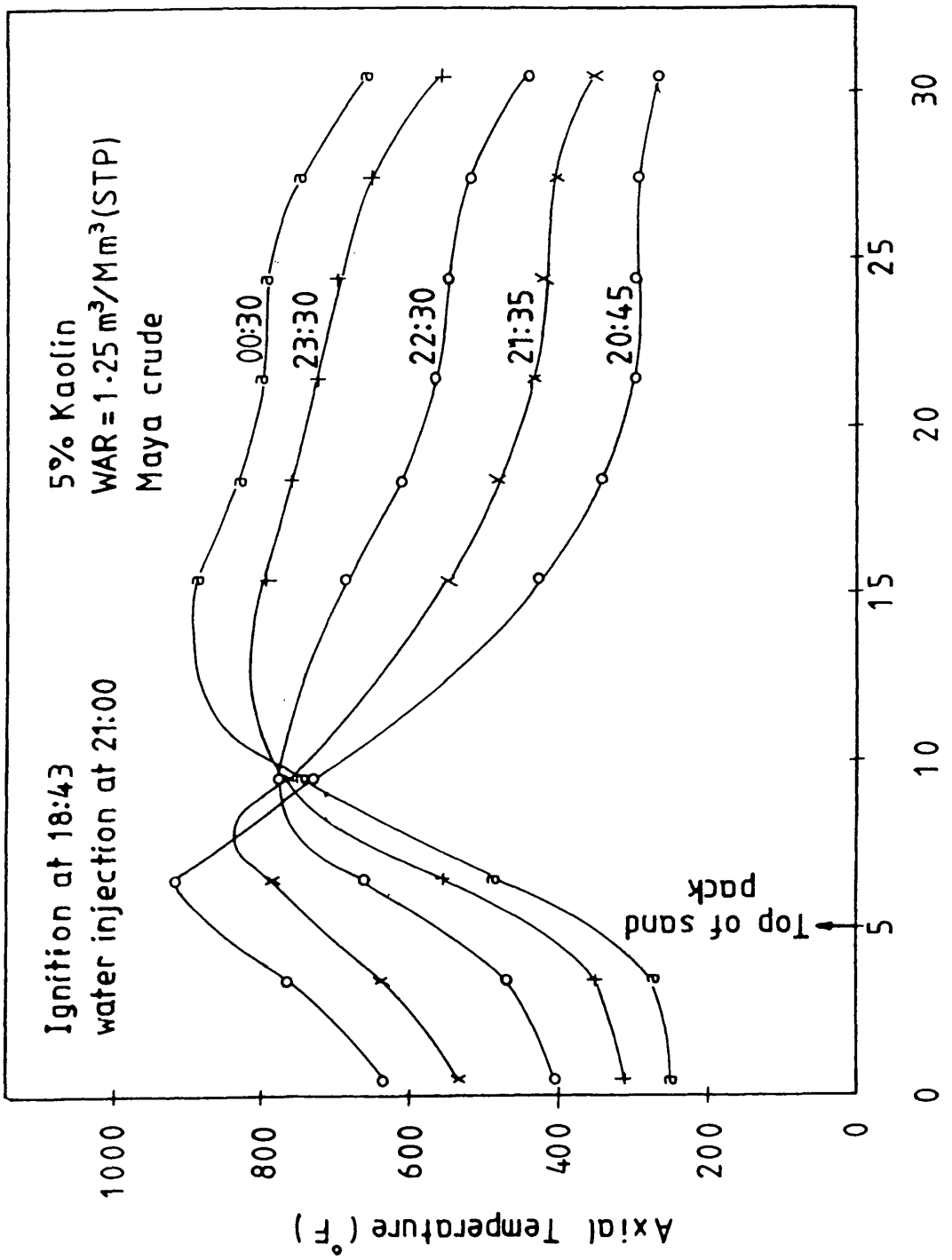

Figure 4.7 Axial temperature of sand pack *versus* distance along the combustion tube (run No.7).

even narrower steam plateau condition was observed 3.75 h after ignition [clock time 12:30, Figure 4.8(a)], when the sand mixture contained 10% amorphous silica. The highest peak temperature was recorded 10.83 h after ignition [clock time 19:35, Figure 4.8(b)], reaching a value of 963° F (517° C). Although this temperature was the highest value obtained for all the runs, the average peak temperature is nevertheless still lower than that for the normal wet combustion run (run 2), which used the same crude oil. The high peak temperature occurring towards the end of the run is again due to the preheating action of the hot combustion gases.

The temperature as a function of time was recorded for every thermocouple at both axial and wall positions. A few selected profiles, which are representative of the temperature history of different zones, are illustrated in Figures 4.9-4.20. For the most part, control was kept within a margin of 15-20° F, with the result that the axial temperature was sometimes higher, and sometimes lower, than the corresponding wall temperature. However, right at the combustion zone, the heating tape was not capable of generating a high enough temperature. Nevertheless, it can be seen that with the exception of run 5 (shown in Figure 4.17), a satisfactory adiabatic condition was achieved in this region.

Manual control, with a single heating tape, is a difficult and crude method of operating the system. It is surprising, therefore, that an apparently satisfactory degree of control was achieved. In addition, severe problems were encountered towards the end of the run, when heat losses became large due to conduction through the tube bottom flange. In one case, failure of the heating tape caused the temperature difference to increase to approximately 150° F, which rapidly destroyed the adiabtic regulation. The result was that the combustion could not be sustained.

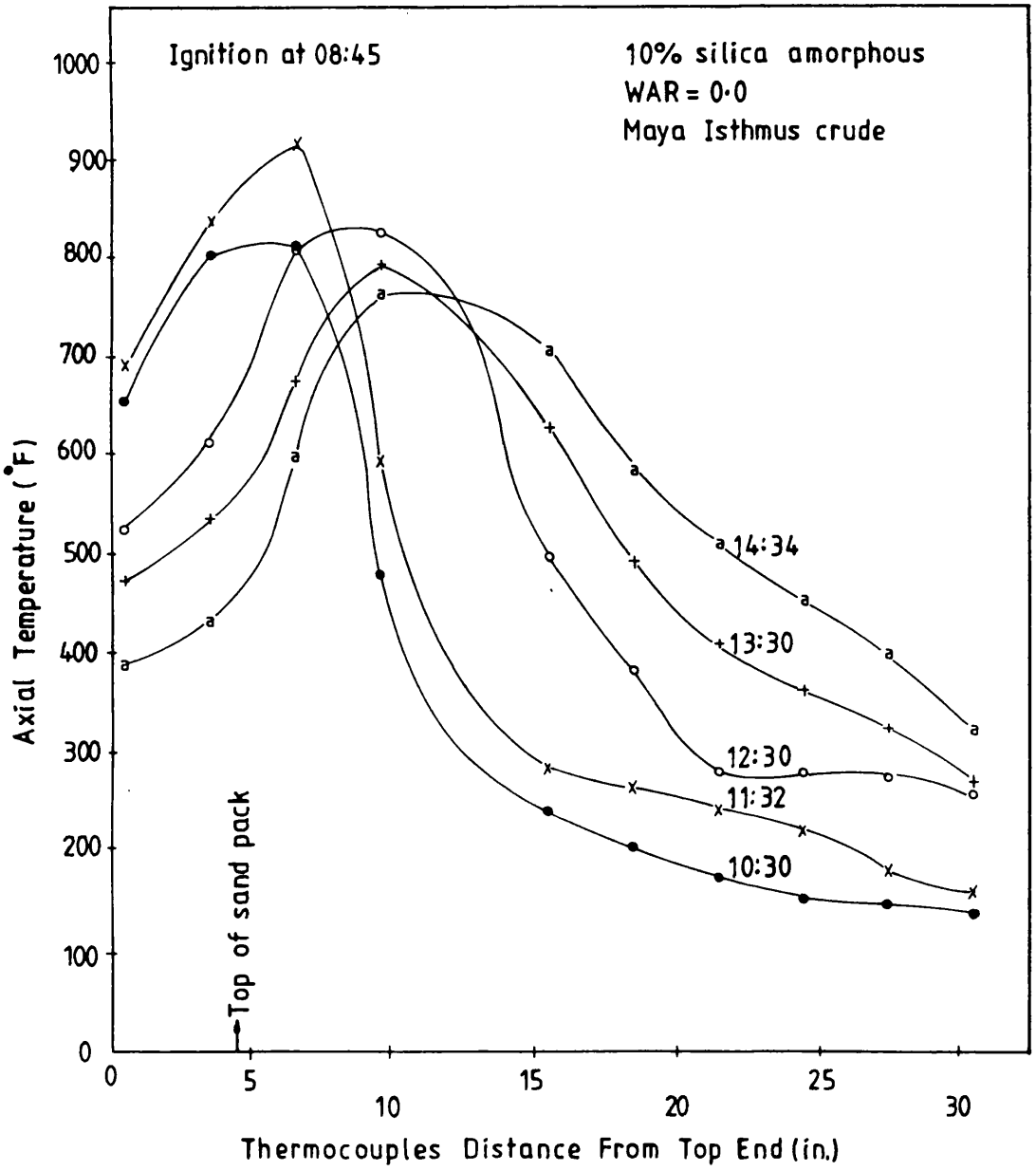

Figure 4.8(a) Axial temperature of sand pack *versus* distance along the combustion tube (run No.8)

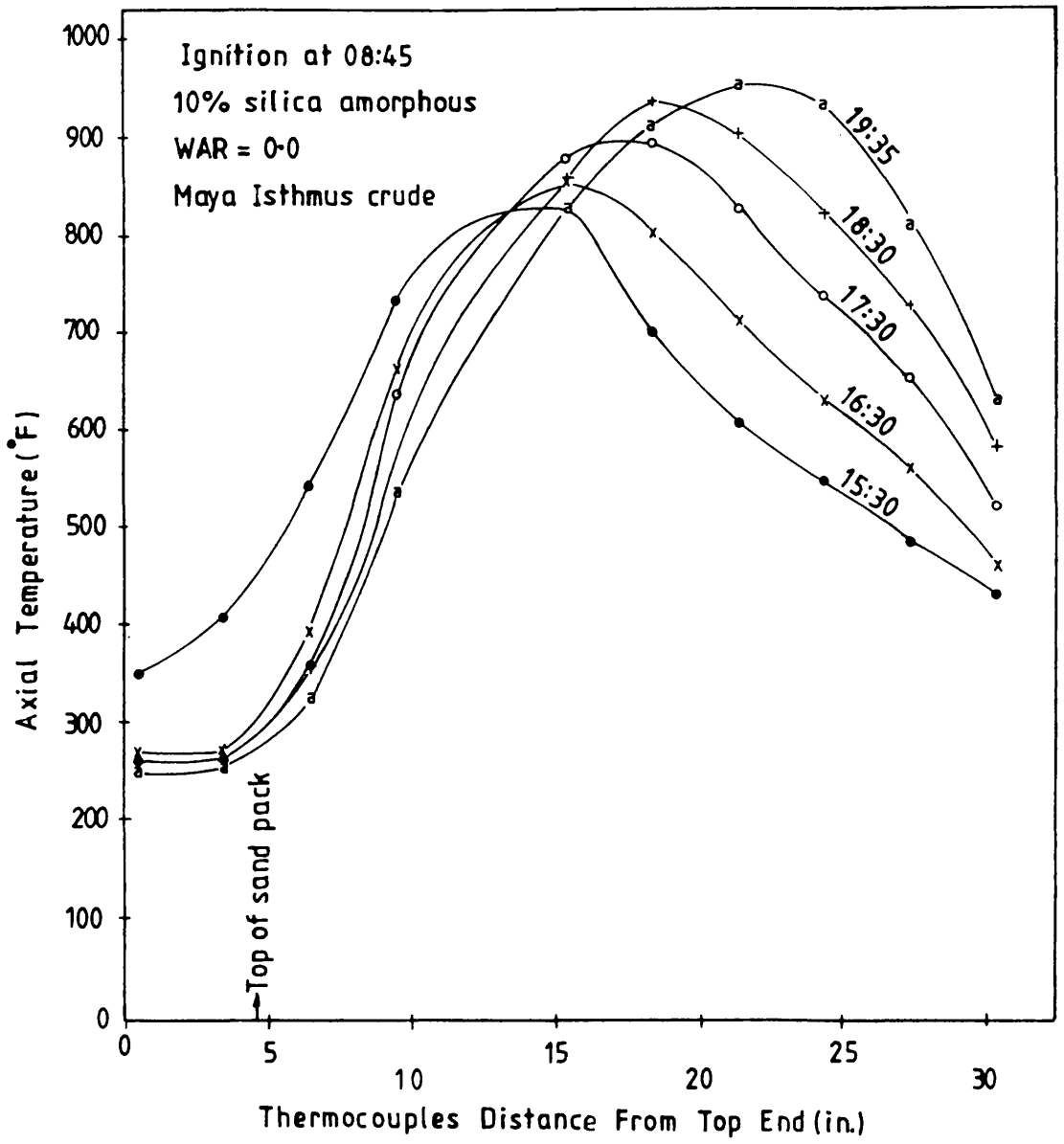

Figure 4.8(b) Axial temperature of sand pack *versus* distance along the combustion tube (run No.8).

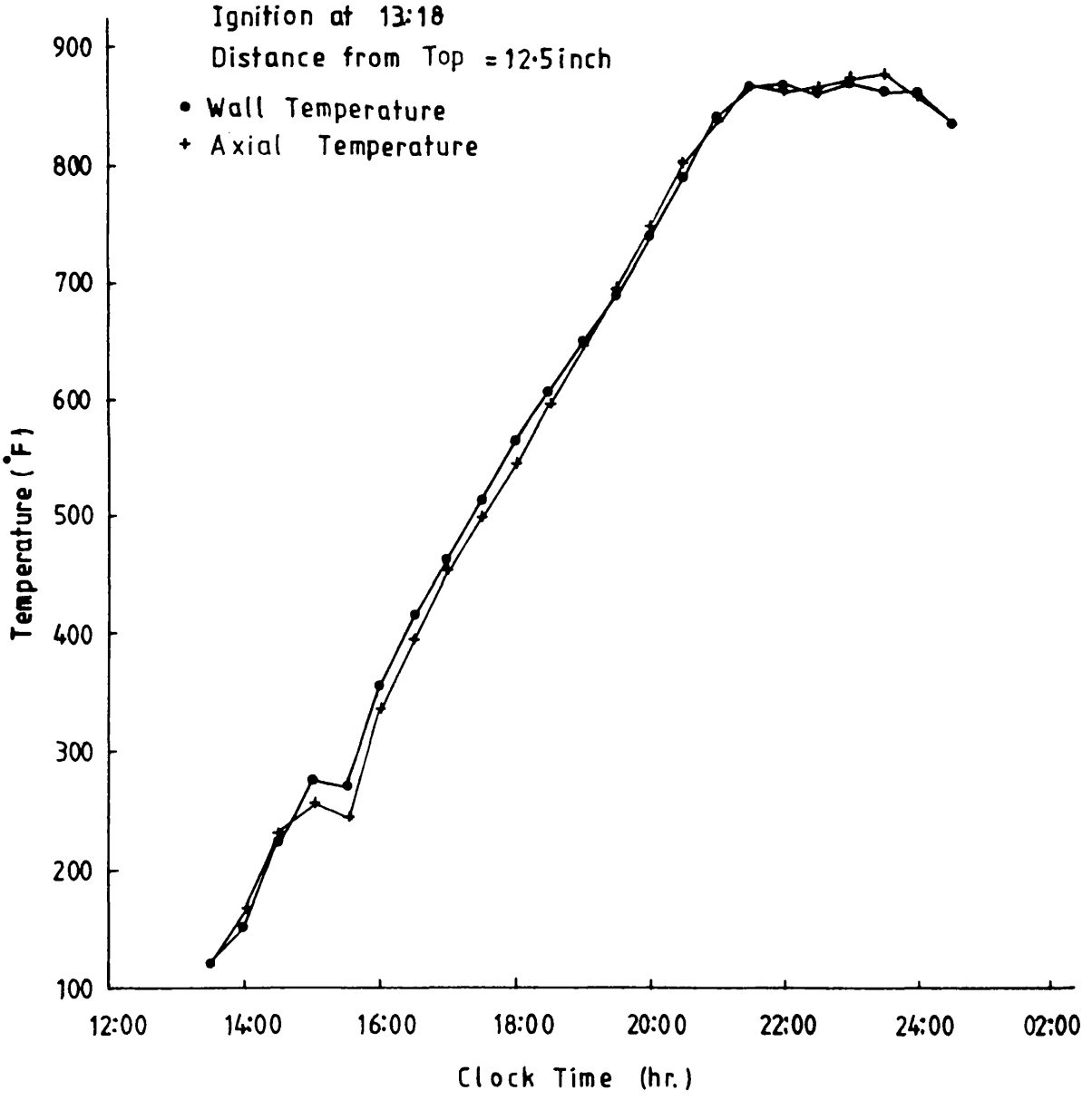

Figure 4.9 Temperature history for the combustion of the Maya Isthmus crude (run No.1).

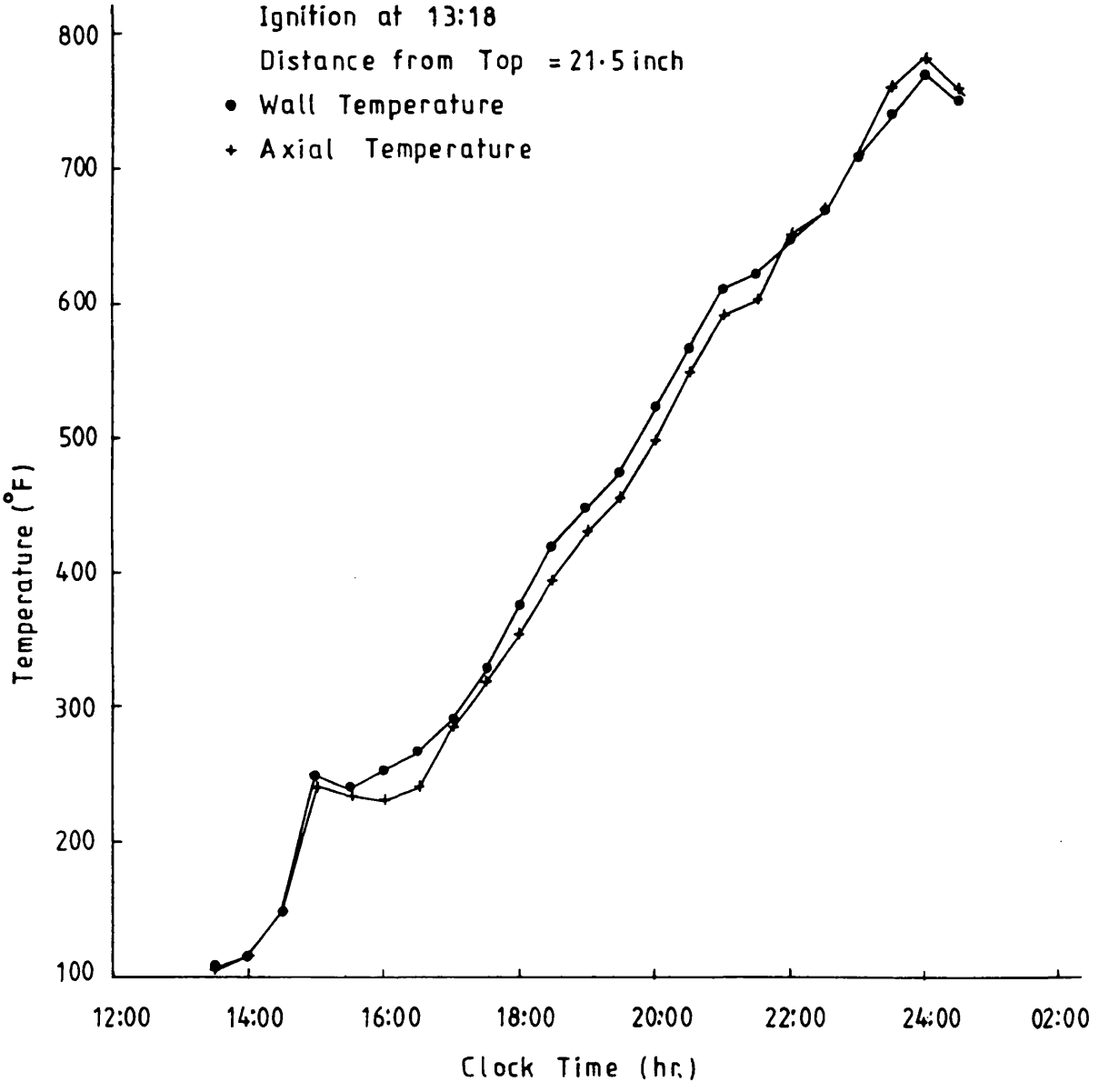

Figure 4.10 Temperature history for the combustion of the Maya Isthmus crude (run No.1).

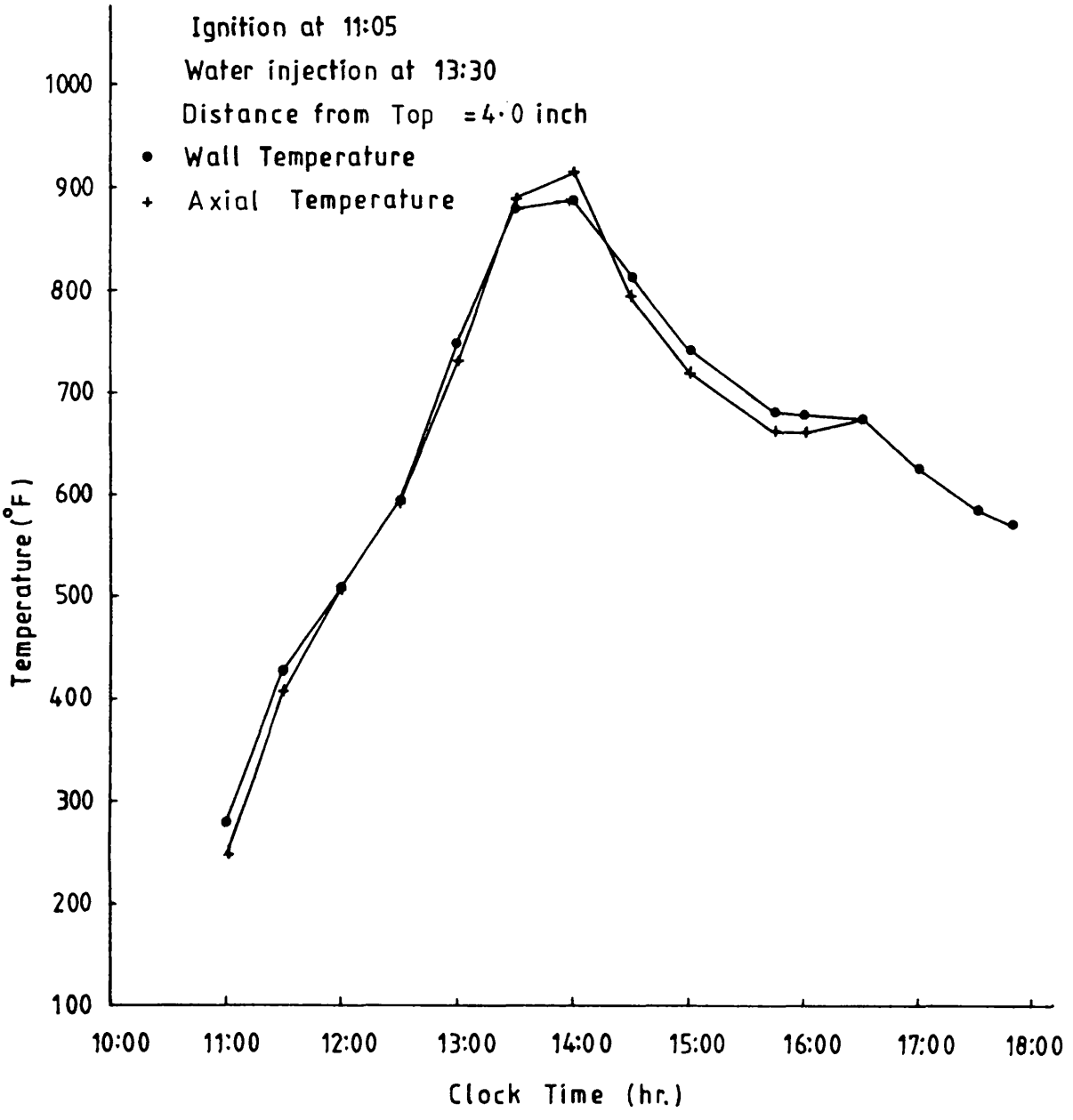

Figure 4.11 Temperature history for the combustion of the Maya Isthmus crude (run No.2).

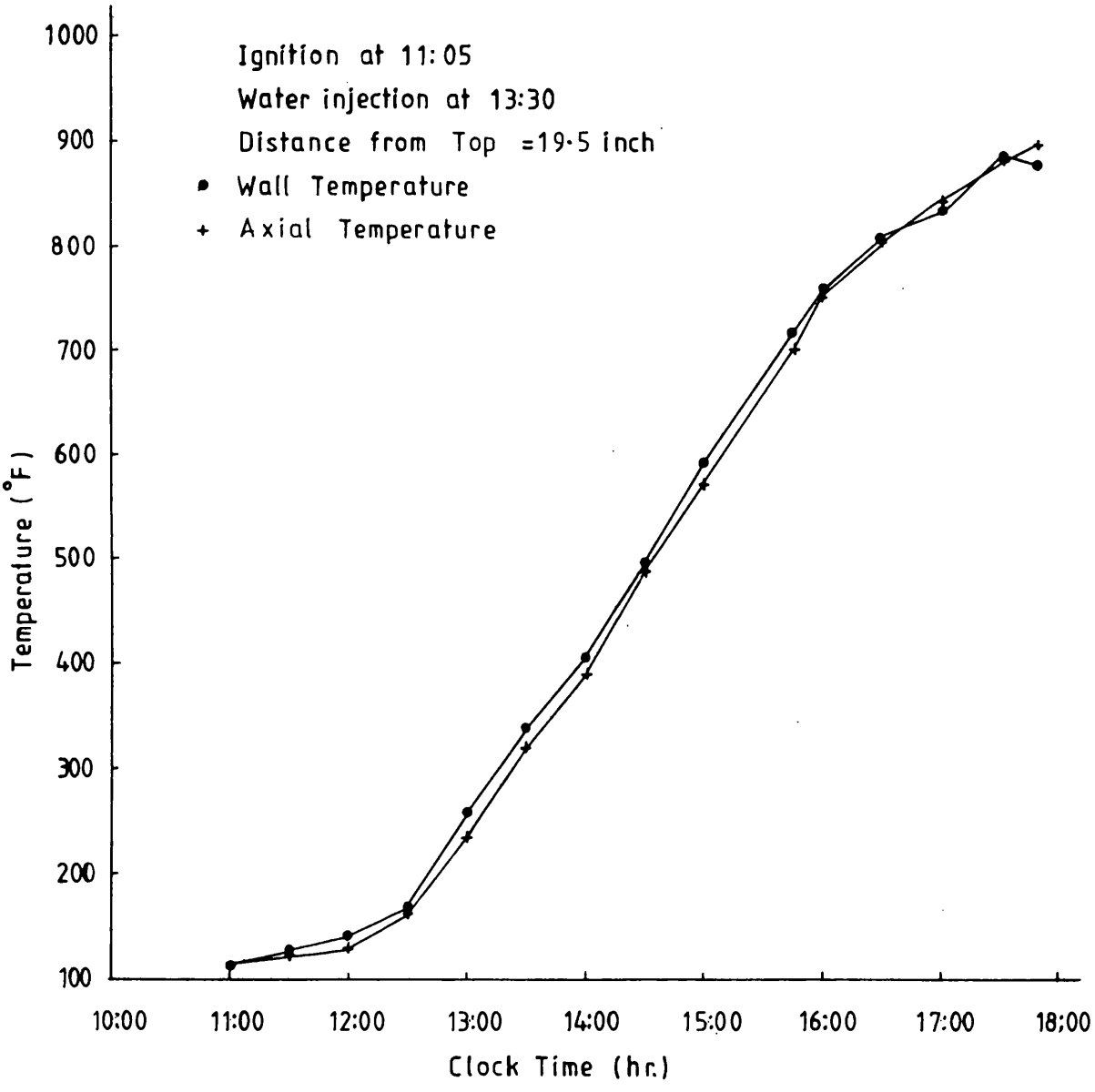

Figure 4.12 Temperature history for the combustion of the Maya Isthmus crude (run No.2).

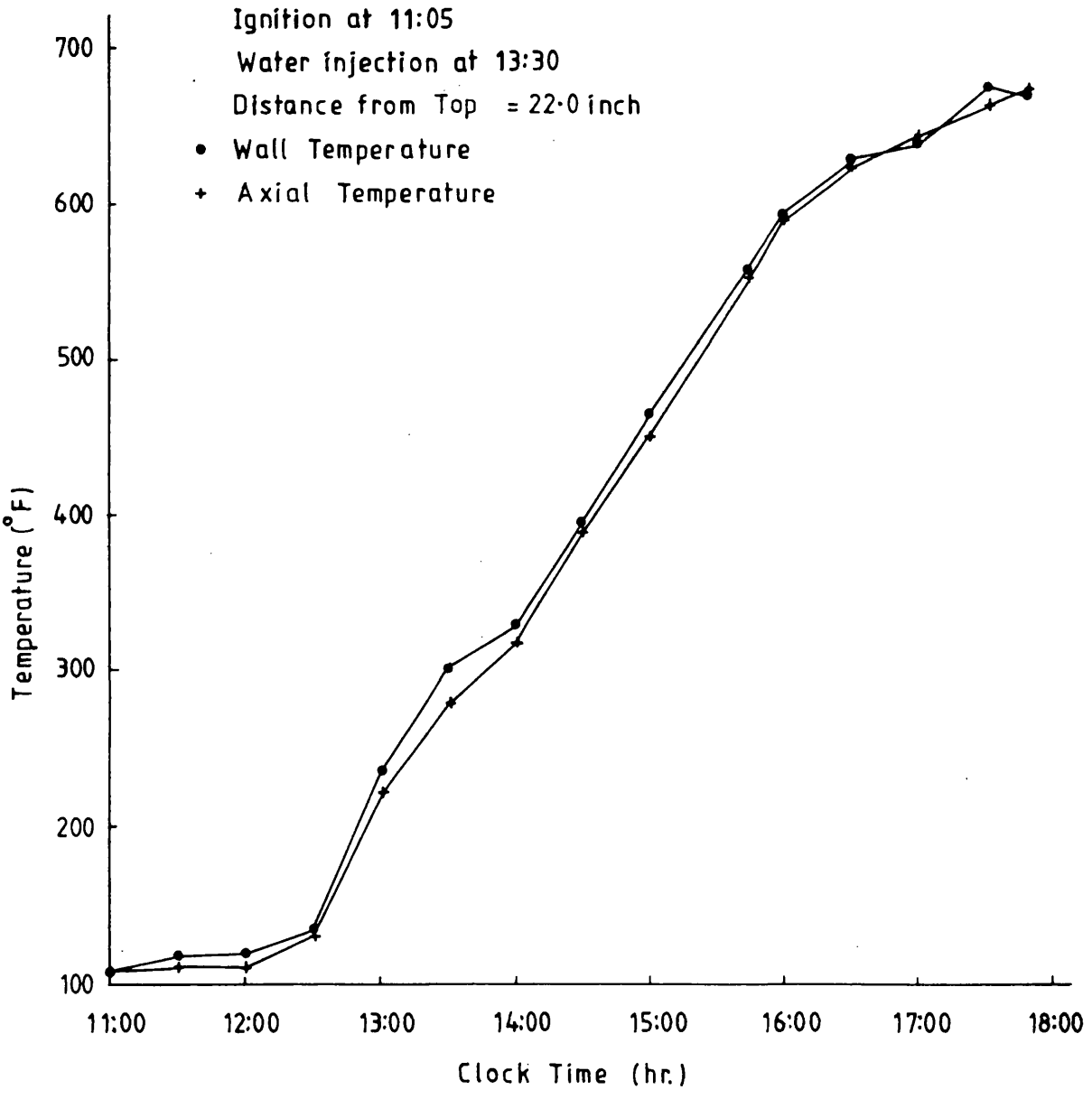

Figure 4.13 Temperature history for the combustion of the Maya Isthmus crude (run No.2).

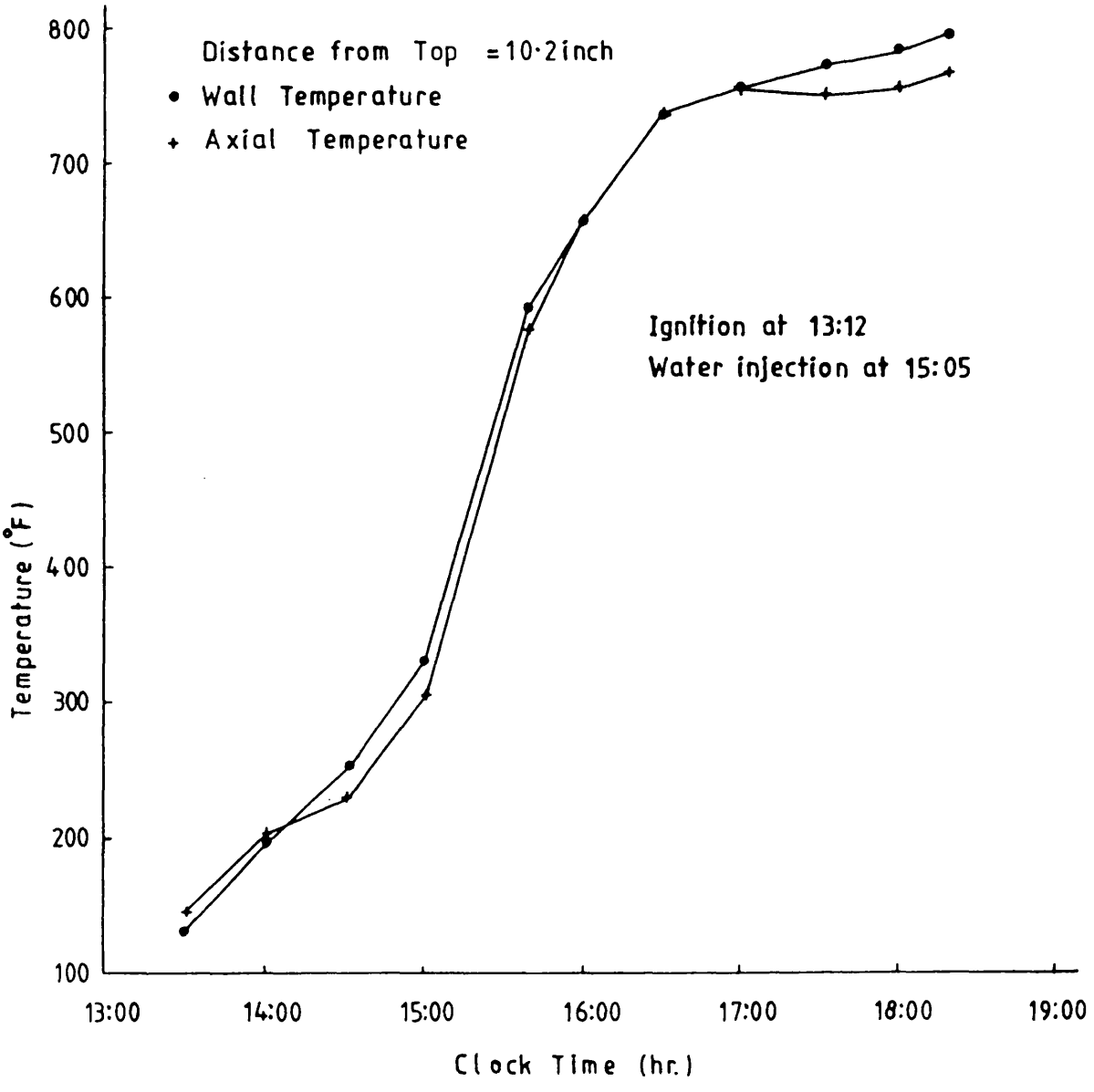

Figure 4.14 Temperature history for the combustion of the Maya Isthmus crude (run No.3).

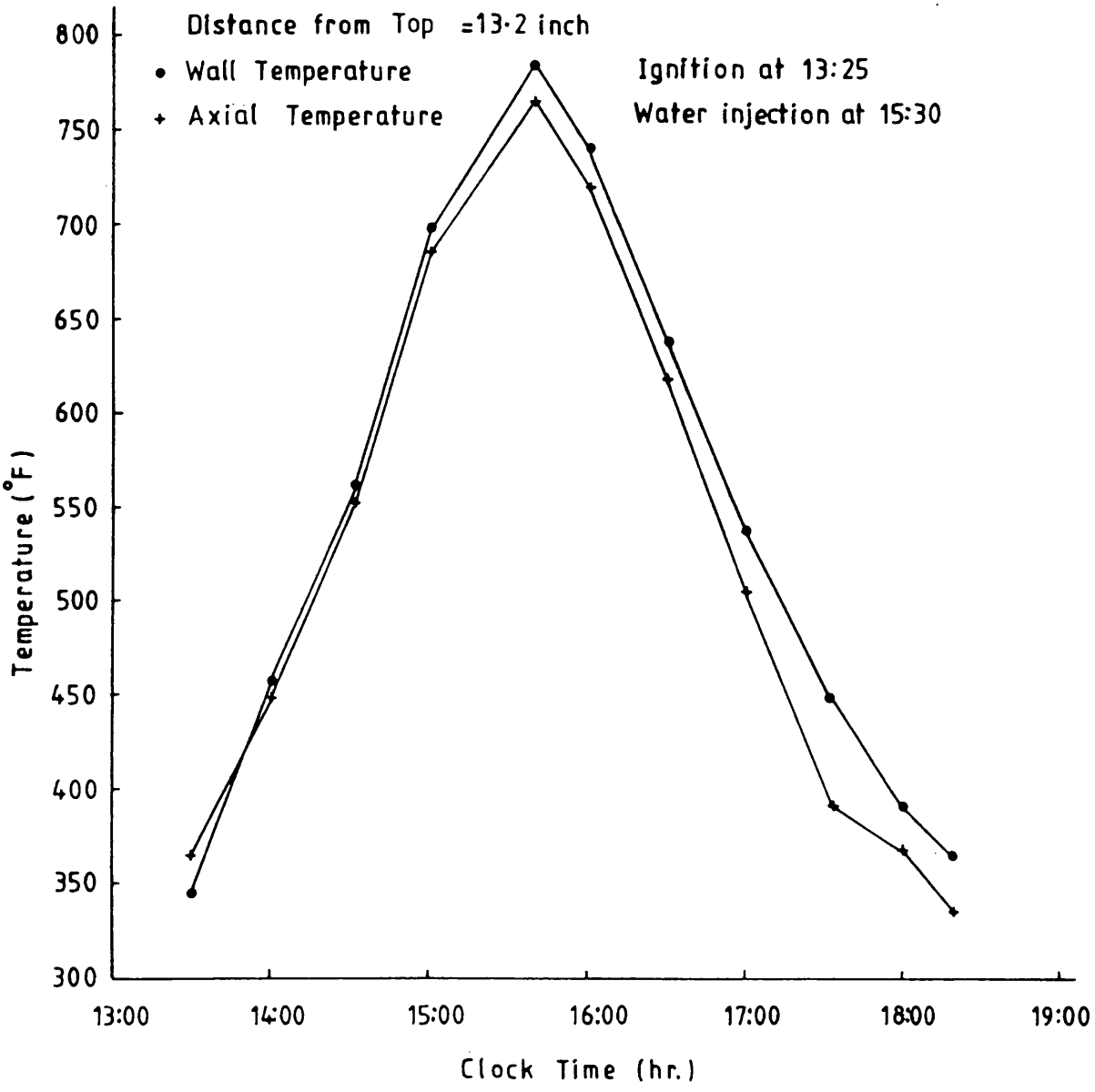

Figure 4.15 Temperature history for the combustion of the Maya Isthmus crude (run No.4).

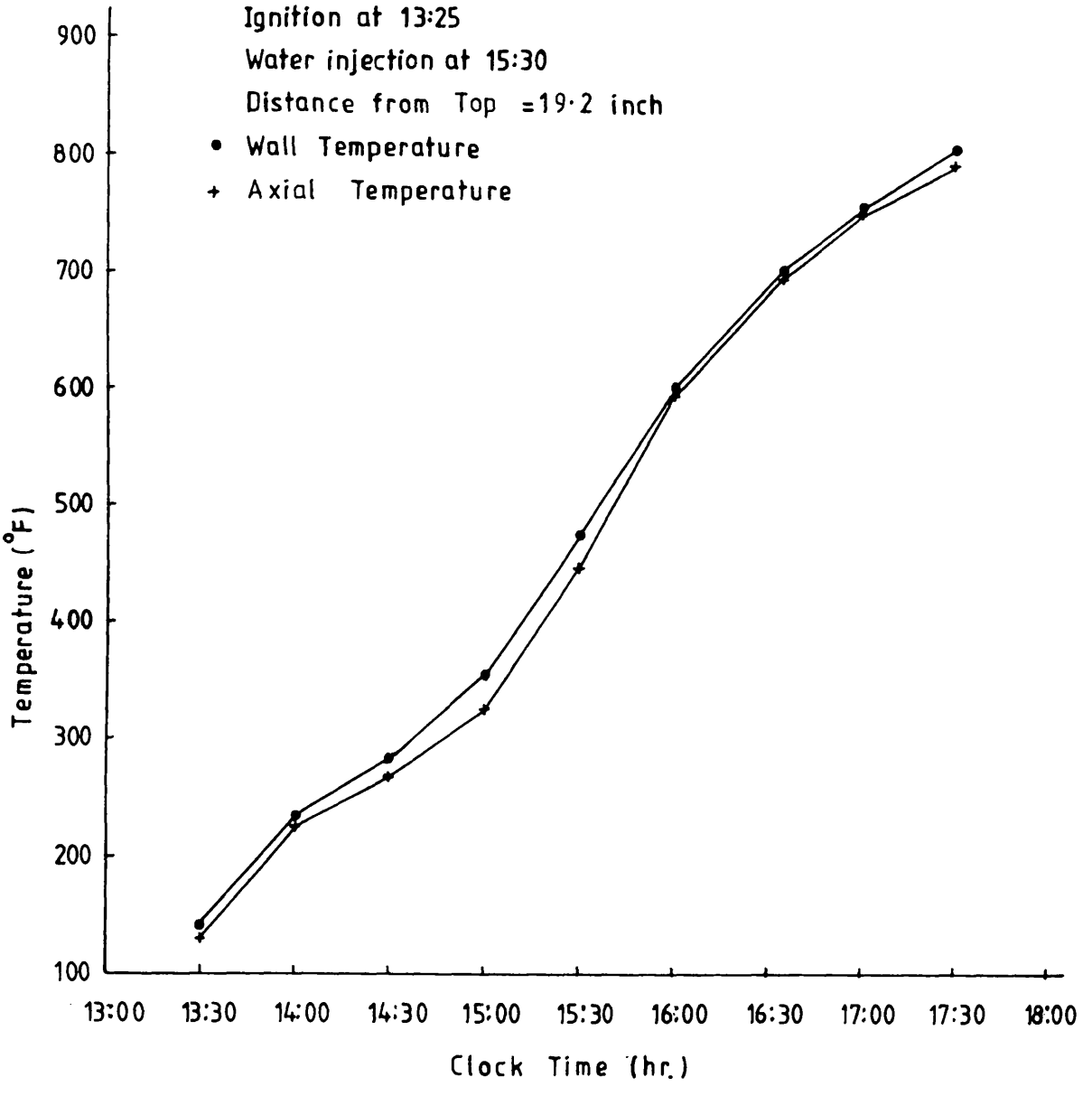

Figure 4.16 Temperature history for the comhustion of the Maya Isthmus crude (run No.4).

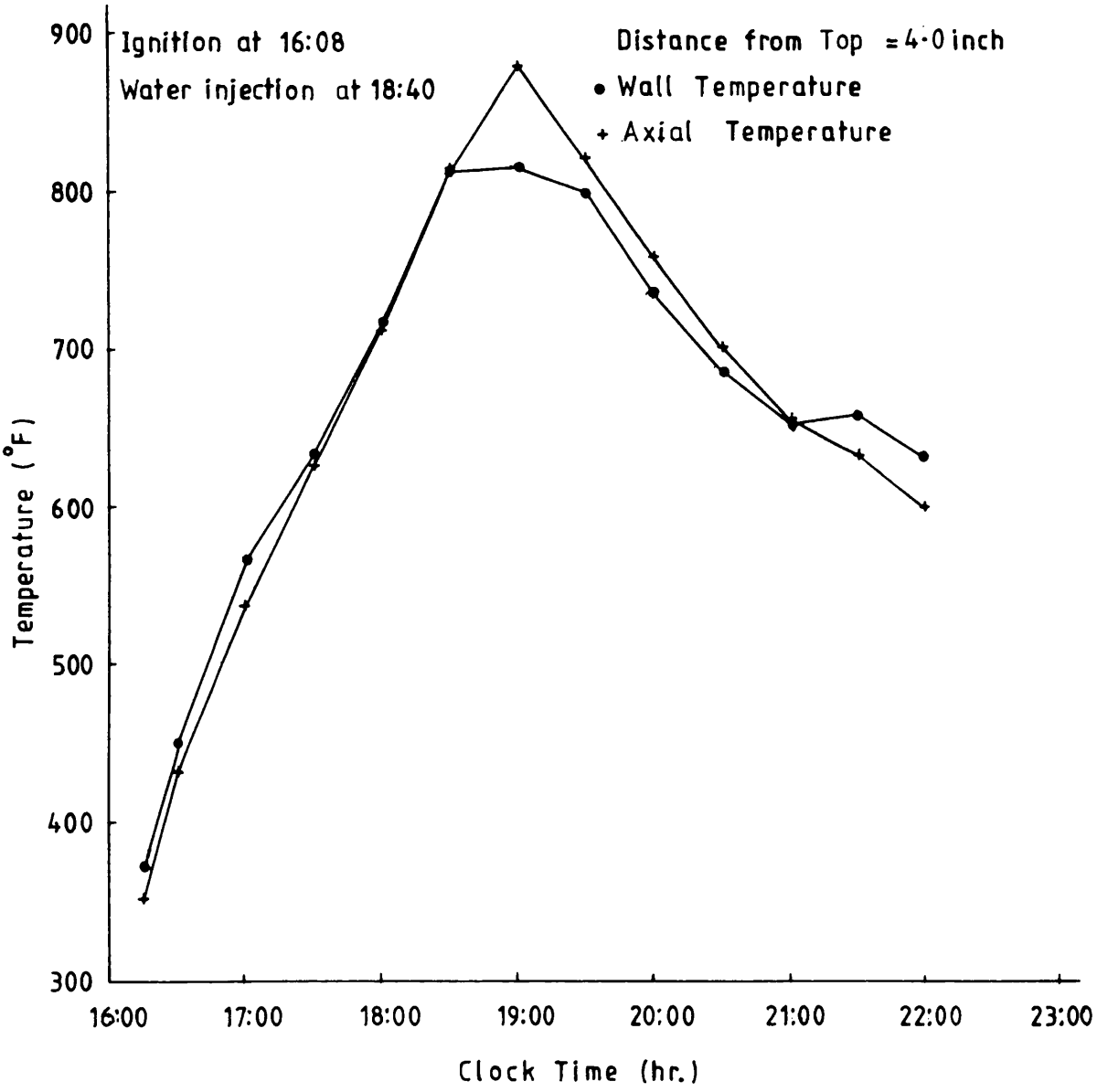

Figure 4.17 Temperature history for the combustion of the Maya Isthmus crude (run No.5).

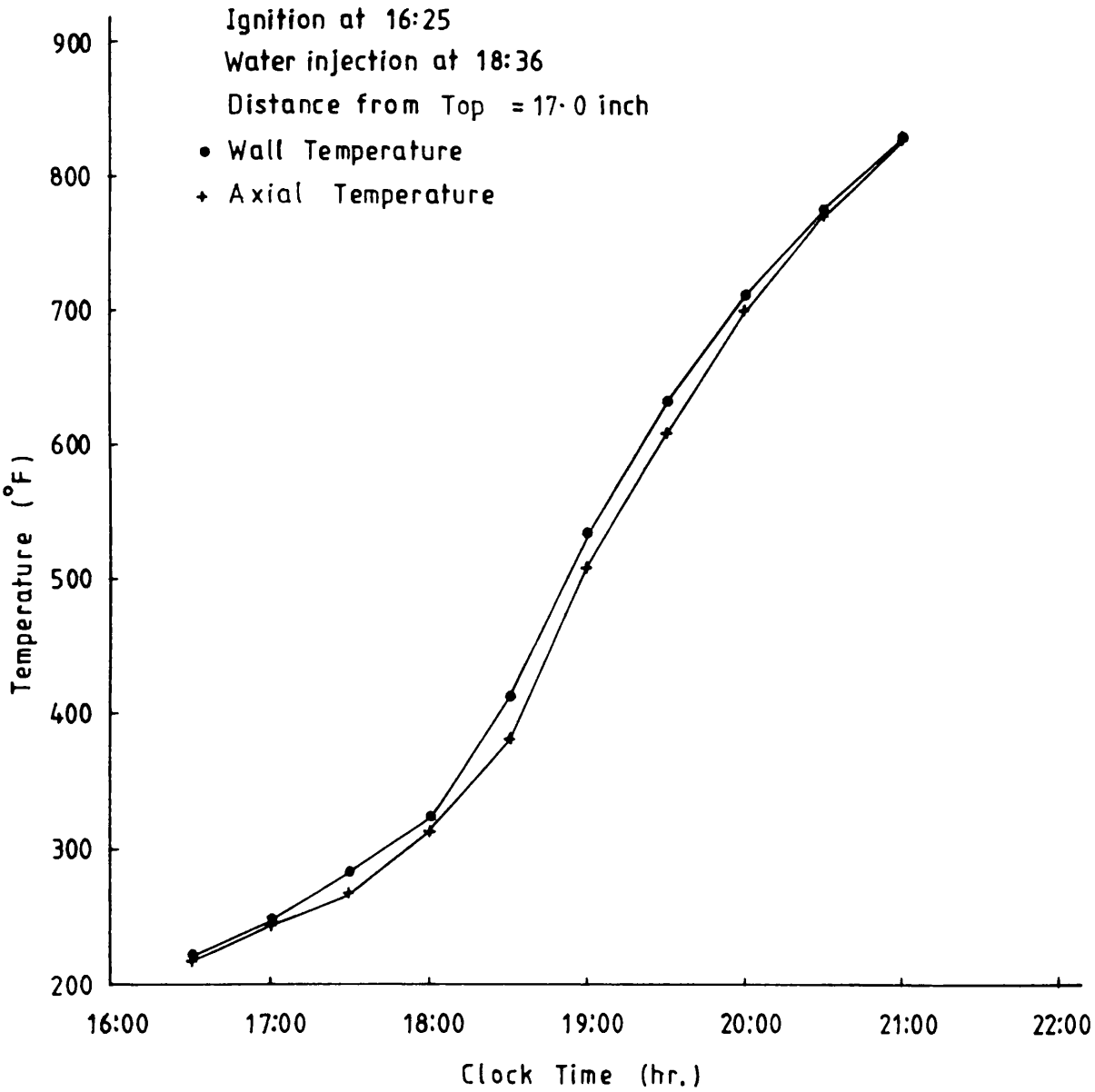

Figure 4.18 Temperature history for the comhustion of Forties crude (run No.6).

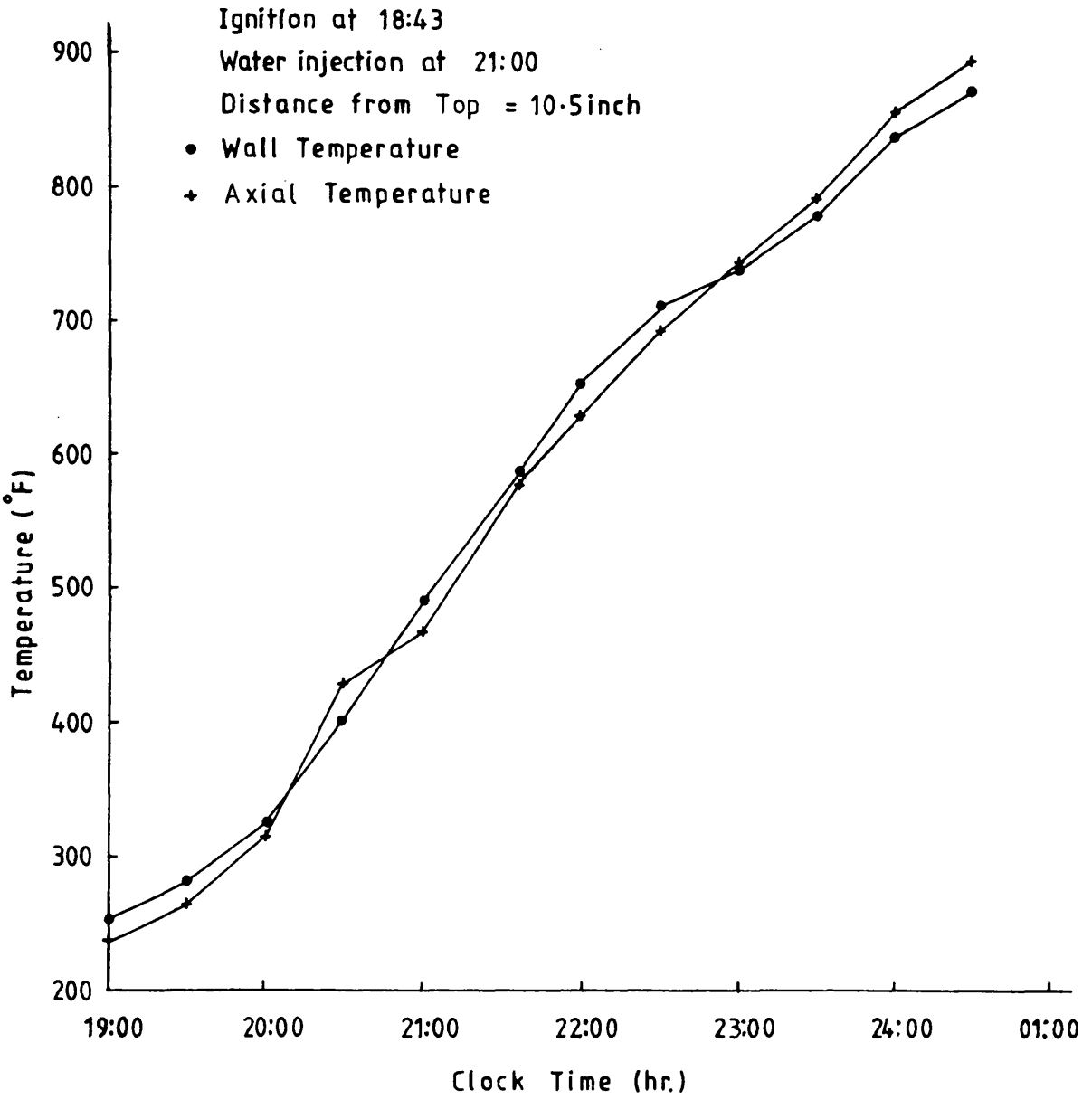

Figure 4.19 Temperature history for the combustion of Maya crude (run No.7).

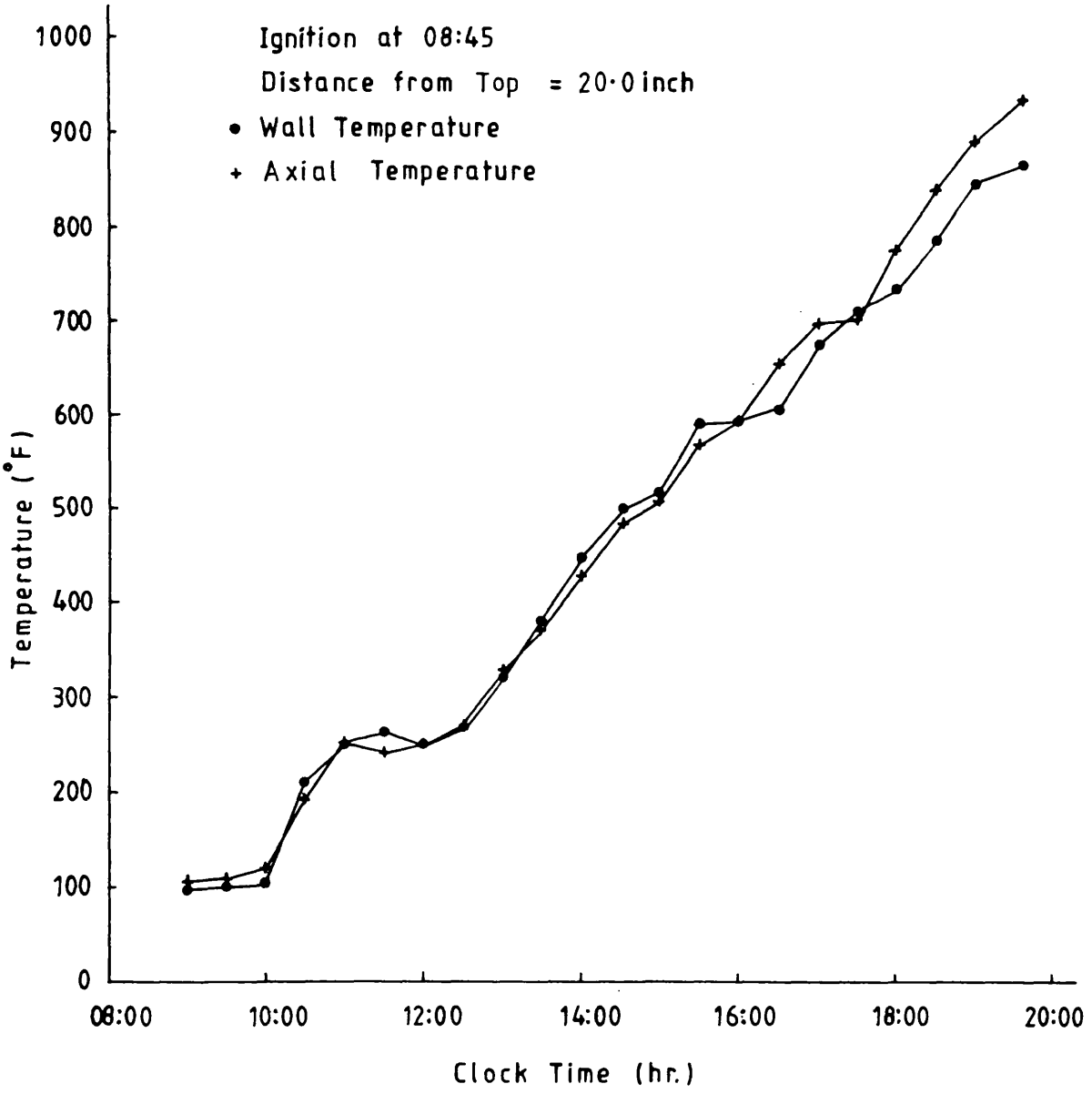

Figure 4.20 Temperature history for the combustion of the Maya Isthmus crude (run No.8).

Compared with results obtained by other workers elsewhere (Harding, 1976; Ejiogu, 1979; and Parrish and Craig, 1969), the degree of adiabatic control appears to be very reasonable.

4.3 Exit gas composition

Figures 4.21-4.28 illustrate the composition of the produced gases as a function of time from ignition.

In run 1 (Figure 4.21), the concentration of CO_2 and CO tends to increase generally over the combustion period, while the oxygen shows a decreasing trend. The oxygen concentration decreases sharply to a low level of 1.9 % 2.2 h after ignition, then averages approximately 1.6 %, whilst at the same time, CO_2 mole fraction increases gradually and reaches a value of 16.9 % 5 h after ignition. The CO mole fraction varied from 2.5 to 3.5 %. CO_2 and CO concentrations start to drop again to lower values of 11.7 % and 2.0 % respectively, 6.25 h after ignition. The oxygen concentration is then 3.0 %. As the peak temperature increases towards the end of the run [see Figure 4.1(b)], the CO_2 and CO concentration increases to 17.8 and 3.0 % respectively, while oxygen averages 1%. The analysis of the dry combustion gases shows no evidence of the presence of light hydrocarbon or hydrogen being produced.

For the normal wet combustion run (run 2, Figure 4.22), the level of carbon monoxide production is higher than that of the carbon dioxide immediately after ignition. Later on, the CO_2 and CO production appears to follow the same trend throughout the run. The carbon dioxide concentration increases after the wet combustion has stabilised and reaches a maximum value of 14.5 % 3.25 h after water injection (5.67 h after ignition). At the same time, the oxygen concentration fraction is 0.94% and the carbon monoxide concentration is 5.0%. Very small traces of methane and

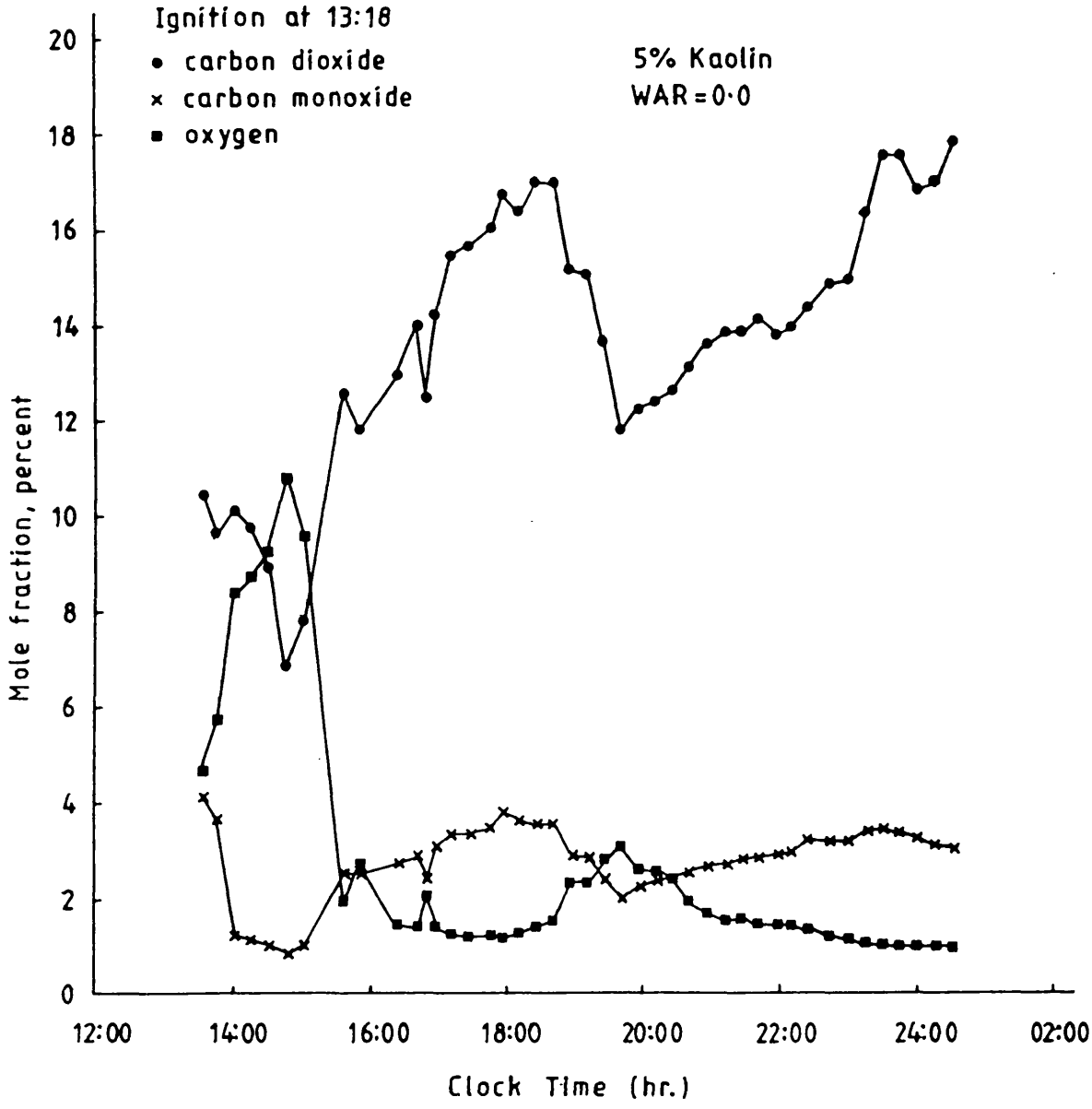

Figure 4.21 Exit gas composition *versus* time for Maya Isthmus crude (run No.1).

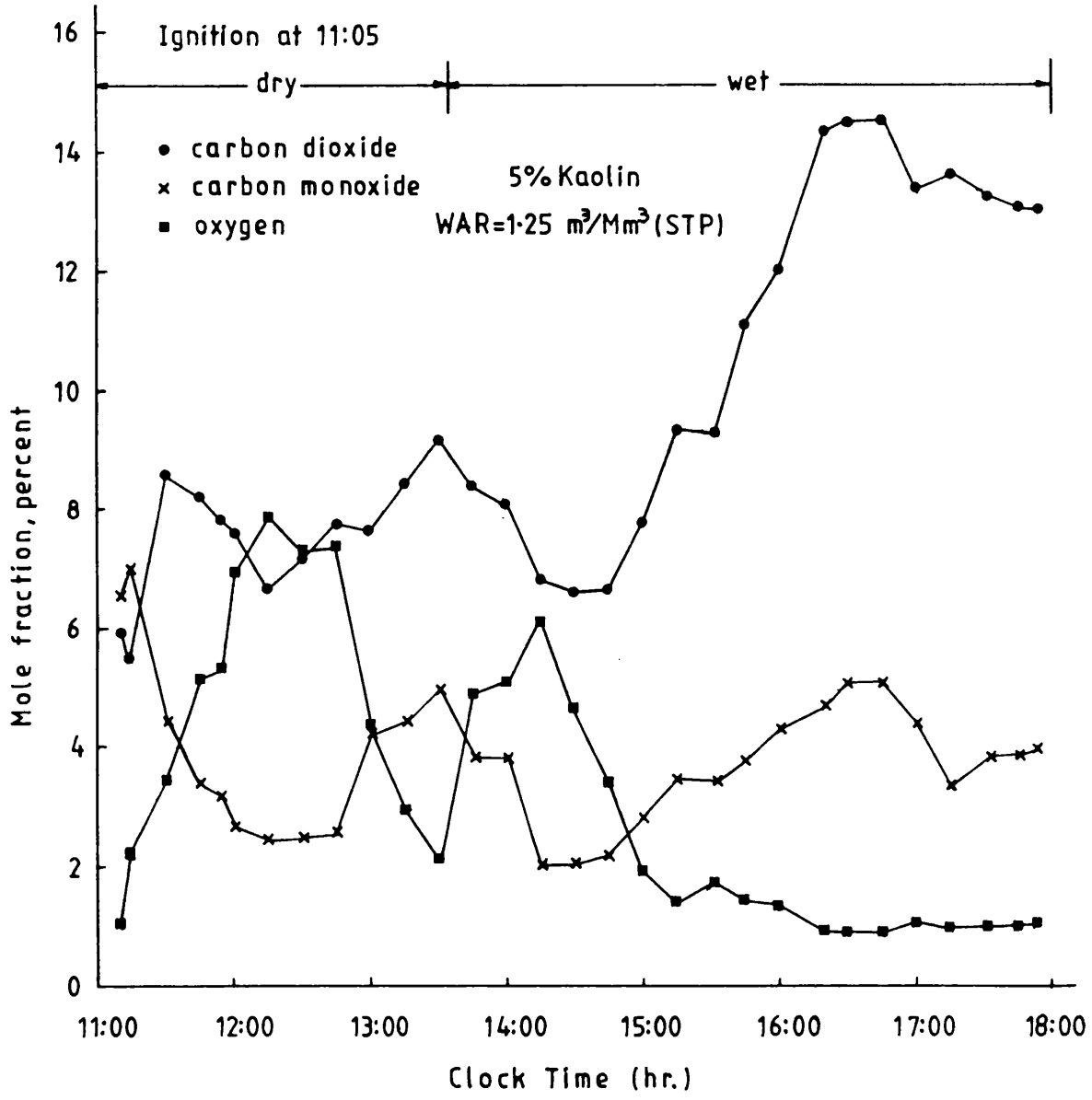

Figure 4.22 Exit gas composition *versus* time for Maya Isthmus crude (run No.2).

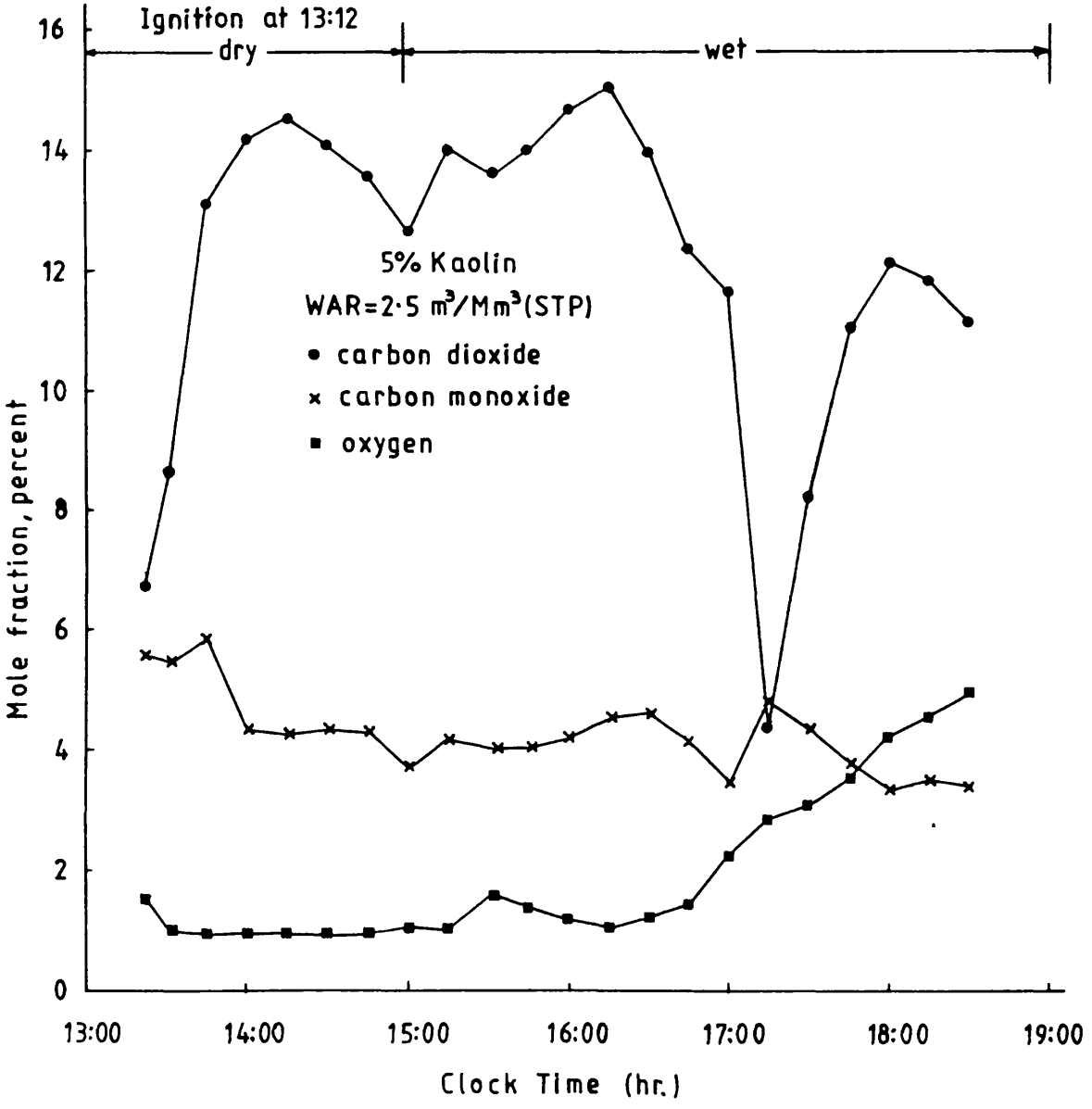

Figure 4.23 Exit gas composition *versus* time for Maya Isthmus crude (run No.3).

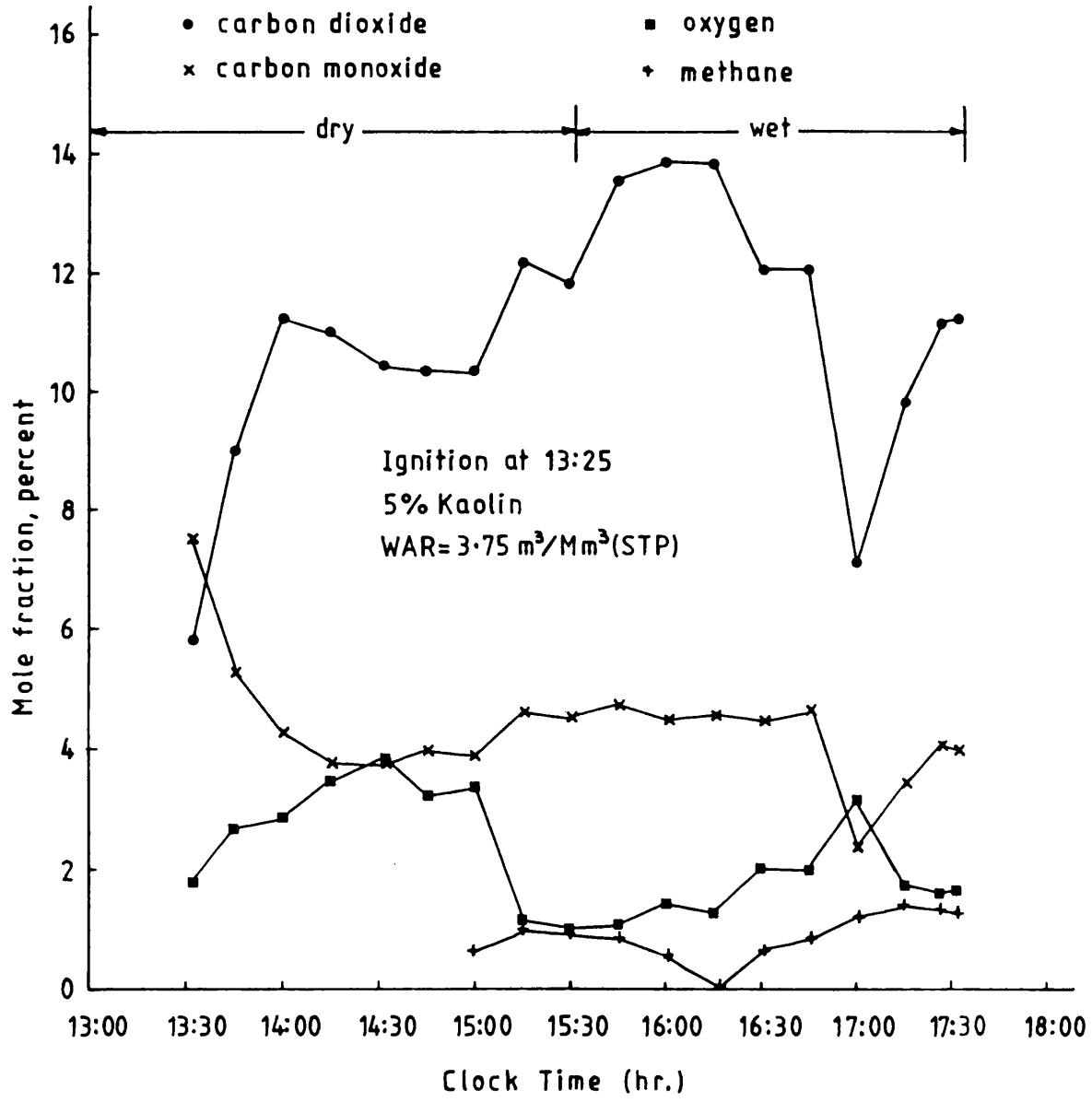

Figure 4.24 Exit gas composition *versus* time for Maya Isthmus crude (run No.4).

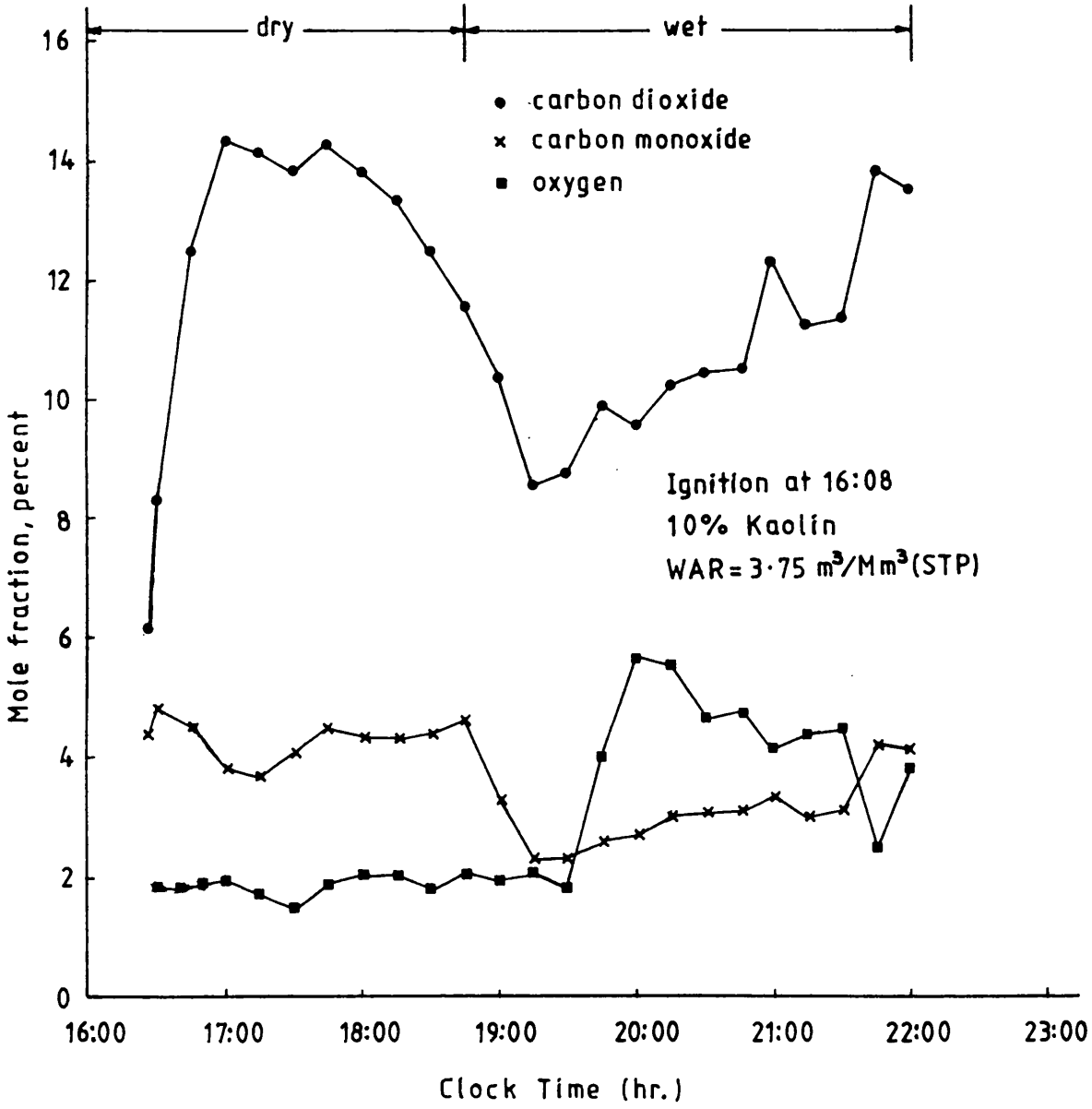

Figure 4.25 Exit gas composition *versus* time for Maya Isthmus crude (run No.5).

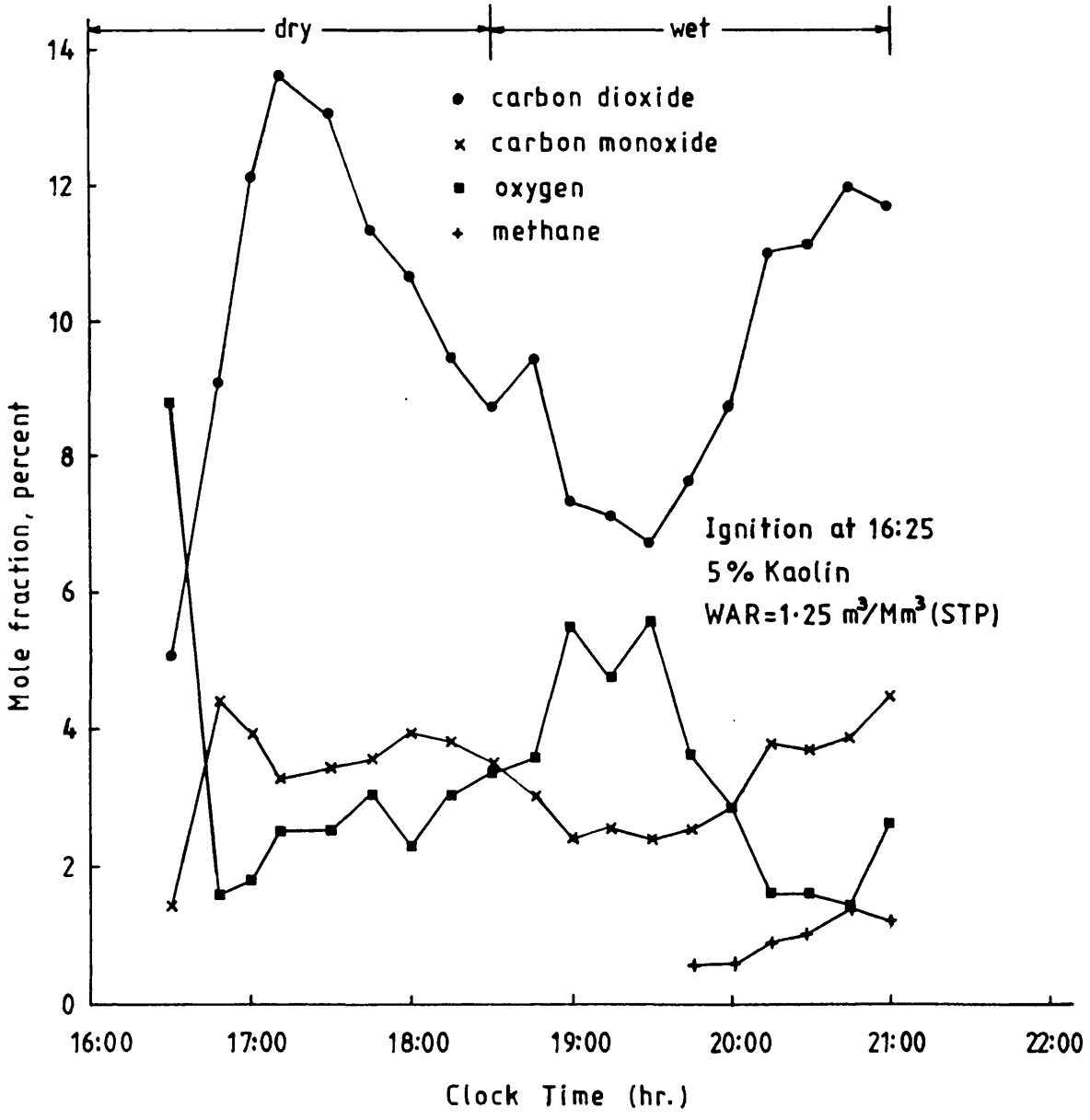

Figure 4.26 Exit gas composition *versus* time for Forties crude (run No.6).

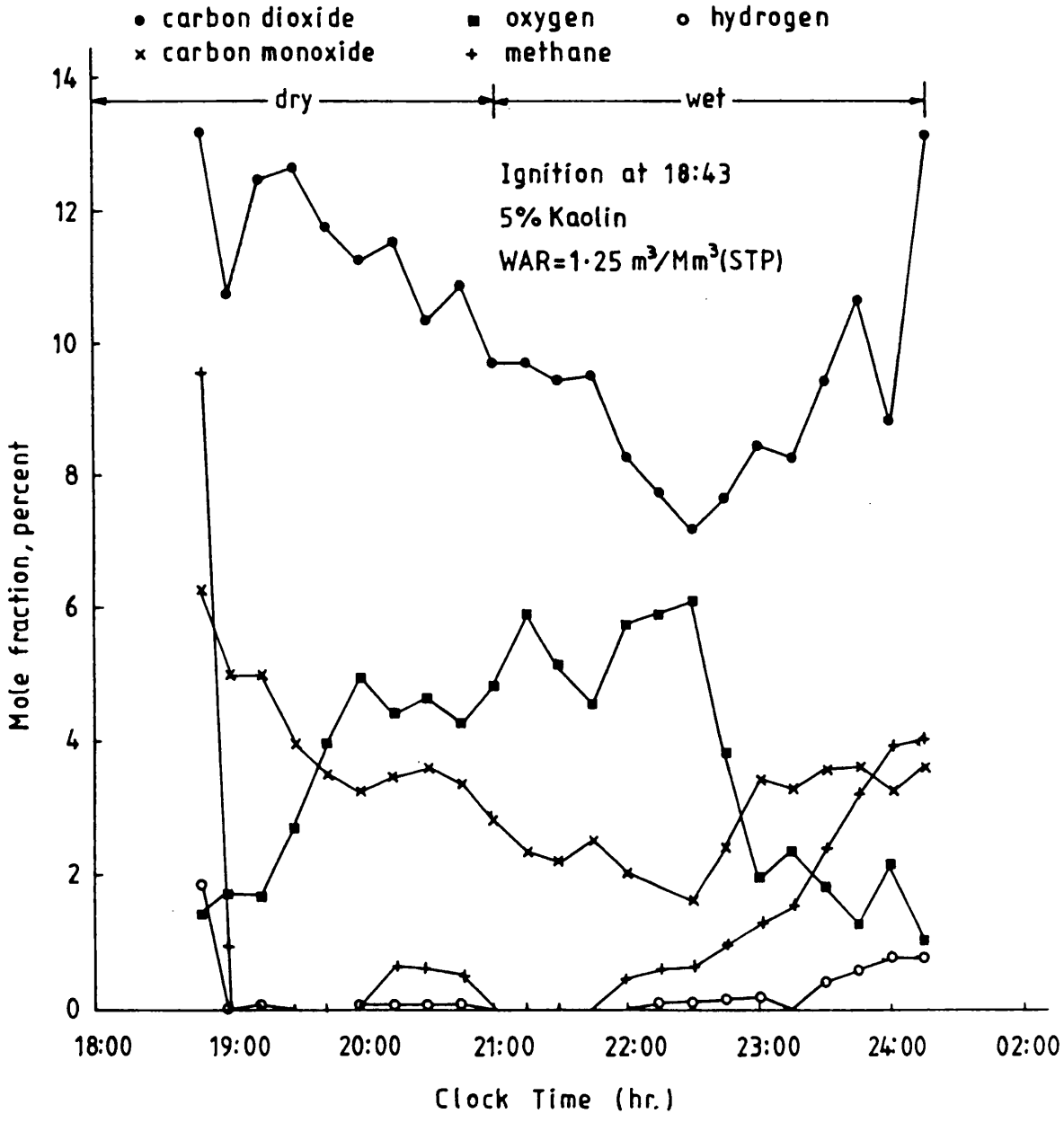

Figure 4.27 Exit gas composition *versus* time for Maya crude (run No.7).

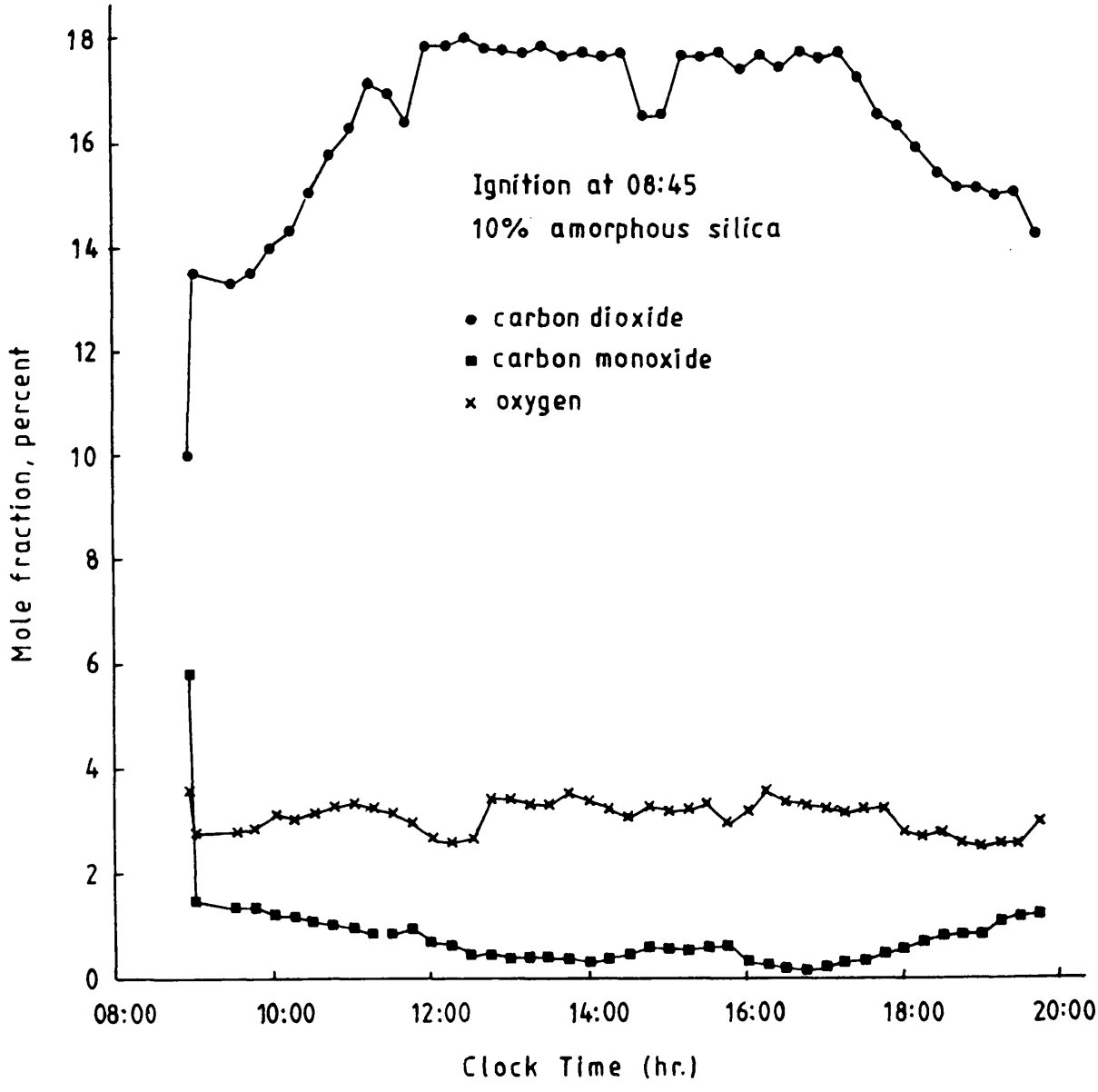

Figure 4.28 Exit gas composition *versus* time for Maya Isthmus crude (run No.8).

hydrogen were observed during the run (see Appendix D). Compared with run 1 (dry combustion), the level of carbon dioxide is much lower overall, whereas the carbon monoxide production level is higher.

In run 3 (Figure 4.23), normal wet combustion is taking place at a higher WAR of 2.5 m^3/Mm^3 (STP). Shortly after ignition, stable levels were reached and the composition of the product gases averaged 13±1.5% CO_2, 4±0.5% CO and 1.1% O_2. This indicates that most of the oxygen has been consumed by combustion. The carbon dioxide level decreased sharply after about 4 h from ignition to a very low value of 4.33%, while the CO mole fraction was 4.85%, thus giving a correspondingly high CO/CO_2 ratio of 1.12 (see Section 4.5). This indicates that a significant amount of oxygen was consumed by low temperature oxidation reactions as the oxygen entered the steam zone.

In run 4 (Figure 4.24), the CO_2 and CO concentration increased after the water was injected, reaching maximum values of 13.45% and 4.76% respectively and oxygen was consumed at the super heated steam temperature. The CO_2 concentration then fell sharply to a value of 7.0 % 3.59 h after ignition, whilst the CO mole fraction decreased to 2.4 %. There is therefore a short period during which LTO reactions took place, probably due to the cooling effect of the water passing through the combustion zone. Substantial amounts of methane, together with traces of hydrogen, were produced during the wet combustion period, producing 0.5-1% of methane, and 0.1-0.25% of hydrogen.

For the sand mixture containing 10% clay (run 5), the produced gas analysis during the first part of the dry burn period showed a low CO_2 concentration (Figure 4.25), due to LTO reactions. After 1.62 h from ignition, carbon oxides increased to 14.2 % and 4.2 % for CO_2 and CO res-

pectively, while O_2 was only 1.8 %. A greater oxygen concentration was produced after water injection, but the CO_2 concentration decreased to less than 10% and the CO decreased to less than 3%. The wet combustion became more stable after about 4 h from ignition, so that the product gas composition then corresponded closely to that of normal wet combustion.

Figure 4.26 shows the exit gas composition for the light Forties oil. Here, the normal wet product gases exhibit a similar condition to that of the combustion gases for the Maya Isthmus (run 2), where LTO reactions were initially present. However, the gas analysis corresponded to that of a typical dry combustion, immediately after ignition. In other words, CO_2 and CO now increase as the combustion becomes more stabilised. Thus, after a period of about 1.5 h from ignition, the carbon dioxide starts to decline, reaching a value of 8.7 % just before the water injection is commenced. The cooling effect of the injected water also increases the concentration of oxygen to about 5.6% and decreases the CO_2 and CO concentrations to 6.7% and 2.4 % respectively after about 2 h from the commencement of water injection. Methane ranging from 1±0.5% is produced and traces of hydrogen are also observed at the end of the run.

The product gas analysis for run 7 is shown in Figure 4.27. Significant amounts of methane and detectable amounts of hydrogen were produced throughout this run, with a similar trend for both gases. Thermal cracking seems to be the only reason for this. The carbon dioxide and carbon monoxide mole fractions averaged at 11.7 and 3.7% respectively for the dry period, while the oxygen mole fraction averaged at 3.3%. In the wet combustion period, CO_2 and CO mole fractions decreased to a lower value and averaged at 8.9 and 2.8% respectively. The oxygen which was produced was slightly higher than that of the dry period and was approximately 3.7%.

Figure 4.28 presents the gas profile for the dry combustion run (run 8), in which 10% amorphous silica was added to the sand mixture. The variations exhibited by the gas profiles in this case were less frequent and were smaller. The analysis of CO_2, CO and O_2 showed that the mole fractions averaged 16.30. 3.1 and 0.85% respectively. Thus the level of carbon dioxide was higher and the oxygen levels were much lower, compared with the other runs.

4.4 Oxygen utilisation and peak temperature

Oxygen utilisation is a measure of the combustion efficiency. The instantaneous and overall values were calculated from the exit gas analysis (computer program, Appendix B). Figures 4.29-4.36 show the percentage of oxygen utilisation and the combustion front temperature, as a function of the operating time for the combustion runs 1-8. The lowest oxygen utilisation values occurred in the period just after ignition. Thereafter, the oxygen utilisation reached significantly higher values, as the combustion front became established. The results show that the oxygen utilisation profiles tend to follow the same overall behaviour as the peak temperature. However, when there is a large drop in front temperature, this does not cause a similar sharp decrease in the oxygen utilisation.

For the wet combustion runs, the injected water produces a cooling effect in the combustion zone. Combined with the lower residence time for the oxygen in the combustion zone, this causes a lowering of the peak temperature, resulting in greater oxygen breakthrough. Thus, increased oxygen flow downstream of the combustion front leads to further LTO reactions taking place.

Table 4.3 summarises the overall oxygen utilisation and average peak temperature conditions for each of the eight combustion runs. According to this table, the oxygen utilisation is almost the same as for the

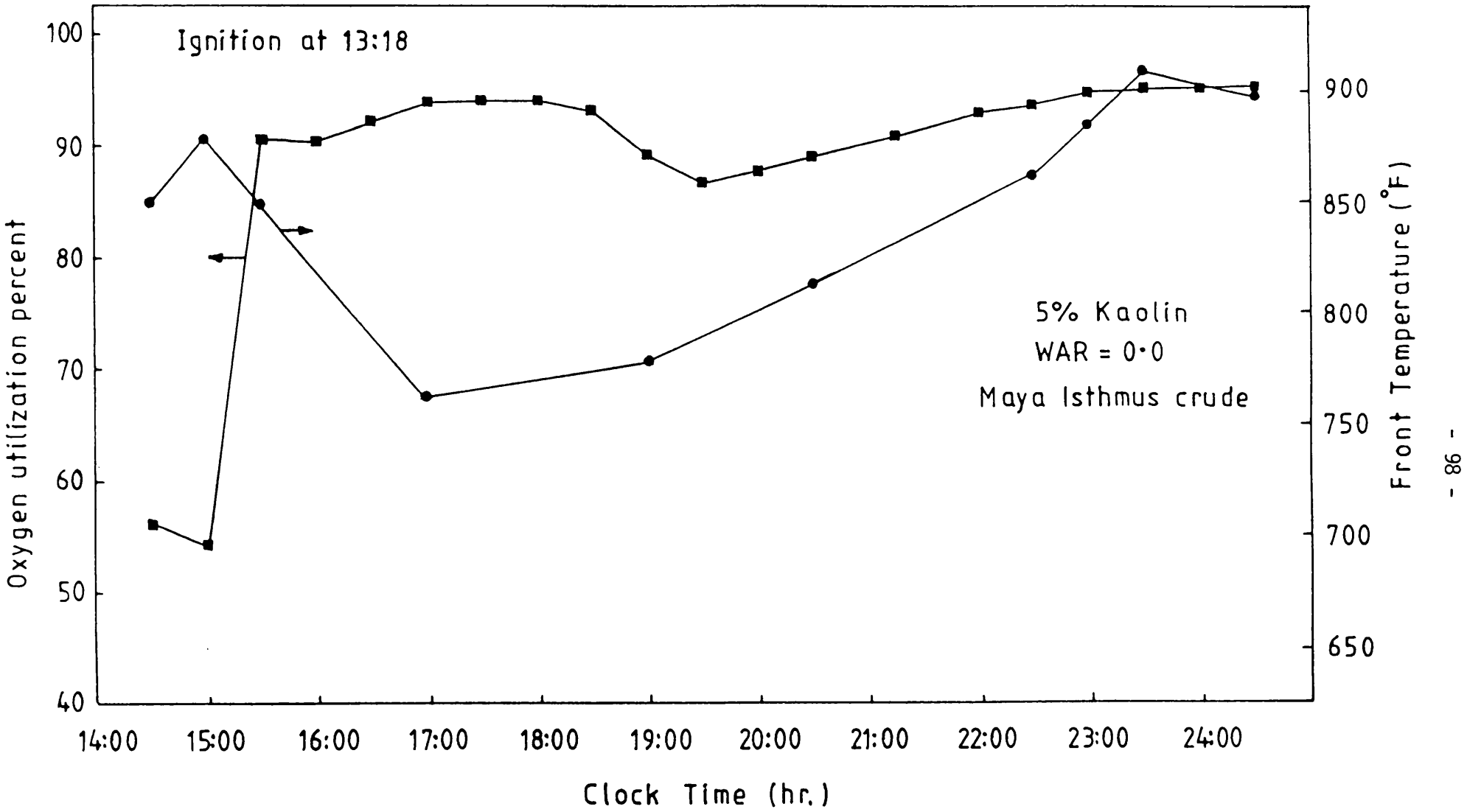

Figure 4.29 Percentage of oxygen utilisation and combustion front temperature (run No.1).

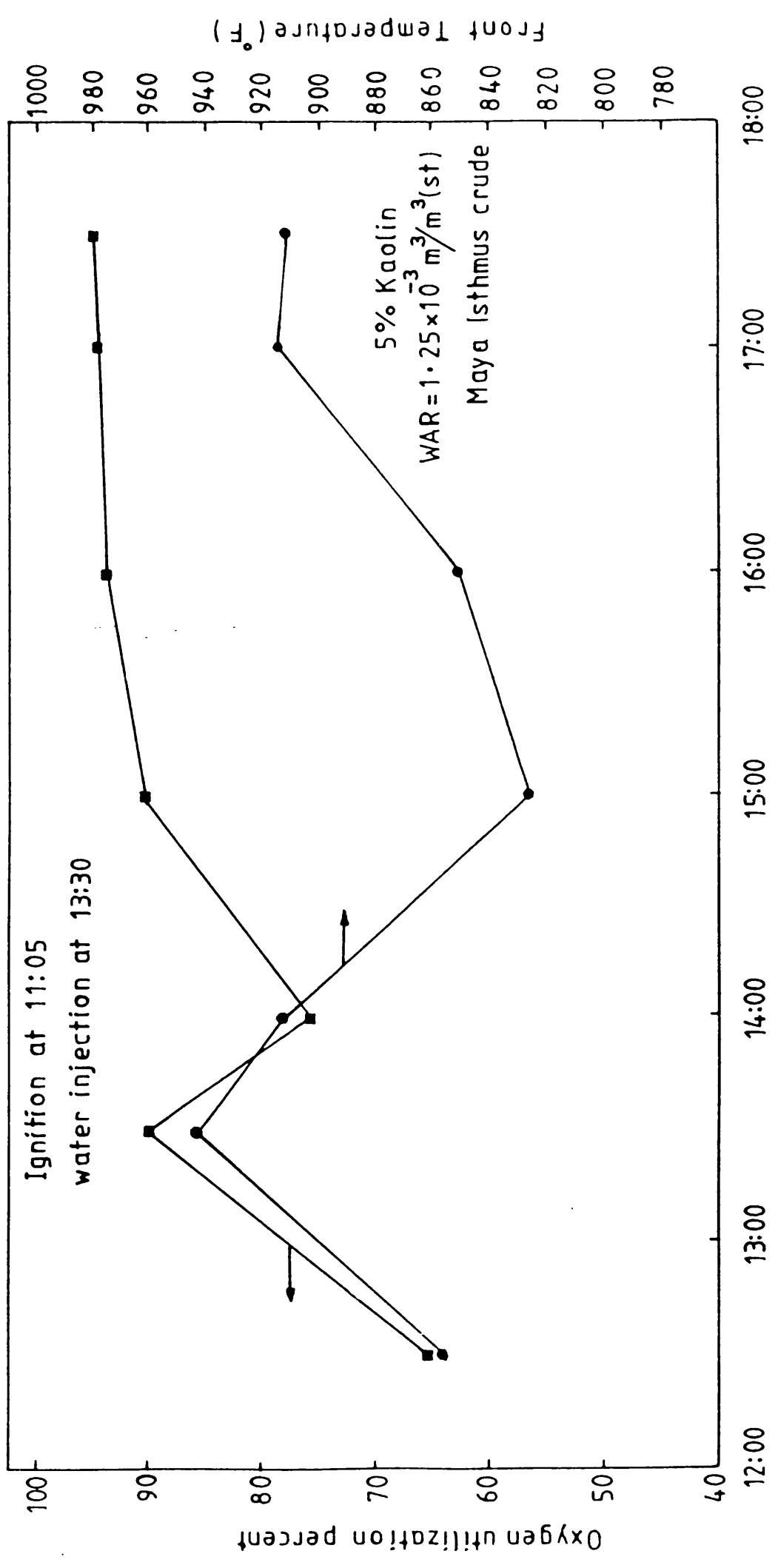

Figure 4.30 Percentage of oxygen utilisation and combustion front temperature (run No.2).

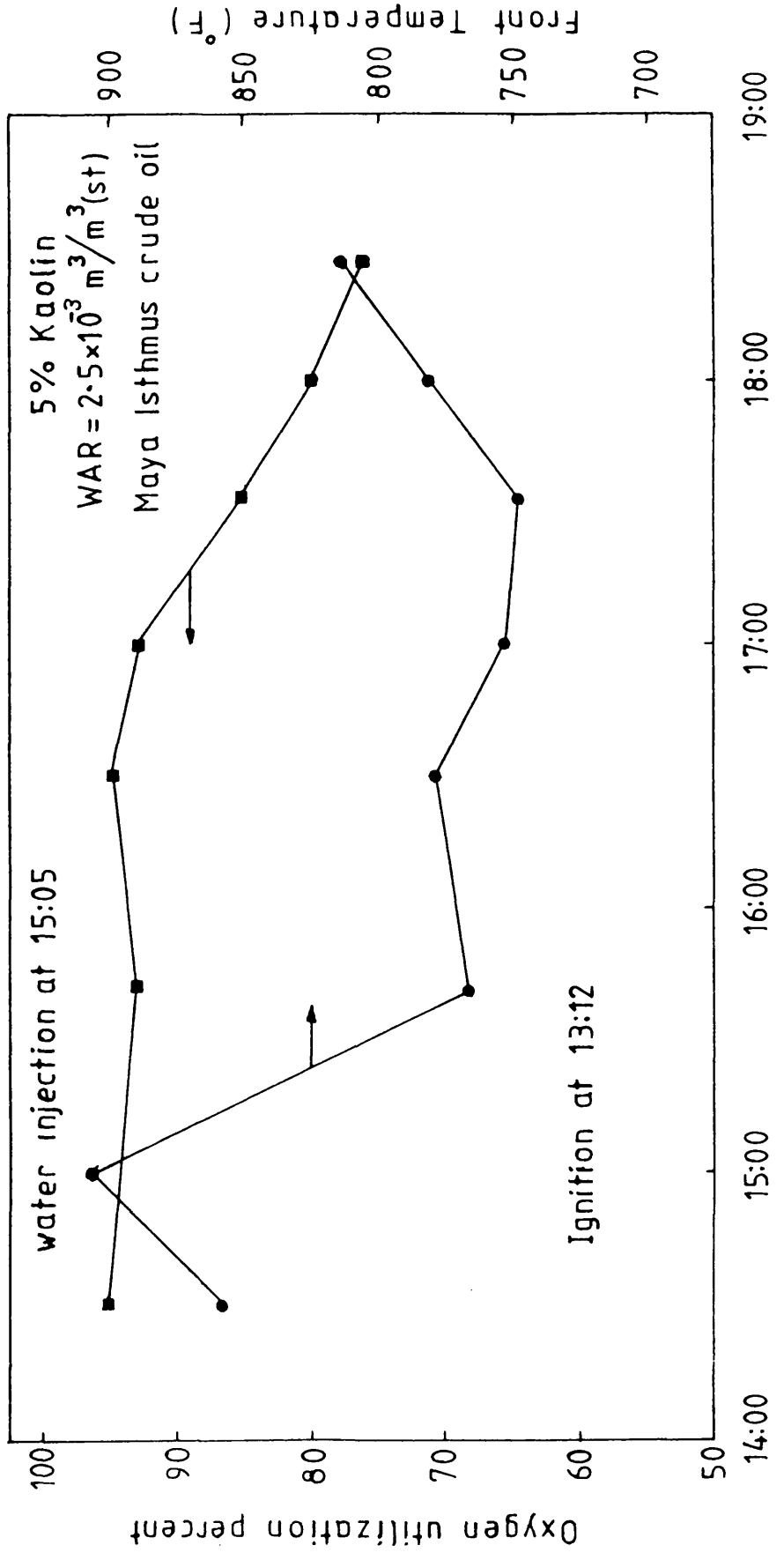

Figure 4.31 Percentage of oxygen utilisation and conbustion front temperature (run No.3).

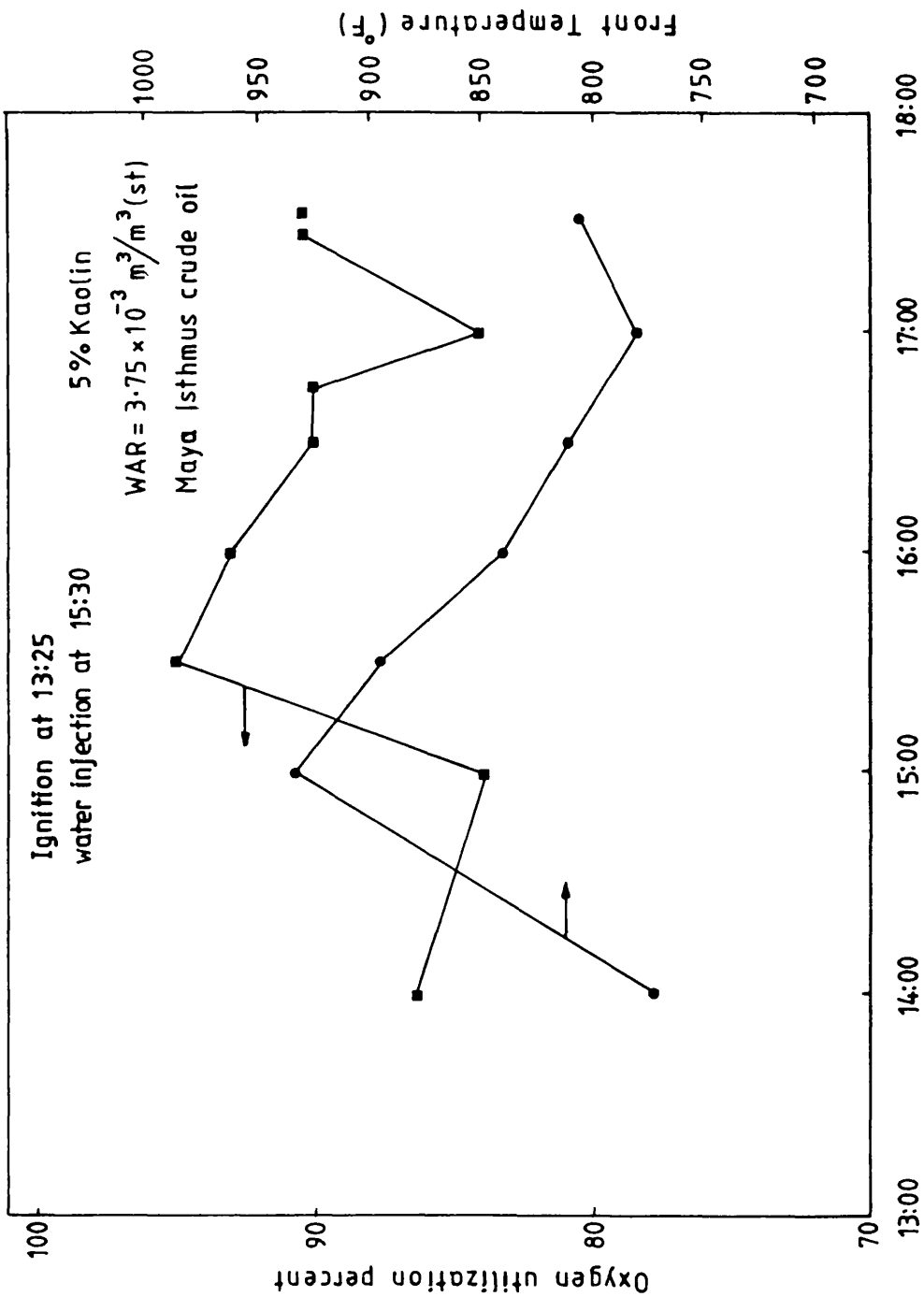

Figure 4.32 Percentage of oxygen utilisation and combustion front temperature (run No.4).

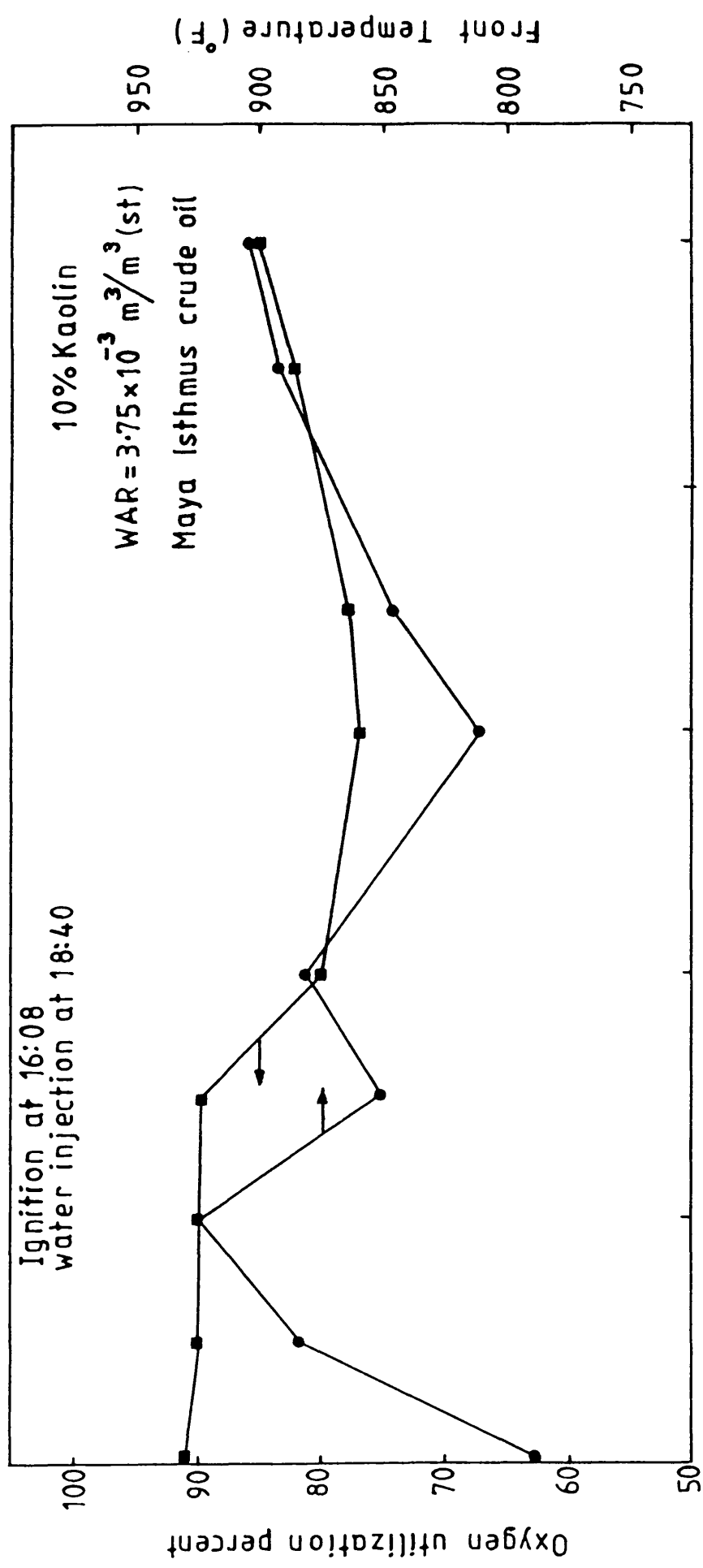

Figure 4.33 Percentage of oxygen utilisation and combustion front temperature (run No.5).

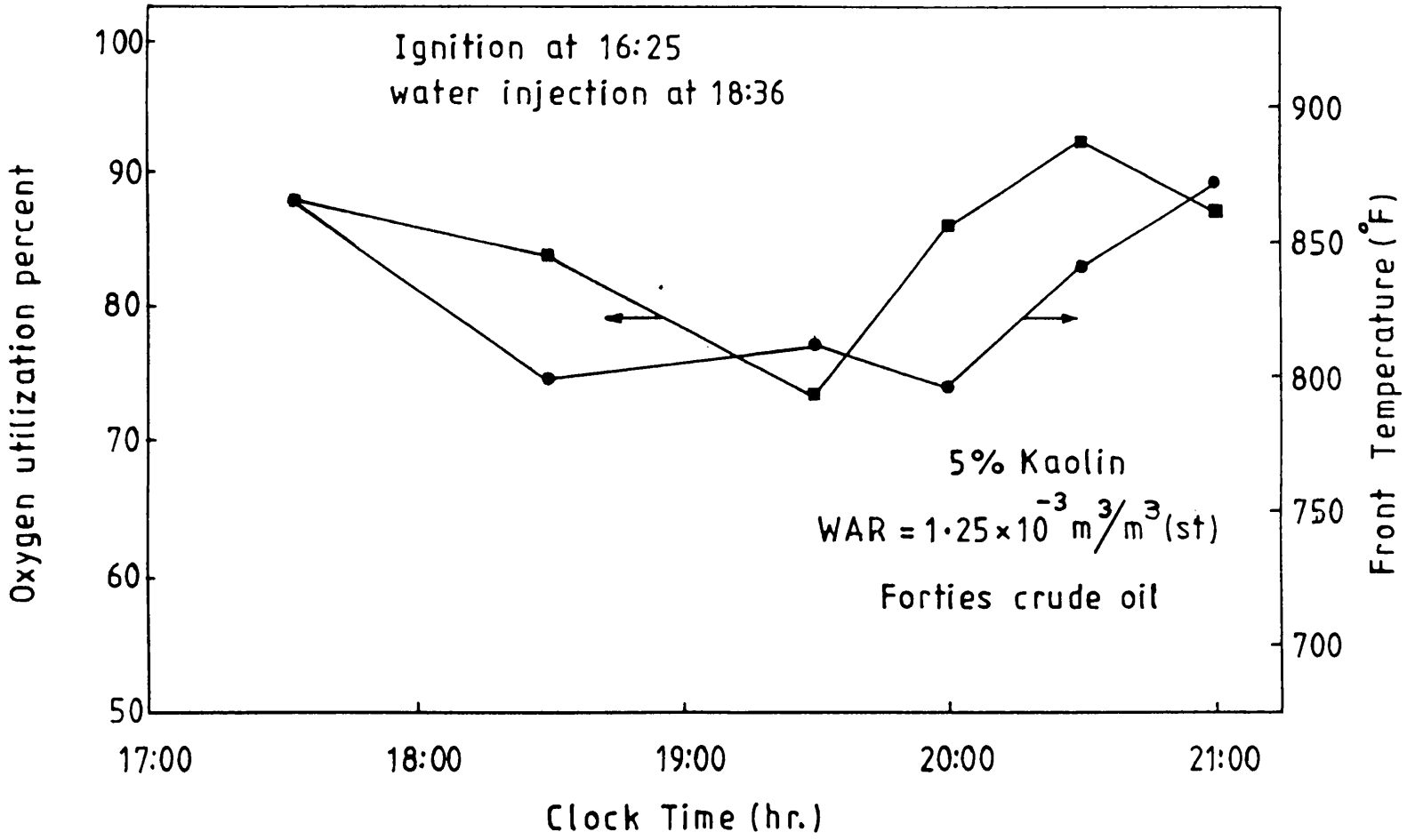

Figure 4.34 Percentage of oxygen utilisation and combustion front temperature (run No.6).

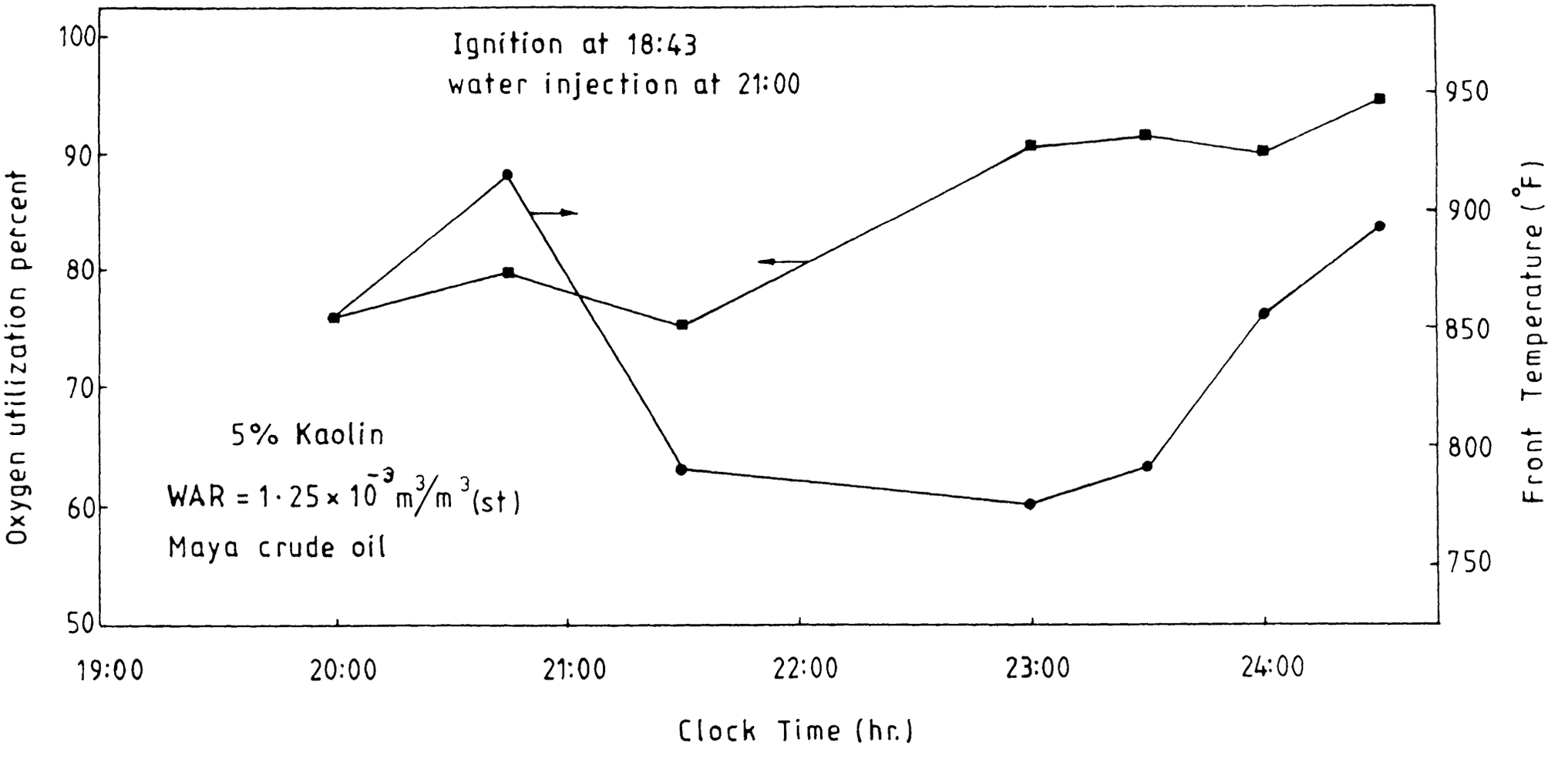

Figure 4.35 Percentage of oxygen utilisation and combustion front temperature (run No.7).

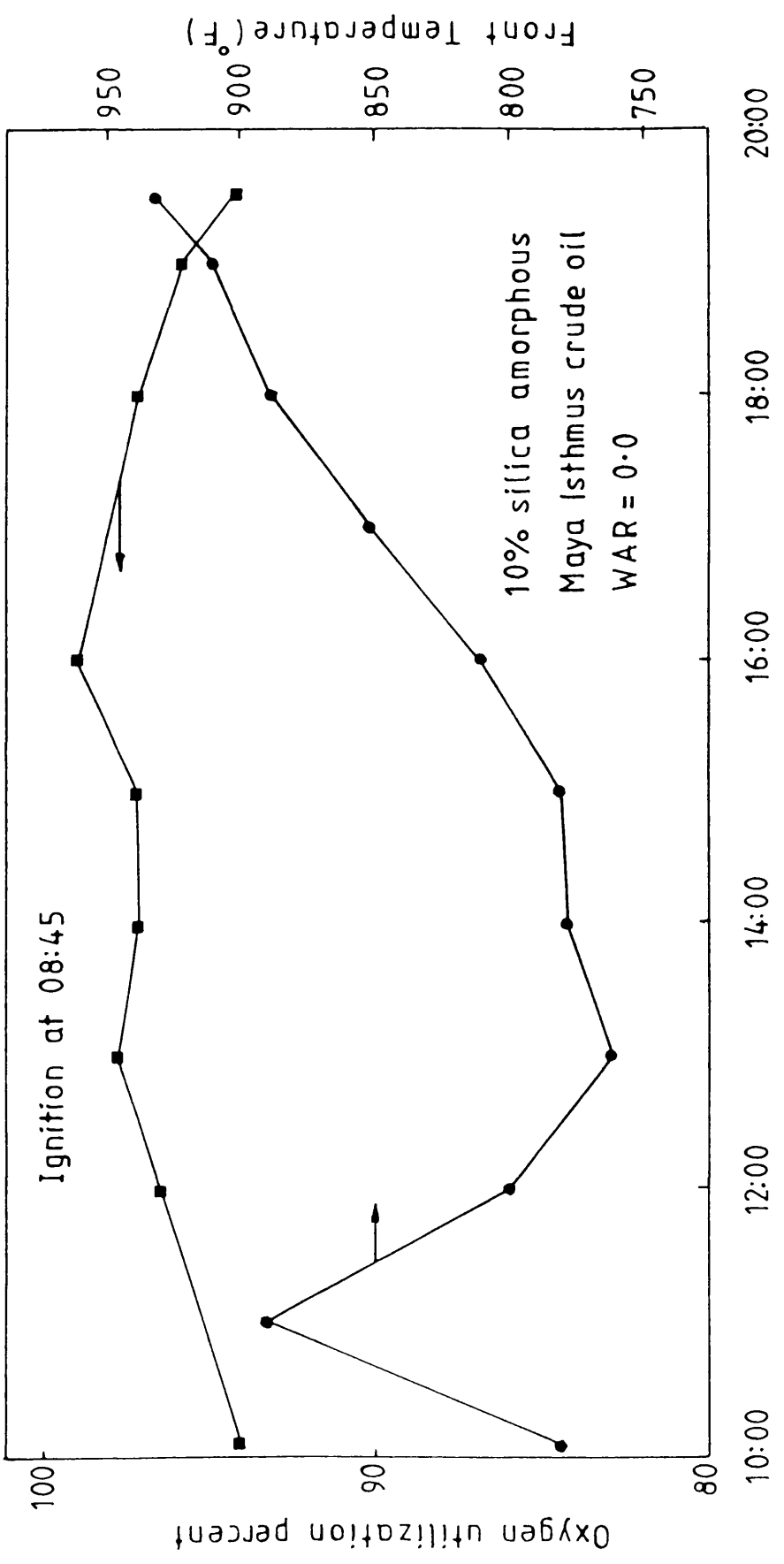

Figure 4.36 Percentage of oxygen utilisation and combustion front temperature (run No.8).

Table 4.3

Overall oxygen utilisation and average peak temperature

Run No.	Sand mixture characteristics	Crude oil	Combustion mode	Oxygen utilisation (%)	Average peak temperature (° F)
1	5% kaolin	Maya Isthmus	dry	85.8	844
2	5% kaolin	Maya Isthmus	normal wet	85.6	885
3	5% kaolin	Maya Isthmus	normal wet	91.1	797
4	5% kaolin	Maya Isthmus	partially quenched	89.7	844
5	10% kaolin	Maya Isthmus	partially quenched	85.9	875
6	5% kaolin	Forties	normal wet	86.3	829
7	5% kaolin	Maya	normal wet	83.5	846
8	10% amporphous silica	Maya Isthmus	dry	95.8	865

normal wet combustion of the two light oils (Forties and Maya Isthmus), but is approximately 2% lower for the heavier Maya oil. The wet combustion runs 3 and 4 with WAR 2.5 and 3.75 m^3/Mm^3 (STP) respectively, which have lower average peak temperatures, exhibit improved oxygen utilisation. Therefore, in spite of the increased water flux effect on the combustion temperature, a considerable amount of oxygen was consumed at the steam zone temperature.

The highest oxygen utilisation obtained occurred in run 8, in which 10% amorphous silica was incorporated into the sand matrix. This is in agreement with values obtained by Guvenir (1980), using similar material (see Table 4.4). By comparison with the data presented in this table, it would appear that wet combustion exhibited improved oxygen utilisation for air flux less than 20 $m^3(st)/m^2$ h for all pressures. Therefore, the air flux must be low enough so that the residence time of the oxygen is long enough for all the oxygen to be consumed within the combustion zone (McKay, 1982). Burger and Sahuquet (1976) have suggested that a high temperature zone of 100 cm (3.3 ft) in length is sufficient to ensure complete oxygen consumption. In another study of wet combustion, Dietz and Weijdema (1968) stated that for steam zone temperatures greater than 200° C (400° F), the oxygen was consumed in less than 100 cm.

4.5 Apparent H/C ratio and CO/CO_2 volume ratio

The apparent H/C ratio and CO/CO_2 ratio were calculated from the analysis of the produced gases, on an instantaneous and overall values basis (computer program, Appendix B). The H/C ratio was calculated on the assumption that all of the oxygen which did not appear in the exit gases had reacted to form water. This may not be strictly true, however, because of the possibility of LTO reactions occurring. Any LTO reaction

Table 4.4

Comparisons of oxygen utilisation efficiency

Author	Porous medium	Pressure (psig)	Comb. tube length (cm)	Air flux [m^3(st)/m^2 h]	WAR [m^3/Mm^3 (STP)]	Oxygen utilisation (%)
Sterner and Wertman (1976)	Crushed Berea sand	100	93.98	17.68-45.4	0.0	49-90.95
Satman (1979)	Ottowa sand + 1-8.9% fire clay	100	99.54	28.32-39.6	0.0	79-94.76
Guvenir (1980)	sand + various amounts of kaolin	200	101.6	13.83	0.0	85.0
	+ amorphous silica	200		13.83	0.0	97.0
Ejiogu *et al.* (1979)	Cardium sandstone, Alberta	864	185.4	31.36-37.75	0-2.67	76.42-99.1
Harding *et al.* (1976)	Athabasca sand	834-843	182.88	16.34-19.2	1.87-2.25	97-99
Burger and Sahuquet (1973)	(silica sand)	160	210.8	9.0	0.0	86-100
	(silica sand)	160		18	0.0	81
	(reservoir rock)	530		9	1-3	98-100

effect would be evidenced by a low level of CO_2 and CO in the exit gases. In other words, more oxygen will have reacted with hydrocarbons than can be found in the exit gases.

The plots of H/C and CO/CO_2 ratios for the fuel burned are shown in Figures 4.37-4.44. In run 1, the instantaneous value of H/C just after ignition was very high at 26.06 (Appendix D). The corresponding CO/CO_2 ratio was equal to zero, since the CO concentration was equal to zero. However, these values have not been included in the calculation of the average H/C and molar CO/CO_2 ratios. For the period 15:35-24:00 in Figure 4.37, the CO/CO_2 ratio averages 0.2±0.01. This means that both CO and CO_2 are being produced by the same principle reaction. The lowest H/C and CO/CO_2 ratios are observed towards the end of the run and are the result of the extended high temperature zone due to preheating. The overall H/C ratio for run 1 is 0.88, with the CO/CO_2 ratio averaging only 0.195 (see Table 4.5).

For normal wet combustion (run 2), the average H/C ratio is 2.15. In this case, the CO/CO_2 ratio is higher than that achieved during the dry combustion run (run 1). Although the average peak temperature is the highest for this run at 885.0° F (475° C), the H/C ratio also has a high value. Careful examination of the results reveals that there is strong evidence of some LTO reactions taking place during the period 14:15-15:30. Figure 4.38 shows that the highest H/C ratio is 5.49, which occurs at 14:45. At the same time, the peak temperature reaches its lowest value of the run, at 825.0° F (440° C). The combination of higher nitrogen production (≈86%) and lower CO production (< 10%) during the period 14:15-15:30 is further evidence of LTO reaction.

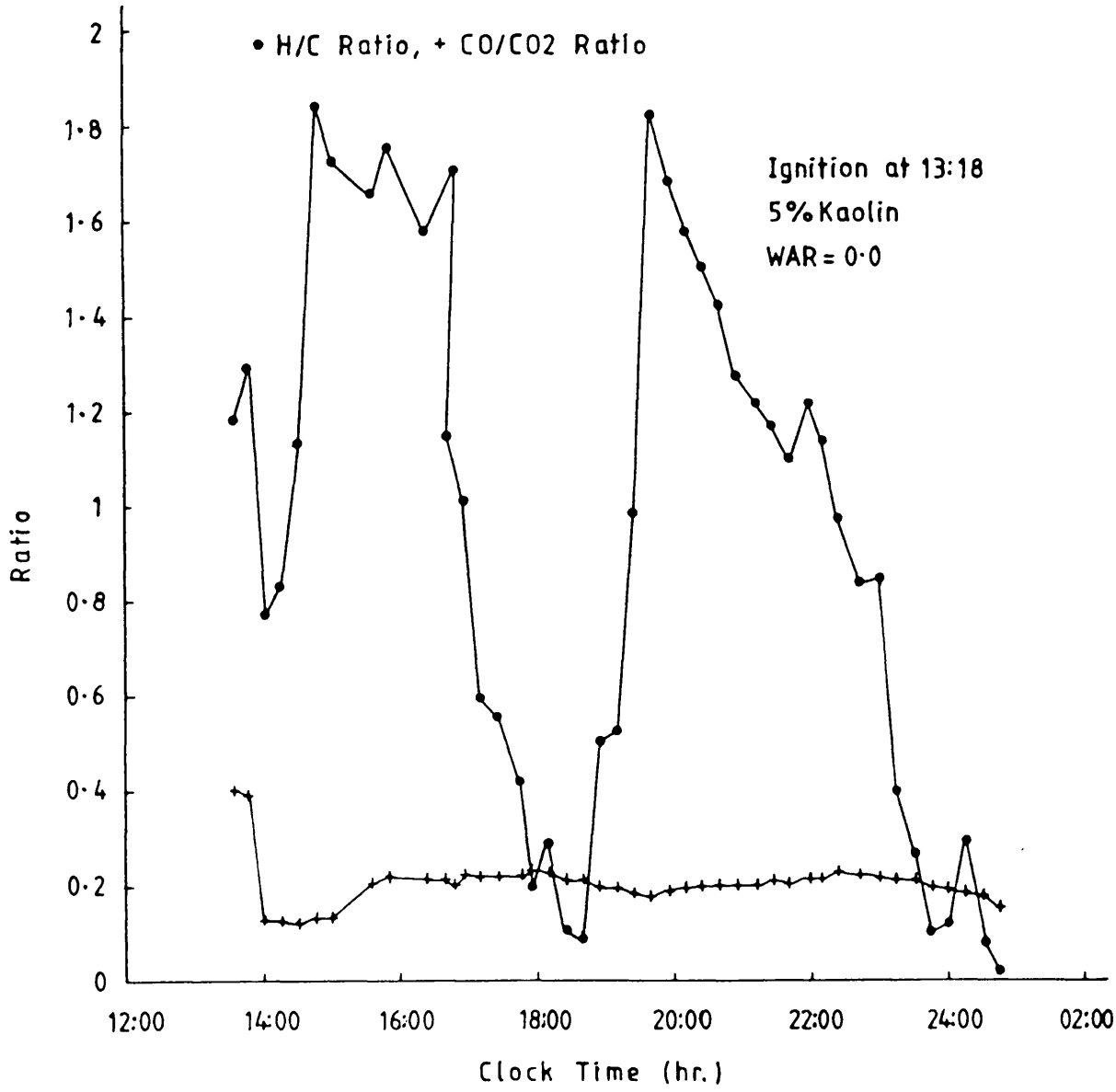

Figure 4.37 Hydrogen-carbon ratio and carbon monoxide-carbon dioxide ratio of the fuel burned for the Maya Isthmus crude (run No.1).

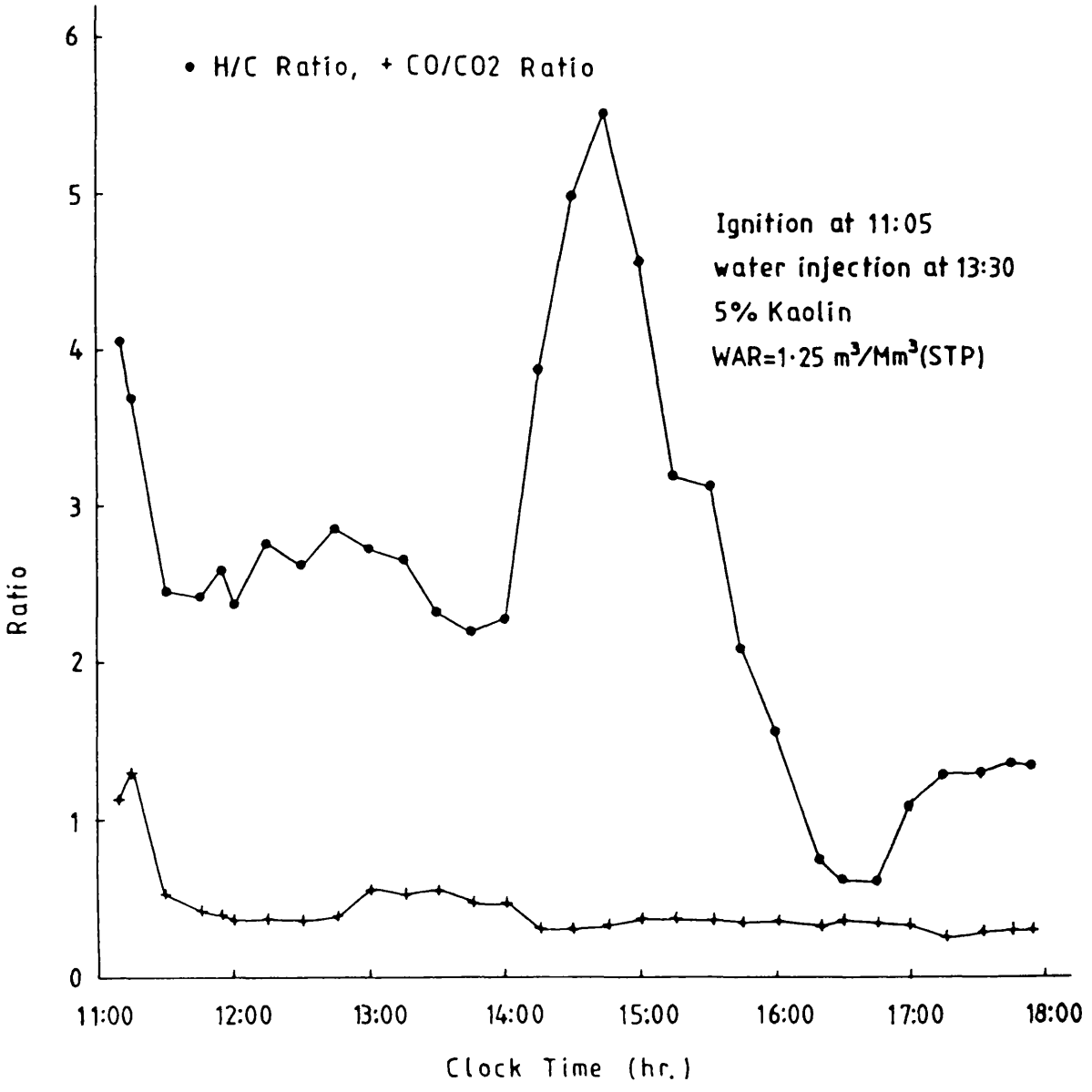

Figure 4.38 Hydrogen-carbon ratio and carbon monoxide-carbon dioxide ratio of the fuel burned for the Maya Isthmus crude (run No.2).

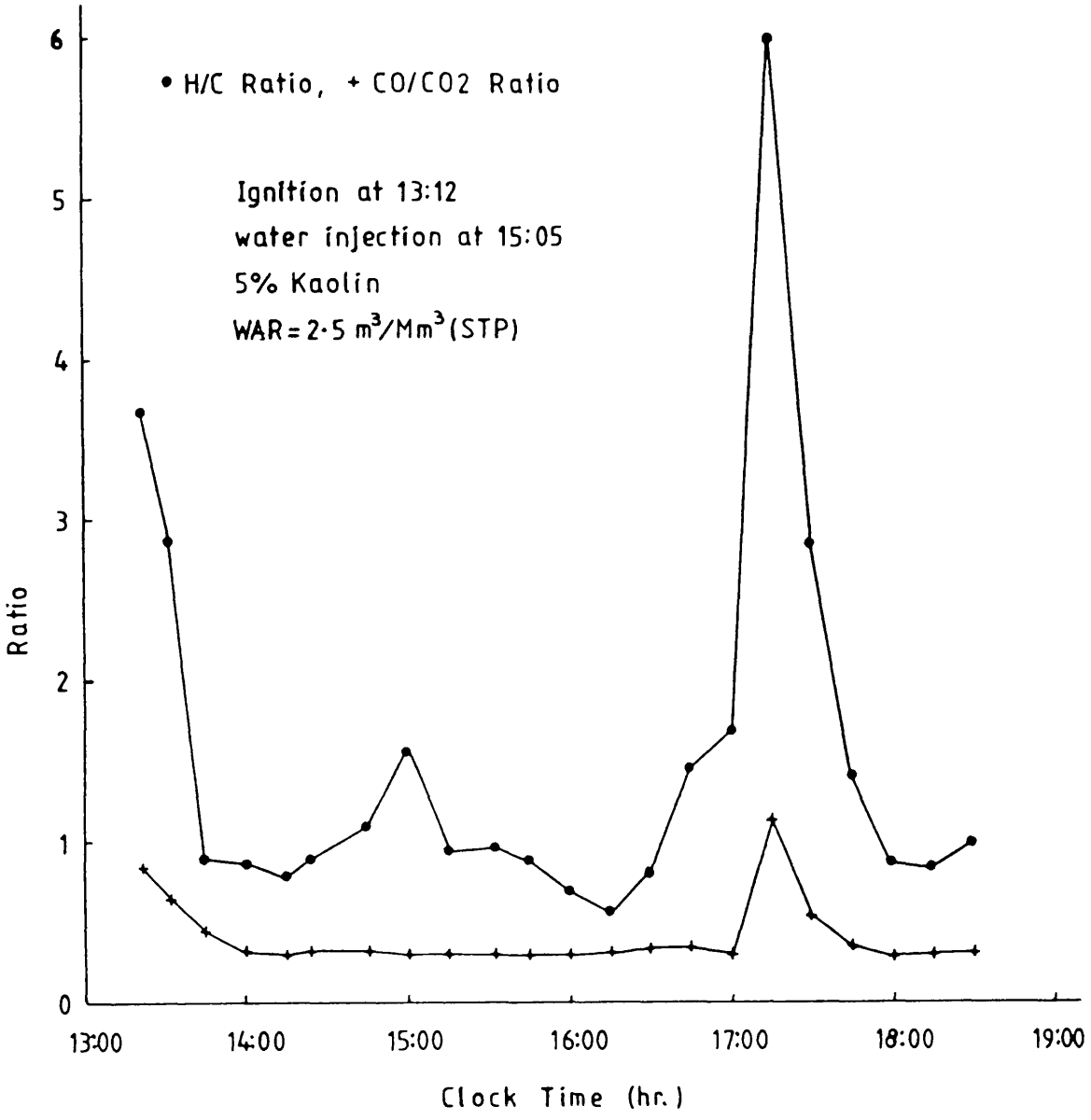

Figure 4.39 Hydrogen-carbon ratio and carbon monoxide-carbon dioxide ratio of the fuel burned for the Maya Isthmus crude (run No.3).

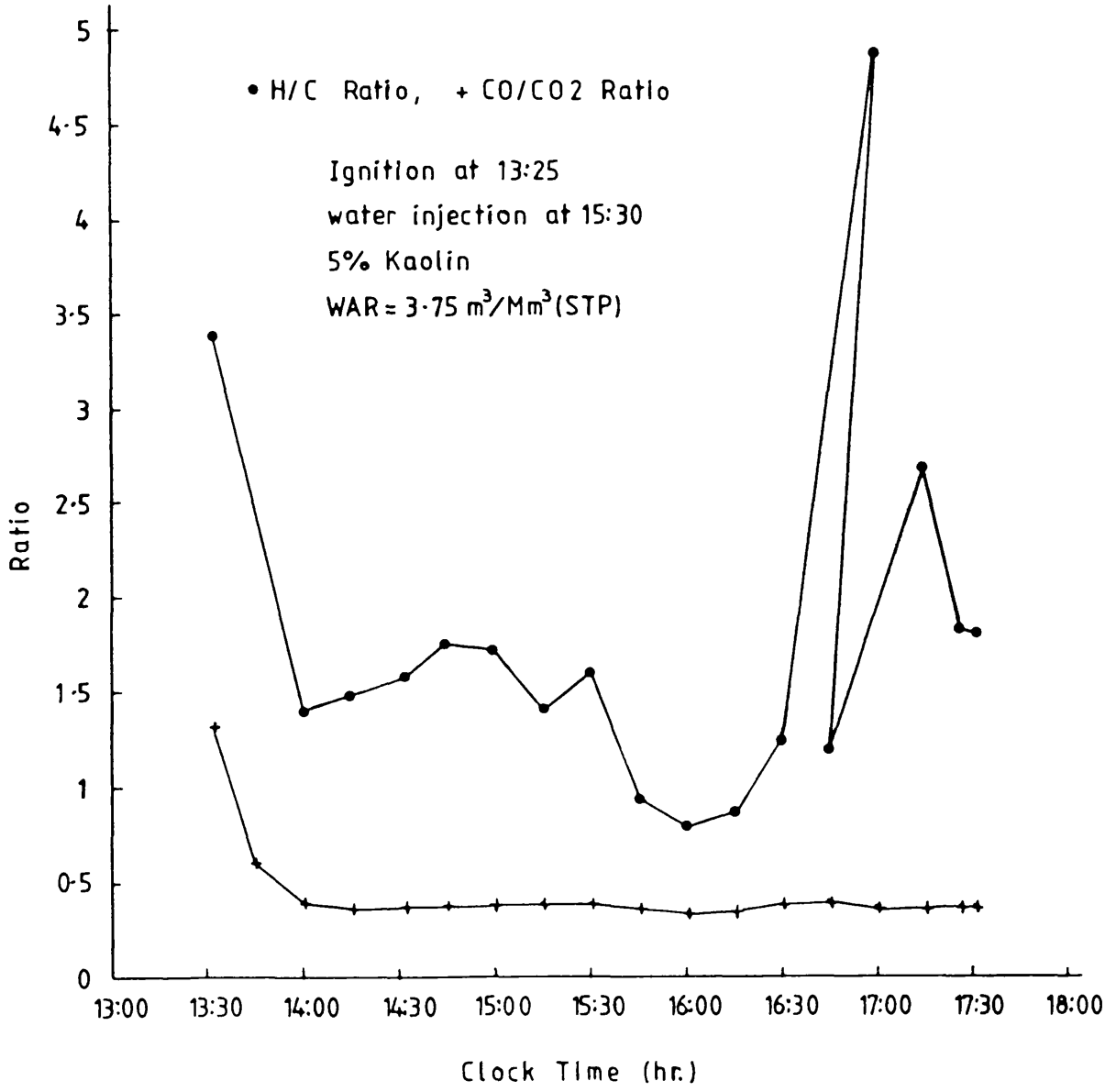

Figure 4.40 Hydrogen-carbon ratio and carbon monoxide-carbon dioxide ratio of the fuel burned for the Maya Isthmus crude (run No.4).

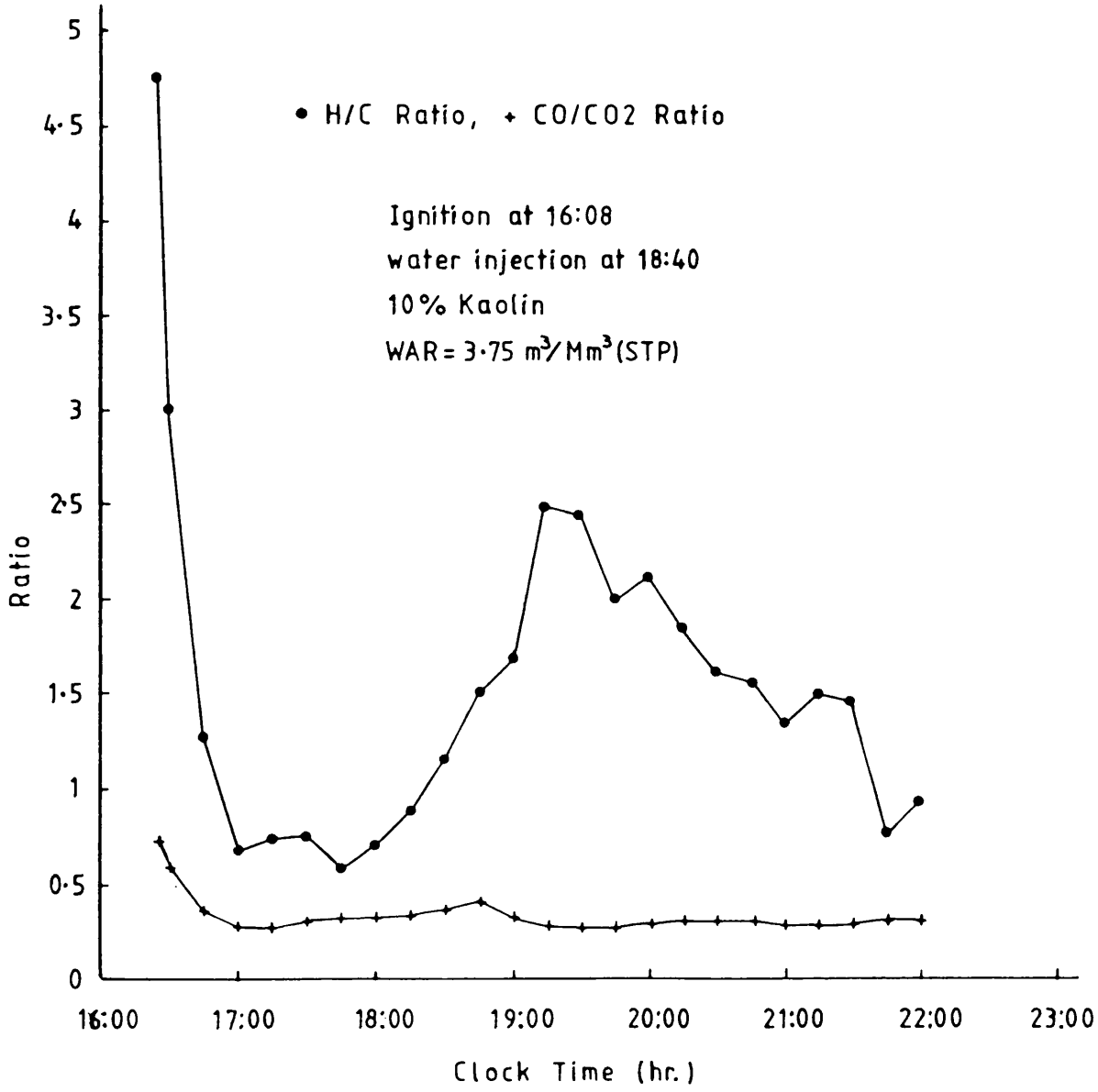

Figure 4.41 Hydrogen-carbon ratio and carbon monoxide-carbon dioxide ratio of the fuel burned for the Maya Isthmus crude (run No.5).

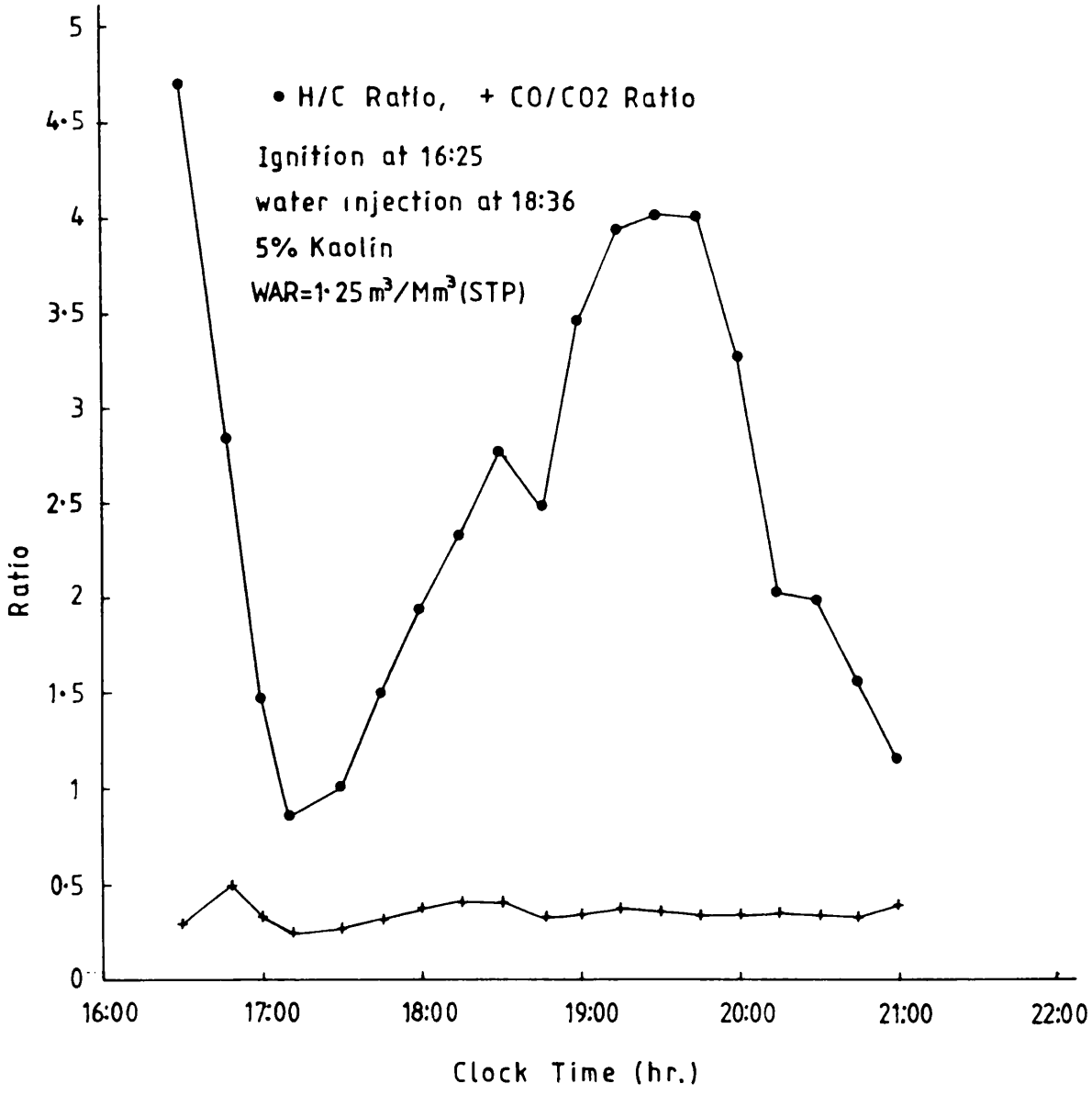

Figure 4.42 Hydrogen-carbon ratio and carbon monoxide-carbon dioxide ratio of the fuel burned for the Forties crude (run No.6).

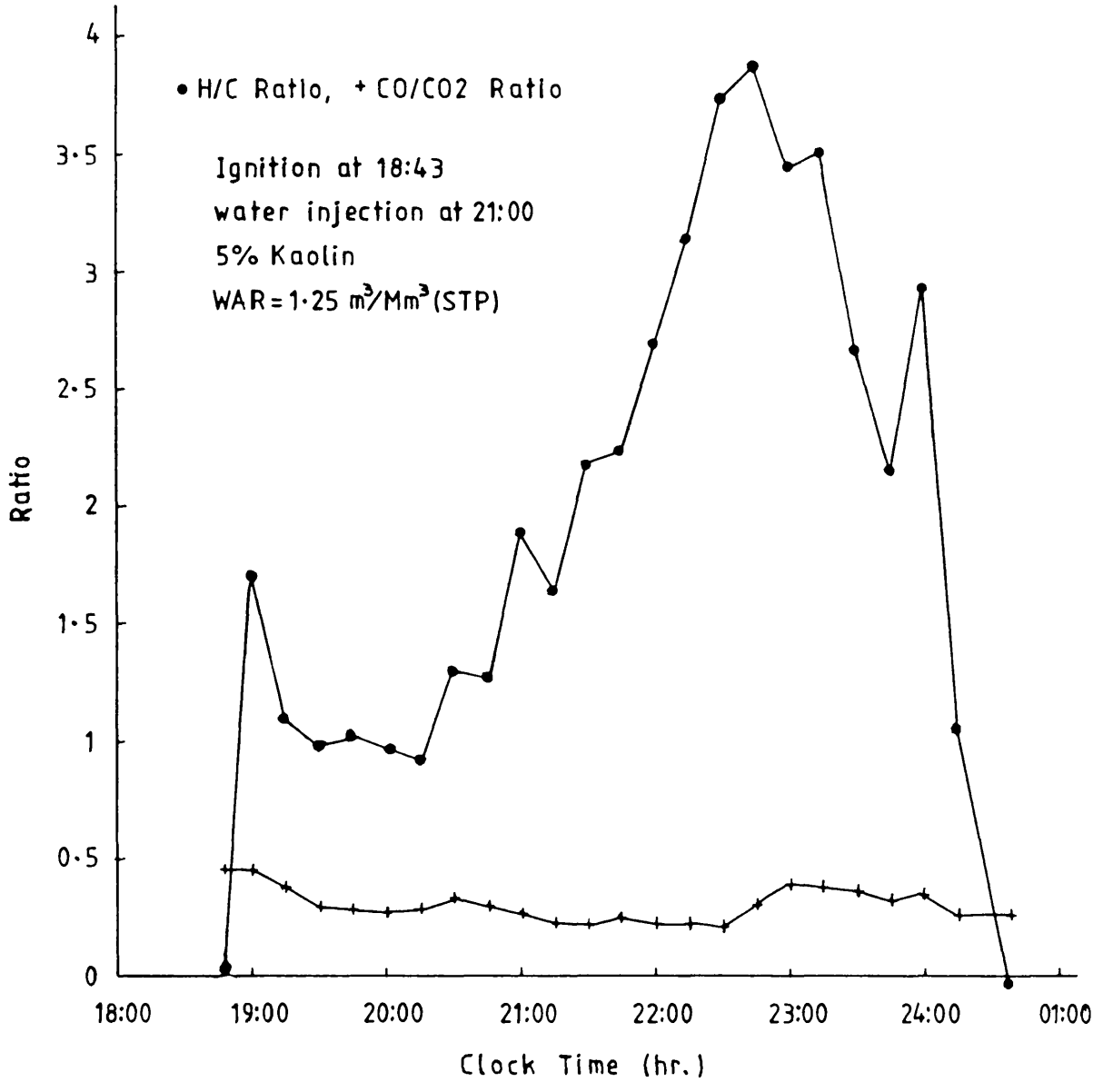

Figure 4.43 Hydrogen-carbon ratio and carbon monoxide-carbon dioxide ratio of the fuel burned for the Maya crude (run No.7).

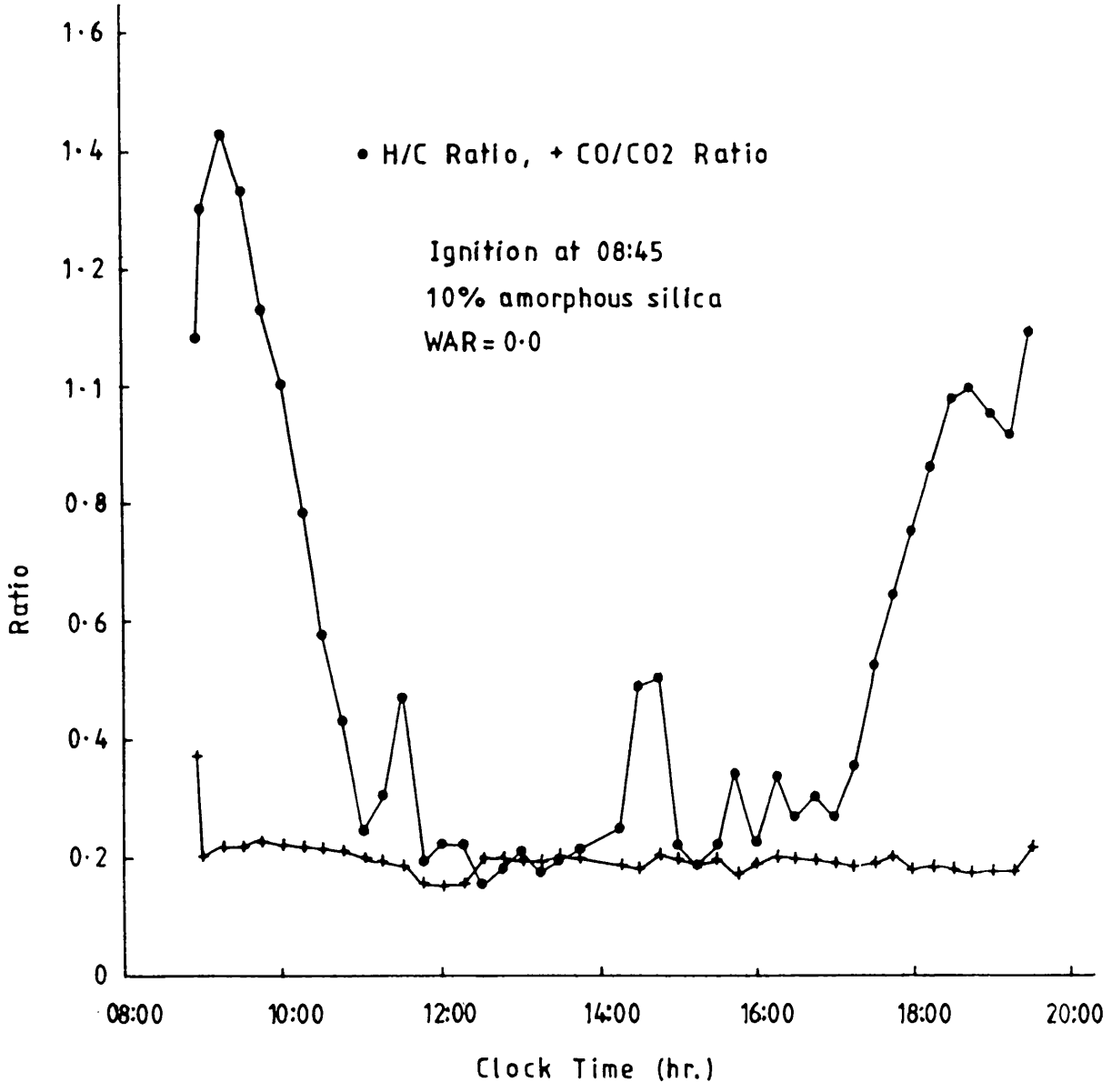

Figure 4.44 Hydrogen-carbon ratio and carbon monoxide-carbon dioxide ratio for the fuel burned for the Maya Isthmus crude (run No.8)

Table 4.5

H/C and CO/CO_2 ratios and the corresponding peak temperatures

Oil-sand mixture characteristics	Mode of combustion	Average apparent H/C ratio	Average CO/CO_2 ratio	Peak temperature (° F)
Maya Isthmus (5% kaolin)	dry	0.88	0.195	843
Maya Isthmus (5% kaolin)	normal wet	2.15	0.435	885
Maya Isthmus (5% kaolin)	normal wet	1.25	0.4	797
Maya Isthmus (5% kaolin)	partially quenched	1.63	0.37	844
Maya Isthmus (10% kaolin)	partially quenched	1.32	0.33	875
Forties (5% kaolin)	normal wet	2.16	0.345	829
Maya (5% kaolin)	normal wet	1.91	0.325	846
Maya Isthmus (10% amorphous silica)	dry	0.51	0.194	865

For normal wet combustion with WAR of 2.5 m^3/Mm^3 (STP) (run 3, Figure 4.39), the highest H/C ratio value occurred (17:15). Simultaneously the CO/CO_2 ratio achieved its value of 1.12, which is the highest recorded for the entire investigation.

With the higher water:air ratio in run 4 (Figure 4.40), the CO/CO_2 volume ratio is nearly constant from 14:00 until the end of the run. The H/C and CO/CO_2 profiles appear to follow the same behaviour as those for run 3.

For partially quenched wet combustion with 10% kaolin (run 5), Figure 4.41 shows that the average H/C and CO/CO_2 ratio are both lower than those of run 4, which had only 5% kaolin. Thus more fuel is burned, probably consisting mainly of carbon. The higher clay content therefore leads to increased fuel deposition (discussed in the next section).

Figures 4.42 and 4.43 present results for the Forties and Maya crude oils respectively. Table 4.5 shows that for the Forties crude, the fuel burned has the same H/C value as that for the Maya Isthums for the same WAR, namely 1.25 m^3/Mm^3 (STP). On the other hand, with heavy Maya, the fuel burned exhibits a lower H/C ratio than either of the two light crudes. The dry burn period for the heavy Maya has an average H/C value of 1.12. Thus more carbon is burned during this period, due to the high carbon residue content of the oil (11%, see Table 3.4). As stated in Section 4.3, a small but significant amount of CH_4 and H_2 were produced during run 7, because of cracking reactions. This gives rise to a negative H/C value at the very end of the run (Appendix D). It is believed that this is due to negative values in the hydrogen consumption obtained in this period. The amount of hydrogen consumed is simply based on the oxygen balances calculation, which is calculated by the computer program given in Appendix B,

low nitrogen mole fraction and at the same time, higher CO_2 and CO production introduced the negative value.

Figure 4.44 shows both H/C and CO/CO_2 ratios for run 8, where 10 w/w% of amorphous silica powder was added to the sand mixture. The fuel burned had an average H/C of 0.51 and CO/CO_2 of 0.19. They are the lowest values obtained in any of the runs. These low values indicate preferential oxidation of carbon, with a higher conversion to form CO_2, rather than CO.

Examination of the data presented in Table 4.5 shows that there is an expected scatter of the H/C values in the case of the wet combustion, when compared with the trend of the peak temperature. Thus run 2 shows a high average H/C ratio with a high corresponding peak temperature of 885 ° F, while dry runs 1 and 8 have lower H/C ratios and relatively high peak temperatures.

Generally, the fuel burned in wet combustion exhibits a higher H/C ratio than that in dry combustion. The cooling action of the injected water alters the chemical reaction conditions. Produced fluid may react further in the heated zone, resulting in additional chemical and physical changes (Fulton, 1980; and Alderman and Osoba, 1971). Parrish and Craig (1969) stated that the reaction mechanisms of water-fire flooding (COFCAW) are very complicated and the crude oil is subjected to an extensive period of steam distillation. They investigated a wide range of API gravities, but they were unable to establish any correlation with the cracking characteristics of the particular crude oil. Dietz and Weijdema, (1968) also obtained higher H/C ratios for partially quenched combustion, with a sharp decrease in CO_2 production when the combustion became locally quenched. Their values of H/C ratio averaged 8.3 for partially quenched combustion and just 3.8 for the dry and normal wet modes.

Low temperature oxidation reactions are more likely to occur during a wet combustion burn, when more oxygen enters the steam zone downstream (McKay, 1982). Burger and Sahuquet (1976) showed that an H/C ratio > 2 indicates LTO reactions, while H/C ratios < 2 are an indication of predominantly gas-solid reactions ($C + O_2 \rightarrow CO_2$). Harding (1976) observed high H/C ratios for evaluation of Athabasca oil sand, which were due to LTO reactions occurring during some periods. In another test, cracked products (light hydrocarbon and hydrogen) were obtained, due to the development of high temperature zones. Guvenir (1980) has also pointed out the important effect of the porous medium itself, and particularly the effect of clay and other minerals on the oxidation reaction. These effects need to be taken into account, because they affect the apparent H/C ratio of the fuel burned.

Each of the three crude oils used (Forties, Maya Isthmus and Maya) produced some catalytic products. As mentioned in Section 4.3, some methane and hydrogen production occurred in runs 2, 4, 5 and 6 (Appendix D), while very significant amounts of CH_4 and H_2 were produced during run 7, using the heavy Maya crude. Also, the negative value of H/C ratios towards the end of the run indicates that thermal cracking was taking place as the front approached the coke zone. The oxidation reaction may also have been affected by the presence of vanadium and nickel in the Maya crude, which contained 267 ppm and 52 ppm respectively, of these metals. However, since the Maya crude contains 3.91% of sulphur as well, this could appreciably affect the level of catalytic activity, due to poisoning.

Guvenir (1980) showed that the H/C ratio decreases with increased clay content during dry combustion. It seems that the H/C ratio exhibits the same trend during wet combustion. For partially quenched combustion, however, the average H/C ratio for the fuel burned is lower with 10% clay (run 5, Table 4.5), compared with run 4, which had only 5% kaolin.

Higher CO/CO_2 ratios are obtained for wet combustion, compared with dry combustion runs (Table 4.5). Typical CO/CO_2 and H/C values for dry and normal wet combustion of heavy oil are 0.25 and 1.38 respectively, as found by the Computer Modelling Group (1982; 1.55-1.82). For dry combustion, Showalter (1963) reported H/C values ranging from 0.9-2.22 and CO/CO_2 from 0.1-0.34 for 11-40° API crude oils. Guvenir (1980) obtained a rather constant CO/CO_2 ratio of 0.36-0.38 for 19.3 API crude, in a sand mixture which contained various percentages of clay. Dabbous and Fulton (1974) indicated that LTO reactions produce CO_2 and CO, the amounts depending on the type of crude oil used. The average CO/CO_2 values were 0.8 and 0.5 for crude oils of 27.1 and 19.9 API respectively.

4.6 Fuel consumption

Fuel consumption was calculated on the basis of the stoichiometric relationship given by Nelson and McNeil (1961). This method does not include the porosity effect. In addition, therefore, a comparison was made using the empirical porosity factor developed by McKay (1982). The fuel consumption values obtained by these two methods are compared in Table 4.6, showing that they are analogous, *i.e.*, exhibit the same trend. Table 4.6 also gives the fuel consumption as a percentage of the original oil in place. The heat released due to combustion and the heat available to 100 gm sand matrix was calculated according to the Burger and Sahuquet (1972) approach.

For the dry combustion runs (1 and 8), all of the deposited fuel was completely burned. This is justified by the clean, light colour of the burnt sand removed from the combustion tube. On the other hand, the term 'fuel consumption' in wet combustion means that only part of the fuel which is available is consumed to sustain the combustion. The remaining part of the fuel forms a coke residue, which depends on the water:air ratio.

Table 4.6

Fuel consumption and heat of combustion

Run No.	Crude oil	Clay content (%)	WAR [m^3/Mm^3 (STP)]	Mode of combustion	Cumulative carbon burned (gm)	Cumulative hydrogen burned (gm)	Fuel consumption % OOIP	Fuel consumption kg/m^3	Fuel consumption lb/100 lb sand*	Av. heat of combustion** (cal/gcHx)	Heat available cal/g sand	Heat available kJ/kg sand
1	Maya Isthmus	5	0.0	dry	38.164	2.8	11.38	19.98	1.465	8897	130.3	31.13
2	Maya Isthmus	5	1.25	normal wet	18.514	3.31	5.79	10.43	0.729	10358	75.6	18.06
3	Maya Isthmus	5	2.5	normal wet	16.08	1.68	4.67	8.33	0.597	8949	52.8	12.61
4	Maya Isthmus	5	3.75	partially quenched	11.49	1.56	3.48	6.19	0.444	9386	41.6	9.94
5	Maya Isthmus	10	3.75	partially quenched	15.16	1.67	4.42	8.0	0.562	9207	51.5	12.3
6	Forties	5	1.25	normal wet	10.16	1.82	3.19	5.51	0.407	10507	42.1	10.05
7	Maya	5	1.25	normal wet	12.87	2.05	3.88	6.99	0.495	9914	48.6	11.61
8	Maya Isthmus	10	0.0	dry	38.75	1.65	10.6	18.57	1.212	7937	96.0	22.93

* Fuel lb/100 lb rock = $0.0638\ kg/m^3 \times \frac{1}{1-\phi} \times \frac{100}{160}$; ϕ = porosity, $\rho r = 160\ lb/ft^3$.

** Heat of combustion in cal/gcHx = $\frac{265{,}700 + 197{,}850\ CO/CO_2}{(1+CO/CO_2)(12+H/C)} + \frac{31{,}175\ H/C - 171{,}700}{12 + H/C}$ (Burger and Sahuquet, 1972).

According to Table 4.6, the fuel availability is higher for dry combustion runs, irrespective of the water:air ratio. As mentioned previously, an increase in WAR decreases the residence time for the oxygen in the combustion zone. This decreases the fuel consumption, as shown in Figure 4.45.

The fuel burned in run 5 (with 10% kaolin) is 8.0 kg/m^3 of reservoir, or 0.562 lb/100 lb, which is 4.4% of the original oil in place. This is more than the value of 6.19 kg/m^3 (0.44 lb/100 lb) obtained for run 4 (5% kaolin) at the same WAR, which is 3.5% of OOIP. This is primarily due to the high surface area of the kaolin (12-14 m^2/g), which gives higher fuel deposition and causes a higher fraction of the fuel to be burnt. Therefore, in wet combustion, the clay minerals present in the reservoir rock, in addition to the selected WAR, act to control the fuel consumption.

Comparing the fuel burned for different API gravity crudes (runs 2, 6 and 7) under normal wet combustion, it can be seen that the fuel consumption is lowest for the North Sea Forties crude at 5.51 kg/m^3 (0.4 lb/100 lb). This indicates that wet combustion can be sustained in high gravity oil reservoirs, with a relatively low fuel consumption (3.19% OOIP). For dry combustion, however, a much higher figure is expected, as shown by runs using Maya Isthmus. The highest fuel consumption was obtained for the Maya Isthmus crude (10.43 kg/m^3 or 0.73 lb/100 lb), due to LTO reactions. It seems, therefore, that API gravity does not correlate with fuel consumption. This finding agrees with that of Bae (1976), who attributed the increased fuel consumption to LTO reactions. Fassihi *et al.* (1980b) and Alexander *et al.* (1962) also found that LTO reactions could increase fuel deposition. Dabbous and Fulton (1974) found that light crudes are more susceptible to LTO than are heavy oils.

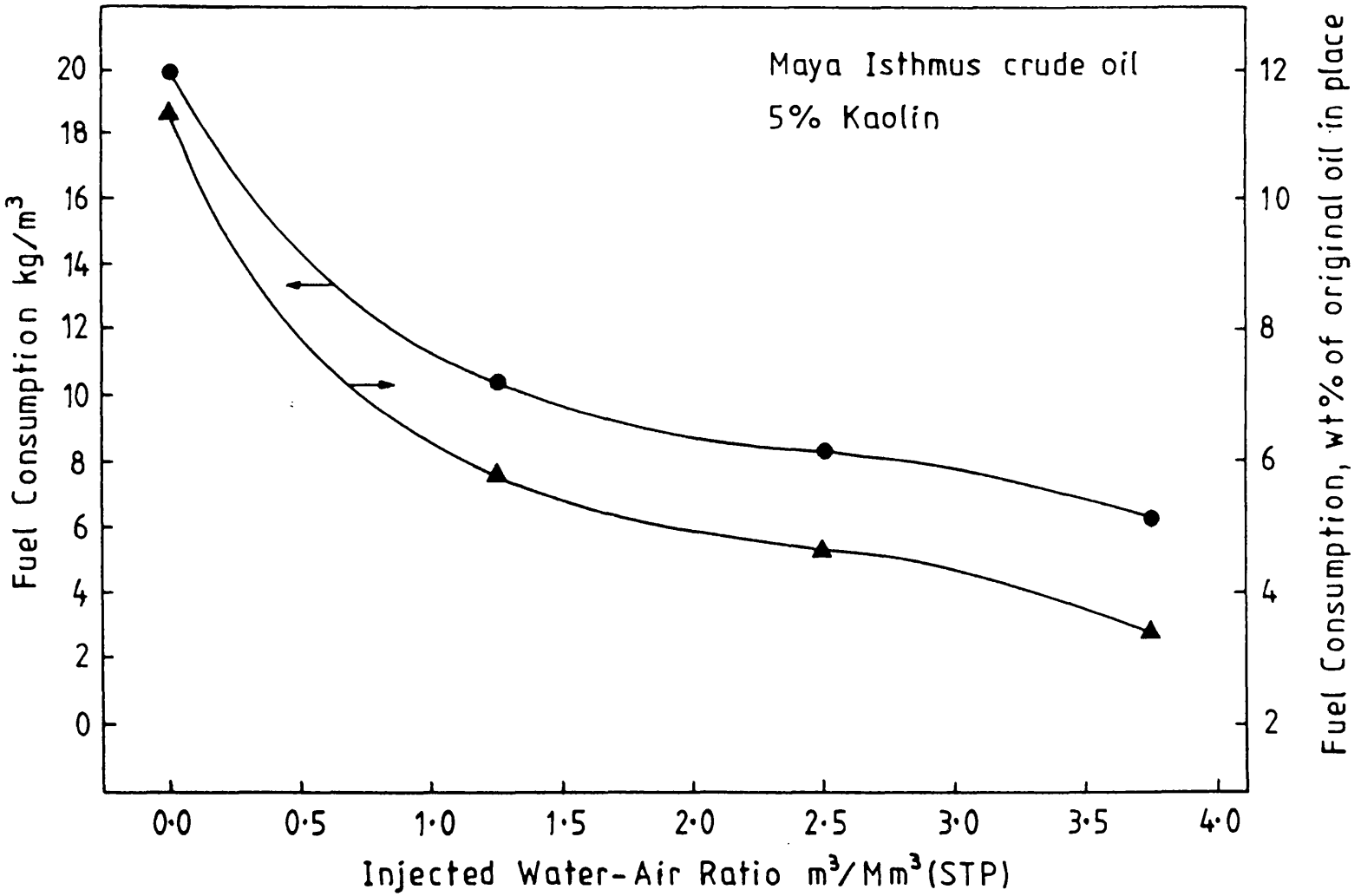

Figure 4.45 Fuel consumption against injected water-air ratio (runs No.s 1,2,3 and 4).

For run 8, using 10% amorphous silica, the fuel available is 18.57 kg/m^2 (1.21 lb/100 lb). This is less than runs for dry combustion with only 5% kaolin, using the same Maya Isthmus crude oil. This is due to the higher surface area of kaolin (12-14 m^2/g), compared with amorphous silica (2.0 m^2/g). In run 5, the fuel available with 10% kaolin gave a value of 19.6 kg/m^3 (1.372 lb/100 lb) during the dry burn phase. These results are within the range values reported elsewhere (Burger and Sahuquet, 1973; Garon and Wygal, 1974; Guvenir, 1980; and McKay, 1982). For dry combustion, Guvenir (1980) reported values of 1.33 lb/100 lb, using 15% amorphous silica dust (1.4 m^2/g surface area), 1.4 lb/100 lb for 10% kaolin, and 1.11-1.28 lb/100 lb for 5% kaolin. Burger and Sahuquet (1973) gave the average fuel burned as 1.05 lb/100 lb for 27 API crude and 1.45 lb/100 lb for 16 API crude with dry combustion. For wet combustion, a value of 0.762 lb/100 lb was obtained for a 16 API crude using a WAR 2-6 m^3/Mm^3 (STP). Garon and Wygal (1974) obtained a fuel consumption of 0.86 and 0.9 lb/100 lb for a 20.3 API crude with dry combustion at 0 and 1000 psi respectively, 0.79-0.56 lb/100 lb using WAR 1.01-5.94 m^3/Mm^3 (STP) at atmospheric pressure. At 1000 psi, values ranging from 0.74 to 0.33 lb/100 lb were obtained for WAR 0.94-6.98 m^3/Mm^3 (STP).

The conclusions arising out of the results presented in this chapter are summarised as follows:-

(1) Under near-adiabatic temperature conditions, a self-sustained combustion front could not be established, unless clay material or amorphous silica was present in the oil-sand mixture. However, the minimum clay content to sustain combustion was not determined. This property affects the fuel availability and other combustion characteristics, so that native reservoir rock must be used for field project investigation.

(2) Vigorous combustion of light North Sea Forties oil (36.6 API) and Maya Isthmus oil (32.4 API) was sustained with a WAR equal to 1.25 m^3/Mm^3 (STP) (normal wet combustion) under a pressure of 50 psig. The fuel consumption for the Forties oil was the lowest achieved in any experiment. Vigorous self-sustained combustion was also achieved with the Maya Isthmus oil under partially quenched operation conditions (WAR = 3.75 m^3/Mm^3 (STP).

(3) The average value of the combustion front temperature was not appreciably affected by the injected water at low water:air ratios [WAR < 2 m^3/Mm^3 (STP)]. Under partially quenched operating conditions the combustion-steam zone temperature attains high values compared with results which have been obtained at much higher pressures. In the latter case, the adiabatic operation of the combustion tube may have been much less effective, or else totally absent.

(4) For a given crude oil, the fuel consumption falls very steeply as the mode of combustion changes from dry to wet. As the WAR was further increased, there was a continued decrease in the fuel consumption. In the case of Maya Isthmus crude oil, the fuel consumption was reduced by 40.6 % for a three-fold increase in WAR from 1.25 to 3.75 m^3/Mm^3 (STP). At a WAR = 3.75 m^3/Mm^3 (STP), the fuel consumption was only 30.9 % of that required for dry combustion.

(5) Oxygen utilisation was not significantly affected by either the clay content (up to 10% kaolin), or the API gravity of the oil. However, there was evidence of some improvement of oxygen utilisation efficiency under wet combustion conditions, as the WAR was increased.

Very high oxygen utilisation was obtained with the addition of 10% amorphous silica, reaching almost 100%.

(6) Significant LTO reaction effects were obtained in many of the experiments during the period immediately after ignition. The occurrence of LTO effects was most pronounced, however, under wet combustion conditions with the light Maya Isthmus crude. This gave a high H/C value and consequent increased fuel consumption.

(7) Significant amounts of light components (CH_4 and H_2) were produced from wet combustion of both light and heavy oils. This was the result of steam cracking reactions taking place in the high temperature steam zone. Any catalytic activity was mainly derived from the addition of the clay material. The amount of hydrogen and methane produced was greatest for the heavy Maya crude.

CHAPTER 5

IN SITU COMBUSTION PERFORMANCE PARAMETERS

Introduction

As discussed in Chapter 2, the parameters obtained from laboratory combustion tube experiments provide extremely important parameters which can be employed to assess the technical and economic viability of field project operations. The important parameters to be determined are the air required, WAR, fuel consumption and fluid production history (oil, water). These have been obtained for the eight combustion tests in this investigation and their significance is analysed with respect to the condition of each experiment. Comparisons are made with other work and detailed material balance information is presented.

5.1 Combustion front velocity

Figures 5.1-5.8 show the location of the combustion front as a function of the time of arrival of the front at successive thermocouple positions along the combustion tube. This is determined from the peak combustion temperatures data presented in Chapter 4. The stabilised burning period for each case is identified by the constant rate section AA on the graphs. For wet combustion runs, it corresponds to the stabilised wet burn period and is therefore easily recognised from the temperature rate profiles. However, it is also possible to confirm that the combustion front has attained a constant velocity by examination of the oxygen utilisation during this period (Figures 4.29-4.36). The combustion zone velocity, normalised by division with the air flux, is a measure of the volume of reservoir burned per unit of air injected [m^3/Mm^3 (STP)]. Table 5.1 shows the overall and stabilised values of the combustion front velocity, together with the normalised front velocities. The fuel consumption for

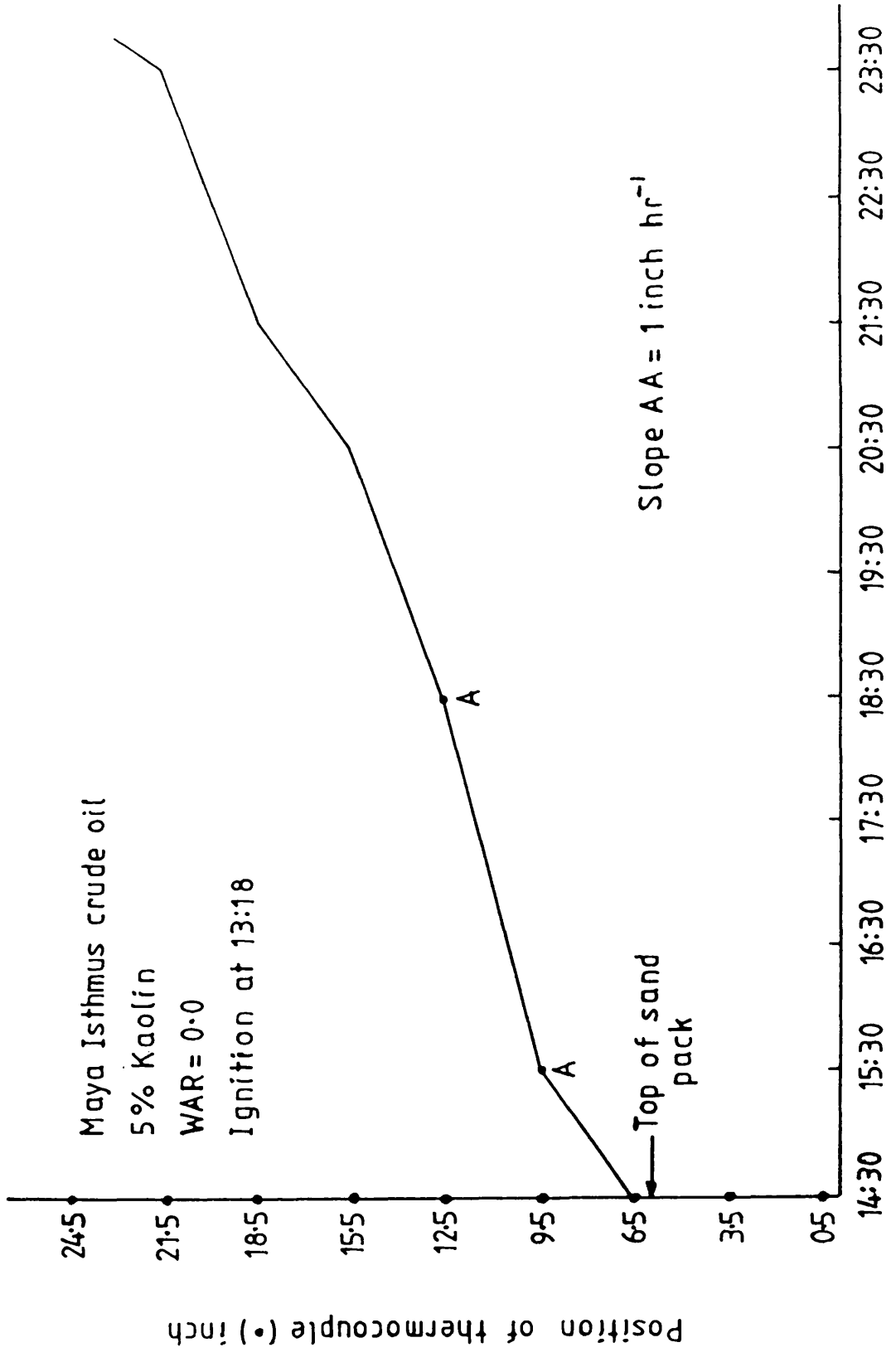

Figure 5.1 Combustion front position *versus* time (run No.1).

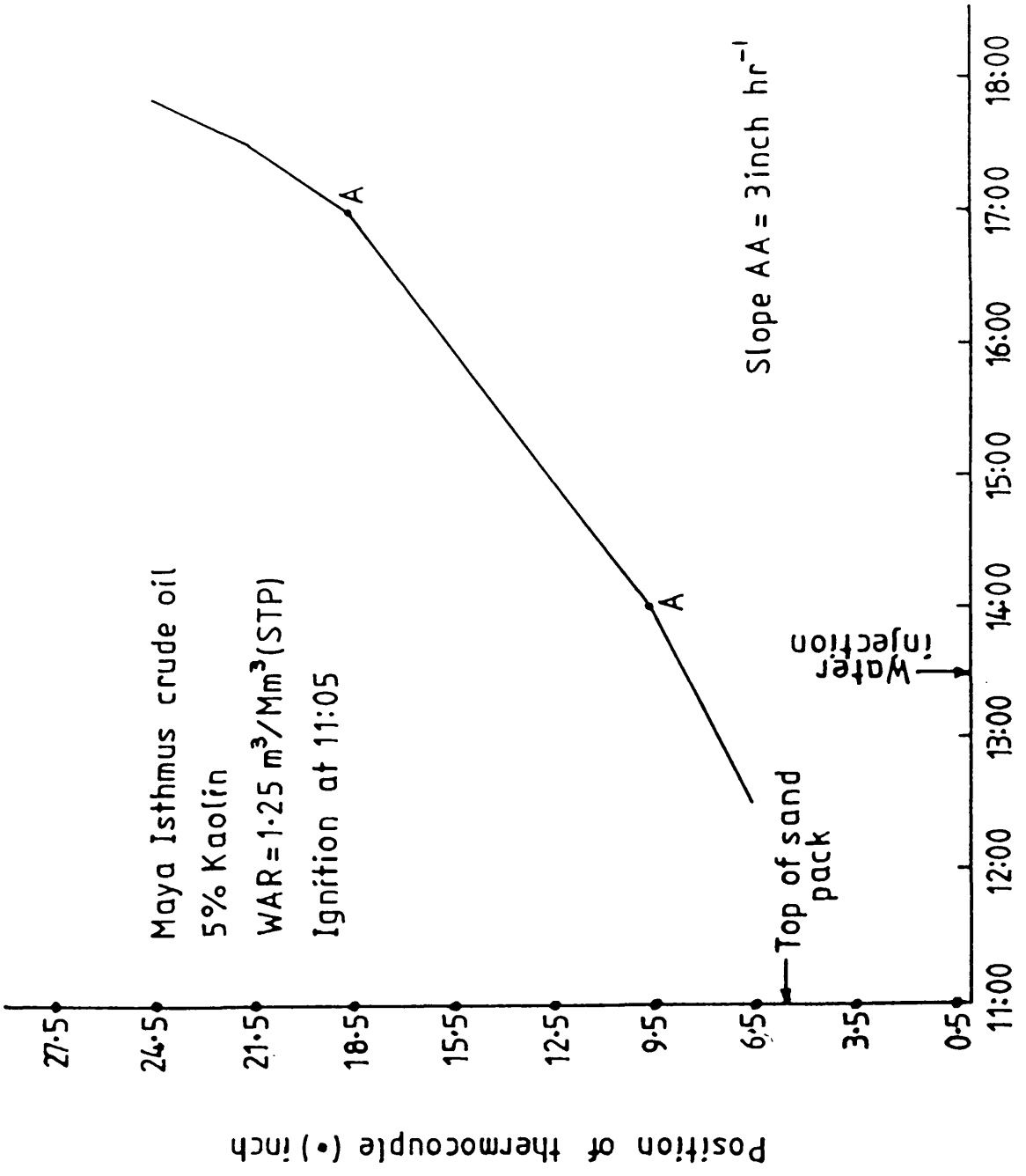

Figure 5.2 Combustion front position *versus* time (run No.2).

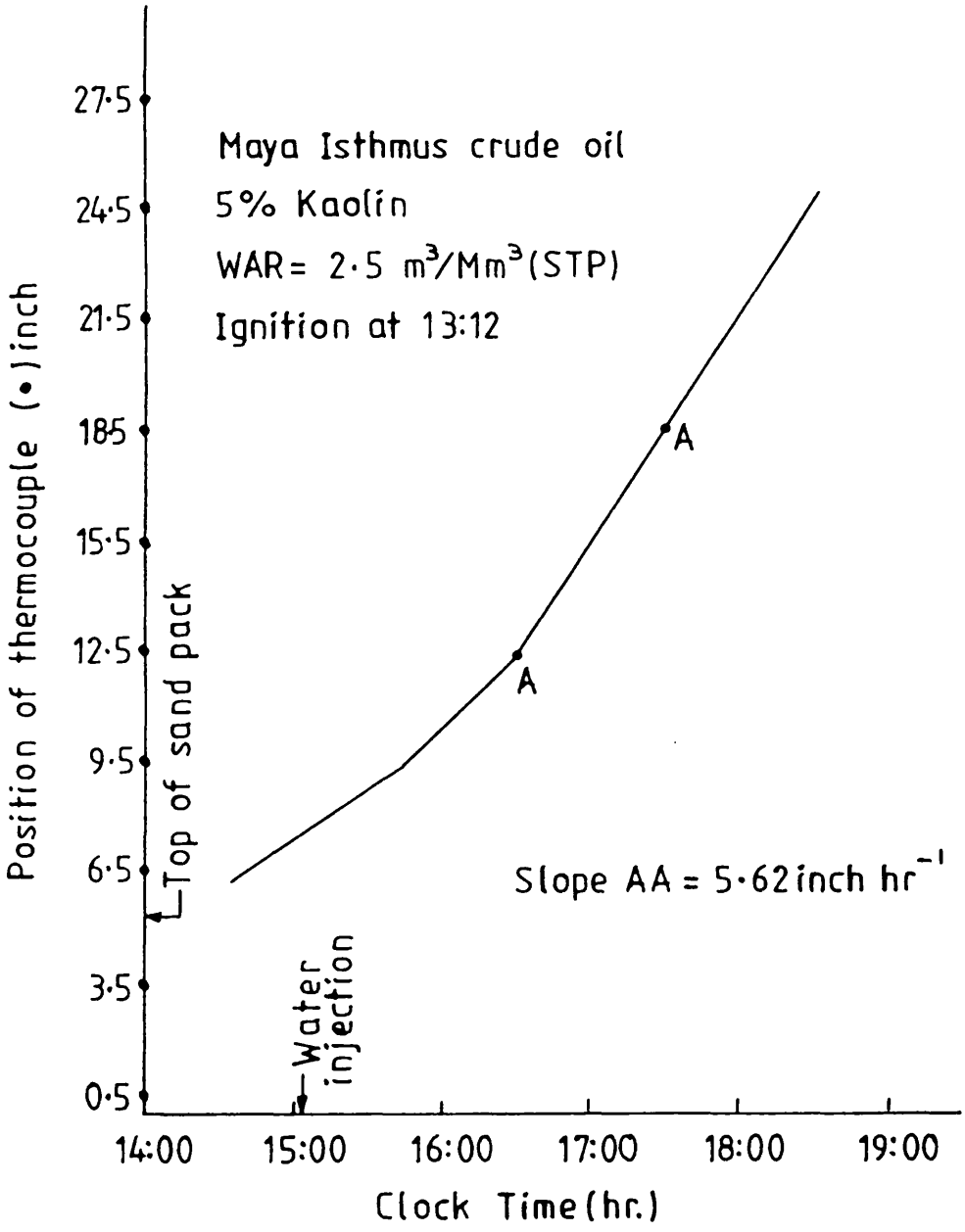

Figure 5.3 Combustion front position *versus* time (run No.3).

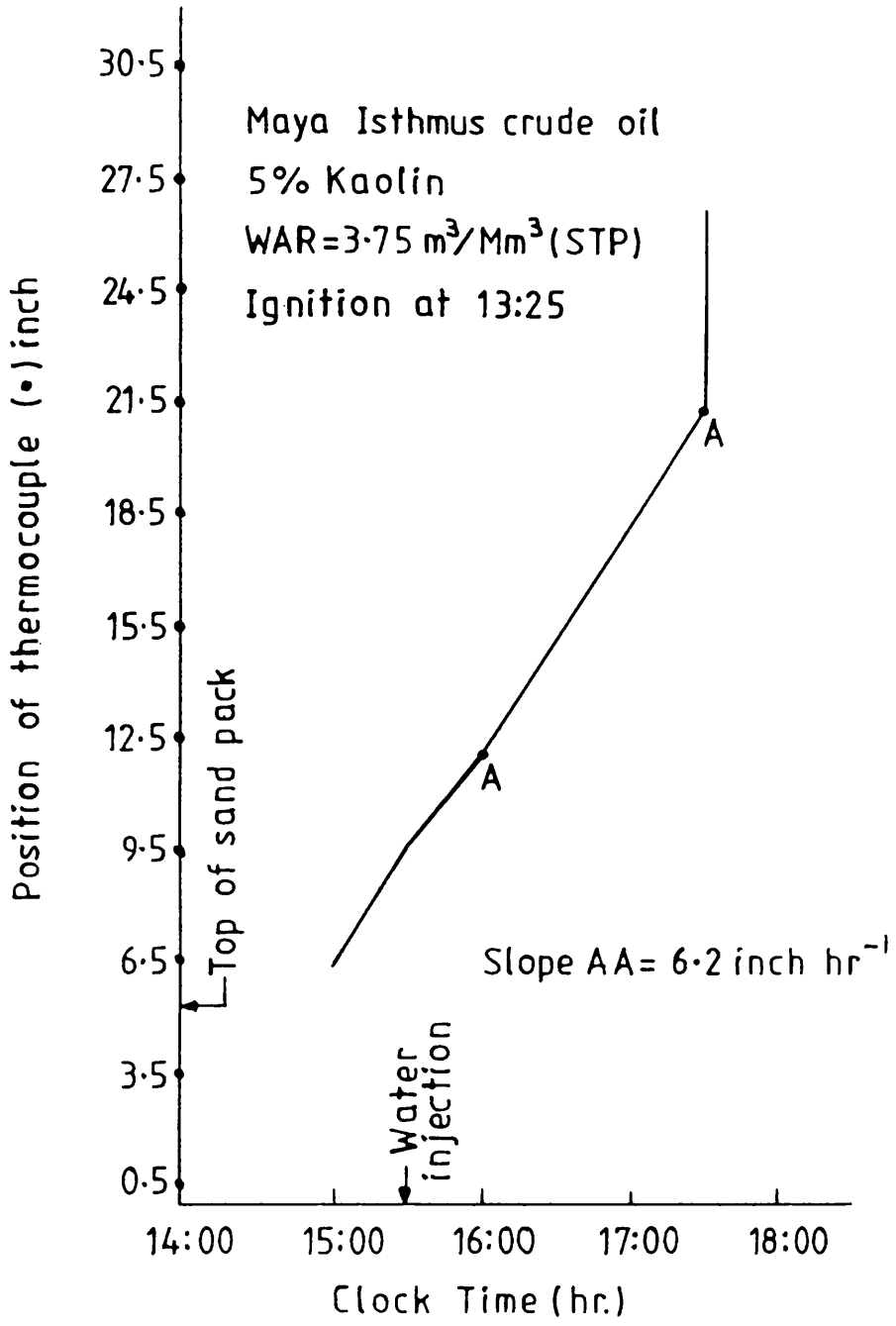

Figure 5.4 Combustion front position *versus* time (run No.4).

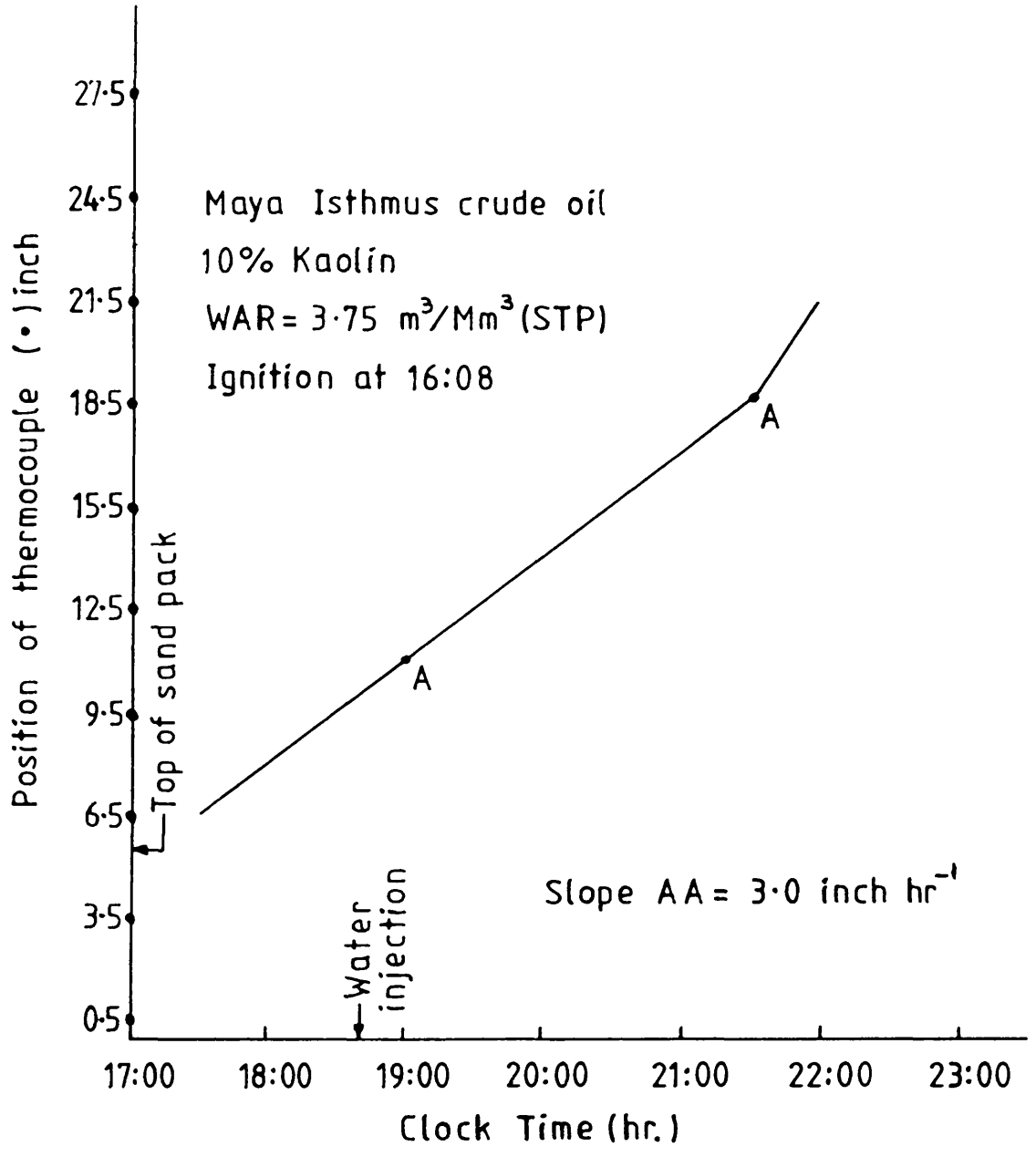

Figure 5.5 Combustion front position *versus* time (run No.5).

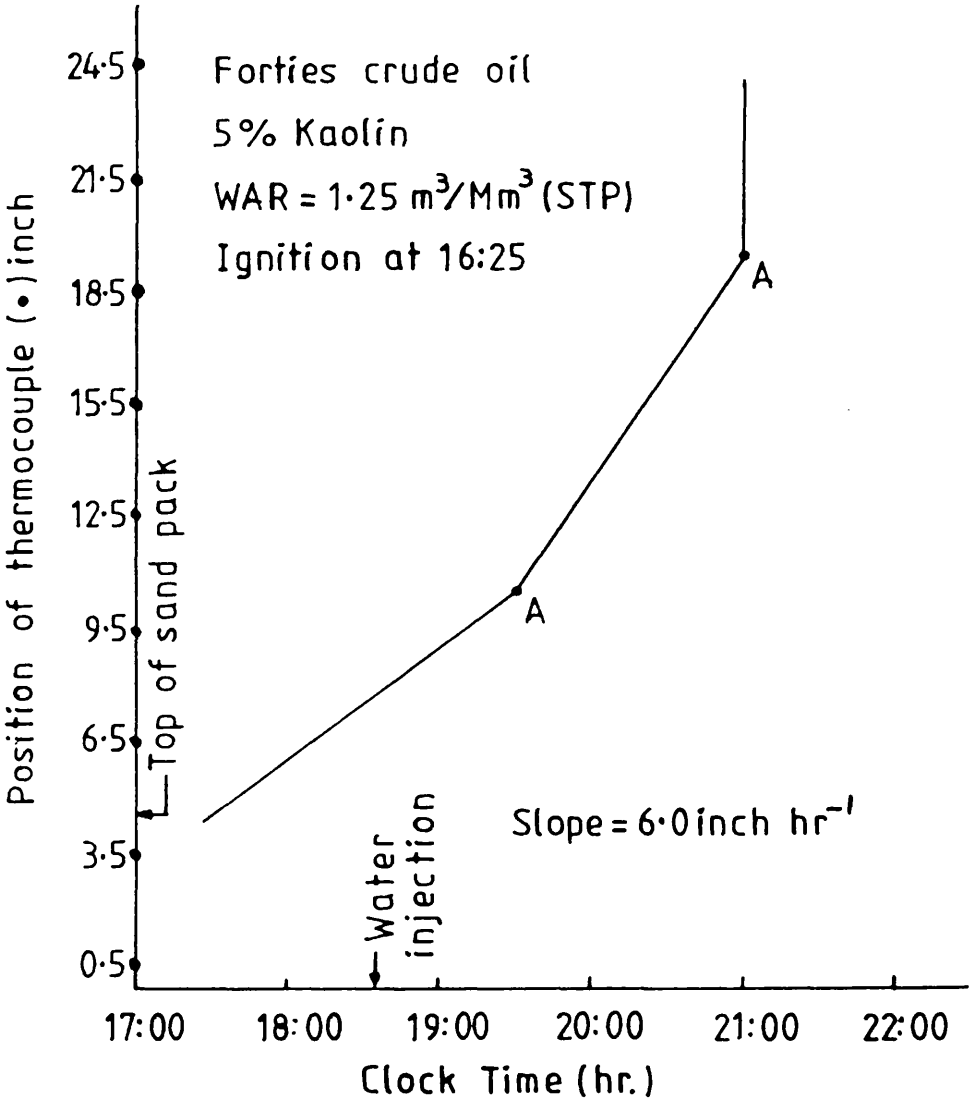

Figure 5.6 Combustion front position *versus* time (run No.6).

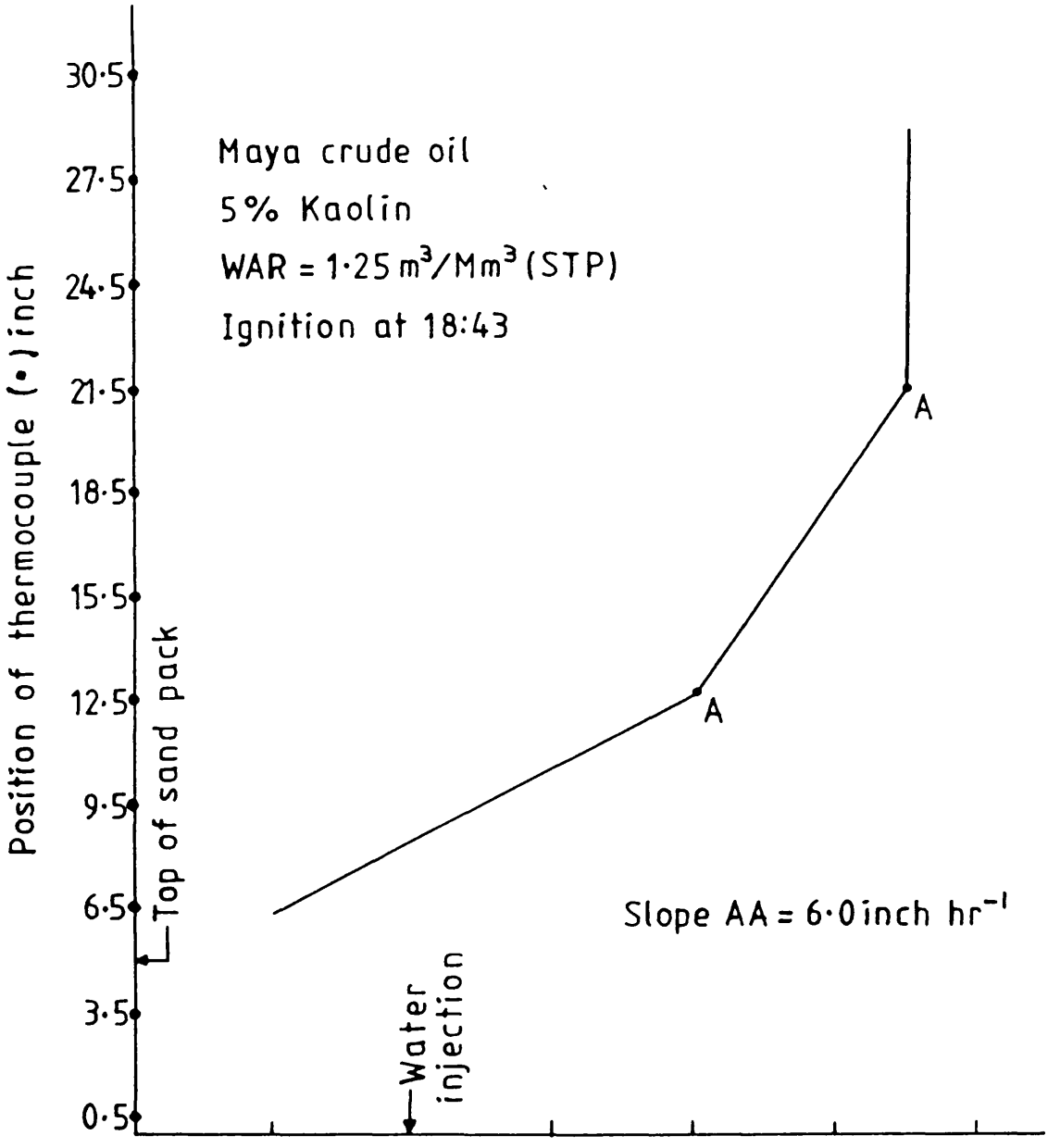

Figure 5.7 Combustion front position *versus* time (run No.7).

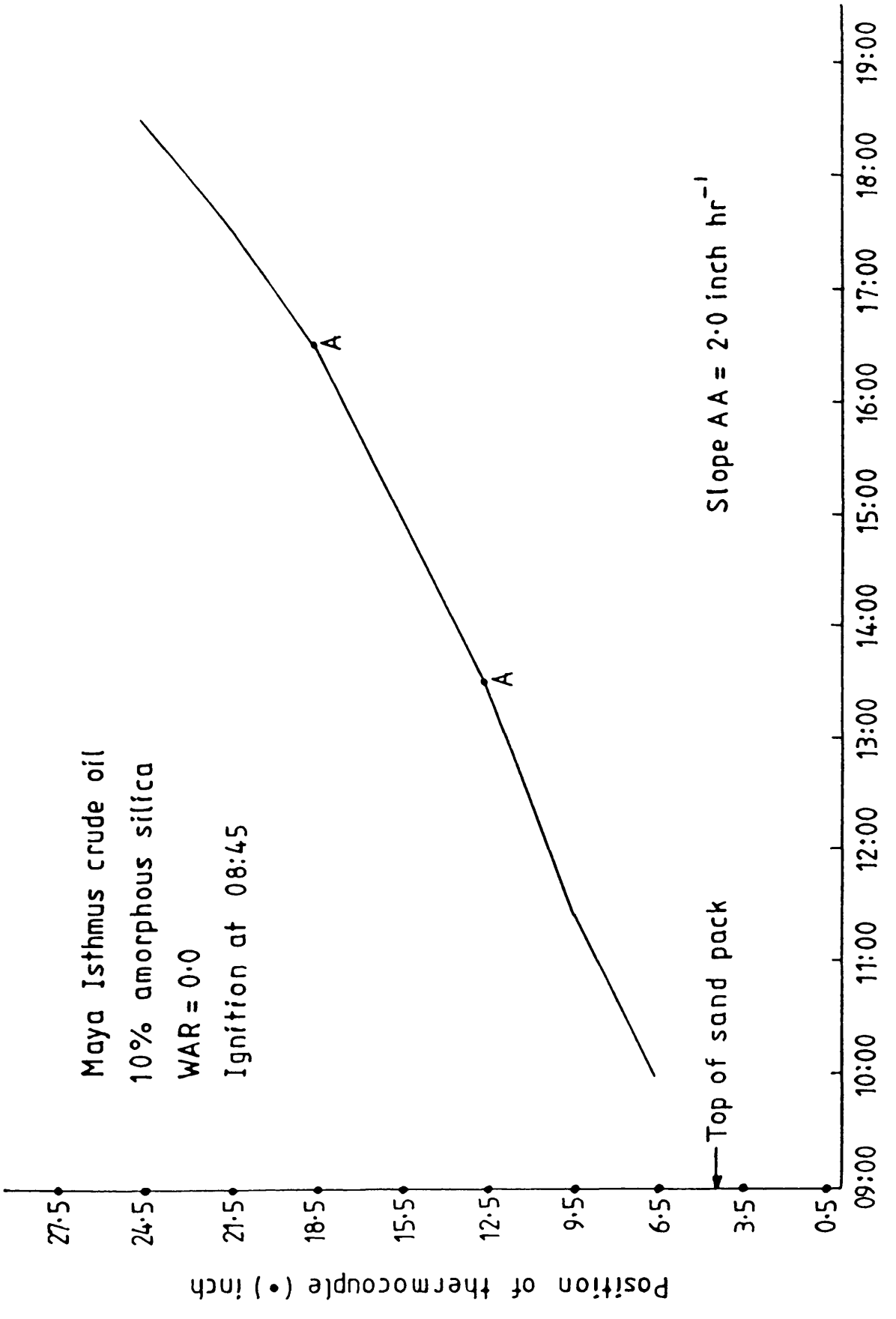

Figure 5.8 Combustion front position *versus* time (run No.8).

Table 5.1

Combustion front velocity and fuel consumption

Run number	1		2		3		4		5		6		7		8	
Oil type	Maya Isthmus		Maya Isthmus		Maya Isthmus		Maya Isthmus		Maya Isthmus		Forties		Maya		Maya Isthmus	
Clay content (%)	5		5		5		5		10		5		5		10 (amorphous silica)	
WAR [m^3/Mm^3(STP)]	0.0		1.25		2.5		3.75		3.75		1.25		1.25		0.0	
Combustion mode	dry		normal		normal		partially quenched		partially quenched		normal		normal		dry	
Combustion front velocity	Overall	Stabilised	Overall	Stabilised	Overall	Stabilised	Overall	Stabilised	Overall	Stabilised	Overall	Stabilised	Overall	Stabilised	Overall	Stabilised
(cm/h)	5.33	2.54	9.14	7.62	12.8	14.27	15.24	15.75	9.65	7.62	13.33	15.24	10.67	15.24	5.58	5.08
(in/h)	2.1	1	3.6	3	5.04	5.62	6	6.2	3.8	3	5.25	6	4.2	6	2.2	2
Normalised combustion velocity [m^3/Mm^3(STP)]	3.66	1.74	6.27	5.23	5.78	9.8	10.45	10.8	6.62	5.23	9.15	10.46	7.32	10.46	3.83	3.48
Fuel consumption (kg/m^3)	19.98	34.8	10.43	14.37	8.17	7.8	5.95	6.5	8.0	10.61	5.51	5.75	6.86	7.0	18.57	24.0

both the overall and stabilised periods is also noted in Table 5.1. As expected, the combustion front velocity increases with increasing WAR. A similar trend is observed for the normalised combustion front velocity. Fuel consumption, however, decreases with increasing WAR. Combustion front velocity for run No.5 (10% kaolin) is much lower than that for run No.4 (5% kaolin) at the same WAR. This is directly attributable to the much higher fuel consumption for run No.5.

For the normal wet combustion mode (runs Nos. 2, 6 and 7), the light Forties crude (36.6 °API) gave the highest combustion velocity, compared with Maya Isthmus crude (32.4 °API), which gave the lowest. The low combustion velocity with Maya Isthmus crude is due to the high fuel consumption, as discussed in Section 4.5. This is in accordance with the results of Garon and Wygal (1974), who found that an increase in the amount of fuel burned caused a reduction in the combustion velocity. The surface area effect of the kaolin affecting combustion is similar to the extra affinity of the native rock. Burger and Sahuquet (1973) showed that unextracted rock material gave the highest fuel burned and the lowest combustion velocities.

For the range of WAR investigated (runs Nos. 1, 2, 3 and 4), the combustion front velocities generally increased with WAR, at a fixed air flux. This trend is compared with the correlating line determined by Dietz and Weijdema (1968), as shown in Figure 5.9. The latter figure also shows the results obtained by Burger and Sahuquet (1973) and Garon and Wygal (1974). Dietz's general line is designated as a partially quenched combustion (super wet combustion). The slope of the line of the present work shows good agreement with Dietz's line, but the line is displaced to the left, which means it does not pass through the origin. However, the dry combustion run value of normalised combustion velocity

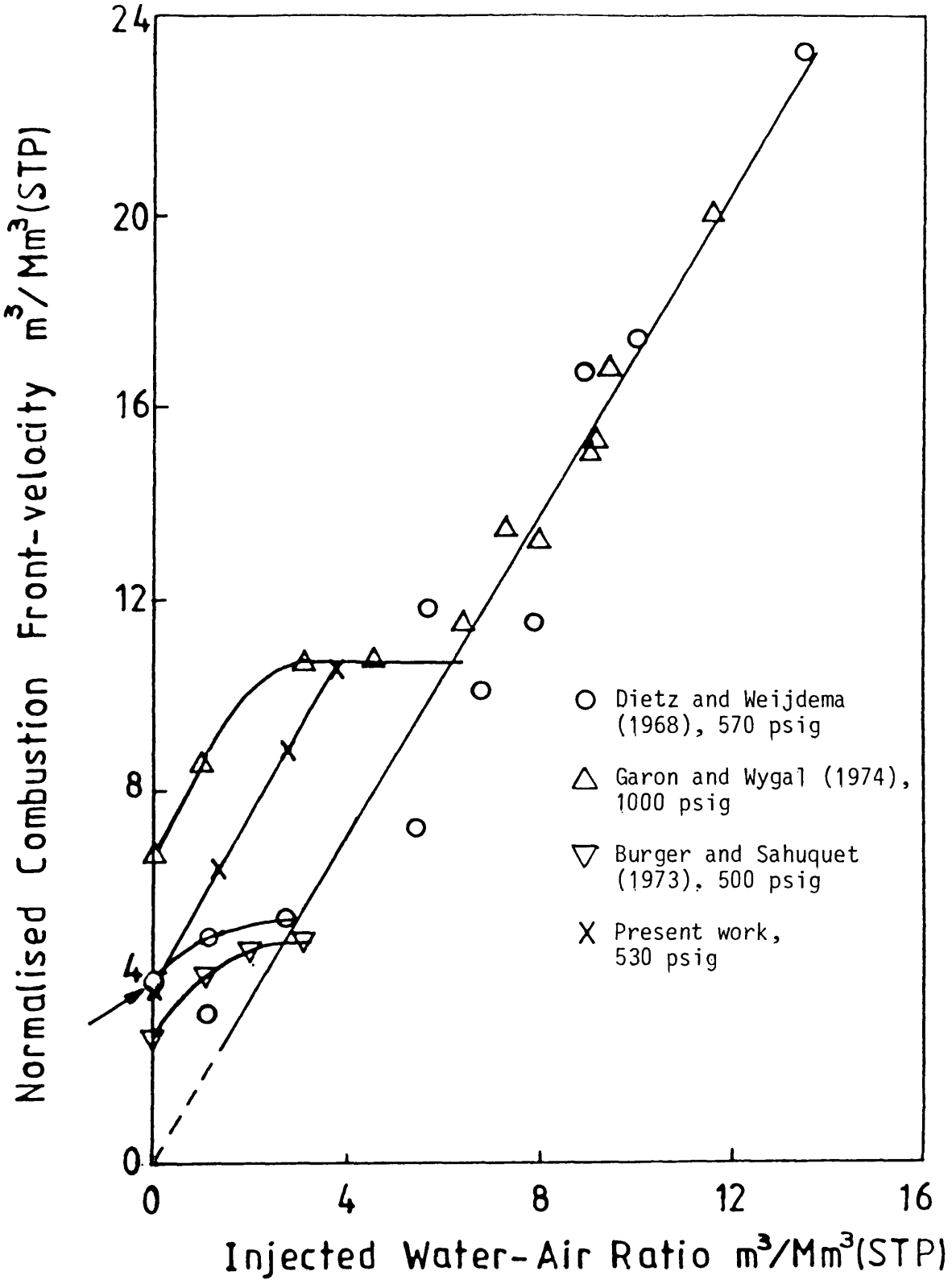

Figure 5.9 Normalised combustion velocity as a function of injected water-air ratio.

coincides exactly with the experimental value of Dietz and Weijdema. There is a general scatter of Dietz and Weijdema results, partially quenched, occurring even to the left of the diagonal line. In any event, those results were obtained under high pressure (570 psig) and non-adiabatic conditions.

The much higher normalised velocity values of the present work, and the values obtained in the work carried out by Garon and Wygal (1974) reflect the fact that heat dissipation also plays an important role, compared with the non-adiabatic experimental values found by Dietz and Weijdema (1968). Dietz observed a small increase in normalised combustion velocity values at water-air ratios less than that required for partially quenched combustion.

Furthermore, Garon and Wygal's result shows a very wide range of normal wet combustion to the left of the general line, while the present work exhibits partially quenched combustion at a similar WAR. This means that the higher the pressure, the wider the range of normal wet combustion, *i.e.*, the transition from normal wet, to partially quenched, combustion.

5.2 Overall and stabilised air requirement

The air compression cost is a major component of the total cost of an *in situ* combustion process. Therefore, the amount of air required to recover 1 m^3 of oil, or air-to-oil ratio (AOR), as well as the air consumed per 1 kg of fuel or air-to-fuel ratio (AFR), are the basic parameters needed to determine the economics of a combustion project. A sample of calculations of the air requirement, for both the overall and stabilised period of combustion, is given in Appendix C. The air requirement in standard cubic meters per cubic meter of burnt sand pack, the AFR and the AOR, are given in Table 5.2, for all the experiments.

Table 5.2

Air requirement, air-to-fuel ratio and air-to-oil ratio

Run number	1		2		3		4		5		6		7		8	
Oil type	Maya Isthmus		Maya Isthmus		Maya Isthmus		Maya Isthmus		Maya Isthmus		Forties		Maya		Maya Isthmus	
Clay content (%)	5		5		5		5		10		5		5		10% amorphous silica	
WAR [m^3/Mm^3(STP)]	0.0		1.25		2.5		3.75		3.75		1.25		1.25		0.0	
Air requirement [m^3(st)/m^3]	Overall	Stabilised	Overall	Stabilised	Overall	Stabilised	Overall	Stabilised	Overall	Stabilised	Overall	Stabilised	Overall	Stabilised	Overall	Stabilised
	231.7	372.6	135.7	179.3	92.1	95.3	72.2	73.5	92.2	130.9	71.6	80.7	90.3	93.9	182.6	223.4
AFR [m^3(st)/kg]	11.6	10.7	13.0	12.2	11.05	12.2	12.14	11.33	11.52	12.33	12.99	14.0	13.42	13.42	9.83	9.3
AOR [m^3(st)/m^3]	1380.8	663.7	874.8	782.2	597.8	448.6	540.2	422.4	677.2	635.6	471.0	320.3	820.9	822.7	1200.4	1119.4

In the calculation of the overall air requirement, the last section of unburnt coke zone is not included as part of the burnt section of the sand pack. Table 5.2 illustrates that there is a decrease in the air requirement for runs Nos. 1, 2, 3 and 4 at a fixed clay content of 5% as the WAR increases. Compared with dry combustion, the air requirement is reduced to 58.5% with a WAR of 1.25, 38.9 % with a WAR of 2.5, and approximately 31.2% with a WAR of 3.75 m^3/Mm^3 (STP).

The effect of clay content on the air requirement is demonstrated by runs Nos. 4 and 5. As shown in Table 5.2, the air requirement is 92.2 $m^3(st)/m^3$ for run No.5 with 10% kaolin, which is approximately 21.7% higher than for run No.4 [72.2 $m^3(st)/m^3$] using 5% kaolin. Similarly, the AOR is 677.2 $m^3(st)/m^3$ which is approximately 20.2 % higher than that found for run No.4 [540.2 $m^3(st)/m^3$].

In runs Nos. 2, 6 and 7, using a WAR of 1.25 m^3/Mm^3 (STP) and 5% kaolin, the highest air requirement and AOR is obtained for the Maya Isthmus crude (run No.2). These are, respectively, 135.7 $m^3(st)/m^3$ and 874.8 $m^3(st)/m^3$. The lowest air requirement of 71.6 $m^3(st)/m^3$ is obtained for the Forties crude, giving an AOR of 471.0 $m^3(st)/m^3$. The Maya crude (run No.7) gave similar values for both air requirement and AOR during both the stabilised and overall periods.

Generally, the air requirement is greater during the stabilised period, since more fuel is burned (see Table 5.1). However, less air is required to produce the oil, as evidenced by the smaller AOR for the stabilised period, compared with the overall result. The two exceptions to this are runs Nos. 7 and 8, for which the AOR is approximately the same. This means that more oil is produced during the stabilised periods.

The overall values of AFR's are plotted as a function of WAR, as shown in Figure 5.10. At a WAR of 1.25 m^3/Mm^3(STP), the AFR for the two light crudes (Forties and Maya Isthmus) is very similar, whilst the heavy Maya has the highest AFR value. The overall trend of the plot can only be considered to be approximate, since the low WAR's values lie above the line and the high WAR (excluding run No.8) lie below it.

Table 5.3 lists the AFR values obtained by various authors and these are compared with those obtained in this study for both dry and wet combustion modes. Figures 5.11 and 5.12 were produced from the Table in order to show the trend of AFR for various porous media and operating pressures. In Figure 5.11, there is a considerable scatter of the dry AFR values as a function of combustion temperature. The data obtained by Showlater (1963), however, appears to be inconsistent. Thus there is a slight increase in AFR values with combustion temperature, but lower results are obtained at a pressure of 470 psig. In the present work, there is reasonable agreement with the general trend exhibited by Showlater's result (1963), particularly for the run with 5% kaolin. Martin *et al.* (1958) obtained a high degree of scatter for both their AFR values and fuel consumption values. Despite the scatter of AFR values found by Burger and Sahuquet (1973), there is an increase in AFR with combustion temperature (McKay, 1982). However, AFR values for the same combustion temperature are different at different operating pressures.

In the case of wet combustion, the effect of combustion temperature is not important when compared to WAR (Garon and Wygal, 1974). Figure 5.12 indicates the general trend of the results obtained by Burger and Sahuquet (1973). From this, it seems that there is a slight increase in AFR with WAR, so that AFR is higher at higher pressures. The AFR

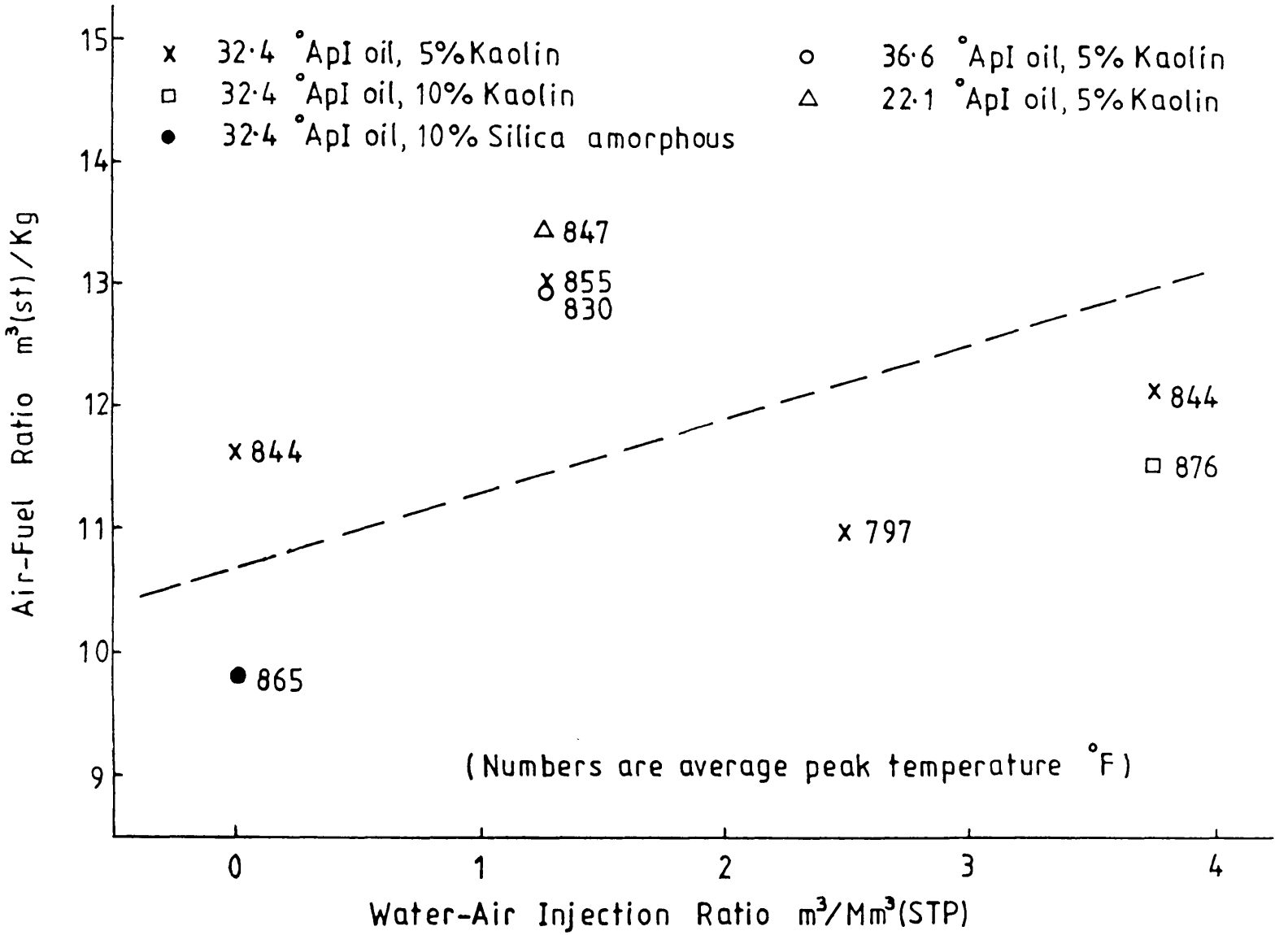

Figure 5.10 Summary of air-fuel ratios of wet and dry combustion.

Table 5.3

Comparison of air-fuel ratios

		Pressure (psig)	°API	WAR [$(m^3/Mm^3$ STP]	AFR* [m^3(st)/kg fuel]
Present work	Silica sand + 5% kaolin	50	32.4	0	11.6
				1.25	13.0
				2.5	11.0
				3.75	12.14
Present work	Sand pack + 5% kaolin	50	36.6	1.25	13.0
Present work	Sand pack + 5% kaolin	50	22.1	1.25	13.42
Martin *et al.*	Sand pack	80	21.2	0	13.66
(1958)		600	21.2	0	11.66-17.15
Burger and	Silica sand	160	16	0	12.0
Sahuquet (1973)				2	11.0
				4	11.6
Burger and	Treated reservoir rock	160	27	2	12.16
Sahuquet (1973)				4	12.3
Burger and	Untreated reservoir	530	27	0	11.9
Sahuquet (1973)	rock			1	10.98
				2	11.6
				3	11.6
Parrish and	Nelliebiy sandstone	500	13.5	2.31	9.17
Craig (1969)			25.2	3.43	10.17
			30.5	3.34	9.8
			28.9	2.23	10.42
			40.9	2.31	14.47
Ejiogu (1978)	Reservoir rock	860	37	0	13.42
	Alberta			0.99	10.54
				1.93	9.27
				2.73	9.36
Harding *et al.*	Athabasca oil sand	834	7.84	1.87	12.6
(1976)		843	7.84	2.255	10.0

*AFR's calculated for this table.

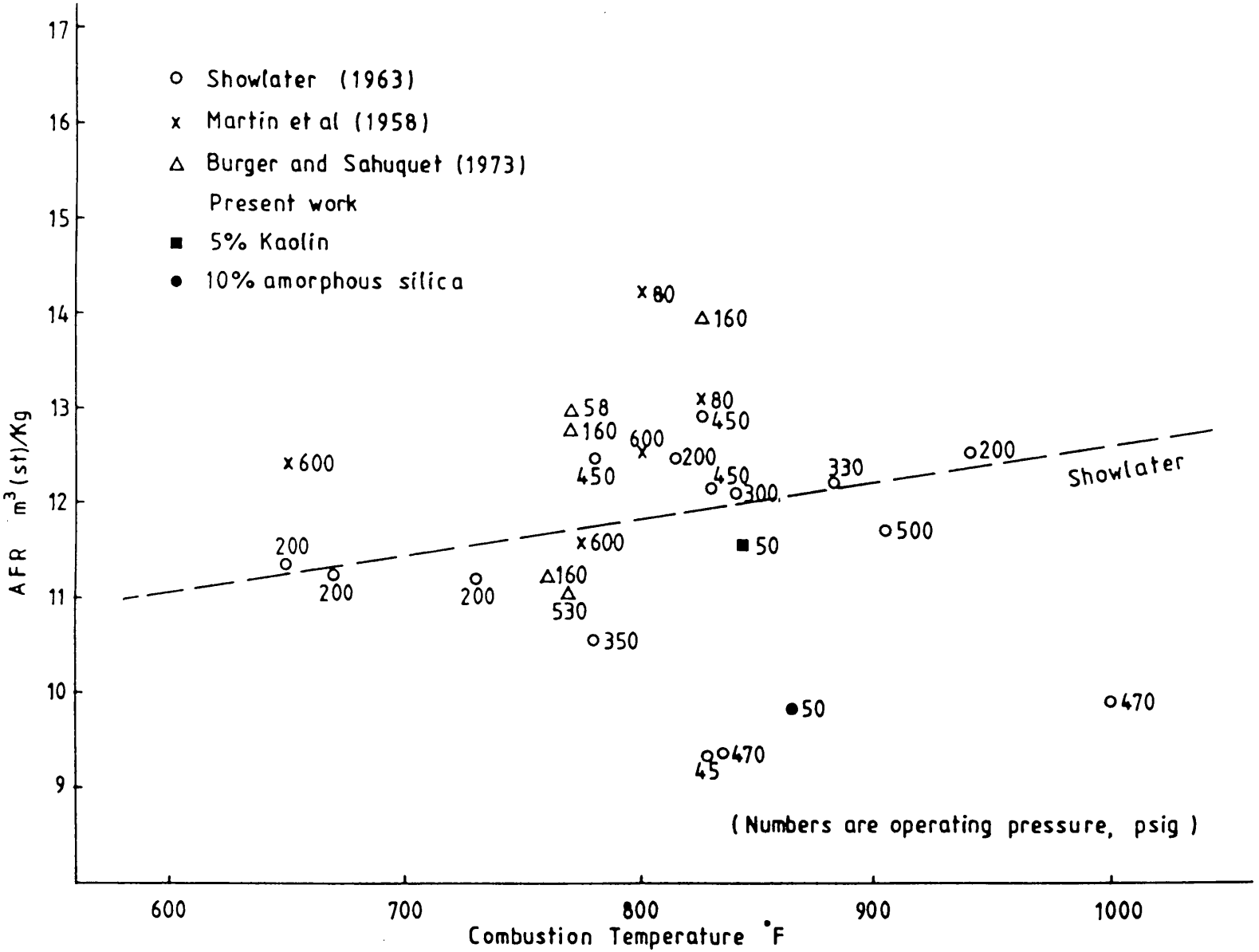

Figure 5.11 Air-fuel ratio (dry combustion).

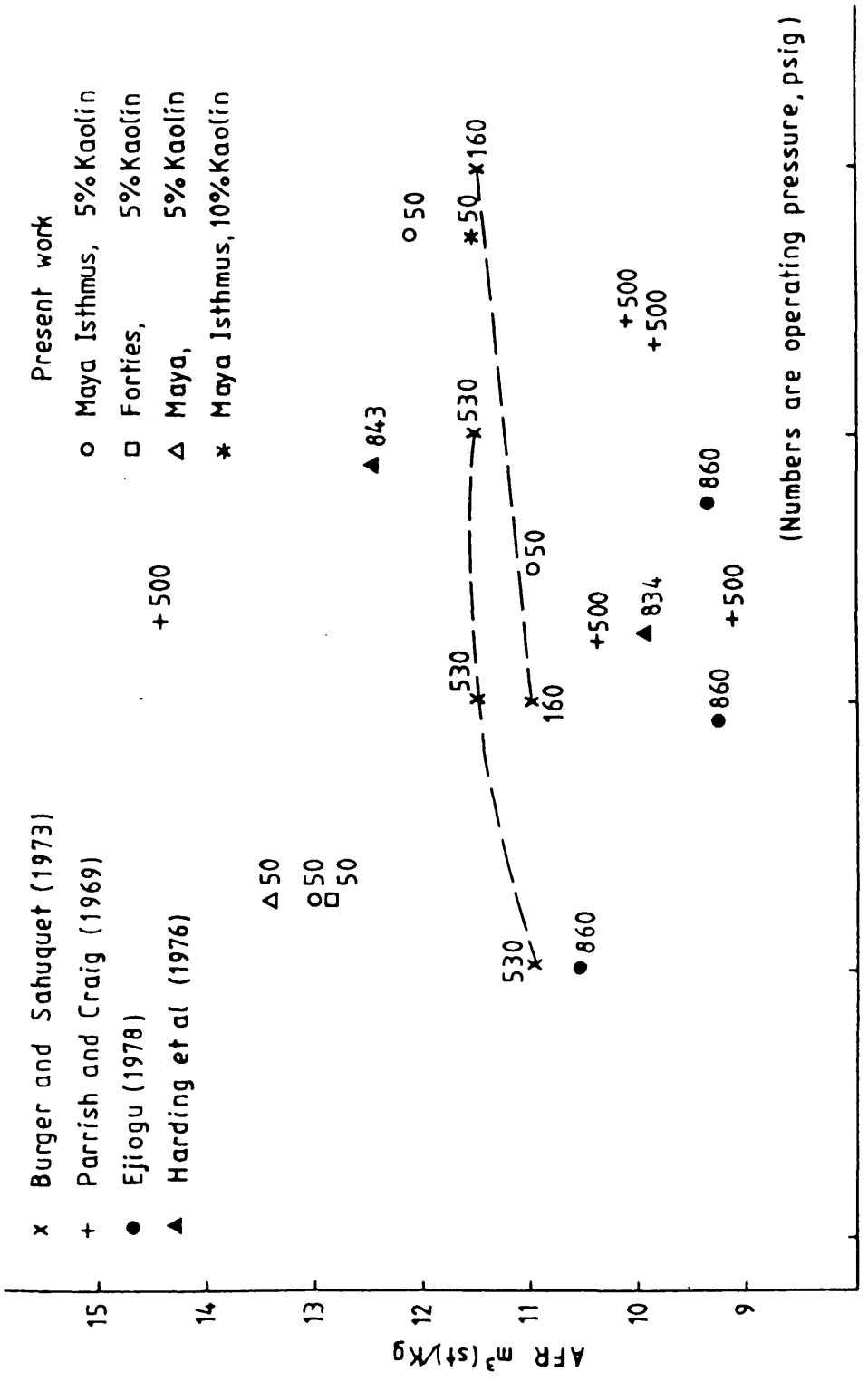

Figure 5.12 Air-fuel ratio (wet combustion).

values for the present work are higher with lower WAR ratios. However, when WAR > 2 m^3/Mm^3(STP), there is closer agreement with the trend of the results obtained by Burger and Sahuquet's results. Parrish and Craig (1969) and Harding (1976) published AFR data which are too scattered to show any significant trend and values obtained for AFR by Ejiogu in 1978 show a different trend to that of Burger and Sahuquet, decreasing as the WAR increases.

5.3 Other combustion parameters (stabilised and overall period)

Sand mixtures containing 10% amorphous silica exhibited high oxygen utilisation. The fuel consumption was also almost the same as that combusted in run No.1 with 5% kaolin. In an attempt to understand the mode of this behaviour, the carbon burning period is presented for the stabilised dry burning periods only (Table 5.4). This therefore assumes that the combustion front only advances when all of the available fuel is consumed. This raises some uncertainty, because the dry period for the wet runs is relatively small. However, it is obvious that the carbon burning rate is higher with the amorphous silica (run No.8), compared with the runs which contained 5% and 10% kaolin, even though the amorphous silica possesses a smaller surface area (2.0 m^2/g) than the kaolin (12–14 m^2/g). A similar trend was obtained by Guvenir (1980) in a combustion run with amorphous silica dust IMSIL-10 (1.42 m^2/g in surface area), but no definite explanation was given. Drici and Vossoughi (1984) have indicated that there is a reduction in the activation energy using amorphous silica (IMSIL-10) and other solid additives (silica sand, silica, alumina, kaolinite and montmorillonite) having different surface areas. They concluded that the surface area of solid additives affected the oxidation of the oil regardless of their chemical composition. In this respect, the effectiveness of the

Table 5.4

Combustion parameters for overall and stabilised periods

Run No.	Clay content (%)	WAR [m^3/Mm^3 (STP)]	^oAPI gravity	Carbon burning rate* (gm/h)	O_2 utilisation Stab.† (%)	O_2 utilisation Overall (%)	Av.apparent H/C ratio Stab.†	Av.apparent H/C ratio Overall	Fuel consumption Stab.† (kg/m^3)	Fuel consumption Overall (kg/m^3)	Heat of combustion Stab.† (cal/g_{CH_x})	Heat of combustion Overall (cal/g_{CH_x})
1	5	0.0	32.4	3.0	92.46	85.83	0.97	0.88	34.8	19.98	8511	8897
2	5	1.25	32.4	2.3	88.52	85.63	2.62	2.15	14.37	10.43	10555	10358
3	5	2.5	32.4	3.27	89.47	91.17	2.54	1.25	7.79	8.17	10177	8949
4	5	3.75	32.4	2.24	90.43	89.77	1.78	1.63	6.49	5.95	9341	9387
5	10	3.75	32.4	3.08	79.3	85.94	1.8	1.32	10.61	8.0	9782	9208
6	5	1.25	36.6	2.5	85.26	86.38	3.05	2.16	5.75	5.51	11352	10528
7	5	1.25	22.1	2.49	90.7	83.5	2.95	1.91	7.0	6.86	11176	9914
8	10 amorphous silica	0.0	32.4	3.64	97.69	95.85	0.27	0.51	24.0	18.57	7463	7937

*Carbon burning rate was calculated from the slope of plotting cumulative carbon burnt *versus* time according to Vossoughi *et al.* (1981).

†Stabilised values were calculated from programme (Appendix B).

solid additives depends on the nature of the surface and not on its availability, *i.e.*, surface area.

In Guvenir's discussion (1980), fuel deposition processes in porous media containing clays occur, due to the cracking of large hydrocarbon molecules within the intrapore space of the particles, which imposes a diffusional limitation. On the other hand, the fuel deposition process in amorphous silica mixture provides less resistance for oxygen diffusion, due to the larger pore diameter and smaller surface area.

Photographs taken by a scanning electron microscope are shown in Figures 5.13 and 5.14, with magnification of 1000 and 2000 respectively. These reveal the very porous nature of the surface of the amorphous silica, whereas the kaolin has a very distinctive plate-like structure (smaller pore diameter). The flocculation properties (aggregation) of clay minerals may also give rise to close particle packing with less accessibility to fluid. On the contrary, the more open structure of the amorphous silica makes it more accessible to fluid, *i.e.*, with less diffusional resistance. Then the oxygen which readily diffused into the pores might have been consumed totally upon contacting the carbonaceous fuel.

5.4 Production history

The cumulative liquid production history for the oil and water is presented in Figures 5.15-5.22 for each run. The density of the produced oil is also given in these plots.

In the case of dry combustion and runs with low WAR, there is an initial delay in water production. This is due to the low initial water saturation in the pack and the time required to produce a condensated water bank. However, as the WAR increases, this delay effect is reduced.

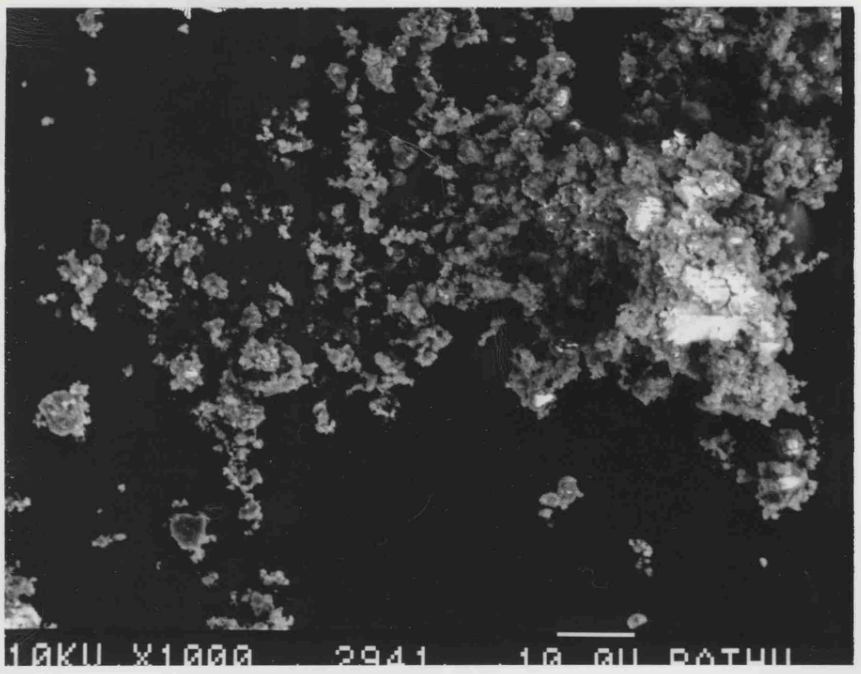

(a) amorphous silica

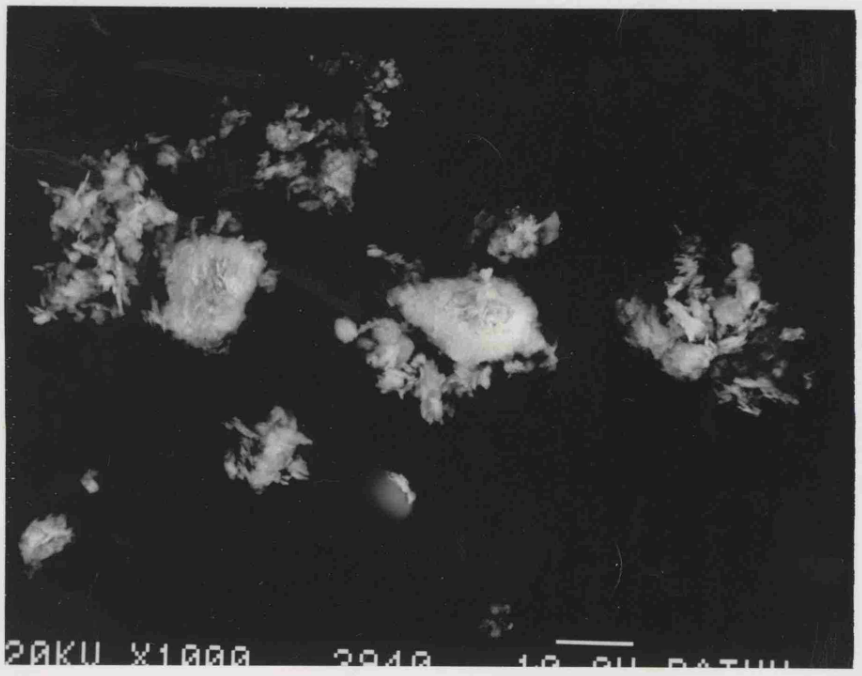

(b) kaolin

Figure 5.13 Scanning electron microscope photographs at 1000 magnification.

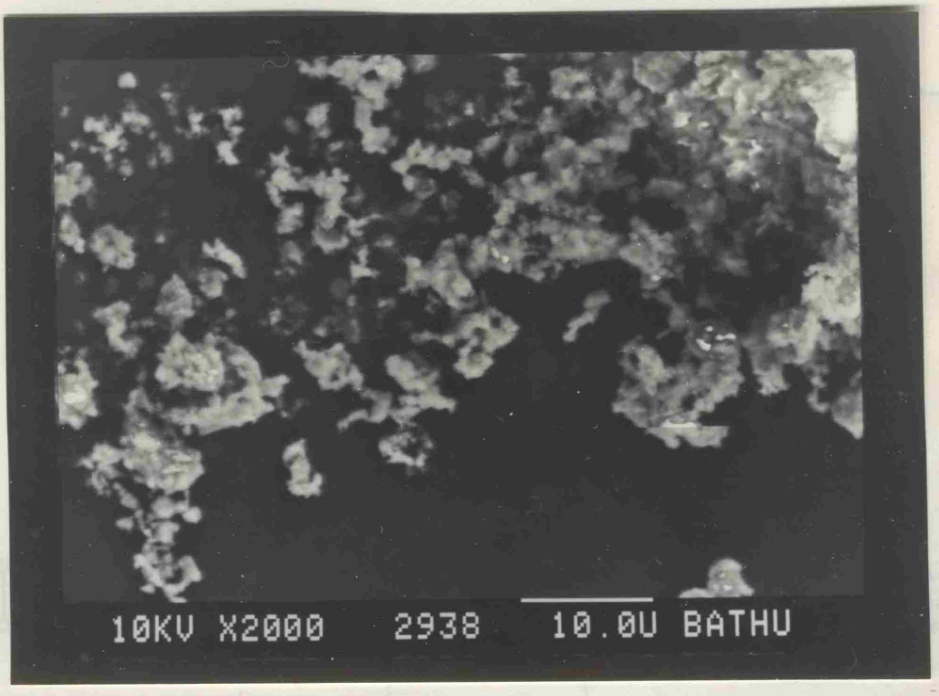

(a) amorphous silica

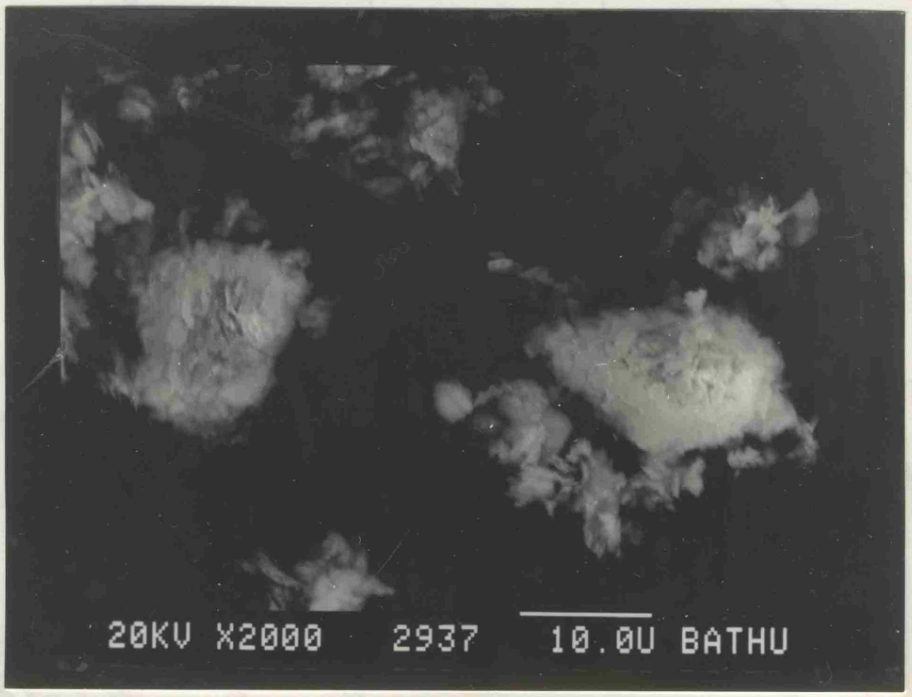

(b) kaolin

Figure 5.14 Scanning electron microscope photographs at 2000 magnification.

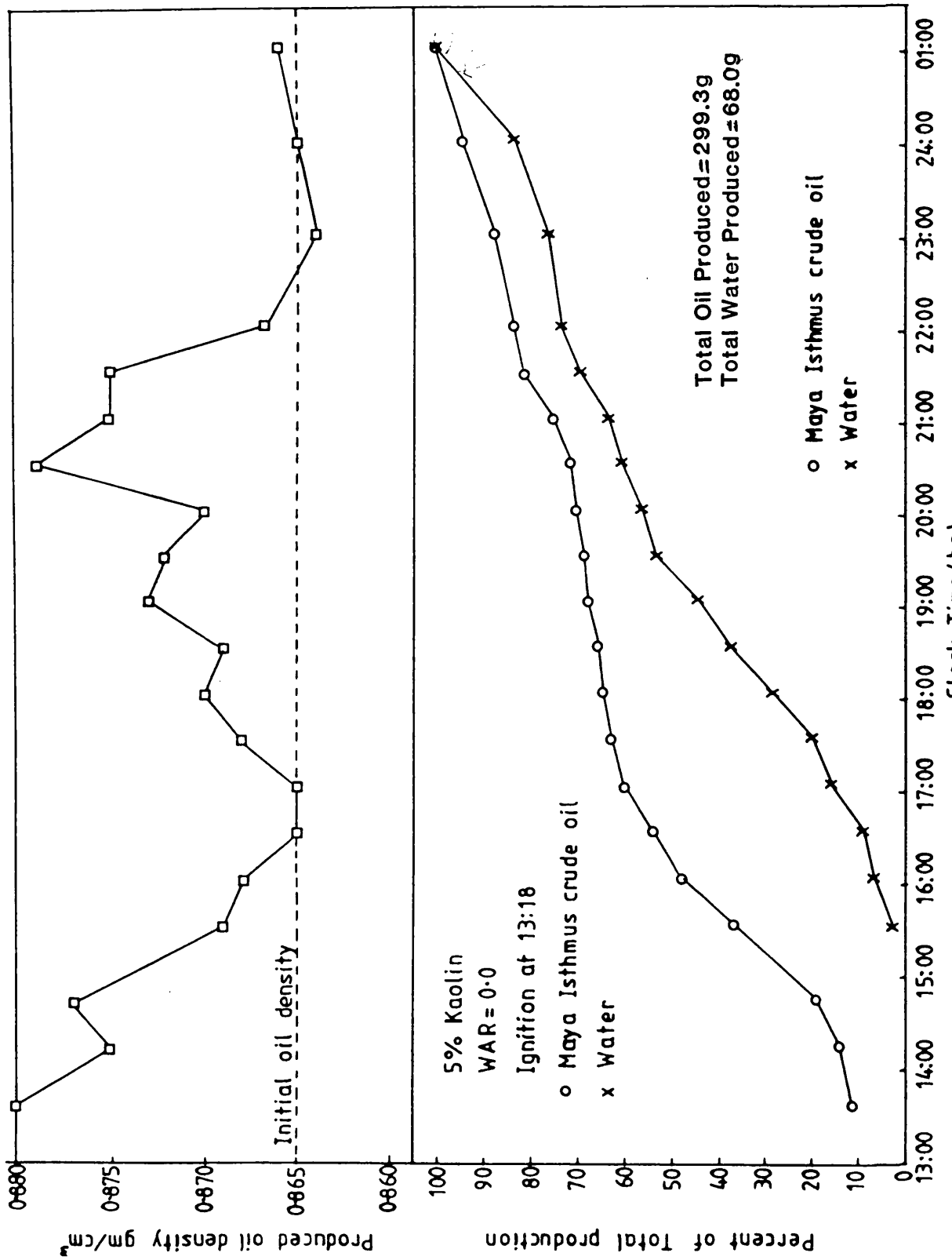

Figure 5.15 Cumulative production history and oil densities (run No.1).

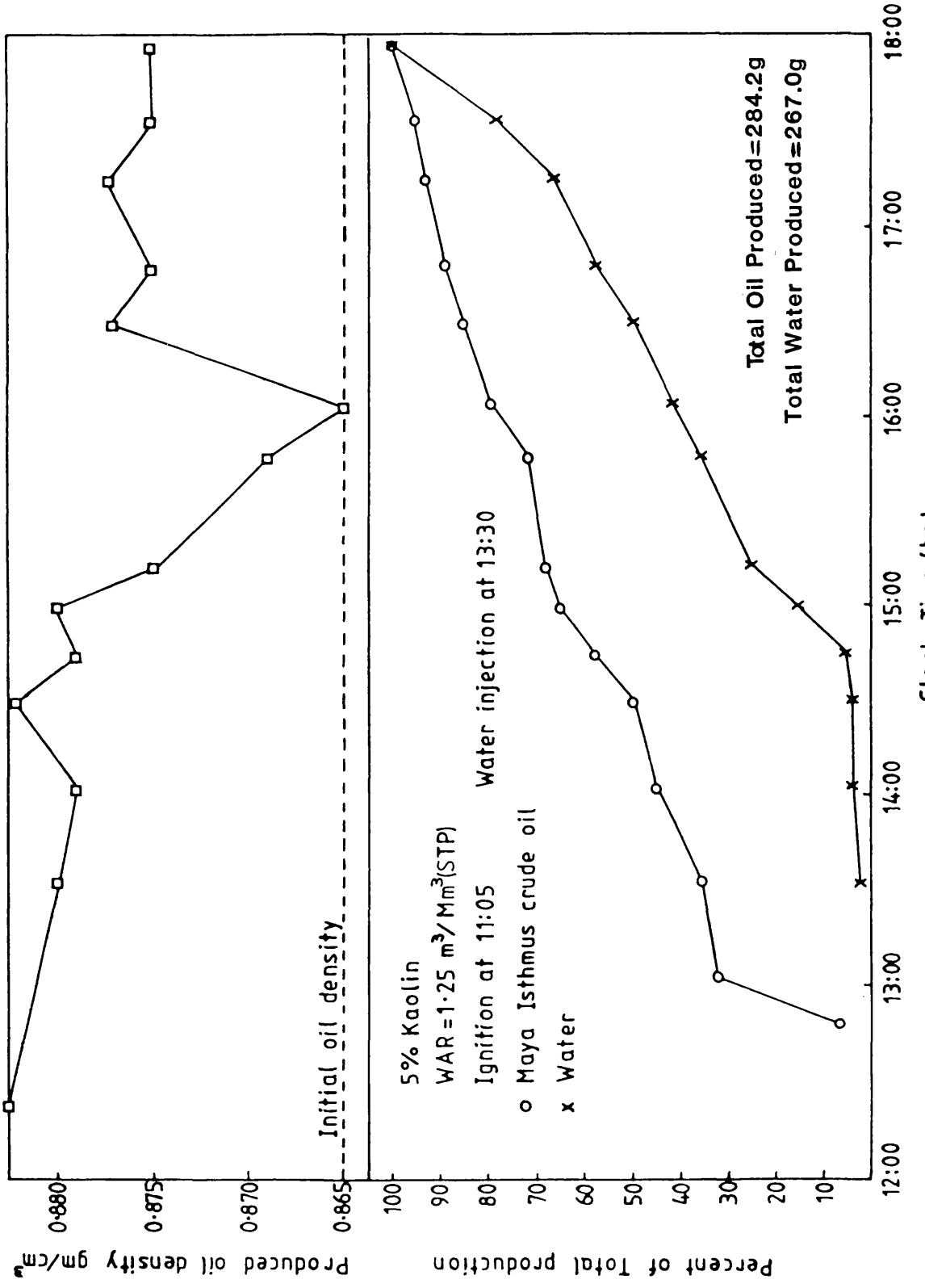

Figure 5.16 Cumulative production history and oil densities (run No.2).

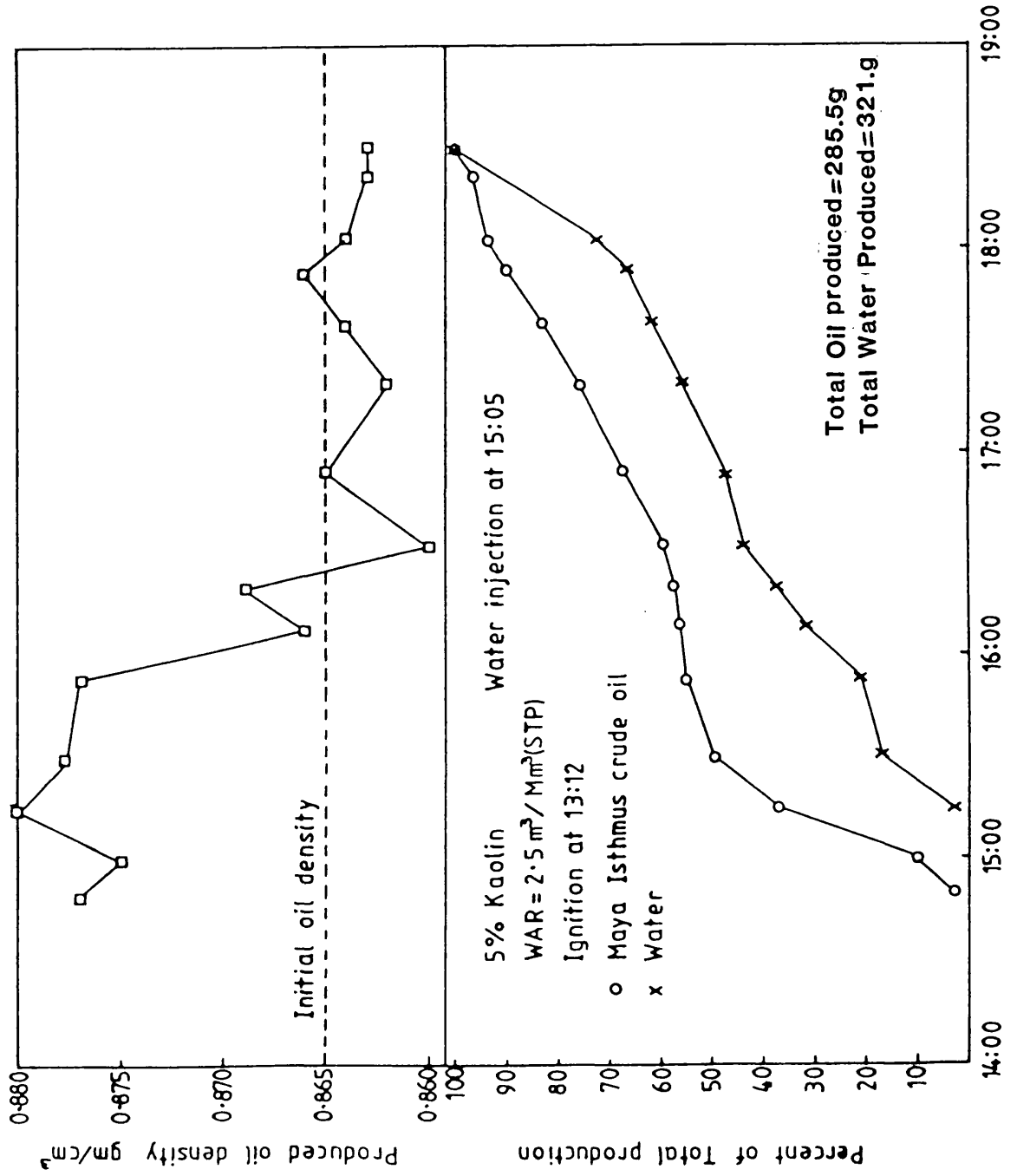

Figure 5.17 Cumulative production history and oil densities (run No.3).

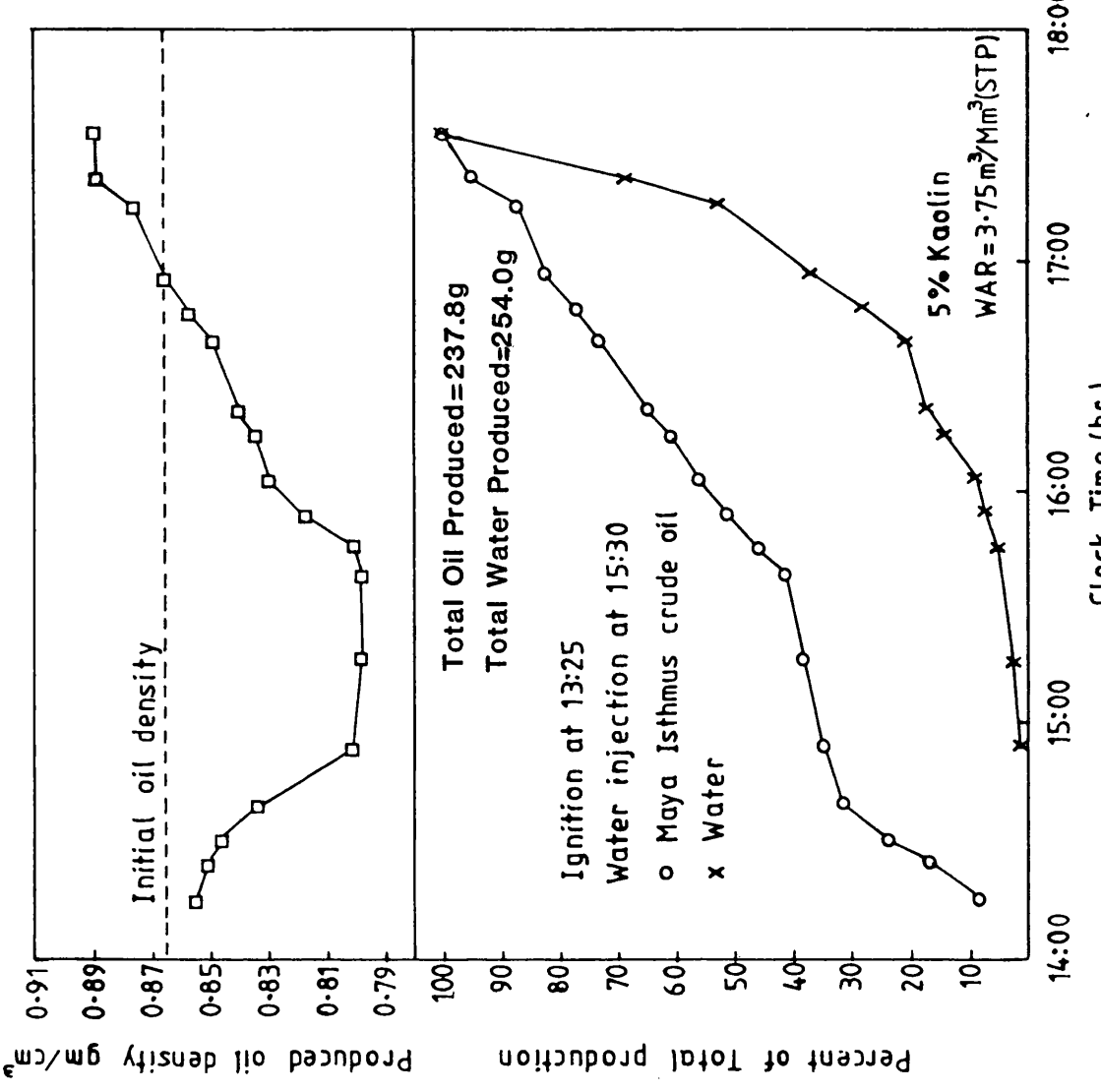

Figure 5.18 Cumulative production history and oil densities (run No.4).

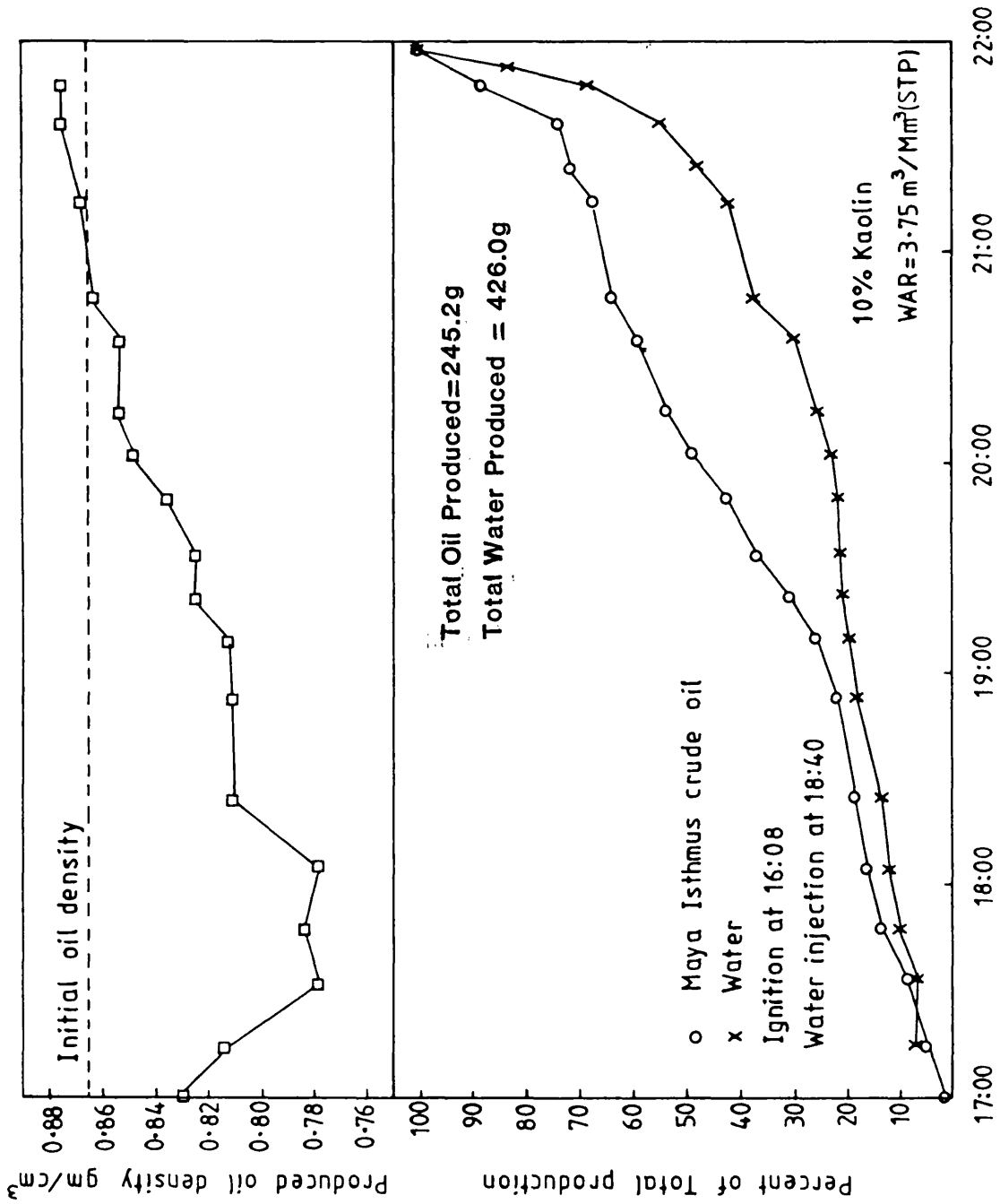

Figure 5.19 Cumulative production history and oil densities (run No.5).

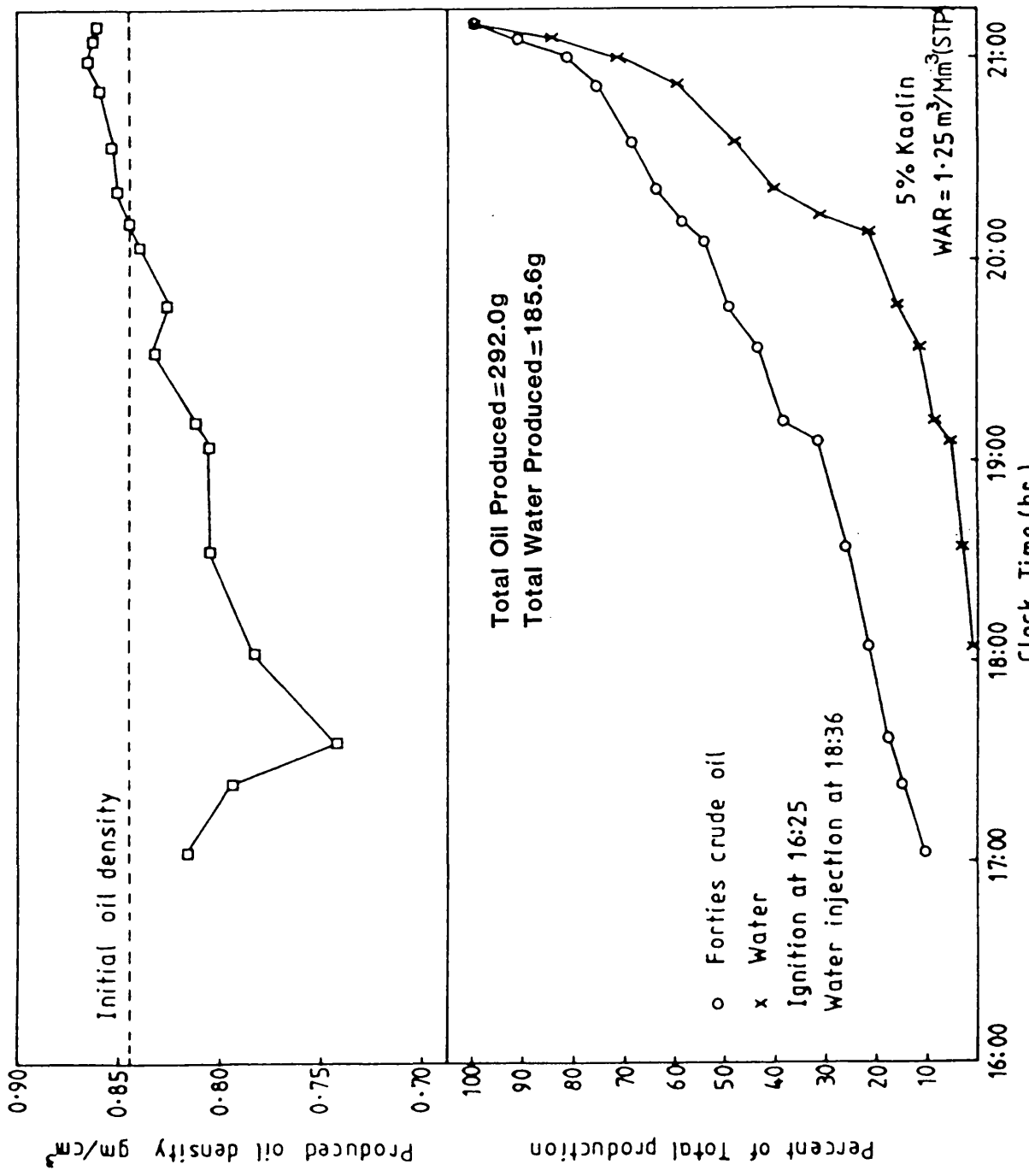

Figure 5.20 Cumulative production history and oil densities (run No.6).

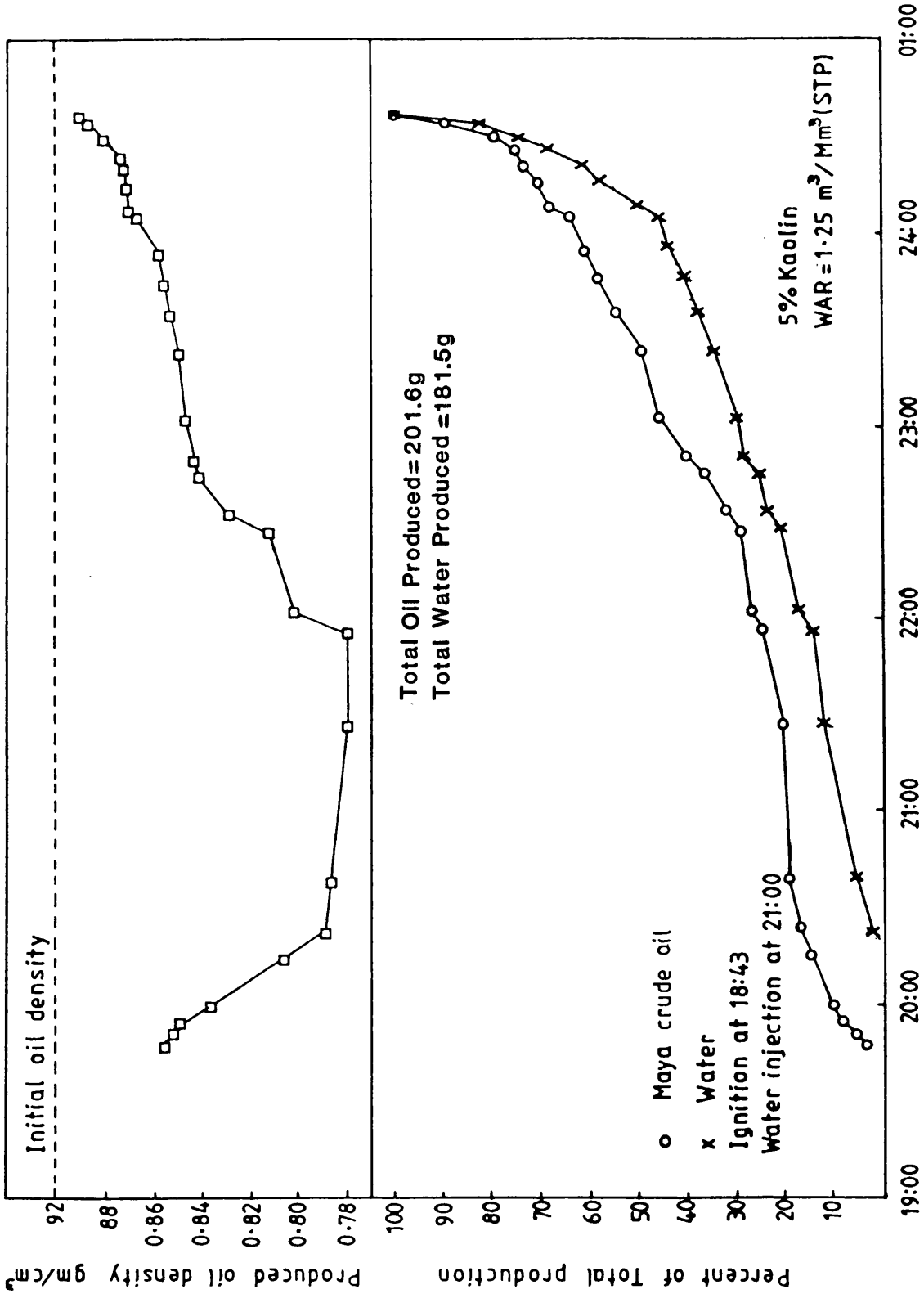

Figure 5.21 Cumulative production history and oil densities (run No.7).

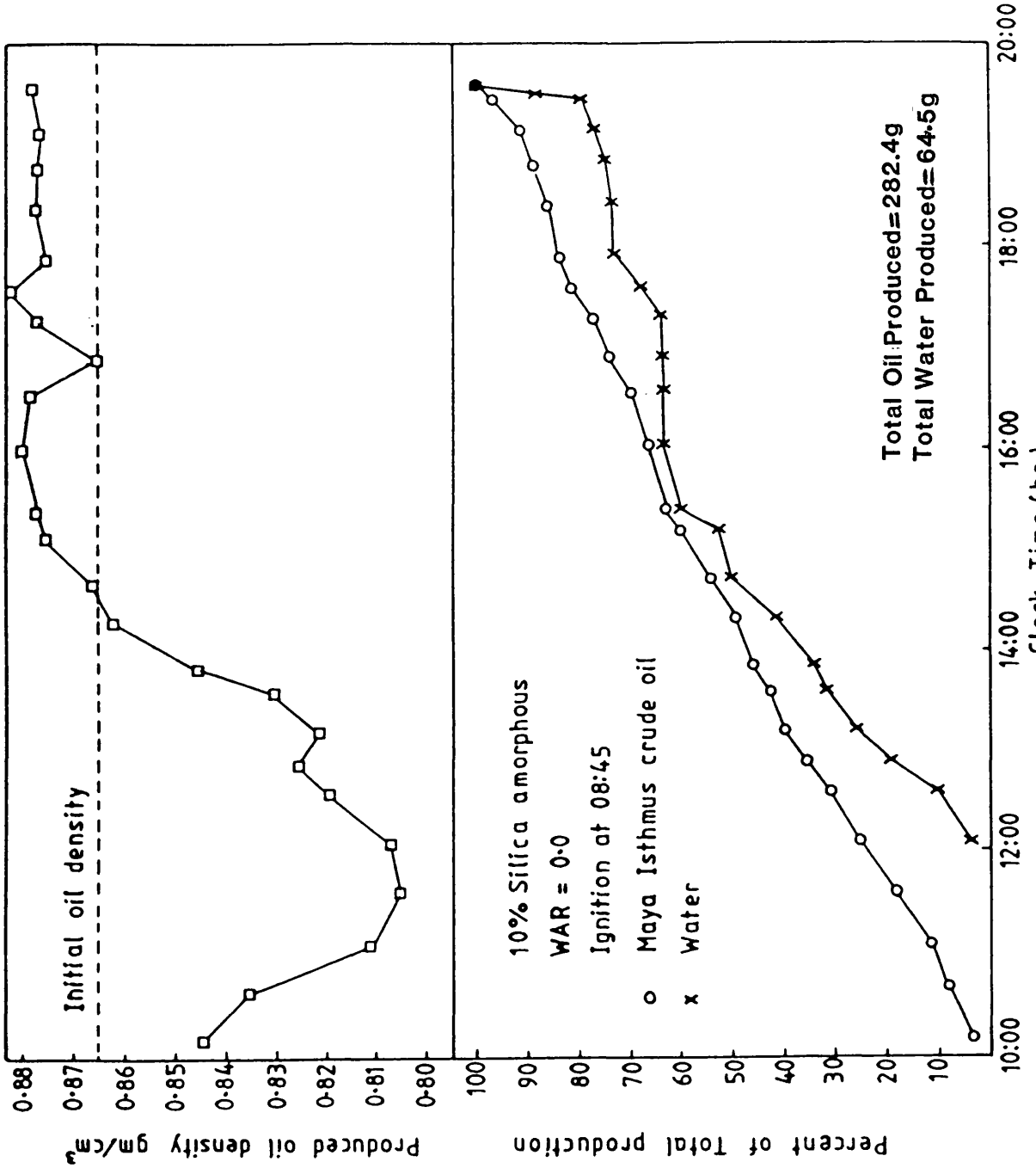

Figure 5.22 Cumulative production history and oil densities (run No.8).

The formation of an extended steam bank leads to efficient displacement of the oil, with consequent increase in oil production.

Stable emulsion and clay were produced for all the runs, except No.6, which was conducted with the Forties oil. Different crude oils have different tendencies to form emulsions, particularly heavy crudes. The latter are more susceptible to emulsification due to the presence of high molecular weight compounds and perhaps a high acid number. Severely emulsified oil samples were obtained with runs Nos. 1 and 2. These gave a produced oil density higher than that of the original oil densities shown in Figures 5.15 and 5.16. This emulsified density is included in the calculation of the oil recovery and will affect the AOR and the overall oil mass balance. This aspect will be discussed later.

Table 5.5 gives the oil recovery as a percentage of the original volume of oil-in-place for both the overall and stabilised periods. It also gives the highest API observed throughout each run. More oil is produced during the stabilised period of combustion, and this varies from 24 to 45 volume % of the OOIP. Also, in runs Nos. 1, 2 and 3, for Maya Isthums crude, the maximum API had approximately the same value as that of the original crude (°32.4). In runs Nos. 4, 5 and 8, higher values of API were obtained. For run No.6, using Forties crude, the produced API gravity decreased towards the end of the run. It also gave a high oil recovery of 79.3 volume % of OOIP. The heavy Maya crude gave the lowest oil recovery (57.2 volume % of OOIP) with API gravity higher than the original. This can be explained as follows: the light oil fractions produced by cracking and distillation are carried down-stream with the combustion gases and condense in the region of the combustion tube. At the same time, considerable amounts of heavy residual hydrocarbons are left unburnt, forming very viscous products in

Table 5.5

Oil recovery

Run No.	Initial crude oil °API gravity	Stabilised oil recovery (vol. % OOIP)	Overall oil recovery (vol. % OOIP)	Max. °API gravity of produced oil
1	32.4	45.2	82.6	32.3
2	32.4	39.6	74.4	32.0
3	32.4	24.2	74.7	33.0
4	32.4	20.8	65.0	45.8
5	32.4	29.3	67.3	50.3
6	36.6	28.5	79.3	58.4
7	22.1	13.7	57.2	49.9
8	32.4	22.7	75.1	44.3

the last residual coke zone of the combustion tube. This effect, coupled with severe emulsion, is the main reason for the large pressure drop and the low oil recovery with the heavy Maya crude.

Figure 5.23 is produced from Tables 5.2 and 5.5, to show the effect of WAR on the AOR ratio and the oil recovery (runs Nos. 1, 2, 3 and 4). It can be seen that the AOR ratio decreases with increasing WAR. Although initially rapid, the decrease becomes more gradual towards the highest WAR [3.75 m^3/Mm^3(STP)] investigated. The oil recovery, as a percentage of the OOIP, is apparently at its maximum when WAR = 0.0 (run No.1) and decreases with increasing WAR. However, this is likely to be in error, because of the emulsification problem mentioned previously. The trend towards lower oil recovery with higher WAR has also been reported by Ejiogu (1978). This suggests that maximum oil recovery does not necessarily occur when the size of the steam zone is at a maximum.

In a study of the effect of WAR on the oil recovery and the amount of fuel burned, Alderman and Osoba (1971) found an increase in oil production with a corresponding decrease in fuel consumption. Oil recoveries varied from 60.8% to 76.8% of OOIP. In the combustion test reported by Sterner and Wertman (1976), the oil consumed as fuel was 43.7% weight of OOIP, the lowest being 35.1% oil recovery for the Pensylvania crudes of 32.1 and 44.3 °API gravity.

5.5 Oil and water mass balances

The oil mass balance is determined from the amount of oil originally in the pack, the fuel burned and the residual oil saturation. The amount of vaporised hydrocarbons produced is mostly in the form of methane. The concentrations are too low to have any significant effect on the mass balances. An example of the calculation of the oil and water mass balance

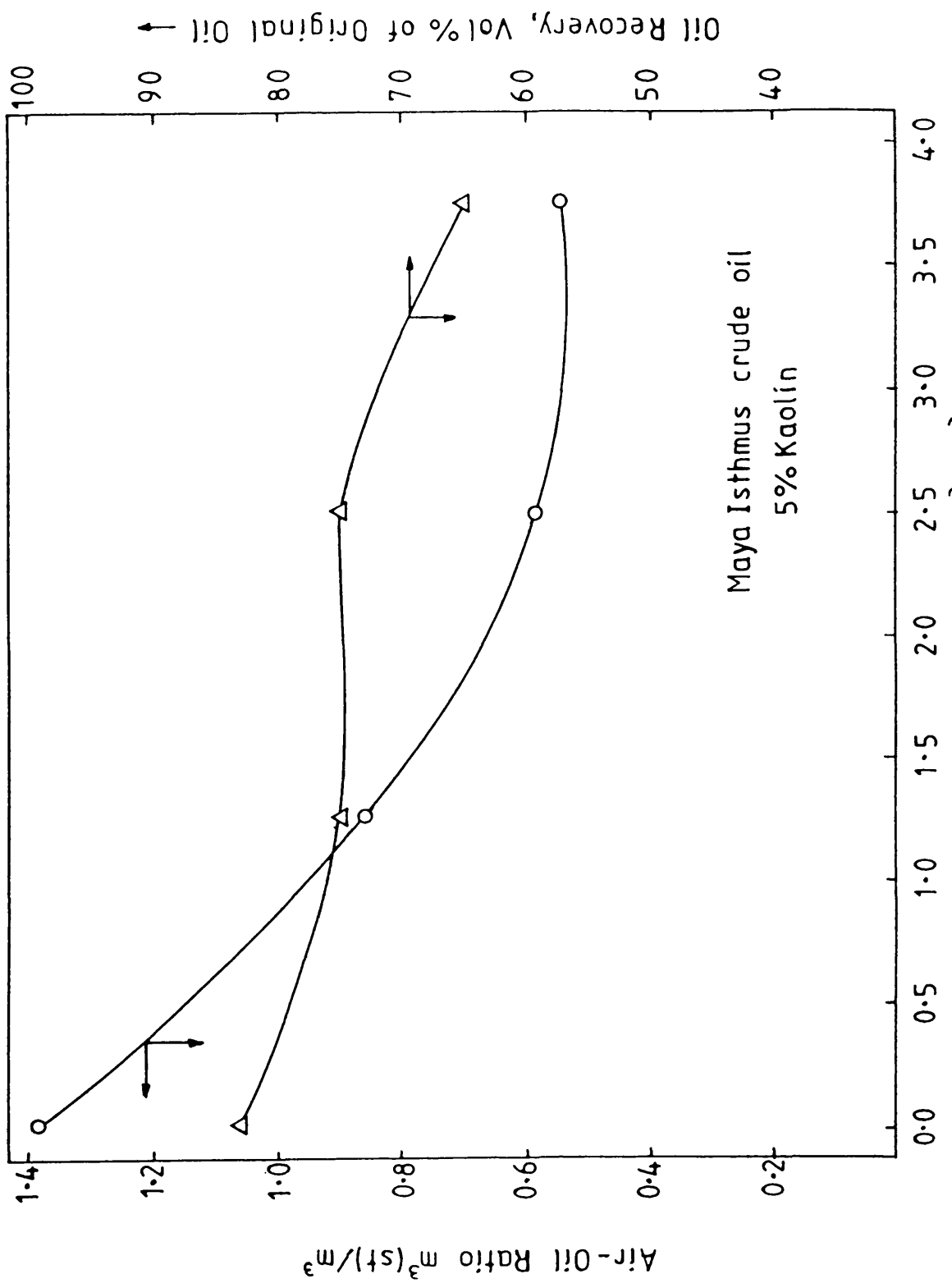

Figure 5.23 Oil recovery and air-oil ratio against injected water-air ratio.

is given in Appendix C2. A summary of the oil and water mass balances for each run is presented in Table 5.6. The differences in the oil balances varies from 0.86 to 9.7% respectively. It can be seen from Table 5.6 that the differences in the water balances are higher for the combustion runs where the calculated oil weight is more than the initial oil in the pack (runs Nos. 1, 3 and 7). This is mainly due to the difficulties experienced in separating the water from the oil-clay emulsion produced and also to other cumulative errors, which will be discussed later.

It is very interesting to note that the percentage of unburnt fuel (residue) increases with the water:air ratio, whereas the fuel burned (consumed) decreases with WAR (runs Nos. 1, 2, 3 and 4). The residual water saturation also increases with WAR, as in runs Nos. 1, 2, 3 and 4.

In run No.5, in which the porous media contained 10% kaolin, the unburnt fuel as a percentage of the total calculated weight is lower than that of run No.4 with 5% kaolin. However, the fuel burned is higher for the same WAR. In run No.5, there is an error of 9.7% in oil mass balance and 11.8% in the water mass balance. Again, this is mainly attributed to high clay production and its effect on the density of the produced oil.

In run No.7, for Maya crude, the difference in the oil balance is 23 g, which represents 6% of OOIP and less water is produced during the experiment. The oil residue amount is 46.5% of the total amount of calculated oil, which gives a very low recovery, as mentioned previously. The composition of the Maya crude (high carbon residue and asphaltene content - see Table 3.4), is thought to be the reason for this low recovery efficiency. McKay (1982) has pointed out that the amount of produced oil appears to be a function of the composition of the original oil-in-place, as well as the displacement mechanism.

Table 5.6

Overall oil and water mass balances

OIL	Run 1	Run 2	Run 3	Run 4	Run 5	Run 6	Run 7	Run 8
Oil content of sand pack (gm)	359.93	376.86	380.42	374.7	380.54	374.8	384.72	380.9
Fuel burned (wt %)	10.87	6.04	4.63	3,62	4,9	3.45	3.66	11.23
Unburnt fuel (wt %)	9.69	15.3	20.95	30.31	23.75	12.17	46.5	10.27
Oil produced as liquid (wt %)	79.45	78.65	74.4	65.92	71.35	84.12	49.39	78.5
Oil produced as vapour (wt %)	-	-	-	0.157	-	0.234	0.44	-
Average produced oil density (gm/cm^3)	0.8704	0.876	0.8686	0.8436	0.8278	0.828	0.8422	0.8534
TOTAL	376.87	361.296	383.7	360.858	343.65	347.0	407.8	359.71
Weight difference (gm)	-16.947	15.563	-3.28	13.846	37.0	27.82	-23	21.18
Error (%)	4.7	4.13	0.86	3.7	9.7	7.42	6.0	5.56
WATER								
Initial water content of sand pack (gm)	59.5	60.8	61.5	61.0	61.84	60.5	62.0	61.5
Water injected (gm)	-	264	323	348	510	141.0	210	-
Water formed by combustion (gm)	25.22	29.876	15.196	14.056	15.054	16.46	18.523	14.858
Total amount of water (gm)	84.72	354.74	400.0	374.056	587.0	217.96	290.52	76.355
Water produced as liquid (wt %)	91.7	84.65	84.9	72.42	82.3	86,6	74	92.2
Residual water in pack (wt %)	5.32	14.93	14.85	27.36	17.7	13.2	25.62	5.2
Water produced as vapour (wt %)	3.03	0.414	0.244	0.203	0.182	0.336	0.376	2.73
TOTAL	74.26	315.97	278.65	350.747	517.6	214.26	245.31	70.0
Weight difference (gm)	10.46	38.77	21.3	23,3	69.0	3.7	45.22	6.35
Error (%)	12.34	10.93	5.34	6.23	11.8	1.5	15.56	8.32

In the case of dry combustion runs (Nos. 1 and 8), the residue (fuel unburned) was calculated for the last zone (coke zone) only, while clean sand was left in the swept pack.

5.6 Overall mass balance consideration

The cumulative air injected (moles) as measured by the inlet rotameter, differed from that of the produced gas, which was measured by the wet test meter, under standard conditions. This indicated that more gas was fed to the combustion tube, which was varied from 12 to 26% in different runs. This difference is believed to be the result of a cumulative error. Part of this error is due to the difference between the volume of the injected air and that of the gas produced according to stoichiometric considerations. This difference was referred to as a gas shrinkage, which, according to Penberthy (1965), amounted to about 4.2%. Ejiogu (1978) and Harding (1976) have also reported a difference of 11.4 and 20% by volume respectively, between the inlet injected air and the produced gas. They considered the gas shrinkage of 4.2% to be a part of this error. Showalter (1963) indicated that the produced gas volume will usually be smaller than the corresponding injected air volume, as a result of the fact that some of the O_2 is used in the formation of water. This effect is offset to a degree by the fact that 1 mole of O_2 will produce 2 moles of CO, but the CO content of produced gas is usually so small that the net effect is a produced gas volume, which is less than the injected air volume at standard conditions. However, after careful consideration of the overall stoichiometry, calculations were carried out for both overall and instantaneous difference values. Table 5.7 shows the overall difference between the calculated moles of air injected (consumed) and the

Table 5.7

The overall difference between the air consumed (mole) and the number of moles of gas produced, based on the measurement by the wet test meter

Run number	Overall difference (%)	Overall average H/C ratio	Overall average CO/CO_2 ratio
1	2.95	0.88	0.195
2	4.99	2.15	0.435
3	2.97	1.25	0.4
4	3.48	1.63	0.37
5	3.02	1.32	0.33
6	4.99	2.16	0.345
7	3.14	1.91	0.325
8	0.95	0.51	0.194

total moles of gas produced, based on the wet test meter measurement, as well as the average overall H/C ratio and CO/CO_2 ratio. Instantaneous difference values are given in Appendix D. It can also be seen from Table 5.7 that the difference percentage is higher when the H/C and CO/CO_2 ratio is high. This, in turn, is strong evidence of LTO reactions occurring. Furthermore, a simple stoichiometric calculation is given in Table 5.8 for run No.2 as an example. Since nitrogen is not involved in any of the reactions, *i.e.*, the moles of N_2 in are equal to the moles of N_2 out, the only difference will be in the O_2 balance. The moles of O_2 disappeared are assumed to be used in the formation of water. Therefore, in order to substitute that difference in the O_2 balance, the known number of O_2 moles used in H_2O formation is added to the total moles of O_2 in the produced gases. As a result, the error in the O_2 balance is a negative value, which probably means that more CO is produced during the LTO reaction.

The need for frequent bleed-off gas during sampling from the separator was especially problematical when using the heavy Maya crude in run No.7, due to the difficulty in recognising that the liquid level is also attributed to the cumulative error in the gas balance. Manual adjustment of the inlet air flowrate, in order to maintain constant air flux, also introduced some error. Any approximation in the calculation of the mole fraction of each gas component will have introduced small errors in the measured data and consequently in the gas balance.

The main difficulty with regard to the liquid mass balance is associated with the problem of separating the oil-water emulsions formed, especially in runs Nos. 1 and 2. The separation is affected by the amount of clay which is produced with the oil. Clay production was worse at high water injection rates and as the clay content increased,

Table 5.8

Overall stoichiometric material balance for run 2

	Cumulative air injected (moles) = 11.762 (calculation based on the wet test meter)						Cumulative gas produced (moles) = 11.177 (measured by the wet test meter)				
Compound	Mole fraction (%)	No. of moles	Atoms C	Atoms H	Atoms O	Atoms N	No. of moles	Atoms C	Atoms H	Atoms O	Atoms N
N_2	79	9.292	-	-	-	18.584	9.2915	-	-	-	18.583
O_2	21	2.47	-	-	4.94	-	0.3564	-	-	0.7128	-
CO							0.42	-	-	0.42	-
CO_2							1.0916	-	-	2.1832	-
TOTAL					4.94(1)*	18.584				3.316(2)*	18.583

*No. of moles of H_2O formed by combustion = 1.66, therefore no. of O_2 moles disappeared = 1.66.(3)

Total O_2(4) = (2) + (3) = 4.976 mole.

Difference on O_2 balance = $\frac{(1) - (4)}{(1)} \times 100 = -0.73\%$.

Difference in N_2 balance = 0.0

so did the migration of fines. Similar effects were obtained with silica powder in run No.8 (10% amorphous silica). Because of the low density of this material (1.13 gm/cm^3), it is easily displaced by the flowing fluid, even under a dry combustion condition. No problems were encountered in separating liquid samples for the light Forties crude in run No.6.

It is almost impossible to eliminate the inaccuracy introduced in the handling of the produced liquids, since they have to be transferred continuously to small centrifuge tubes. However, the latter was avoided when sampling directly from the separator by centrifuge tubes during the operation of runs Nos. 7 and 8. It is important to ensure that the liquids in the production line are completely displaced. This was achieved by disconnecting the lines and displacing the oil with nitrogen. This method avoided any disturbance of the residual liquid remaining in the sand pack.

The amount of water produced as a vapour was based on the assumption that the exit gas was saturated with water vapour at 0 °C. As mentioned previously (Chapter 3), the uncontrollable high steam production gave rise to difficulties in the operation, as well as in the cooling of the production line. Frequent supplies of ice were needed to cool down the condenser and the production line. Therefore, special care should be taken in the operation of combustion runs with high water injection rates.

As mentioned earlier, errors in the gas chromatography analysis could lead to inaccuracies in the amount of fuel burned and also in the hydrocarbons which were produced as gas.

In the determination of water and oil residues using the extraction method, some error is introduced unless the sample is representative of the bulk volume from which it has been taken. Also, some clay loss

results when the samples were flushed with toluene. The same argument applies to the determination of the coke in the post-burn samples. There is a loss on ignition of the kaolin of about 12% (see Table 3.3, Chapter 3). This introduces an error of 1.2% for a 100 g coke sample, containing 10% kaolin. This assumes that the coke sample contained the initial weight percentage of kaolin, but it could be affected by migration of the clay fines, which would tend to accumulate in the last coke zone.

The material balances demonstrate a reasonable level of accuracy having been achieved, in line with other results reported in the literature. No production history or mass balance information was presented by Guvenir (1980), due to difficulties in separating the viscous oil-water-clay emulsions. Values obtained for the present work show discrepancies ranging from 0.86 to 9.7% in the oil mass balances, and 1.5 to 15.56% in the water mass balance. Values reported by Ejiogu (1978) show discrepancies ranging from 2.67 to 14.03% in the oil mass balances and 1.97 to 3.62% in the water mass balances. Oil recoveries ranged from 68.3 to 84% by weight of OOIP. Harding (1976) reported an oil recovery of 60.34 and 87.23% for the Athabasca bitumen, with a discrepancy of 1.98 to 12.12% in oil mass balances and 5.2 to 9.15% in water mass balances.

Conclusions

The conclusions to be drawn from the data presented in this chapter are as follows:-

1. For sand packs containing 5% kaolin, the air requirement (per m^3 of sand pack) decreases with increasing WAR. The AOR also decreases initially, but then levels off as WAR is increased further. Increasing the kaolin content to 10% leads to higher values of both air requirement and AOR.

2. The overall trend of AFR values shows an increasing effect with increasing WAR. For WAR > 2.0 m^3/Mm^3 (STP), there is a reasonably close agreement with the trends shown in the results obtained by Burger and Sahuquet (1973), but AFR values obtained at lower WAR's depart significantly from this. The higher AFR was obtained with the heavy Maya crude oil at a water injection ratio of 1.25 m^3/Mm^3 (STP).

3. Oxygen utilisation and also carbon burning rate are higher in porous media containing 10% amorphous silica, compared with those containing kaolin. This is because the amorphous silica has a more open crystalline structure, which provides less resistance for oxygen diffusion.

4. The North Sea oil Forties (36.6 °API) gave the highest oil recovery at 79.3 % by volume of the original oil in place, whilst the heavy Mexican Maya oil (22.1 °API) gave the lowest recovery value of 57.2 % , for the normal wet combustion mode.

CHAPTER 6

RECOMMENDATIONS

1. In order to study combustion effects at high water-air ratios [WAR > 2.5 m^3/Mm^3(STP)], it will be necessary to use either a longer combustion tube or higher pressure. With the present length of combustion tube and low operating pressure, the transition to partially quenched combustion occurs at relatively low values of WAR.

2. Detailed studies should be undertaken of the kinetics of wet combustion using TGA, DSC and also combustion cell tests, particularly to investigate surface area and catalytic effects when other materials are incorporated into the sand matrix. The nature of the surface of solid additives could be studied by scanning electron microscopy using samples which have been burned isothermally (combustion cell).

3. The range of material additives should be extended to include those which have larger and more active surface areas, such as illite and montmorillonite. Comparison with reservoir rock material should be undertaken, but this will involve detailed identification and characterisation of the constituent (clays, *etc.*) and properties of the rock. The increased swelling tendency of montmorillonite, for example, may cause permeability restriction, but this could be offset using higher water salination.

4. More extensive studies using heavier crude oils (API < 15°) should be made to investigate fuel deposition and the ability to achieve self-sustained combustion without addition of clays, *etc.* to the sand matrix.

5. Adiabatic temperature control could be improved by installing band heaters along the length of the combustion tube. Very close control of the temperature should be achieved, since adiabatic conditions imply that no heat is lost to the surroundings and no heat is added to the system, except from combustion.

6. A semi-automation system is quite feasible for temperature control and data collection. An automatic control of inlet flowrate could be used to achieve a more precise control and consequently the desired air flux.

7. Modified techniques could be used to collect liquid samples from the separator by means of a sampling bomb, provided that gaseous components are injected through the wet test meter. This would avoid disturbance of the process and eliminate errors introduced in the overall mass balance due to flushing of gases.

REFERENCES

Aalund, L. (1983), "North sea crudes: Flotta to Thistle", *Oil and Gas J.*, 6th June, pp.75-79.

Alderman, J.H. and Osoba, J.S. (1971), "A study of oil recovery *in situ* combustion with the addition of water", SPE paper 3684, SPE of AIME 42nd Annual California Regional Meeting, Los Angeles, (4-5 November).

Alexander, J.D., Martin, W.L. and Dew, J.N. (1962), "Factors affecting fuel availability and composition during *in situ* combustion", SPE 296 Production Research Symp., Tulsa, Oklahoma, April.

Al-Saadoon, F.T. (1970), "An experimental and statistical study of residual oil saturation after gas, water and steam drive, and fuel availability for the *in situ* combustion process", PhD Thesis, University of Pittsburgh.

Anthony, M.J., Taylor, T.D. and Gallagher, B.J. (1982), "Fire-flooding in a high-gravity crude in a watered-out West Texas sandstone", *J. Pet. Tech.*, 34, (10), (October) pp.2244-2250.

Aymx, J.W., Bass, D.M.Jr. and Whiting, R.L. (1960), "Petroleum Reservoir Engineering", McGraw-Hill Book Company Inc. (New York).

Bae, J.H. (1977), "Characterisation of crude oil for fire-flooding using thermal analysis methods", *Soc. Pet. Engr. J.*, (June) pp.211-218

Bailey, H.R. and Larkin, B.K. (1960), "Conduction-convection in underground combustion", *Trans.AIME*, 219, pp.321-331.

Bousaid, I.S. (1967), "Oxidation of crude oil in porous media", PhD Thesis, Texas A & M University.

Bousaid, I.S. and Ramey, H.J.Jr. (1968), "Oxidation of crude oil in porous media", *Soc. Pet. Engr. J.*, (June) pp.137-148.

Buesse, H. (1971), "An experimental investigation of the formation of fuel in underground combustion oil recovery", *Erd. Erdgas Zeitschrift*, 87, (12), (December), p.414 (in German).

Burger, J.G. and Sahuquet, B.C. (1972), "Chemical aspects of *in situ* combustion - heat of combustion and kinetics", *Soc. Pet. Engr. J.*, 12, (5) (October), pp.410-422.

Burger, J.G. and Sahuquet, B.C. (1973), "Laboratory research on wet combustion", *J. Pet. Tech.*, 25, (16), (October) pp.1137-1146.

Burger, J.G. (1976), "Spontaneous ignition in oil reservoirs", *Soc. Pet. Engr. J.*, (April) pp.73-81.

Buxton, T.S. and Craig, F.F.Jr. (1972), "Wet *in situ* combustion aid recovery of oil, AICHE told", *Oil and Gas J.*, 3rd April, pp.50-53.

Buxton, T.S. and Craig, F.F.Jr. (1973), "Effect of injected air-water ratio and reservoir oil saturation on the performance of a combination of forward combustion and water-flooding", AICHE Symp. Ser., No.127, 69, pp.27-30.

Computer Modelling Group (1982), "Computer simulation of thermal enhanced oil recovery schemes", Calgary, Alberta, Canada and the Oil Recovery Division, AEE Winfrith, England, Dorchester, England, June (Section 10).

Dabbous, M.K. (1971), "*In situ* oxidation of crude oils in porous media", PhD Thesis, University of Pittsburgh.

Dabbous, M.K. and Fulton, P.F. (1974), "Low temperature oxidation reaction kinetics and effects on the *in situ* combustion process", *Soc. Pet. Engr. J.*, 4, (3), (June) pp.253-262.

Dietz, D.N. and Weijdema, J. (1968), "Wet and partially quenched combustion", *J. Pet. Tech.*, 20, (4), (April) pp.411-415.

Drici, O. and Vossoughi, S. (1984), "Study of the surface area effect on crude oil combustion by thermal analysis techniques", 13th Ann. Conf. North American Thermal Analysis Soc., (September 23-26), Philadelphia, Penn.

Emery, L.W. (1962), "Results from a multi-well thermal-recovery test in Southeastern Kansas", *J. Pet. Tech.*, 14, (6), (June), 671.

Ejiogu, G.C. (1978), "Wet combustion - a tertiary recovery process for light oil", MSc Thesis, University of Alberta, Calgary, Canada.

Ejiogu, G.C., Bennion, D.W., Moore, R.G. and Donnelly, J.K. (1979), "Wet combustion - a tertiary recovery process for the Pembina Cardium reservoir", *J. Can. Pet. Tech.*, July-September, Montreal, pp.58-65.

Fassihi, M.R., Ramey, H.J. and Brigham, W.E. (1980a), "The frontal behaviour of *in situ* combustion", SPE paper 8907, 50th Ann. California meeting Soc. Pet. Engrs AIME, Los Angeles, California, April (9-11).

Fassihi, M.R., Brigham, W.E. and Ramey, H.J. (1980b), "The reaction kinetics of *in situ* combustion", SPE paper 9454, 55th Ann. Tech. Conf. and Exhibition Soc. Pet. Engrs AIME, Dallas, Texas, September (21-24).

Fassihi, M.R., Brigham, W.E. and Ramey, H.J. (1984), "Reaction kinetics of *in situ* combustion: Part 2 - modelling", *Soc. Pet. Engr. J.*, (August) pp.408-416.

Fuchida, T. (1959), "Laboratory and field experiments on fire-flooding recovery methods", *Prod. Monthly*, 23, (9), pp.30-35.

Fulton, R.S. (1980), "Produced fluid changes during a fire-flood", SPE paper 9005, 5th Int. Symp. Oil Field and Geothermal Chem., Stanford, California, May (25-30).

Gadelle, C.P., Burger, J.G., Bardon, C.P., Machedon, V., Carcoana, A. and Petcovici, V. (1981), "Heavy-oil recovery by *in situ* combustion - two field cases in Rumania", *J. Pet. Tech.*, (November) pp.2057-2066,

Garon, A.M. and Wygal, R.J. (1974), "A laboratory investigation of fire-water flooding", *Soc. Pet. Engr. J.*, 14, (6), (December) pp.537-544.

Gates, C.F. and Ramey, H.J.Jr. (1958), "The South Belridge thermal recovery experiment", *Trans. AIME*, 213, pp.236-244.

Grant, B.F. and Szasz, S.E. (1954), "Development of an underground heat wave for oil recovery", *Trans. AIME*, 201, (23), pp.108-118.

Gray, D.H. and Rex, R.W. (1966), "Formation damage in sandstone caused by clay dispersion and migration", 14th Nat. Conf. Clays and Clay Minerals, Pergamon Press,

Grim, R.E. (1962), "Applied Clay Mineralogy", McGraw-Hill Book Company Inc., (Illinois).

Guvenir, I.M. (1980), "The development of an automated *in situ* combustion assembly to study effects of clay on the dry-forward *in situ* combustion process", PhD Thesis, University of Kansas, Lawrence.

Harding, W.C., Fletcher, P.B., Shopard, J.C., Dittman, E.W. and Zodow, D.W. (1972), "*In situ* combustion in a thin reservoir containing high-gravity oil", *J. Pet. Tech.*, 24, (2), (February) pp.199-208.

Harding, T.G. (1976), "A combustion tube for investigation of *in situ* oil recovery", MSc Thesis, University of Calgary.

Harding, T.G., Moore, R.G., Bennion, D.W. and Donnelly, J.K. (1976), "Adiabatic combustion tube evaluation of *in situ* processes for oil sands", Proc. Symp. Tar Sands, 26th Can. Chem. Eng. Conf., Toronto, Ontario, October (3-6).

Hester, D.V. and Menzie, D.E. (1954), "Development of subsurface combustion drive", *Pet. Eng.*, 26, (12), (November), B-82.

Holbrook, G.W., Hungerford, T.E. and Rankin, M.R. (1959), "A fire-flooding experiment in the Bradford-Allegany area", *Prod. Monthly*, 23, (12), (October), pp.26-28.

Horne, J.S., Bousaid, I.S. Dore, T.L. and Smith, L.B. (1982), "Initiation of an *in situ* combustion project in a thin oil column underlain by water", *J. Pet. Tech.*, 34, (10), (October) pp.2233-2243.

Howard, F.A. (1923), "A method of operating an oil well", U.S. Patent 1,473,348.

Huffman, G.A., Benton, J.P., El-Messidi, A.E. and Riley, K.M. (1983), "Pressure maintenance by *in situ* combustion, West Heidelberg Unit, Jasper County, Ms.", *J.Pet.Tech.*, 35, (10) (October) pp.1877-1883.

Kharrat, R. and Vossoughi, S. (1984), "Feasibility study of the *in situ* combustion process using TGA/DSC techniques", SPE/DOE paper 12678, SPE/DOE 4th Symp. Enhanced Oil Recovery, Tulsa, April (15-18).

Kuhn, C.S. and Koch, R.L. (1953), "*In situ* combustion - newest method of oil recovery", *Oil and Gas J.*, 52, (14), 10th August, pp.92-96.

Langnes, G.L. and Besson, C.M. (1964), "*In situ* combustion combined with water-flooding", 39th Ann. Full Meeting, Houston, October (11-14), preprint SPE 952, 10 pp.

Martin, W.L., Alexander, J.D. and Dew, J.N. (1958), "Process variables of *in situ* combustion", *Trans. AIME*, 231, pp.28-35.

McKay, W.N. (1982), "A discussion of fire-flooding", Petroleum Recovery Institute, Calgary, Alberta, Canada.

McNiel, J.S. and Nelson, T.W. (1959), "3 ways to improve oil recovery", *Oil and Gas J.*, 57, (3), (January) pp.86-98.

Mekhtibeili, R.M. and Sultanov, Z.A. (1978), "The effect of rock properties on the specific oxidant requirement in fire-flooding", translated from Russian, *Neft, Khoz*, No.2, pp.31-34.

Mills G.A. (1947), "Process of activating kaolin clay", U.S. Patent 2,477,639.

Moss, J.T., White, P.D. and McNeil, J.S.Jr. (1959), "*In situ* combustion process - results of a five well field experiment in Southern Oklahoma", *Trans. AIME*, 216, pp.55-64.

Mungen, N. (1965), "Permeability reduction through changes in pH and salinity", *Trans. AIME*, 234, p.1449.

Nahin, P.G., Merrill, W.C., Grenal, A. and Crog, R.S. (1951), "Mineralogical studies of California oil-bearing formations. I. Identification of clays", *Trans. AIME*, 192, pp.151-158.

Nelson, T.W. and McNeil, J.S. (1961), "How to engineer an *in situ* combustion project", *Oil and Gas J.*, (June 5), 59, (23), 58.

Okandan, E., Bağci, S., Demiral, B., Parlaktuna, M., Topkaya, I. and Gürpinar, Ö. (1982), "Laboratory dry combustion tests for limestone crude oil", 2nd European Symp. on Enhanced Oil Recovery, Paris, November (8-10), pp.489-494.

Parrish, D.R., Rausch, R.W., Beaver, K.W. and Wood, H.W. (1962), "Underground combustion in the Shannon pool, Wyoming", *J. Pet. Tech.*, 255, (14), (February), pp.197-205.

Parrish, D.R. and Craig, F.F.Jr. (1969), "Laboratory study of combination of forward combustion and water flooding - the COFCAW process", *J. Pet. Tech.*, 21, (6), (June) pp.753-761.

Penberthy, W.L.Jr. (1965), "The design and operation of a combustion tube for investigation of combustion oil recovery", MSc Thesis, Texas A & M University.

Poettman, F.J., Schilson, R.E. and Surkalo, H. (1967), "Philosophy and technology of *in situ* combustion in light oil reservoirs", *World Oil*, 165, pp.487-497.

* Rall, C.G. and Taliaferro, D.B. (1946), "A method for determining simultaneously the oil and water saturation of oil sand", R.I. 4004.

Ramey, H.J. (1971), "*In situ* combustion", 8th World Pet. Cong., Moscow, preprint PD9, (2), (13-19 June), 20P.

Rendi, T.W., Anderson, J.M. and Richard, A.D. (1980), "A duel-phase GC column", *American Laboratory*, reprinted January, 1980.

Satman, A. (1979), "*In situ* combustion models for the steam plateau and for fieldwide oil recovery", PhD Thesis, University of Stanford, California.

Scott, P.H. (1960), "*In situ* combustion - water flooding process", U.S. Patent 3,131,761.

Sheinman, A.B. and Sergeev, A.I. (1958), "Eskperimentalnoe Issledovanie Goreniya v sloe Neftenosnog o peska", *Neft. Acad. Nauk USSR*, 11, p.228.

Showalter, W.E. (1963), "Combustion drive tests", *Soc. Pet. Engr. J.*, 3, (1) (March), pp.53-58.

Smith, F.W. and Perkins, T.K. (1973), "Experimental and numerical simulation studies of the wet combustion recovery process", *J. Can. Pet. Tech.*, 12, (3) (July-September) pp.44-54.

* Prats, M. (1982), "Thermal Recovery", Society of Petroleum Engineers, Dallas, U.S.A.

Sterner, T.E. and Wertman, W.T. (1976), "Laboratory investigation of the *in situ* combustion process for recovery of Pennsylvania Grade crude oil", USBM, R.17044, November, 30P.

Somerton, W.H. and Radke, C.J. (1980), "Role of clays in the enhanced oil recovery of petroleum", SPE paper 8845, 1st Joint SPE/DOE Symp. on Enhanced Oil Recovery, Tulsa, April (20-23).

Strange, L.K. (1964), "Ignition: key phase in combustion recovery", *Pet. Eng.*, 36, (12), pp.105-109; 36, (13), pp.97-106.

Vossoughi, S., Willhite, G.P., Kritikos, W.P., Guvenir, I.M. and Elshoubary, Y. (1981), "Effect of clay on crude oil *in situ* combustion processes", SPE paper 10320, 56th Ann. Fall Tech. Conf. and Exhibition Soc. Pet. Engrs AIME, San Antonio, Texas, October (5-7).

Vossoughi, S., Willhite, G.P., Kritikos, W.P., Guvenir, I.M. and Elshoubary, Y. (1982a), "Automation of an *in situ* combustion tube and study of the effect of clay on the *in situ* combustion process", *Soc. Pet. Engr. J.*, (August) pp.493-502.

Vossoughi, S., Bartlett, G.W. and Willhite, G.P. (1982b), "Effect of the sand grain specific surface area on the performance of the tube *in situ* combustion process", SPE paper 11072, 57th Ann. Fall Tech. Conf. and Exhibition Soc. Pet. Engrs AIME, New Orleans, Los Angeles, September (26-29).

Walter, H. (1957), "Application of heat of recovery of oil: field results and possibility of profitable operation", *J. Pet. Tech.*, 9, (2), (February) pp.16-22.

Wilson, L.A., Reed, R.L., Clay, R.R. and Harrison, J.H. (1963), "Some effects of pressure on forward and reverse combustion", *Soc. Pet. Engr. J.*, June, pp.127-137.

Wolcott, E. (1923), "Method of increasing the yield of oil wells", U.S. Patent 1,457,479.

APPENDIX A

Symbols for flow diagram (Figure 3.1)

A.1

Item No.	Function
I_1	Pressure regulator - air cylinder
I_2	Pressure regulator - nitrogen cylinder
I_3	Drier (molecular sieve)
I_4	Furnace (optional)
I_5	Injection water storage
I_6	Building water supply (in and out)
I_7	Ice water container
I_8	Nylon tubing coil
I_9	Pressure regulator - helium cylinder
I_{10}	Wall thermocouple extension cable
I_{11}	Axial thermocouple extension cable
I_{12}	Band heater power supply
I_{13}	Heating tape power supply
I_{14}	Furnace power supply (optional)
I_{15}	Thermocouple (furnace temperature indication)
I_{16}	Thermocouple (combustion tube inlet temperature indication)
E_1	Combustion tube
E_2	Pressure jacket
C_1	Separator
C_2	Condenser
C_3	Sampling cylinder
VT	Vent
VTH	Vent head

A.2 Pressure gauges

PI_1	Combustion tube inlet pressure
PI_2	Combustion tube exit pressure
PI_3	Separator inlet pressure
PI_4	Wet test meter inlet pressure
PI_5	Gas chromatograph inlet pressure

A.3.1 Flow indication and controlling symbols

Symbol	Function	Type/Model	Manufacturer	Technical Sheet/ Bulletin
FI_1, FI_2	Flowmeters	Series 1100-VAA 300	Fisher Control Ltd. (Surrey)	1708 Fisher Control Series 1100, May 1982
FI_3	Wet test meter	DM3D	Alexander Wright & Co. (Westminster)	Technical data - M79
P_1	Metering pump	E_1 long stroke	Metering Pumps Ltd. (London)	MPI No.A19572
P_2	Rotary pump	BM 10/2	Totton Electrical Sales Ltd.	-
PC_1	Pressure regulator	MIR 700 series	Scientific Glass Engineering (UK) Ltd.	Catalogue, March 1982
PC_2	Pressure regulator	T class	The British Steam Specialists Ltd.	Catalogue ref. 7:81
PIC_1	Back pressure regulator	BPR series 30-50	Scientific Glass Engineering Ltd.	Catalogue, March 1982
PIC_2	Back pressure regulator	BPR series 30-10	Scientific Glass Engineering Ltd.	Catalogue, March 1982

A.3.2 Valves

Valve	Type	Catalogue No./ model	Manufacturer	Technical Sheet/ Bulletin	Panel mounted
V_1	Nupro C series	B-4C-10 10 psi cracking	Bristol Valve & Fitting Co. Ltd.	Nupro Company NW-273	No
V_2-V_6 incl.	Whitey series	B-IRS4	Bristol Valve & Fitting Co. Ltd.	Whitey Company NW-972	Yes
V_7	Nupro C series	S-4C-⅓ ⅓ psi cracking	Bristol Valve & Fitting Co. Ltd.	Nupro Company MW-273	No
V_8	Nupro C series	S-4C-1 1 psi cracking	Bristol Valve & Fitting Co. Ltd.	Nupro Company NW-273	No
V_9	Water container on-off valve	D505X/16/16 brass body, gas tap	Simplifix Couplings Ltd.	-	No
V_{10}	Nupro relief CA series	SS-4CA-50	Bristol Valve & Fitting Co. Ltd.	Nupro Company NW-273	No
V_{11}	Nupro relief CA series	SS-4CA-3	Bristol Valve & Fitting Co. Ltd.	Nupro Company NW-273	No
V_{12}-V_{15} incl.	Stopcocks	Teflon	Springham Ltd.	-	No
V_{16}	Drallim series 40	Single bank 3-way valve	Drallim Controls Ltd.	Drallim Publ.101	Yes

A.4 Temperature controlling and indication symbols

Symbol	Function	Model/Code No.	Manufacturer
T_1	Axial thermowell contains 12 thermocouples	According to our design and specification	PJD Instruments Ltd.
T_2	12 wall thermocouples	PWKZB chromel-alumel type	BICC Ltd.
T_3	Band heater	Knuckle type, 600 watts, 240 volts (according to our specification)	Hedin Ltd. (London)
T_4	Heating tape	HT 354	Electrothermal Engineering Ltd. (London)
T_5	Switch box	3750-SP	Digitron Instrumentation Ltd.
T_I	Microprocessor thermometer	Comark 6600	Comark Electronics Ltd.
TC_1	Temperature controller (for band heater)	Pye ether mini	Pye Ether Ltd.
TC_2	Temperature regulator (for heating tape)	MC227	Electrothermal Engineering Ltd. (London)
TC_3	Temperature controller (furnace)	Series 300 model T350	Thermocouple Instruments Ltd.

A.5 Gas analysis symbols

Symbols	Function	Model	Manufacturer/Technical Information
QIC	Gas chromatograph (thermal conductivity head)	Pye Unicam series 104	Pye Unicam Ltd./Technical Manual Series 104
R_S	Digital integrator	MK.11	Labdata Instrument Services Ltd. (Surrey)
R	Recorder	Pye Vitatron	Pye Unicam Ltd.

A.6 Electrical and temperature insulating material (not shown in Figure 3.1)

No.	Item	Model	Manufacturer
1	Refrasil sleeving	Code No.S-43, nominal bore 40 mm, wall thickness 1 mm	Chemical & Insulating Co. Ltd.
2	Refrasil tape	Code No.T-3	Chemical & Insulating Co. Ltd.
3	"Triton Kaowool" ceramic fibre blanket	Needled blanket type, 12 mm in thickness, with working temperature up to 1260° C	Morganite Ceramic Fibres Ltd. (UK)

APPENDIX B

```
  THIS PROGRAMME CALCULATES INSTANTANEOUS AND
  OVERALL COMBUSTION PARAMETERS
dimension
AN2(300),O2(300),CO2(300),CO(300),CH4(300),VP(300),SUM(3
00),RATIO(300),E(300),VOLN2(300),AIR(300),H2(300),
&TIME(300),VPO2(300),VOLO2(300),F(300),C(300),W(300),HC(
300),Q(300),VOLCO(300),VOLCO2(300),VOLCH4(300),DIFF(300)
*              PARAMETER    DEFINED
*AN2C,O2C,CO2C,COC,CH4C,are calibration values obtained
from gas chromatograph
*AN2(I),O2(I),CO2(I),CO(I),CH4(I),HY(I),are intantaneous
analysis of nitrogen,oxygen,carbon dioxide,carbon
monoxide,methane
& and hydrogen in the produced gases in volume percent
*VP(I)=inst.volume(st.cu.m) of produced gases as
measured by wet test meter
*RATIO(I)=inst.CO/CO2 molar ratio
*E(I)=inst.percent of oxygen utilization efficiency
*VPO2(I)=inst volume(st.cu.m) of unreacted oxygen
produced
*VOLN2(I)=inst.volume(st.cu.m) of nitrogen produced
*VOLO2(I)=inst.volume(st.cu.m) of oxygen injected
*VOLCO(I)=inst.volume(st.cu.m) of carbon monoxide
produced
*VOLCO2(I)=inst.volume(st.cu.m) of carbon dioxide
produced
*VOLCH4(I)=inst.volume(st.cu.m) of methane produced
*AIR(I)=inst.volume(st.cu.m) of air injected
*DIFF(I)=inst.percent of volume difference between
produced gases and inlet gases
*H2(I)=inst.hydrogen in fuel burned in gram
*C(I)=inst.carbon in fuel burned in gram
*F(I)=inst.fuel burned in gram
*HC(I)=inst.hydrogen to carbon ratio
*Q(I)=Inst. heat of combustion related to one gram of
fuel (cal/gCHx)
read(40,100)N,NRUN
read(40,100)AN2C,O2C,CO2C,COC,CH4C,HYC
read(40,100)(TIME(I),AN2(I),O2(I),CO2(I),CO(I),CH4(I),HY
(I),VP(I),I=1,N)
100 format(v)
totalV=0.0
totalV1=0.0
totalV2=0.0
totalv3=0.0
total=0.0
total0=0.0
total1=0.0
total2=0.0
total3=0.0
total4=0.0
total5=0.0
total6=0.0
totalQ=0.0
do 20 I=1,N
AN2(I)=AN2(I)*1.5/AN2C
```

```
O2(I)=O2(I)*1.5/O2C
CO2(I)=CO2(I)*3.0/CO2C
CO(I)=CO(I)*1.5/COC
CH4(I)=CH4(I)*1.5/CH4C
HY(I)=HY(I)*1.5/HYC
SUM(I)=AN2(I)+O2(I)+CO2(I)+CO(I)+CH4(I)+HY(I)
AN2(I)=100.0*AN2(I)/SUM(I)
O2(I)=100.0*O2(I)/SUM(I)
CO2(I)=100.0*CO2(I)/SUM(I)
CO(I)=100.0*CO(I)/SUM(I)
CH4(I)=100.0*CH4(I)/SUM(I)
HY(I)=100.0*HY(I)/SUM(I)
totalV=totalV+VP(I)
RATIO(I)=CO(I)/CO2(I)
E(I)=(21.0-O2(I))/21.0*100.0
VPO2(I)=VP(I)*O2(I)/100.0
total=total+VPO2(I)
VOLN2(I)=VP(I)*AN2(I)/100.0
total0=total0+VOLN2(I)
VOLO2(I)=(21/79)*VOLN2(I)
VOLCO2(I)=VP(I)*CO2(I)/100.0
totalV1=totalV1+VOLCO2(I)
VOLCO(I)=VP(I)*CO(I)/100.0
totalV2=totalV2+VOLCO(I)
total1=total1+VOLO2(I)
VOLCH4(I)=VP(I)*CH4(I)/100.0
totalv3=totalv3+VOLCH4(I)
AIR(I)=VOLO2(I)+VOLN2(I)
DIFF(I)=((AIR(I)-VP(I))/AIR(I))*100.0
total2=total2+AIR(I)
DIFFO=(total2-totalV)/total2*100.0
H2(I)=(4.0*1000.0)/(23.6445*100.0)*VP(I)*((21/79)*AN2(I)
-O2(I)-CO2(I)-0.5*CO(I))
total3=total3+H2(I)
C(I)=(12.0*1000.0)/(23.6445*100.0)*VP(I)*(CO2(I)+CO(I))
total4=total4+C(I)
write(6,200)
write(6,201)TIME(I),total4
F(I)=H2(I)+C(I)
total5=total5+F(I)
W(I)=9.0*H2(I)
total6=total6+W(I)
HC(I)=H2(I)/C(I)*12.0
Q(I)=((265700.0+197850.0*RATIO(I))/((1.0+RATIO(I))*(12.0
+HC(I))))+((31175.0*HC(I)-171700.0)/(12.0+HC(I)))
totalQ=totalQ+Q(I)
continue
AVG=total3/total4*12.0
AVGQ=totalQ/N
EFF=100.0*(total1-total)/total1
write(6,300)N,NRUN
300 format(1x,"N=",I2,22x,"NRUN NO",I2)
write(6,400)
write(6,401)(TIME(I),AN2(I),O2(I),CO2(I),CO(I),CH4(I),HY
(I),VP(I),I=1,N)
400 format(1x,"The clock time,The instantaneous
fractional exit gas composition and The instantaneous
gas produced
```

```
&(st.cu.m)VP(I)
are:"//1x,"TIME(I)",2x,"AN2(I)",2x,"O2(I)",2x,"CO2(I)",3
x,"CO(I)",2x,"CH4(I)",2x,"HY(I)",2x,"VP(I)"/1x,"
&"_______",2x,"_______",2x,"_____",2x"_______",3x,"_____",2
x,"_______",2x,"_______")
401
format(2x,f5.2,3x,f5.2,2x,f5.2,2x,f5.2,5x,f5.2,2x,f5.2,2
x,f5.2,2x,f7.5)
write (6,500)
write(6,501)(TIME(I),RATIO(I),E(I),AIR(I),I=1,N)
500 format(1x,"The clock time TIME(I),The instantaneous
molar ratio(carbon monoxide to carbon dioxide ratio)
RATIO(I),
&The oxygen utilization efficiency% E(I),The
instantaneous (st.cu.m) of air injected AIR(I)
are:"//5x,"TIME(I)",4x,"RATIO(I)"
&,4x,"E(I)",3x,"AIR(I)"/5x,"________",3x,"________",4x,"__
____",3x,"_______")
501 format(5x,f5.2,5x,f7.5,4x,f6.3,2x,f8.6)
write(6,600)
write(6,601)(TIME(I),DIFF(I),I=1,N)
600 format(1x,"The Clock Time TIME(I),The Instantaneous
Volume Difference DIFF(I)
are:"//5x,"TIME(I)",4x,"DIFF(I)"/5x,"____
&_____",4x,"_______")
601 format(5x,f5.2,6x,f7.4)
write(6,700)
write(6,701)(TIME(I),H2(I),C(I),F(I),I=1,N)
700 format(1x,"The clock time TIME(I),The inst. hydrogen
in fuel burned(gm.) H2(I),The inst. carbon in fuel
burned(gm.) C(I),
&and the fuel burned in time interval(gm.) F(I)
are:"//5x,"TIME(I)",3x,"H2(I)",4x,"C(I)",5x,"F(I)"/5x,"_
_______",3x,"_______",
&3x,"_______",3x,"_______")
701 format(5x,f5.2,3x,f7.4,3x,f7.4,2x,f7.4)
write(6,800)
write(6,801)(TIME(I),W(I),HC(I),I=1,N)
800 format(1x,"The clock time TIME(I),The inst. amount
of water formed by combustion in gram W(I),The inst.
apparent
& hydrogen to carbon ratio HC(I)
are:"//5x,"TIME(I)",4x,"W(I)",3x,"HC(I)"/5x,"________",3x
,"_______",2x,"_______")
801 format(5x,f5.2,3x,f8.6,2x,f8.6)
write(6,810)
write(6,811)(TIME(I),Q(I),I=1,N)
810 format(1x,"The clock time TIME(I) and The heat of
combustion related to one gm. of fuel(cal/gCHx)
are:"//5x,"TIME(I)",3x,
&"Q(I)"/5x,"________",3x,"________")
811 format(5x,f5.2,2x,f9.1)
write(6,850)total
850 format(1x,"The Total Vol.(st.cu.m) of Oxygen
Produced,total is"/(1x,f7.4))
write(6,860)total0
860 format(1x,"The Total Vol.(st.cu.m) of Nitrogen
Produced,total0 is"/(1x,f7.4))
```

```
write(6,870)totall
870 format(1x,"The Total Vol.(st.cu.m) of Oxygen
Injected,totall is"/(1x,f7.4))
write(6,880)total2
write(6,890)EFF
890 format(1x,"The Over all Oxygen Utilization
Efficiency %(combustion efficiency),EFF is"/(1x,f5.2))
880 format(1x,"The Total Vol.(st.cu.m) of Air
Injected,total2 is"/(1x,f7.4))
write(6,900)total3
900 format(1x,"The Total amt.(gm) of Hydrogen In Burned
Fuel,total3 is"/(1x,f7.4))
write(6,901)total4
901 format(1x,"The Total amt.(gm) Of Carbon In Burned
Fuel,total4 is"/(1x,f7.4))
write(6,902)total5
902 format(1x,"The Total amt(gm) Of Fuel Burned,total5
is"/(1x,f7.4))
write(6,903)total6
903 format(1x,"The Total amt(gm)Of water formed By
Combustion,total6 is"/(1x,f7.4))
write(6,904)AVG
904 format(1x,"The Average Hydrogen To Carbon (H/C)
Ratio,AVG is"/(1x,f8.4))
200 format(1x,"The clock time and the cumalative carbon
burned(gm.)
is:"//1x,"TIME(I)",5x,"total4"/1x,"_____",5x,"_____")
201 format(1x,f5.2,5x,f7.4)
write(6,905)AVGQ
905 format(1x,"The estimate of the average heat of
combustion (cal/gCHx),AVGQ is:"/(1x,f10.1))
write(6,906)totalV
906 format(1x,"The Total Vol.(st.cu.m) of Cumulative Gas
Produced,totalV is:"/(1x,f7.4))
write(6,907)totalV1
907 format(1x,"The Total Vol.(st.cu.m) of Carbon Dioxide
Produced,totalV1 is:"/(1x,f10.8))
write(6,908)totalV2
908 format(1x,"The Total Vol.(st.cu.m) of Carbon
Monoxide Produced,totalV2,is:"/(1x,f10.8))
write(6,909)totalv3
909 format(1x,"The total Vol.(st.cu.m) of methane
produced,totalv3 is:"/(1x,f9.8))
write(6,910)DIFFO
910 format(1x,"The Overall Difference Value,DIFFO
is:"/(1x,f6.3))
stop
end
```

APPENDIX C

Calculated procedure for air requirement and the oil and water mass balances is illustrated with reference to run No.3. Detailed calculations of total air consumed and fuel consumption have already been given in Appendix B.

Example - Run No.3

Overall period (clock time)	13:12 - 18:30
Stabilised period (clock time)	16:30 - 17:30
Ignition time (clock time)	13:12
Water injection time (clock time)	15:05

Condition of test:

crude oil	Maya Isthmus (32.4 °API)
porous media	silica sand + 5% kaolin
length of pack	0.736 m
cross-sectional area of combustion tube	0.003294 m^2
water-to-air ratio	2.5 m^3/Mm^3(STP)

C-1 Calculation of air required per unit volume of sand pack, air-to-oil and air-to-fuel ratios

(1) Air requirement $m^3(st)/m^3$

(i) Overall

Total air consumed	=	0.1965 m^3(st)
Length of sand pack (combusted section)	=	0.647
Volume of combusted section	=	0.647 x area of tube
	=	0.002133 m^3

Therefore air requirement $= \frac{\text{Total air consumed}}{\text{vol. of combusted section}}$

$= \frac{0.1965}{0.002133}$

$= 92.1\ m^3(st)/m^3$

(ii) Stabilised period

Air consumed $= 0.04776\ m^3(st)$

Length of pack traversed by the combustion front $= 0.152\ m$

Volume of combusted section $= 0.000501\ m^3$

Therefore stabilised air requirement $= \frac{0.04776}{0.000501}$

$= 95.33\ m^3(st)/m^3$

(2) AFR $m^3(st)/kg$

(i) Overall

Total fuel consumed $= 17.78\ gm$

$= 0.01778\ kg$

Therefore air-fuel ratio $= \frac{\text{total air consumed}}{\text{total fuel consumed}}$

$= \frac{0.1965}{0.01778}$

$= 11.05\ m^3(st)/kg$

(ii) Stabilised period

Total fuel consumed $= 3.915\ gm$

Air consumed $= 0.04776\ m^3(st)$

Therefore air-fuel ratio $= \frac{0.04776}{3.915 \times 10^{-3}}$

$= 12.2\ m^3(st)/kg$

(3) AOR $m^3(st)/m^3$

(i) Overall

Total air consumed	=	0.1965 $m^3(st)$
Total oil produced	=	285.5 gm
Average density of oil produced	=	0.8686 gm/cm^3
Volume of oil produced	=	328.7 cm^3
	=	0.0003287 m^3
Therefore AOR overall	=	$\frac{0.1965}{0.0003287}$
	=	597.8 $m^3(st)/m^3$

(ii) Stabilised period

Air consumed	=	0.04776 $m^3(st)$
Oil produced during stabilised period	=	91.93 gm
Average density of the oil produced	=	0.8636 gm/cm^3
Volume of oil produced	=	106.45 cm^3
	=	0.00010645 m^3
Therefore AOR stabilised	=	$\frac{0.04776}{0.00010645}$
	=	448.6 $m^3(st)/m^3$

(4) Fuel consumption per unit volume of sand pack (kg/m^3)

(i) Overall

Total fuel consumed	=	17.78 gm
	=	0.01778 kg
Volume of combusted section	=	0.002133 m^3
Therefore fuel consumption/ volume of sand pack	=	$\frac{0.01778}{0.002133}$
	=	8.33 kg/m^3

(ii) Stabilised period

Fuel consumed	=	3.915 gm
Volume of combusted section	=	0.000501 m^3
Therefore fuel consumption	=	$\frac{0.003915}{0.000501}$
	=	7.8 kg/m^3

C-2 Mass balance check

(1) Oil (weight in gm)

Initial oil content of pack....(1)	=	380.42
Liquid oil produced (separator)	=	278.3
Liquid oil (displaced from production line)	=	7.24
Fuel consumed (oil and coke)	=	17.78
Residual oil and coke	=	80.4
Total.....(2)	=	383.7
Difference (1-2)	=	-3.28
Difference (%)	=	0.86

(2) Water

Initial water content of pack	=	61.5 gm
Volume of water injected	=	324 cm^3
Density of water	=	0.9979 gm/cm^3
Water injected	=	323.32 gm
Water formed by combustion	=	15.196 gm
Total.....(1)	=	400 gm
Liquid water produced (separator)	=	291.0
Water produced (displaced from production line)	=	30.5
Residual water in the pack	=	56.23
Water lost as vapour [Ejiogu (1978)]	=	0.924
Total.....(2)	=	378.65
Difference (1-2)	=	21.35
Difference (%)	=	5.34

APPENDIX D

RUN NO.1

Maya Isthmus crude oil (32.4 °API); 5% kaolin; WAR = 0.0; ignition at 13:18; stabilised period (15:30-18:30)

Clock time	Mole fraction %															
	N_2	O_2	CO_2	CO	CH_4	1*	2*	3*	4*	5*	6*	7*	8*	9*	10*	11*
13.25	87.14	11.27	1.59	0.00	0.00	0.0052	0.091	0.042	0.132	0.810	26.06	0.000	46.31	0.00574	9.40	23795.7
13.33	80.76	4.69	10.40	4.16	0.00	0.0078	0.056	0.576	0.633	0.5105	1.18	0.399	77.68	0.00797	2.13	8454.9
13.45	80.93	5.77	9.58	3.72	0.00	0.0072	0.052	0.486	0.538	0.472	1.29	0.388	72.55	0.00738	2.44	8680.4
14.00	80.22	8.42	10.08	1.28	0.00	0.0093	0.034	0.536	0.570	0.309	0.77	0.127	59.92	0.00944	1.48	8639.5
14.15	80.31	8.75	9.72	1.21	0.00	0.0121	0.046	0.671	0.718	0.418	0.83	0.124	58.33	0.01230	1.63	8756.9
14.30	80.80	9.28	8.86	1.06	0.00	0.0112	0.053	0.564	0.617	0.478	1.13	0.119	55.82	0.01145	2.18	9290.9
14.45	81.44	10.87	6.79	0.89	0.00	0.0133	0.079	0.518	0.598	0.716	1.84	0.131	48.21	0.01371	2.99	10370.5
15.00	81.59	9.62	7.77	1.03	0.00	0.0256	0.164	1.143	1.307	1.477	1.72	0.132	54.21	0.02644	3.17	10185.6
15.35	82.92	1.99	12.53	2.56	0.00	0.0156	0.165	1.195	1.359	1.483	1.65	0.204	90.54	0.01637	4.7	9820.2
15.50	82.94	2.76	11.74	2.55	0.00	0.0085	0.090	0.616	0.706	0.811	1.75	0.217	86.83	0.00892	4.7	9928.1
16.05	83.04	2.08	12.43	2.46	0.00	0.0097	0.104	0.733	0.837	0.936	1.70	0.197	90.12	0.01020	4.9	9919.2
16.22	82.80	1.51	12.93	2.76	0.00	0.0112	0.117	0.892	1.000	1.055	1.58	0.213	92.81	0.01174	4.6	9669.4
16.40	81.67	1.43	13.97	2.93	0.00	0.0120	0.098	1.029	1.127	0.884	1.14	0.209	93.19	0.01241	3.3	8973.0
16.55	81.22	1.47	14.20	3.10	0.00	0.0091	0.067	0.799	0.866	0.605	1.00	0.218	93.01	0.00936	2.77	8708.2
17.10	79.87	1.28	15.47	3.38	0.00	0.0101	0.047	0.966	1.019	0.429	0.59	0.218	93.91	0.01021	1.07	7966.2
17.25	79.74	1.25	15.64	3.37	0.00	0.0087	0.038	0.839	0.874	0.346	0.55	0.215	94.03	0.00878	0.91	7898.2
17.45	79.24	1.28	16.01	3.48	0.00	0.0096	0.033	0.949	0.982	0.298	0.42	0.217	93.93	0.00963	0.31	7643.3
17.55	78.27	1.20	16.71	3.82	0.00	0.0098	0.016	1.021	1.037	0.147	0.1..	0.228	94.30	0.00971	-0.92	7167.2
18.10	78.68	1.31	16.35	3.66	0.00	0.0086	0.021	0.873	0.894	0.187	0.28	0.224	93.76	0.00857	-0.35	7365.2
18.25	78.03	1.44	16.98	3.55	0.00	0.0089	0.008	0.927	0.935	0.074	0.11	0.209	93.15	0.00879	-1.25	7069.4
18.40	77.93	1.55	16.94	3.58	0.00	0.0093	0.007	0.968	0.975	0.061	0.08	0.211	92.60	0.00917	-1.42	7016.9
18.55	79.62	2.35	15.10	2.93	0.00	0.0089	0.034	0.814	0.848	0.304	0.49	0.194	88.81	0.00897	0.78	7880.4
19.10	79.71	2.34	15.03	2.92	0.00	0.0098	0.039	0.893	0.932	0.351	0.52	0.194	88.86	0.00989	0.91	7929.1
19.25	81.14	2.80	13.62	2.44	0.00	0.0082	0.054	0.668	0.728	0.490	0.97	0.178	86.65	0.00842	2.61	8799.4
19.40	83.14	3.09	11.72	2.05	0.00	0.0080	0.085	0.559	0.643	0.763	1.82	0.175	85.29	0.00842	4.98	10177.3
19.55	82.89	2.64	12.20	2.27	0.00	0.0068	0.069	0.499	0.569	0.627	1.67	0.186	87.43	0.00714	4.76	9914.3
20.10	82.66	2.62	12.36	2.36	0.00	0.0086	0.084	0.642	0.724	0.760	1.57	0.190	87.50	0.00900	4.44	9744.9
20.25	82.49	2.44	12.59	2.47	0.00	0.0079	0.075	0.604	0.679	0.680	1.50	0.196	88.36	0.00825	4.24	9603.7
20.40	82.37	1.96	13.08	2.59	0.00	0.0083	0.078	0.660	0.738	0.703	1.42	0.198	90.68	0.00865	4.04	9468.8
20.55	82.02	1.74	13.56	2.69	0.00	0.0073	0.064	0.601	0.665	0.573	1.27	0.198	91.71	0.00758	3.70	9222.1
21.12	81.88	1.59	13.80	2.73	0.00	0.0092	0.078	0.772	0.849	0.702	1.21	0.197	92.44	0.00954	3.56	9129.0
21.26	81.71	1.61	13.83	2.85	0.00	0.0078	0.064	0.660	0.724	0.577	1.16	0.205	92.35	0.00807	3.34	9018.8
21.40	81.55	1.48	14.12	2.85	0.00	0.0074	0.058	0.637	0.695	0.523	1.09	0.202	92.95	0.00764	3.14	8914.2
21.58	81.80	1.46	13.75	2.95	0.00	0.0103	0.088	0.873	0.961	0.793	1.21	0.214	93.05	0.01066	3.37	9065.2
22.10	81.61	1.48	13.92	2.98	0.00	0.0062	0.050	0.532	0.582	0.452	1.13	0.214	92.93	0.00640	3.12	8938.0
22.25	81.07	1.36	14.32	3.25	0.00	0.0086	0.062	0.767	0.828	0.555	0.96	0.227	93.53	0.00882	2.50	8602.1
22.43	80.69	1.27	14.81	3.22	0.00	0.0105	0.067	0.961	1.027	0.600	0.83	0.217	93.95	0.01073	2.14	8402.7
23.00	80.74	1.16	14.90	3.20	0.00	0.0097	0.062	0.892	0.953	0.561	0.84	0.214	94.46	0.00991	2.12	8427.4
23.15	79.17	1.10	16.28	3.44	0.00	0.0085	0.028	0.851	0.878	0.251	0.39	0.211	94.74	0.00852	0.23	7618.6
23.30	78.67	1.07	16.76	3.49	0.00	0.0085	0.019	0.874	0.897	0.174	0.26	0.208	94.81	0.00846	-0.47	7378.4
23.45	78.07	1.04	17.51	3.39	0.00	0.0095	0.008	1.007	1.015	0.079	0.09	0.193	95.06	0.00939	-1.17	7112.0
24.00	78.18	1.02	17.51	3.29	0.00	0.0085	0.009	0.897	0.903	0.078	0.12	0.187	95.14	0.00841	-1.07	7174.0
24.15	78.92	1.04	16.93	3.12	0.00	0.0087	0.021	0.885	0.906	0.192	0.23	0.184	95.06	0.00869	-0.11	7524.8
24.32	78.09	1.01	17.80	3.09	0.00	0.0086	0.006	0.912	0.917	0.052	0.07	0.173	95.16	0.00850	-1.17	7149.0
24.45	78.00	1.02	18.25	2.73	0.00	0.0106	0.002	1.129	1.131	0.015	0.01	0.149	95.16	0.01047	-1.24	7133.5
1.00	79.09	1.04	17.66	2.21	0.00	0.0086	0.017	0.867	0.885	0.153	0.24	0.125	95.03	0.00861	0.12	7682.1
1.20	81.32	1.34	14.91	2.43	0.00	0.0268	0.188	2.359	2.547	1.698	0.95	0.163	93.63	0.02759	2.86	8823.5

*See end of Appendix for notes detailing column headings

RUN NO.2

Maya Isthums crude oil (32.4 °API); 5% kaolin; WAR = 1.25 m^3/Mm^3 (STP); ignition at 11:05; water injection at 13:30; stabilised period (14:00-17:00)

Clock time	Mole fraction %																
	N_2	O_2	CO_2	CO	CH_4	H_2	1*	2*	3*	4*	5*	6*	7*	8*	9*	10*	11*
11:10	86.42	1.08	5.91	6.59	0.00	0.000	0.00514	0.110	0.326	0.436	0.992	4.06	1.114	94.85	0.00562	8.58	11503.3
11:15	85.29	2.27	5.41	7.03	0.00	0.000	0.00261	0.051	0.165	0.216	0.456	3.69	1.299	89.21	0.00282	7.37	10877.3
11:30	83.53	3.46	8.56	4.45	0.00	0.000	0.00912	0.123	0.602	0.725	1.105	2.45	0.519	83.50	0.00964	5.42	10180.6
11:45	83.19	5.16	8.20	3.45	0.00	0.000	0.00980	0.116	0.579	0.696	1.048	2.41	0.420	75.42	0.01032	5.03	10345.6
11:55	83.44	5.37	7.97	3.22	0.00	0.000	0.00640	0.078	0.363	0.442	0.705	2.59	0.404	74.42	0.00676	5.32	10635.2
12:00	82.72	6.97	7.57	2.73	0.00	0.000	0.00490	0.050	0.256	0.307	0.453	2.36	0.361	66.80	0.00513	4.50	10413.6
12:15	82.98	7.91	6.64	2.47	0.00	0.000	0.00900	0.096	0.416	0.511	0.860	2.75	0.372	62.32	0.00945	4.80	10943.9
12:30	83.00	7.33	7.14	2.53	0.00	0.000	0.01070	0.115	0.525	0.640	1.031	2.62	0.354	65.11	0.01124	4.82	10797.9
12:45	83.23	7.43	6.73	2.61	0.00	0.000	0.01030	0.116	0.488	0.604	1.044	2.85	0.387	64.63	0.01085	5.08	11037.3
13:00	83.69	4.42	7.62	4.27	0.00	0.000	0.01040	0.142	0.628	0.769	1.277	2.71	0.560	78.93	0.01102	5.60	10481.5
13:15	83.50	2.99	8.44	4.46	0.61	0.000	0.00930	0.134	0.609	0.743	1.208	2.65	0.529	85.76	0.00983	5.38	10447.9
13:30	82.74	2.17	9.16	5.00	0.93	0.009	0.01040	0.144	0.747	0.891	1.293	2.31	0.546	89.68	0.01089	4.52	9923.8
13:45	82.29	4.91	8.36	3.88	0.56	0.010	0.00680	0.077	0.422	0.499	0.691	2.18	0.464	76.63	0.00708	4.00	9905.1
14:00	82.39	5.12	8.06	3.87	0.56	0.014	0.01020	0.117	0.617	0.734	1.053	2.27	0.480	75.60	0.01064	4.11	10010.5
14:15	84.96	6.16	6.80	2.09	0.00	0.000	0.00940	0.137	0.424	0.560	1.229	3.87	0.307	70.67	0.01011	7.01	12517.2
14:30	86.67	4.69	6.56	2.07	0.00	0.000	0.00880	0.160	0.386	0.546	1.440	4.98	0.316	77.66	0.00965	8.85	13717.2
14:45	87.72	3.44	6.61	2.23	0.00	0.000	0.00840	0.173	0.377	0.549	1.553	5.50	0.337	83.60	0.00933	9.93	14186.6
15:00	87.42	1.98	7.75	2.85	0.00	0.000	0.00840	0.172	0.452	0.624	1.545	4.56	0.368	90.56	0.00929	9.63	13154.8
15:15	85.70	1.46	9.35	3.49	0.00	0.000	0.01140	0.197	0.743	0.940	1.774	3.18	0.373	93.05	0.01237	7.81	11513.3
15:32	85.50	1.74	9.28	3.47	0.00	0.000	0.00900	0.152	0.582	0.734	1.366	3.13	0.374	91.69	0.00974	7.61	11437.1
15:45	83.61	1.49	11.13	3.78	0.00	0.000	0.01460	0.191	1.104	1.295	1.717	2.07	0.339	92.92	0.01545	5.51	10050.0
16:00	81.95	1.32	12.00	4.32	0.42	0.007	0.00650	0.069	0.538	0.608	0.624	1.55	0.360	93.73	0.00674	3.59	9170.5
16:20	79.58	0.97	14.32	4.72	0.41	0.006	0.01010	0.060	0.976	1.036	~~0.539~~	~~0.74~~	0.330	95.40	0.01017	0.73	7861.0
16:30	79.07	0.93	14.48	5.13	0.39	0.005	0.01040	0.054	1.035	1.089	0.482	0.62	0.354	95.59	0.01041	0.09	7574.2
16:45	78.99	0.94	14.53	5.10	0.44	0.006	0.00960	0.048	0.956	1.005	0.435	0.61	0.351	95.52	0.00960	-.02	7557.1
17:00	81.06	1.10	13.39	4.45	0.00	0.000	0.01120	0.092	1.014	1.106	0.824	1.08	0.333	94.76	0.01149	2.54	8471.3
17:15	81.97	1.02	13.63	3.39	0.00	0.000	0.00960	0.088	0.829	0.918	0.726	1.28	0.249	95.16	0.00996	3.62	9066.3
17:32	81.85	1.02	13.25	3.88	0.00	0.000	0.01120	0.105	0.974	1.079	0.948	1.30	0.293	95.16	0.01160	3.48	8953.0
17:45	81.99	1.04	13.07	3.89	0.00	0.000	0.00910	0.088	0.783	0.872	0.795	1.35	0.298	95.02	0.00944	3.65	9031.5
17:54	81.92	1.09	13.00	3.99	0.00	0.000	0.00690	0.066	0.595	0.661	0.598	1.34	0.307	94.82	0.00716	3.57	8984.6

*See end of Appendix for notes detailing column headings

RUN NO.3

Maya Isthmus crude oil (32.4 °API); 5% kaolin; WAR = 2.5 $m^3.Mm^3$ (STP); ignition at 13:12; water injection at 15:05; stabilised period (16:30-17:30)

Clock time	Mole fraction %															
	N_2	O_2	CO_2	CO	CH_4	1*	2*	3*	4*	5*	6*	7*	8*	9*	10*	11*
13:22	83.93	1.56	6.69	5.61	2.21	0.00386	0.073	0.241	0.314	0.661	3.66	0.838	92.57	0.00410	5.87	11309.3
13:32	84.80	1.06	8.64	5.50	0.00	0.00570	0.097	0.409	0.506	0.876	2.85	0.637	94.93	0.00612	6.84	10542.2
13:45	80.02	0.99	13.11	5.88	0.00	0.00790	0.057	0.761	0.818	0.510	0.89	0.449	95.30	0.00800	1.28	7818.4
14:00	80.42	1.00	14.19	4.38	0.00	0.00950	0.064	0.896	0.960	0.577	0.86	0.309	95.22	0.00967	1.76	8147.1
14:15	80.17	1.00	14.52	4.31	0.00	0.00870	0.054	0.831	0.885	0.482	0.77	0.297	95.22	0.00883	1.46	8030.7
14:30	80.49	0.99	14.11	4.41	0.00	0.00950	0.066	0.893	0.959	0.591	0.88	0.313	95.28	0.00968	1.84	8176.9
14:45	81.12	1.01	13.52	4.35	0.00	0.00900	0.074	0.816	0.890	0.666	1.09	0.322	95.18	0.00924	2.62	8513.2
15:00	82.55	1.08	12.64	3.74	0.00	0.00900	0.097	0.748	0.845	0.871	1.55	0.296	94.88	0.00940	4.30	9365.1
15:15	80.70	1.07	14.02	4.22	0.00	0.01120	0.081	1.036	1.117	0.725	0.93	0.301	94.90	0.01144	2.10	8303.6
15:32	80.73	1.61	13.60	4.07	0.00	0.00770	0.055	0.690	0.745	0.494	0.95	0.299	92.33	0.00787	2.14	8348.0
15:45	80.50	1.41	14.00	4.09	0.00	0.01500	0.100	1.377	1.477	0.900	0.87	0.292	93.29	0.01528	1.86	8222.7
16:00	79.88	1.24	14.64	4.25	0.00	0.00890	0.049	0.853	0.902	0.438	0.68	0.290	94.10	0.00900	1.10	7890.8
16:15	79.33	1.08	15.02	4.56	0.00	0.00850	0.039	0.845	0.884	0.349	0.55	0.304	94.84	0.00854	0.41	7597.5
16:30	80.13	1.26	13.96	4.65	0.00	0.00920	0.059	0.869	0.927	0.527	0.81	0.333	94.00	0.00933	1.41	7982.2
16:45	82.04	1.47	12.32	4.16	0.00	0.00940	0.094	0.786	0.881	0.849	1.44	0.337	92.98	0.00976	3.71	9059.3
17:00	82.62	2.28	11.61	3.49	0.00	0.00880	0.094	0.674	0.769	0.847	1.68	0.301	89.13	0.00920	4.38	9545.2
17:15	87.90	2.91	4.33	4.85	0.00	0.00800	0.185	0.373	0.558	1.668	5.97	1.121	86.14	0.00890	10.13	13588.3
17:30	84.32	3.13	8.19	4.36	0.00	0.00990	0.149	0.631	0.780	1.343	2.84	0.532	85.10	0.01057	6.30	10710.6
17:45	81.59	3.58	11.03	3.80	0.00	0.00900	0.079	0.677	0.756	0.709	1.40	0.344	82.93	0.00929	3.17	8969.4
18:00	80.29	4.25	12.11	3.36	0.00	0.00730	0.041	0.573	0.614	0.368	0.86	0.277	79.78	0.00742	1.60	8241.7
18:15	80.12	4.58	11.78	3.52	0.00	0.00850	0.046	0.660	0.706	0.411	0.83	0.299	78.21	0.00862	1.39	8125.6
18:30	80.51	4.98	11.12	3.40	0.00	0.00610	0.037	0.449	0.487	0.335	0.99	0.305	76.30	0.00622	1.87	8397.7

*See end of Appendix for notes detailing column headings

RUN NO.4

Maya Isthums crude oil (32.4 °API); 5% kaolin; WAR = 3.75 m^3/Mm^3 (STP); ignition at 13:25; water injection at 15:30; stabilised period (16:00-17:00)

Clock time	Mole fraction%																
	N_2	O_2	CO_2	CO	CH_4	1*	2*	3*	4*	5*	6*	7*	8*	9*	10*	11*	12*
13:33	84.89	1.82	5.75	7.54	0.00	0.00	0.00435	0.083	0.293	0.376	0.744	3.38	1.312	91.33	0.00467	6.94	10459.3
13:45	83.00	2.69	8.99	5.31	0.00	0.00	0.00780	0.102	0.566	0.668	0.917	2.16	0.591	87.17	0.00820	4.82	9613.7
14:00	81.59	2.89	11.22	4.29	0.00	0.00	0.00900	0.083	0.709	0.791	0.743	1.40	0.382	86.22	0.00930	3.17	8869.2
14:15	81.76	3.51	10.96	3.78	0.00	0.00	0.00840	0.076	0.628	0.705	0.688	1.46	0.345	83.29	0.00869	3.37	9072.4
14:33	81.91	3.88	10.43	3.78	0.00	0.00	0.01070	0.1 1	0.772	0.873	0.909	1.57	0.363	81.54	0.01109	3.55	9201.8
14:45	82.37	3.24	10.37	4.02	0.00	0.00	0.00700	0.074	0.511	0.586	0.669	1.74	0.388	84.58	0.00730	4.09	9415.7
15:00	81.74	3.38	10.31	3.95	0.51	0.12	0.00790	0.081	0.572	0.653	0.732	1.71	0.383	83.89	0.00818	3.47	9371.1
15:15	81.79	1.18	12.16	4.62	1.09	0.24	0.00820	0.081	0.698	0.780	0.733	1.40	0.380	94.37	0.00840	2.40	8875.0
15:30	81.24	1.06	11.81	4.57	1.07	0.25	0.00810	0.089	0.673	0.762	0.803	1.59	0.387	94.96	0.00836	3.06	9172.7
15:45	79.81	1.10	13.52	4.76	0.70	0.12	0.00960	0.069	0.891	0.960	0.619	0.93	0.352	94.77	0.00971	1.14	8139.9
16:00	79.52	1.46	13.85	4.51	0.56	0.12	0.00820	0.050	0.764	0.814	0.451	0.79	0.326	93.07	0.00827	0.79	7967.6
16:15	80.27	1.32	13.80	4.61	0.00	0.00	0.00670	0.044	0.626	0.670	0.399	0.85	0.334	93.72	0.00681	1.58	8055.9
16:30	80.73	2.07	12.05	4.48	0.57	0.11	0.00750	0.065	0.629	0.694	0.585	1.24	0.372	90.16	0.00767	2.26	8629.8
16:45	80.51	2.02	12.05	4.68	0.61	0.12	0.00790	0.067	0.671	0.738	0.604	1.20	0.389	90.36	0.00806	2.02	8516.5
17:00	86.42	3.18	7.06	2.43	0.80	0.11	0.00670	0.131	0.323	0.454	1.177	4.86	0.344	84.85	0.00734	8.70	13536.8
17:15	83.67	1.79	9.85	3.46	1.05	0.18	0.00790	0.119	0.534	0.653	1.072	2.68	0.351	91.46	0.00838	5.78	10889.7
17:26	81.86	1.67	11.15	4.10	1.01	0.22	0.00650	0.076	0.503	0.57	0.687	1.82	0.367	92.03	0.00675	3.73	9589.1
17:32	81.78	1.68	11.21	4.04	1.05	0.25	0.01455	0.169	1.127	1.296	1.525	1.80	0.360	92.00	0.01510	3.67	9583.2

*See end of Appendix for notes detailing column headings

RUN NO.5

Maya Isthums crude oil (32.4 °API); 10% kaolin: WAR = 3.75 m^3/Mm^3 (STP); ignition at 16:08; water injection at 18:40; stabilised period (19:00-21:30)

Clock time	Mole fraction %																
	N_2	O_2	CO_2	CO	CH_4	H_2	1*	2*	3*	4*	5*	6*	7*	8*	9*	10*	11*
16:22	86.09	1.98	6.13	4.43	1.36	0.020	0.00550	0.117	0.295	0.412	1.051	4.75	0.723	90.55	0.00599	8.23	12750.9
16:30	84.36	1.77	8.32	4.86	0.69	0.000	0.00420	0.070	0.281	0.351	0.633	3.00	0.585	91.55	0.00448	6.35	10839.0
16:45	81.45	1.53	12.47	4.54	0.00	0.000	0.00865	0.079	0.747	0.826	0.708	1.26	0.364	92.70	0.00892	3.01	8691.5
17:02	79.90	1.92	14.32	3.86	0.00	0.000	0.01005	0.052	0.927	0.979	0.469	0.67	0.269	90.85	0.01016	1.12	7938.8
17:15	80.10	2.08	14.13	3.70	0.00	0.000	0.00725	0.040	0.656	0.696	0.357	0.73	0.262	90.11	0.00735	1.37	8060.3
17:30	80.00	2.08	13.79	4.13	0.00	0.000	0.00935	0.053	0.850	0.903	0.475	0.74	0.300	90.12	0.00947	1.25	7969.3
17:45	79.39	1.84	14.25	4.52	0.00	0.000	0.00800	0.037	0.762	0.799	0.335	0.59	0.317	91.24	0.00804	0.49	7622.2
18:02	79.79	2.09	13.79	4.34	0.00	0.000	0.00940	0.050	0.865	0.915	0.453	0.70	0.315	90.06	0.00949	0.99	7839.0
18:15	80.35	1.98	13.32	4.35	0.00	0.000	0.00755	0.050	0.677	0.727	0.446	0.88	0.327	90.59	0.00768	1.68	8128.4
18:30	81.05	2.11	12.46	4.38	0.00	0.000	0.01690	0.137	1.444	1.581	1.233	1.14	0.352	89.97	0.01734	2.53	8510.5
18:45	81.78	1.85	11.50	4.63	0.25	0.010	0.00175	0.018	0.143	0.161	0.162	1.51	0.402	91.21	0.00181	3.40	8998.8
19:00	81.97	4.04	10.37	3.32	0.30	0.010	0.00680	0.066	0.472	0.538	0.592	1.67	0.320	80.74	0.00706	3.62	9482.1
19:15	83.14	5.67	8.54	2.34	0.31	0.009	0.00820	0.093	0.453	0.546	0.839	2.47	0.275	73.01	0.00863	4.98	10807.5
19:30	83.38	5.56	8.72	2.34	0.00	0.000	0.00830	0.094	0.466	0.560	0.848	2.43	0.268	73.50	0.00876	5.25	10767.0
19:46	82.85	4.66	9.86	2.62	0.00	0.000	0.00880	0.092	0.557	0.650	0.829	1.98	0.266	77.79	0.00923	4.65	10123.5
20:00	83.02	4.76	9.52	2.71	0.00	0.000	0.00741	0.081	0.460	0.540	0.726	2.11	0.285	77.35	0.00779	4.84	10254.2
20:15	82.58	4.17	10.21	3.04	0.00	0.000	0.00729	0.075	0.490	0.565	0.672	1.83	0.298	80.15	0.00762	4.33	9790.6
20:30	82.05	4.41	10.43	3.11	0.00	0.000	0.00860	0.079	0.591	0.670	0.709	1.60	0.298	79.00	0.00893	3.72	9435.1
20:47	81.89	4.51	10.48	3.12	0.00	0.000	0.00900	0.079	0.621	0.701	0.714	1.53	0.297	78.52	0.00933	3.53	9328.6
21:00	81.78	2.51	12.33	3.37	0.00	0.000	0.00680	0.060	0.542	0.602	0.539	1.33	0.273	88.03	0.00704	3.40	9063.7
21:15	81.98	3.82	11.18	3.03	0.00	0.000	0.00830	0.074	0.598	0.672	0.667	1.49	0.271	81.81	0.00861	3.63	9334.4
21:30	81.84	3.69	11.32	3.14	0.00	0.000	0.00750	0.066	0.551	0.616	0.590	1.43	0.277	82.43	0.00777	3.47	9220.9
21:45	79.42	1.83	13.80	4.24	0.72	0.015	0.00895	0.051	0.819	0.870	0.458	0.75	0.307	91.29	0.00900	0.53	7948.7
22:04	79.75	2.04	13.48	4.15	0.59	0.010	0.00998	0.061	0.893	0.954	0.548	0.82	0.307	90.31	0.01007	0.94	8078.2

*See end of Appendix for notes detailing column headings

RUN NO.6

Forties crude oil (36.6 °API); 5% kaolin; WAR = 1.25 m^3/Mm^3 (STP); ignition at 16:25; water injection at 18:16; stabilised period (19:30-20:30)

Clock time	Mole fraction %																
	N_2	O_2	CO_2	CO	CH_4	H_2	1*	2*	3*	4*	5*	6*	7*	8*	9*	10*	11*
16:31	83.87	8.87	5.05	1.46	0.75	0.009	0.00106	0.014	0.035	0.049	0.123	4.70	0.289	57.77	0.00113	5.81	13496.9
16:48	84.83	1.63	9.07	4.46	0.00	0.000	0.00870	0.142	0.598	0.739	1.274	2.84	0.492	92.23	0.00934	6.88	10795.4
17:00	82.12	1.84	12.09	3.96	0.00	0.000	0.00900	0.090	0.733	0.823	0.811	1.48	0.327	91.26	0.00935	3.79	9148.7
17:10	80.55	2.55	13.60	3.31	0.00	0.000	0.00868	0.053	0.745	0.798	0.477	0.85	0.243	87.87	0.00885	1.92	8353.4
17:30	80.95	2.56	13.03	3.46	0.00	0.000	0.00745	0.053	0.623	0.676	0.476	1.02	0.265	87.82	0.00763	2.41	8567.4
17:45	81.97	3.09	11.33	3.60	0.00	0.000	0.00898	0.085	0.681	0.765	0.761	1.49	0.318	85.28	0.00932	3.63	9198.6
18:00	83.03	2.33	10.66	3.98	0.00	0.000	0.00770	0.092	0.572	0.664	0.831	1.94	0.373	88.89	0.00809	4.85	9754.8
18:15	83.59	3.09	9.46	3.85	0.00	0.000	0.00786	0.103	0.531	0.634	0.926	2.32	0.407	85.30	0.00832	5.49	10250.7
18:30	84.33	3.41	8.72	3.54	0.00	0.000	0.00837	0.120	0.521	0.641	1.084	2.78	0.406	83.75	0.00893	6.32	10894.0
18:47	83.90	3.61	9.42	3.07	0.00	0.000	0.01057	0.138	0.670	0.808	1.245	2.48	0.326	82.80	0.01123	5.84	10678.8
19:00	84.70	5.52	7.32	2.46	0.00	0.000	0.00650	0.093	0.323	0.416	0.836	3.45	0.336	73.73	0.00697	6.73	11945.0
19:15	85.51	4.80	7.11	2.59	0.00	0.000	0.00780	0.126	0.384	0.510	1.132	3.93	0.364	77.17	0.00844	7.61	12458.4
19:30	85.28	5.60	6.70	2.42	0.00	0.000	0.00770	0.119	0.356	0.476	1.073	4.01	0.361	73.33	0.00831	7.36	12560.6
19:45	85.66	3.67	7.61	2.57	0.50	0.008	0.00758	0.131	0.391	0.522	1.178	4.01	0.337	82.52	0.00822	7.77	12611.7
20:00	84.98	2.90	8.72	2.90	0.50	0.006	0.00780	0.126	0.460	0.585	1.130	3.28	0.332	86.17	0.00839	7.03	11732.3
20:15	82.68	1.66	10.98	3.81	0.88	0.009	0.00705	0.089	0.529	0.618	0.798	2.01	0.347	92.10	0.00738	4.45	9935.3
20:30	82.52	1.64	11.11	3.71	1.02	0.008	0.00787	0.098	0.592	0.690	0.878	1.98	0.334	92.21	0.00822	4.26	9920.1
20:46	81.15	1.47	11.98	3.89	1.50	0.009	0.00840	0.088	0.677	0.764	0.790	1.56	0.325	93.00	0.00863	2.65	9285.7
21:00	79.90	2.67	11.67	4.50	1.26	0.018	0.00899	0.071	0.738	0.808	0.635	1.15	0.386	87.27	0.00909	1.12	8435.9

*See end of Appendix for notes detailing column headings.

RUN NO.7

Maya crude oil (22.1 °API); 5% kaolin; WAR = 1.25 m^3/Mm^3 (STP); ignition at 18:43; water injection at 21:00; stabilised period (23:00-24:00)

Mole fraction %

Clock time	N_2	O_2	CO_2	CO	CH_4	H_2	1*	2*	3*	4*	5*	6*	7*	8*	9*	10*	11*
18:50	67.67	1.46	13.17	6.25	9.53	1.91	0.00138	0.001	0.136	0.137	0.005	0.05	0.475	93.06	0.00118	-16.95	6113.4
19:05	81.57	1.76	10.74	5.02	0.92	0.00	0.00750	0.085	0.600	0.684	0.762	1.70	0.467	91.62	0.00774	3.10	9144.4
19:15	80.71	1.72	12.45	5.00	0.00	0.12	0.00480	0.039	0.425	0.464	0.349	1.09	0.402	91.81	0.00490	2.04	8299.3
19:30	80.61	2.75	12.61	3.98	0.00	0.05	0.00880	0.061	0.741	0.802	0.546	0.98	0.316	86.91	0.00898	2.00	8347.0
19:46	80.62	4.04	11.74	3.52	0.00	0.08	0.00988	0.065	0.765	0.830	0.585	1.02	0.300	80.77	0.01008	9.92	8459.7
20:00	80.33	5.02	11.23	3.28	0.05	0.09	0.00858	0.050	0.632	0.682	0.452	0.95	0.292	76.10	0.00872	1.60	8365.3
20:15	79.81	4.45	11.52	3.48	0.63	0.11	0.00787	0.047	0.599	0.646	0.419	0.93	0.302	78.79	0.00795	1.00	8298.2
20:30	80.65	4.68	10.33	3.63	0.60	0.11	0.00806	0.063	0.571	0.634	0.565	1.32	0.351	77.70	0.00823	2.06	8821.9
20:45	80.79	4.29	10.88	3.41	0.52	0.11	0.00880	0.068	0.638	0.707	0.616	1.29	0.313	79.56	0.00900	2.22	8877.5
21:03	82.54	4.86	9.69	2.85	0.00	0.06	0.00890	0.090	0.566	0.656	0.808	1.90	0.294	76.85	0.00930	4.30	9916.6
21:15	82.00	5.94	9.69	2.37	0.00	0.00	0.00748	0.063	0.458	0.521	0.567	1.65	0.245	71.72	0.00776	3.61	9680.6
21:30	83.14	5.18	9.40	2.22	0.00	0.06	0.00698	0.076	0.412	0.487	0.681	2.21	0.236	75.35	0.00735	5.03	10545.7
21:45	83.29	4.60	9.48	2.55	0.00	0.08	0.00800	0.092	0.489	0.580	0.826	2.25	0.269	78.10	0.00843	5.10	10513.0
22:00	83.32	5.78	8.27	2.08	0.45	0.10	0.00870	0.104	0.457	0.561	0.934	2.73	0.251	72.48	0.00918	5.23	11230.6
22:15	83.69	5.92	7.73	1.92	0.61	0.13	0.00670	0.087	0.328	0.415	0.779	3.17	0.248	71.80	0.00710	5.63	11817.7
22:30	84.24	6.13	7.16	1.66	0.65	0.17	0.00840	0.118	0.376	0.493	1.059	3.76	0.232	70.83	0.00896	6.29	12589.7
22:45	84.92	3.86	7.65	2.45	0.94	0.18	0.00750	0.125	0.384	0.509	1.124	3.90	0.321	81.62	0.00806	6.95	12520.1
23:00	84.59	2.06	8.42	3.46	1.23	0.24	0.00800	0.139	0.482	0.621	1.251	3.46	0.411	90.18	0.00857	6.65	11780.4
23:15	84.51	2.39	8.24	3.31	1.52	0.03	0.00730	0.126	0.428	0.554	1.131	3.52	0.402	88.60	0.00781	6.53	11878.3
23:30	82.24	1.88	9.42	3.61	2.39	0.46	0.00880	0.130	0.582	0.712	1.173	2.69	0.384	91.06	0.00916	3.93	10822.0
23:45	80.66	1.23	10.62	3.66	3.19	0.64	0.00700	0.092	0.507	0.599	0.827	2.17	0.344	94.13	0.00715	2.10	10185.9
24:00	81.05	2.19	8.79	3.28	3.89	0.80	0.01410	0.213	0.864	1.077	1.915	2.96	0.373	89.56	0.01447	2.56	11213.5
24:15	77.27	1.10	13.12	3.66	4.04	0.81	0.01680	0.128	1.430	1.558	1.148	1.07	0.279	94.75	0.01643	-2.25	8613.0
24:37	72.20	1.40	15.77	4.48	5.17	0.99	0.00085	-0.00315	0.874	0.871	-0.0283	-0.043	0.243	93.36	0.0077	-9.42	6497.7

*See end of Appendix for notes detailing column headings

RUN NO.8

Maya Isthmus crude oil (32.4 °API); 10 amorphous silica; WAR = 0.0; ignition at 08:45; stabilised period (13:30-16:30)

Clock time	Mole fraction %														
	N_2	O_2	CO_2	CO	CH_4	1*	2*	3*	4*	5*	6*	7*	8*	9*	10*	11*
08:55	80.47	5.88	9.98	3.66	0.00	0.00990	0.062	0.686	0.747	0.556	1.08	0.367	71.98	0.01008	1.82	8371.0
09:05	82.10	1.54	13.52	2.83	0.00	0.00782	0.071	0.649	0.720	0.636	1.31	0.210	92.65	0.00813	3.77	9240.4
09:30	82.43	1.40	13.30	2.86	0.00	0.01030	0.101	0.845	0.946	0.906	1.43	0.215	93.31	0.01075	4.16	9422.3
09:45	82.18	1.42	13.51	2.89	0.00	0.00650	0.060	0.541	0.601	0.541	1.33	0.214	93.23	0.00676	3.87	9270.2
10:05	81.59	1.24	14.02	3.15	0.00	0.00790	0.065	0.688	0.753	0.583	1.13	0.224	94.09	0.00816	3.17	8895.4
10:17	81.36	1.23	14.32	3.10	0.00	0.01040	0.080	0.919	0.999	0.718	1.04	0.216	94.16	0.01071	2.90	8771.1
10:30	80.57	1.16	15.07	3.20	0.00	0.00981	0.060	0.910	0.969	0.536	0.79	0.212	94.49	0.01001	1.95	8339.4
10:45	79.85	1.07	15.75	3.33	0.00	0.00956	0.044	0.926	0.970	0.399	0.57	0.211	94.92	0.00966	1.06	7957.8
11:00	79.32	1.03	16.28	3.38	0.00	0.00854	0.030	0.852	0.882	0.272	0.42	0.208	95.11	0.00857	0.40	7693.2
11:16	78.65	0.92	17.10	3.32	0.00	0.00853	0.018	0.884	0.902	0.158	0.24	0.194	95.60	0.00849	-.45	7386.3
11:30	78.92	0.91	16.96	3.21	0.00	0.00871	0.022	0.892	0.914	0.199	0.30	0.189	95.67	0.00870	-.10	7519.9
11:45	79.60	1.00	16.38	3.02	0.00	0.00865	0.033	0.852	0.885	0.298	0.47	0.185	95.25	0.00872	0.75	7859.0
12:00	78.69	0.76	17.84	2.72	0.00	0.00840	0.014	0.876	0.890	0.123	0.19	0.152	96.40	0.00837	-.40	7455.6
12:15	78.85	0.68	17.84	2.64	0.00	0.00870	0.017	0.904	0.920	0.149	0.22	0.148	96.76	0.00868	-.20	7537.0
12:30	78.81	0.51	17.96	2.72	0.00	0.00950	0.018	0.997	1.015	0.162	0.22	0.152	97.59	0.00948	-.24	7515.2
12:45	78.25	0.50	17.77	3.48	0.00	0.00975	0.013	1.052	1.065	0.117	0.15	0.196	97.63	0.00966	-.96	7204.6
13:00	78.36	0.45	17.72	3.47	0.00	0.00980	0.015	1.054	1.069	0.138	0.18	0.196	97.86	0.00972	-.81	7256.7
13:15	78.52	0.47	17.65	3.37	0.00	0.00863	0.016	0.920	0.936	0.141	0.20	0.191	97.78	0.00858	-.61	7334.4
13:30	78.38	0.46	17.80	3.35	0.00	0.00860	0.013	0.923	0.936	0.117	0.17	0.188	97.81	0.00853	-.79	7274.0
13:45	78.39	0.44	17.61	3.56	0.00	0.00811	0.014	0.871	0.885	0.124	0.19	0.202	97.89	0.00805	-.78	7261.2
14:00	78.51	0.37	17.67	3.45	0.00	0.00850	0.016	0.911	0.927	0.142	0.21	0.195	98.22	0.00845	-.63	7322.9
14:15	78.73	0.45	17.58	3.24	0.00	0.00880	0.019	0.930	0.949	0.171	0.25	0.184	97.86	0.00877	-.55	7437.5
14:30	78.71	0.53	17.64	3.12	0.00	0.00830	0.017	0.874	0.891	0.151	0.23	0.177	97.49	0.00827	-.37	7438.6
14:45	79.60	0.63	16.46	3.31	0.00	0.00910	0.037	0.913	0.951	0.334	0.49	0.201	97.02	0.00917	0.75	7833.5
15:00	79.66	0.62	16.50	3.22	0.00	0.00954	0.039	0.955	0.994	0.355	0.50	0.195	97.03	0.00962	0.83	7873.3
15:16	78.60	0.58	17.58	3.23	0.00	0.00874	0.016	0.923	0.940	0.148	0.21	0.184	97.22	0.00870	-.51	7379.7
15:32	78.43	0.64	17.58	3.35	0.00	0.00950	0.015	1.009	1.024	0.138	0.18	0.190	96.95	0.00943	-.73	7291.2
15:45	78.69	0.67	17.64	2.99	0.00	0.00840	0.016	0.880	0.895	0.142	0.21	0.169	96.81	0.00837	-.39	7438.5
16:00	79.08	0.37	17.31	3.22	0.02	0.00867	0.025	0.903	0.928	0.229	0.34	0.186	98.24	0.00868	0.11	7610.6
16:17	78.50	0.30	17.61	3.60	0.00	0.00830	0.016	0.893	0.910	0.147	0.22	0.204	98.59	0.00825	-.64	7310.4
16:30	78.98	0.23	17.35	3.42	0.03	0.00790	0.023	0.832	0.855	0.206	0.33	0.197	98.91	0.00790	-.03	7552.0
16:45	78.76	0.22	17.66	3.36	0.00	0.00756	0.018	0.806	0.824	0.158	0.26	0.191	98.94	0.00754	-.31	7445.9
17:03	78.92	0.25	17.55	3.28	0.00	0.00860	0.022	0.909	0.932	0.201	0.30	0.187	98.82	0.00859	-.10	7524.4
17:15	78.82	0.34	17.66	3.18	0.00	0.01100	0.025	1.163	1.189	0.227	0.26	0.180	98.36	0.01097	-.23	7485.2
17:30	79.13	0.40	17.23	3.24	0.00	0.00870	0.026	0.904	0.930	0.236	0.35	0.188	98.08	0.00871	0.16	7620.6
17:45	79.74	0.52	16.50	3.24	0.00	0.00910	0.039	0.912	0.951	0.354	0.52	0.196	97.53	0.00919	0.93	7911.4
18:00	80.27	0.61	16.25	2.86	0.00	0.00880	0.045	0.854	0.899	0.407	0.64	0.176	97.07	0.00894	1.58	8203.8
18:15	80.67	0.76	15.84	2.73	0.00	0.00760	0.045	0.716	0.761	0.402	0.75	0.172	96.38	0.00776	2.06	8419.9
18:30	80.97	0.85	15.37	2.82	0.00	0.00690	0.045	0.637	0.682	0.409	0.86	0.183	95.97	0.00707	2.43	8571.7
18:46	81.38	0.89	15.10	2.63	0.00	0.00760	0.056	0.684	0.740	0.500	0.97	0.174	95.77	0.00783	2.92	8810.5
19:00	81.46	0.88	15.11	2.55	0.00	0.00930	0.069	0.833	0.902	0.621	0.99	0.169	95.81	0.00959	3.02	8865.5
19:15	81.26	1.14	14.97	2.63	0.00	0.00960	0.068	0.858	0.925	0.610	0.95	0.176	94.58	0.00987	2.78	8759.7
19:33	81.14	1.21	15.03	2.62	0.00	0.00910	0.062	0.815	0.877	0.557	0.91	0.174	94.22	0.00935	2.64	8700.6
19:45	81.51	1.25	14.20	3.05	0.00	0.01590	0.126	1.392	1.518	1.137	1.03	0.215	94.07	0.01640	3.07	8857.7

*See end of Appendix for notes detailing column headings

Footnotes to Appendix D

1 = Volume of gas produced m^3 (st) (as measured by wet test meter).

2 = Amount of hydrogen burned, g.

3 = Amount of carbon burned, g.

4 = Amount of fuel burned, g.

5 = Amount of water formed by combustion, g.

6 = Hydrogen:carbon ratio.

7 = Carbon monoxide:carbon dioxide ratio.

8 = Oxygen utilisation percentage.

9 = Volume of air consumed, m^3 (st).

10 = Volume difference factor, percentage.

11 = Heat available (released from combustion), cal/gcH_x.